

**Proceedings of the Symposium**  
**on the**  
**ECONOMIC MINERAL DEPOSITS OF THE**  
**SOUTHEAST: METALLIC ORE DEPOSITS**

**Sponsored by the Southeastern Section of the  
Geological Society of America, Atlanta, Georgia  
April 6, 1989**

**Edited by**  
**Robert B. Cook**

**Georgia Department of Natural Resources  
Environmental Protection Division  
Georgia Geologic Survey**

**BULLETIN 117**

The papers presented herewith have not undergone review procedures of the Georgia Geologic Survey's Quality Assurance Plan. They do not necessarily reflect the technical opinions of the Georgia Geologic Survey.

**Proceedings of the Symposium**  
**on the**  
**ECONOMIC MINERAL DEPOSITS OF THE**  
**SOUTHEAST: METALLIC ORE DEPOSITS**

**Sponsored by the Southeastern Section of the  
Geological Society of America, Atlanta, Georgia  
April 6, 1989**

**Edited by  
Robert B. Cook  
Department of Geology  
Auburn University**

**Georgia Department of Natural Resources  
Lonice C. Barrett, Commissioner**

**Environmental Protection Division  
Harold F. Reheis, Assistant Director**

**Georgia Geologic Survey  
William H. McLemore, State Geologist**

**Atlanta  
1990**

**BULLETIN 117**

## PREFACE

This Bulletin contains 10 of the 11 papers presented in the symposium "Economic Mineral Deposits of the Southeast: Metallic Ore Deposits" held as part of the Geological Society of America Southeastern Section Annual Meeting in Atlanta, April 6-7, 1989. Also included is an invited paper by Peng Sha and C. Michael Lesher that complements two other volume papers on the gold occurrences of the Goldville District of Tallapoosa County, Alabama.

Seven of the volume's papers deal with various aspects of specific gold districts or occurrences including Georgia's Dahlonga district and Royal Vindicator deposit. Depositional types vary widely and include probable synmetamorphic, meta-epithermal, shear zone-hosted epigenetic, and placer. Other papers present details of such varied topics as the tin occurrences related to the Rockford Granite of the Alabama Northern Piedmont, the metallogeny of a central Piedmont accretionary plate margin, Zn-Pb resources of the central Kentucky district, and the geochemistry of America's first known PtAs occurrence.

The idea for this proceedings volume is not unique. It represents the second in what hopefully will be regularly though intermittently published collections of papers based on similar symposia dealing with the economic geology of the metallic resources of the southeastern United States. The first such work, "Volcanogenic Sulfide and Precious Metal Mineralization in the Southern Appalachians" (edited by Kula C. Misra), is still available as Studies in Geology #16 of the University of Tennessee Department of Geological Sciences.

My sincere appreciation is expressed to the authors who have taken the time to formalize and revise the text and illustrations of their symposium presentations. Special thanks go to the numerous reviewers who were invariably thorough, prompt and unselfish in their constructive criticism. Publication of this bulletin would not have been possible without the continued support of the Georgia Geologic Survey and in particular the editorial assistance of Ms. Patricia Allgood. The diligent efforts and word-processing skills of Ms. Eva Lilly and Ms. Sheila Arington contributed markedly to the successful completion of this volume.

Robert B. Cook  
Department of Geology  
Auburn University  
Auburn, AL 36849-5305

## TABLE OF CONTENTS

Thermobarometry of Synmetamorphic Gold Deposits, Goldville District, Northern Piedmont, Alabama (Harold H. Stowell and C. Michael Lesher) .....	1
Microthermometry of Fluid Inclusions in Auriferous Quartz Veins, Northern Piedmont, Alabama (Peng Sha and Michael Lesher) .....	18
Stable Isotope Geochemistry of Lode Gold Deposits, Northern Piedmont, Alabama (C. Michael Lesher, Harold H. Stowell, and Nathan L. Green) .....	32
The Royal Vindicator Gold Deposit, Haralson County, Georgia: A Metamorphosed Epithermal Hot-Springs Type Gold Deposit (Travis A. Paris) .....	50
Gold Deposits of the Dahlongea Belt, Northeast Georgia (George V. Albino) .....	85
Paleoplacer Gold in the Lilesville Sand and Gravel Deposits, North Carolina (James R. Craig and John E. Callahan) .....	121
The Use of Relict Phases with Placer Gold in Characterizing Lodes (Alan J. Driscoll, Jr., Donald L. Hall, and James R. Craig) .....	142
A Geochemical Investigation of the Mason Mountain Sperrylite Occurrence, Macon County, North Carolina (Robert B. Cook and James R. Burnell) .....	163
The Central Piedmont Metallogenic Province, South Carolina (Steven K. Mittwede) .....	177
The Rockford Tin District, Alabama Piedmont: A Result of Na-Metasomatism Associated with Trondhjemitic Alteration of the Rockford Granite? (David J. Wesolowski and Mark S. Drummond) .....	208
Polymetallic Sulfide/Fluorspar Mineralization in Western Kentucky: Lead and Zinc Reserves for the 21st Century (Ed L. Schrader, D. E. Gann and A. D. Bishop) .....	229



# THERMOBAROMETRY OF SYNMETAMORPHIC GOLD DEPOSITS, GOLDVILLE DISTRICT, NORTHERN PIEDMONT, ALABAMA

Harold H. Stowell and C. Michael Leshner  
Department of Geology, University of Alabama  
Tuscaloosa, AL 35487-0338

## ABSTRACT

The Goldville district comprises a 16 km long, northeast-trending group of inactive gold mines and prospects in the southeast part of the Ashland-Wedowee belt. Host rocks are metasedimentary rocks of the Wedowee Group that are polydeformed and have been metamorphosed to garnet zone (low- to medium-grade). Gold mines and prospects are associated exclusively with multi-generation quartz±plagioclase±pyrrhotite veins that are variably boudinaged, folded, sheared, and transposed into an  $S_2$  axial planar fabric. Many veins are bordered by very thin (<1 cm) selvages of massive chlorite and/or biotite. Veins, vein selvages, and host rocks are locally sheared by "late" chlorite-muscovite rich shear zones that apparently postdate quartz vein emplacement and peak metamorphism.

The chemistry and texture of garnets in vein selvages, host rocks, and shear zones suggest prograde metamorphic growth with compositional control by host lithologies followed by minor "retrograde" modification. Garnet grains within late shear zones are rimmed with chlorite suggesting retrograde replacement.

Synmetamorphic vein emplacement is indicated by thermobarometric data from veins, vein selvages, host rocks in the Goldville district, and a sample from the Wedowee Group. Garnet-biotite, plagioclase-muscovite, and plagioclase-biotite-muscovite-garnet equilibria yield metamorphic conditions of  $490\pm 50^\circ\text{C}$  ca. 5.8 kb for the Goldville district. Results from all textural occurrences in the district and within the Wedowee Group are indistinguishable. Garnet-biotite and plagioclase-biotite-muscovite-garnet equilibria yield higher metamorphic temperatures of about  $575^\circ\text{C}$  ca. 6.7 kb for Emuckfaw Group schists within the Alexander City fault zone suggesting that this fault zone is a boundary between low-grade (greenschist facies) and medium-grade (amphibolite facies) metamorphic rocks.

Textural relationships, mineral chemistry, and thermobarometric data indicate that the present distribution of gold results from mobilization during near-peak metamorphism and progressive  $D_1$ - $D_2$  deformation.

## INTRODUCTION

The Goldville district comprises a linear group of 17 inactive mines and prospects trending northeast for 16 km across north-central Tallapoosa County (Fig. 1). The regional geology of the Northern Piedmont is described by Tull (1978), Thomas and others (1980), and Guthrie and Leshner (in press).

Gold mineralization in the district is hosted primarily by metasedimentary rocks of the Wedowee Group (Neathery and Reynolds, 1973; Guthrie and Leshner, in press), although the Dutch Bend and Hog Mountain deposits to the west are hosted by tonalite plutons (see Guthrie and Leshner, in press). The rocks in the Goldville district have experienced polyphase deformation (Muangnoicharoen, 1975; Guthrie and Dean, 1989) and greenschist to amphibolite facies

metamorphism (Neathery and Reynolds, 1973; Muangnoicharoen, 1975; Guthrie and Dean, 1989; Stowell et al., in press).

Gold mines and prospects in the Goldville and Hog Mountain districts are associated exclusively with quartz±plagioclase±sulfide veins (Adams, 1930; Pardee and Park, 1948). Adams (1930) interpreted the mineralization as epigenetic, derived from granitic magmas at depth. Paris (1986) interpreted some of the host lithologies as volcanoclastic rocks, considered the gold mineralization to be strata-bound, and favored an exhalative origin for the mineralization. Neal (1986) and Neal and Cook (in press) also interpreted the gold to be strata-bound and syngenetic, but interpreted the host rocks as metapelites. Recent work suggests that vein emplacement/mineralization within metamorphic rocks in the Goldville district occurred during greenschist facies metamorphism (Stowell et al., in press). The mineralogy, and K/Ar and Rb/Sr ages from alteration zones at Hog Mountain and at the Lowe mine suggest that mineralization at both locations likely occurred during the early stages of metamorphism (Green, Leshner, and Stowell, unpublished data).

The principal aim of this report is to characterize temperatures and pressures during vein emplacement/gold mineralization and compare these with metamorphic conditions calculated for rocks in the Wedowee and Emuckfaw Groups adjacent to the district. Diamond drill core from the Jones, Lowe, and Tallapoosa mines, and samples from the Wedowee and Emuckfaw Groups provided the basis for detailed petrographic, mineralogical, and petrological studies.

This study confirms that vein emplacement/gold mineralization occurred at  $490\pm 50^{\circ}\text{C}$  and  $5.8\pm 1$  kb, and indicates that metamorphism of the Emuckfaw Group, south of the Goldville district, in the Alexander City fault zone occurred at somewhat higher temperatures and pressures of  $575\pm 50^{\circ}\text{C}$  and  $6.7\pm 1$  kb.

## GEOLOGIC SETTING

### Host Lithologies

Metasediment-hosted gold deposits in the Goldville district occur in greenschist to amphibolite facies lithologies of the Wedowee Group described by Guthrie and Dean (1989; Fig. 1). Lithologic associations and compositions, thin parallel bedding, and rarely-preserved graded bedding suggest that the rocks were deposited as distal turbidites (Thomas and others, 1980; Guthrie and Dean, 1989; Stowell et al., in press).

South of the Goldville district the Wedowee Group is truncated by the Alexander City fault zone (Fig. 1). The Emuckfaw Group within this zone contains amphibolite facies metamorphic mineral assemblages (Maungnoicharoen, 1975; Guthrie and Dean, 1989). The proximity of these schists to phyllites which contain greenschist facies mineral assemblages has been attributed to widespread retrograde metamorphism of the Wedowee Group (Tull, 1978; Steltenpohl and Moore, 1988).

### Deformation

Five phases of deformation have been recognized based on local cross-cutting relationships in the Goldville district (Guthrie and Dean, 1989): isoclinal folds ( $D_1$ ), close to isoclinal quasi-flexural folds and ductile to semi-brittle shear zones with northwest-directed transport ( $D_2$ ), upright to inclined quasi-flexural slip folds ( $D_3$ ), upright open folds ( $D_4$ ), and dextral strike-slip faults ( $D_5$ ). The regional deformations correlate in a general manner with structures recognized by Tull (1978; cf. Guthrie and Leshner, in press).  $D_1$  through  $D_3$  structures are interpreted to result from progressive deformation during northwest-southeast oriented shortening (Stowell et al., in press).

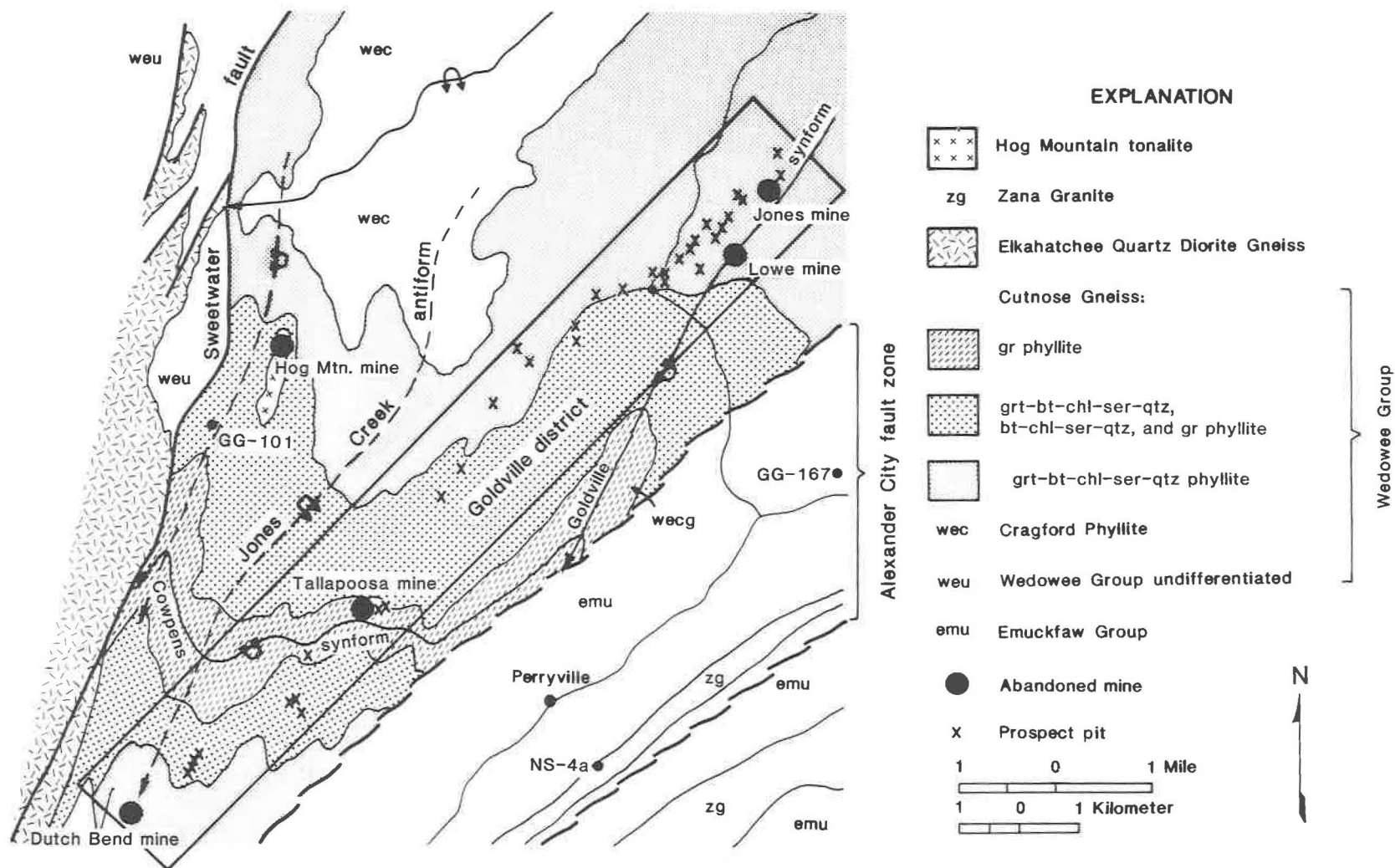


Figure 1. Generalized geologic map of the New Site quadrangle showing mines in the Goldville district and locations of samples used for thermobarometry (modified after Guthrie and Dean, 1989).

## Mineralization

Gold mines and prospects in the district are associated exclusively with multi-generation quartz±plagioclase±sulfide veins that cross-cut compositional layering and the S<sub>1</sub> schistosity (Stowell et al., in press). Veins are variably boudinaged, folded, sheared, and transposed into an S<sub>2</sub> axial planar fabric, suggesting emplacement during S<sub>2</sub> development. Many veins are bordered by very thin (<1 cm) selvages of massive chlorite and/or biotite, and a few are bordered by "late" chlorite-, muscovite-, and quartz-rich shear zones that apparently post-date quartz vein emplacement and peak metamorphism. These sharply defined shear zones locally truncate layering and veins, contain helicitic garnet porphyroblasts which are locally altered to chlorite, and commonly contain significantly smaller grain sizes than host rocks and adjacent vein selvages.

## Metamorphism

Regional metamorphic mineral assemblages in the Wedowee Group have been attributed to an early amphibolite facies event during D<sub>1</sub>, followed by widespread greenschist facies retrograde metamorphism coeval with D<sub>2</sub> (Tull, 1975, 1978; Steltenpohl and Moore, 1988). The earliest metamorphic event generated staurolite to kyanite zone assemblages (Neathery and Reynolds, 1973; Muangnoicharoen, 1975; Steltenpohl and Moore, 1988). Sillimanite zone was attained adjacent to some intrusive bodies (Drummond, 1986). Retrograde chlorite-muscovite zone assemblages occur locally (Steltenpohl and Moore, 1988).

Phyllites and schists in the Wedowee Group contain garnet to sillimanite zone assemblages (Drummond, 1986; Steltenpohl and Moore, 1988). Many of the phyllites and schists in the Goldville district are characterized by garnet-biotite-muscovite-quartz and garnet-chlorite-muscovite-quartz assemblages (Stowell et al., in press). A single sample (LO-2) containing partially replaced staurolite in a vein selvage suggests that metamorphic conditions locally reached those of staurolite zone. Peak metamorphic assemblages are locally retrograded to chlorite-sericite-quartz±biotite. This biotite zone assemblage indicates low grade conditions of the greenschist facies and is similar to "late" metamorphic assemblages recognized elsewhere in the Wedowee Group (Muangnoicharoen, 1975; Tull, 1978; Steltenpohl and Moore, 1988; Guthrie and Dean, 1989).

## ANALYTICAL METHODS

Microanalyses of mineral grains were obtained by wavelength dispersive spectrometry on a CAMECA SX-50 electron microprobes at the University of Tennessee, Knoxville and the University of South Carolina, Columbia, or a JEOL 733 electron microprobe at Southern Methodist University, Dallas. All of the analyses were performed at 15 kV accelerating voltage, 15-20 nA specimen current, maximum of 30 second/100,000 counts on peaks, 10 second counts on backgrounds, and a beam diameter of 1-10 μm. PAP (Pouchou and Pichoir, 1985) and Bence-Albee (Bence and Albee, 1968) data reduction methods were used on the CAMECA and JEOL instruments, respectively. Comparison of analyses of a single grain obtained from two of the instruments and averaging of multiple analyses from one spot obtained on one instrument indicates a precision better than ±2% (relative) for major elements, and a precision better than ±5% (relative) for minor elements.

## PETROGRAPHY AND MINERAL CHEMISTRY

The textural relationships and chemistry of minerals provide considerable information about equilibrium between veins and host rocks, different generations of veins, coexisting vein minerals, and regional metamorphic minerals. These data provide a basis for constraining the timing of vein emplacement, metamorphic conditions during vein emplacement, and the conditions of regional metamorphism.

## Garnet

Garnet occurs as anhedral to euhedral grains within all common lithologies, as well as most vein selvages (Stowell et al., in press). Many grains contain helicitic structures, which are discordant with the fabric outside the porphyroblasts, indicating growth over an early foliation defined by ilmenite and quartz. Garnets commonly have sharp contacts with biotite, muscovite, and early chlorite. Some grains within shear zones are replaced by chlorite along margins and fractures; none of these grains were analyzed.

All of the garnets can be modeled as four component aluminum garnets which are composed predominantly of almandine with lesser amounts of spessartine, grossular, and pyrope (Table 1). Garnet grains from the Tallapoosa mine are strongly zoned, whereas grains from the Lowe mine show only weak zonation (Stowell et al., in press). All zoned garnets exhibit zoning patterns consistent with prograde metamorphic growth (see Stowell et al., in press).

**Table 1. Representative garnet analyses from the Goldville district, Wedowee Group, and Emuckfaw Group, Tallapoosa County, Alabama**

Sample Grain	Lowe mine					Tallapoosa mine		Wedowee Gp.	Emuckfaw Gp.	
	LO-2 G2e 6	LO-13 G1e	LO-15 G3e 4	LO-18 G1e	LO-31d G4e 1	TA-11 G2e	TA-14 G1e	GG-101 G2e	GG-167 G1e 5-6	NS-4a G2e
SiO <sub>2</sub>	37.03	37.13	36.89	36.93	36.99	37.50	37.21	37.19	37.09	37.46
Al <sub>2</sub> O <sub>3</sub>	20.57	20.81	20.88	20.67	21.18	21.44	20.97	21.20	21.36	21.48
TiO <sub>2</sub>	0.10	0.04	0.09	0.06	0.01	0.05	0.06	0.04	0.03	0.05
FeO <sup>1</sup>	26.37	35.71	27.05	35.07	36.58	30.30	33.25	34.11	36.43	28.07
MgO	1.86	1.99	1.68	1.93	1.60	1.66	1.51	2.67	2.50	1.78
MnO	7.29	1.51	9.27	2.45	1.71	4.52	3.44	1.06	1.14	0.92
CaO	6.29	2.97	4.77	2.68	3.66	4.35	3.79	3.36	3.29	10.91
<b>total</b>	<b>99.51</b>	<b>100.14</b>	<b>100.63</b>	<b>99.77</b>	<b>101.74</b>	<b>99.82</b>	<b>100.23</b>	<b>99.63</b>	<b>101.85</b>	<b>100.66</b>
Cations based on 12 oxygens										
Si	2.996	3.003	2.973	3.002	2.963	3.014	3.005	2.996	2.954	2.966
Al	1.962	1.983	1.983	1.980	2.000	2.031	1.995	2.013	2.005	2.004
Ti	0.006	0.002	0.005	0.003	0.000	0.003	0.004	0.002	0.002	0.003
Fe <sup>+2</sup>	1.784	2.415	1.823	2.384	2.451	2.037	2.245	2.299	2.426	1.859
Mg	0.224	0.239	0.202	0.233	0.192	0.199	0.182	0.321	0.297	0.210
Mn	0.499	0.104	0.633	0.169	0.116	0.308	0.235	0.072	0.077	0.062
Ca	0.545	0.257	0.412	0.233	0.315	0.375	0.328	0.290	0.281	0.926
<b>total</b>	<b>8.017</b>	<b>8.004</b>	<b>8.030</b>	<b>8.005</b>	<b>8.036</b>	<b>7.967</b>	<b>7.994</b>	<b>7.994</b>	<b>8.042</b>	<b>8.029</b>
Mg# <sup>2</sup>	0.112	0.090	0.100	0.089	0.073	0.089	0.075	0.122	0.109	0.101
Alm	0.584	0.801	0.594	0.790	0.798	0.698	0.751	0.771	0.787	0.608
Pyr	0.074	0.079	0.066	0.077	0.062	0.068	0.061	0.108	0.096	0.069
Sps	0.164	0.034	0.206	0.056	0.038	0.105	0.079	0.024	0.025	0.020
Grs	0.179	0.085	0.134	0.077	0.102	0.128	0.110	0.097	0.091	0.303

<sup>1</sup> total Fe calculated as FeO

<sup>2</sup> Mg# = Mg/(Mg+Fe)

The almandine content of garnets ranges from 0.58 to 0.80; compositions from both extremes may be found within 75 m at the Lowe mine. Despite large variations in almandine, spessartine, and grossular contents (Table 1), garnets within vein selvages and those within the host rocks

cannot be readily distinguished chemically, suggesting that bulk rock chemistry controlled garnet compositions, not externally-derived fluids.

### Phyllosilicates

Phyllosilicates occur both as disseminated grains and segregations (<1 mm max. dimension) within the host rocks, and as coarse (1-2 mm) aggregates in selvages adjacent to veins. Within the Wedowee Group, biotite-muscovite and chlorite-sericite±biotite define the S<sub>1</sub> and S<sub>2</sub> foliations, respectively. Biotite and muscovite are the dominant phyllosilicates defining the most prominent foliation in the Emuckfaw Group.

### Biotite

Biotite is common within the district and throughout phyllites in the Wedowee Group. Small grains (<1 mm) are found disseminated in most samples and coarse-grained (1-2 mm) selvages are found adjacent to many quartz veins. Biotite is not found in retrograde shear zones.

Biotite compositions in vein selvages, in the matrix of host rocks, and in the Wedowee and Emuckfaw Groups outside the Goldville district were compared (Fig. 2, Table 2). All of the trioctahedral mica analyzed contain between 2.46 and 2.58 tetrahedral Al cations and 0.69 to 0.86 octahedral Al cations per 22 oxygen atoms (Fig. 2). These compositions are very close to Al annite-Al phlogopite solid solution, but will be called biotite for convenience. The Mg# [Mg# = Mg/(Mg+Fe)] of these biotites varies between 0.37 and 0.51. Biotite from the Lowe and Tallapoosa mines are compositionally indistinguishable from biotite in the host rocks.

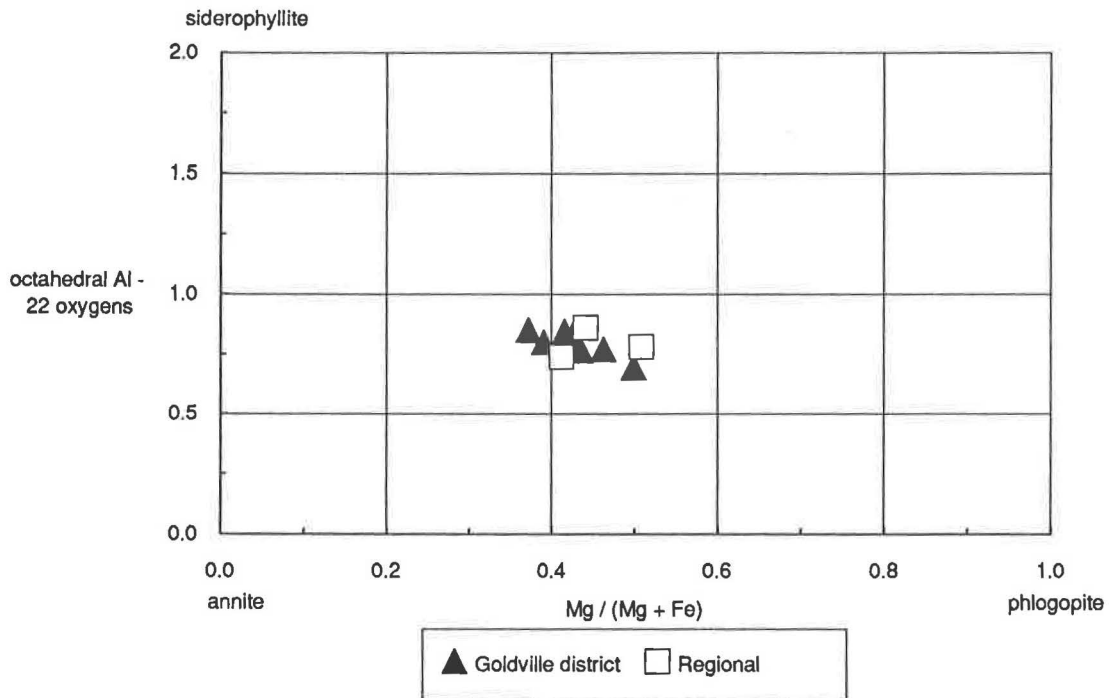


Figure 2. Biotite compositions from Table 2 plotted in terms of octahedral Al vs. Mg/(Mg+Fe).

**Table 2. Representative biotite analyses from the Goldville district, Wedowee Group, and Emuckfaw Group, Tallapoosa County, Alabama**

Sample Grain	Lowe mine					Tallapoosa mine		Wedowee Gp.	Emuckfaw Gp.	
	LO-2 B2	LO-13 B2	LO-15 B4	LO-18 B1	LO-31 B5 2	TA-11 B9 1	TA-14 B 1	GG-101 B2 1	GG-167 B2 1	NS-4a B3
SiO <sub>2</sub>	35.67	35.45	35.50	35.38	35.46	36.41	34.97	36.27	35.73	35.58
Al <sub>2</sub> O <sub>3</sub>	17.67	18.48	17.86	18.06	19.11	18.46	18.22	18.38	18.62	18.18
TiO <sub>2</sub>	1.53	1.43	1.87	1.75	1.50	1.84	1.47	1.48	1.64	2.28
FeO <sup>1</sup>	19.23	21.59	19.76	20.99	23.58	21.61	22.73	19.11	20.36	21.40
MgO	10.78	8.99	9.56	9.10	7.83	8.64	8.17	11.12	9.03	8.42
MnO	0.11	0.06	0.13	0.05	0.07	0.11	0.10	0.07	0.00	0.13
CaO	0.02	0.02	0.02	0.02	0.00	0.01	0.04	0.01	0.00	0.00
Na <sub>2</sub> O	0.15	0.23	0.11	0.16	0.00	0.08	0.19	0.24	0.18	0.13
K <sub>2</sub> O	8.94	8.08	8.60	8.79	8.99	8.37	8.26	7.91	8.98	9.59
Cl	0.01	0.00	0.00	0.01	0.03	0.00	0.00	0.00	0.00	0.01
F	0.00	0.25	0.10	0.00	0.00	0.09	0.00	0.25	0.00	0.00
H <sub>2</sub> O <sup>2</sup>	3.90	3.76	3.81	3.88	3.92	3.90	3.85	3.83	3.90	3.93
<b>total</b>	<b>97.99</b>	<b>98.21</b>	<b>97.25</b>	<b>98.17</b>	<b>100.49</b>	<b>99.48</b>	<b>98.00</b>	<b>98.56</b>	<b>98.43</b>	<b>99.62</b>
Cations based on 11 oxygens										
Si	2.744	2.734	2.753	2.736	2.706	2.768	2.726	2.748	2.744	2.727
Al	1.603	1.680	1.632	1.646	1.718	1.654	1.673	1.641	1.685	1.642
Ti	0.089	0.083	0.109	0.102	0.086	0.105	0.086	0.084	0.095	0.131
Fe <sup>+2</sup>	1.237	1.392	1.281	1.358	1.505	1.374	1.482	1.211	1.308	1.372
Mg	1.236	1.034	1.105	1.049	0.890	0.979	0.949	1.256	1.033	0.962
Mn	0.007	0.004	0.008	0.003	0.004	0.007	0.007	0.004	0.000	0.009
Ca	0.001	0.002	0.002	0.002	0.000	0.001	0.003	0.001	0.000	0.000
Na	0.022	0.034	0.017	0.024	0.000	0.012	0.029	0.035	0.026	0.020
K	0.877	0.795	0.850	0.867	0.876	0.812	0.821	0.765	0.880	0.937
H	1.999	1.939	1.975	1.999	1.996	1.978	2.000	1.940	2.000	1.999
Cl	0.001	0.000	0.000	0.001	0.004	0.000	0.000	0.000	0.000	0.001
F	0.000	0.061	0.025	0.000	0.000	0.022	0.000	0.060	0.000	0.000
<b>total</b>	<b>7.816</b>	<b>7.758</b>	<b>7.756</b>	<b>7.785</b>	<b>7.786</b>	<b>7.712</b>	<b>7.776</b>	<b>7.747</b>	<b>7.771</b>	<b>7.799</b>
Mg <sup>#3</sup>	0.500	0.426	0.463	0.436	0.372	0.416	0.391	0.509	0.441	0.412
Al <sup>IV</sup>	1.256	1.266	1.247	1.264	1.294	1.232	1.274	1.252	1.256	1.273
Al <sup>VI</sup>	0.346	0.414	0.385	0.381	0.425	0.422	0.399	0.390	0.429	0.369

<sup>1</sup> total Fe calculated as FeO

<sup>2</sup> H<sub>2</sub>O calculated assuming 2 OH, Cl, and/or F for every 10 oxygens

<sup>3</sup> Mg# = Mg/(Mg+Fe)

Al<sup>IV</sup>, Al<sup>VI</sup> = tetrahedral and octahedral aluminum, respectively

### White Mica

White mica is abundant throughout the Wedowee Group in fine-grained (<0.5 mm) foliated masses in strongly deformed samples, and coarse (<1 mm) randomly oriented intergrowths with biotite and chlorite in vein selvages within the district. In addition, coarse white mica is locally intergrown with large feldspar crystals in veins at the Lowe and Tallapoosa mines. White mica is

less abundant in the Emuckfaw Group; some amphibole-bearing schists only contain secondary sericite.

White micas from both host rocks and veins are close to muscovite-paragonite mixtures and are 79 to 85% muscovite (Table 3). All of the white micas will be subsequently referred to as muscovite.

**Table 3. Representative muscovite analyses from the Goldville district, Wedowee Group, and Emuckfaw Group, Tallapoosa County, Alabama**

Sample Grain	Lowe mine		Tallapoosa mine	Emuckfaw Gp.	
	LO-2 M1 1	LO-13 M3 1	LO-15 M1 1	TA-14 M2	GG-167 M7
SiO <sub>2</sub>	46.13	47.45	45.99	45.50	48.03
Al <sub>2</sub> O <sub>3</sub>	34.32	34.41	33.44	34.14	35.68
TiO <sub>2</sub>	0.34	0.37	0.40	0.24	0.54
FeO <sup>1</sup>	1.37	1.93	1.59	4.13	1.17
MgO	0.96	0.94	0.99	1.58	0.75
MnO	0.01	0.00	0.01	0.00	0.00
CaO	0.02	0.01	0.10	0.04	0.00
BaO	0.34	0.27	0.97	0.33	0.00
Na <sub>2</sub> O	0.80	1.11	1.00	1.26	0.81
K <sub>2</sub> O	9.25	9.31	8.28	7.37	7.50
Cl	0.01	0.00	0.00	0.00	0.00
F	0.00	0.00	0.00	0.00	0.00
H <sub>2</sub> O <sup>2</sup>	4.44	4.53	4.38	4.46	4.57
<b>total</b>	<b>97.98</b>	<b>100.33</b>	<b>97.15</b>	<b>99.03</b>	<b>99.04</b>
Cations based on 11 oxygens					
Si	3.119	3.138	3.145	3.062	3.152
Al	2.734	2.682	2.695	2.707	2.760
Ti	0.017	0.018	0.021	0.012	0.027
Fe <sup>+2</sup>	0.077	0.107	0.091	0.232	0.064
Mg	0.097	0.093	0.101	0.158	0.073
Mn	0.001	0.000	0.001	0.000	0.000
Ca	0.001	0.001	0.007	0.003	0.000
Ba	0.009	0.007	0.026	0.009	0.000
Na	0.105	0.142	0.133	0.164	0.102
K	0.798	0.785	0.722	0.633	0.628
Cl	0.001	0.000	0.000	0.000	0.000
F	0.000	0.000	0.000	0.000	0.000
<b>total</b>	<b>6.958</b>	<b>6.973</b>	<b>6.941</b>	<b>6.980</b>	<b>6.807</b>
Mg# <sup>3</sup>	0.555	0.465	0.526	0.405	0.532
Al <sup>IV</sup>	0.881	0.862	0.855	0.938	0.848
Al <sup>VI</sup>	1.853	1.820	1.840	1.769	1.912

<sup>1</sup> total Fe calculated as FeO

<sup>2</sup> H<sub>2</sub>O calculated assuming 2 OH, Cl, and/or F for every 10 oxygens

<sup>3</sup> Mg# = Mg/(Mg+Fe)

Al<sup>IV</sup>, Al<sup>VI</sup> = tetrahedral and octahedral aluminum, respectively

## Feldspar

Feldspar occurs as small grains (<1 mm) disseminated within the host rocks of the district, medium-sized grains (1-2 mm) within vein selvages, and large grains (<10 mm) within veins in the district. Many of these large grains are partly replaced by sericite and/or calcite. Schists from the Emuckfaw Group contain numerous lenses and disseminated coarse grains (1-2 mm) of feldspar.

All of the analyzed grains are albite-rich plagioclase with most compositions ranging from An<sub>16</sub> to An<sub>35</sub> (Table 4). Most plagioclase is zoned from core to rim; grains from host rocks are weakly zoned with higher anorthite content in rim compositions. Grains from samples containing quartz veins vary from strongly to weakly zoned with greater or lesser anorthite in rim compositions (Stowell et al., in press).

**Table 4. Representative plagioclase analyses from the Goldville district, Wedowee Group, and Emuckfaw Group, Tallapoosa County, Alabama**

Sample Grain	Lowe mine		Tallapoosa mine		Emuckfaw Gp.
	LO-2 P1e	LO-13 P1	LO-15 P5	TA-14 P4e	GG-167 P1
SiO <sub>2</sub>	59.23	63.40	61.13	62.80	62.95
Al <sub>2</sub> O <sub>3</sub>	24.85	23.20	24.12	22.17	23.70
Fe <sub>2</sub> O <sub>3</sub> <sup>1</sup>	0.06	0.04	0.20	0.14	0.07
CaO	7.22	4.12	5.27	3.20	4.47
Na <sub>2</sub> O	7.52	9.41	8.62	9.64	8.32
K <sub>2</sub> O	0.12	0.06	0.06	0.06	0.07
<b>total</b>	<b>98.99</b>	<b>100.24</b>	<b>99.42</b>	<b>98.01</b>	<b>99.58</b>
Cations based on 8 oxygens					
Si	2.669	2.795	2.730	2.827	2.785
Al	1.320	1.205	1.269	1.176	1.236
Fe <sup>+3</sup>	0.002	0.001	0.006	0.005	0.002
Ca	0.349	0.193	0.251	0.154	0.212
Na	0.657	0.803	0.746	0.840	0.714
K	0.007	0.002	0.002	0.002	0.004
<b>total</b>	<b>5.002</b>	<b>5.000</b>	<b>5.004</b>	<b>5.003</b>	<b>4.953</b>
An	0.345	0.194	0.251	0.155	0.228
Ab	0.649	0.804	0.747	0.843	0.768
Or	0.006	0.002	0.002	0.002	0.004

<sup>1</sup> total Fe calculated as Fe<sub>2</sub>O<sub>3</sub>

## METAMORPHISM

The textural arguments presented above and in Stowell and others (in press) for vein emplacement during metamorphism allow the direct use of metamorphic minerals to determine conditions during mineralization. If the gold was locally derived from syngenetic deposits in the Wedowee Group as suggested by Paris (1986), Neal (1986), and Neal and Cook (in press),

pressure and temperature conditions determined in this manner could represent conditions during syndeformational remobilization of gold.

### **Equilibrium Mineral Assemblages and Petrogenetic Grids**

Mineral assemblages in the Wedowee and Emuckfaw Groups (Table 5) are generally divariant in pressure-temperature space. Host rock and vein selvage minerals from the Goldville district, and mineral assemblages in the Wedowee Group indicate low to medium grade metamorphism: almandine-rich garnet+chlorite+muscovite zone. Although the assemblage garnet+chlorite+biotite is common, chlorite and biotite compositions vary appreciably (Stowell et al., in press). The variability of mineral chemistry in vein samples suggests a strong lithologic control on vein selvage chemistry.

Staurolite occurs as a trace phase within a single vein selvage implying that metamorphism reached amphibolite facies or medium grade at the Lowe mine (Stowell et al., in press). The stability of quartz with muscovite in peak metamorphic assemblages in many of the samples from the Wedowee and Emuckfaw Groups requires that temperatures did not exceed those required for the reaction muscovite + quartz = potassium feldspar + aluminum silicate + vapor (Fig. 3).

The Emuckfaw Group includes amphibolite facies mineral assemblages containing staurolite and kyanite (Maungnoicharoen, 1975). Sample NS-4a contains abundant hornblende compatible with amphibolite facies or medium grade metamorphism.

### **Thermobarometry**

Metamorphic temperatures and pressures were estimated using experimentally- or empirically-calibrated elemental exchange equilibria. The calibrations and activity models used for thermobarometric calculations are discussed by Stowell and others (in press). Only coexisting grains exhibiting no textural evidence of disequilibrium were selected for thermobarometric study. Mineral assemblages for samples used for thermobarometry are given in Table 5. All calculations are based on electron microprobe analyses of individual mineral grains.

Most of the errors quoted below for temperature and pressure calculations are based on analytical and thermodynamic uncertainties. Errors in the relative differences between results based on one thermobarometer may be estimated from analytical uncertainty alone. These relative errors are  $\geq 50\%$  less than absolute errors.

### **Garnet-Biotite Thermometry**

Metamorphic temperatures were calculated for host rocks and vein selvages from the Lowe and Tallapoosa mines, and for the parts of the Wedowee and Emuckfaw Groups outside the district (Fig. 1) using analyzed mineral compositions and Fe-Mg exchange between garnet and biotite (Ferry and Spear, 1978; Ganguly and Saxena 1984, 1985). The uncertainty in temperature determinations based on this exchange is about  $\pm 50^\circ\text{C}$  (Ferry and Spear, 1978).

Drill core samples from the Lowe and Tallapoosa mines containing adjacent unaltered grains of garnet and biotite were selected for geothermometry. Samples were collected from directly adjacent to veins (LO-2, LO-13, and TA-14), some of which have anomalous gold values, and 5 m or more from veins (LO-18, LO-15, and TA-11). In addition, samples were selected from outside the district (GG-101, GG-167, NS-4a) to insure that a valid comparison was made between temperatures calculated for minerals adjacent to the mineralization and regional metamorphic conditions.

**Table 5. Mineral assemblages of samples used for thermobarometry**

	Equilibrium Assemblages	Minor or trace phases
<b>LOWE AND TALLPOOSA MINE</b>		
<b>Veins</b>		
LO-2:	1) pl-qtz 2) car-qtz-sul	ser <sup>1</sup> , op <sup>1</sup>
TA-14:	1) ms-pl-qtz-ap	ser <sup>1</sup>
<b>Vein selvages adjacent to quartz and sulfide veins</b>		
LO-2:	1) grt-bt-ms-pl-qtz 2) grt-bt-st	ilm, po, py
LO-13b:	1) grt-bt-chl-ms-pl-qtz 2) grt-bt-ms-qtz	ilm, py
<b>Host rocks</b>		
LO-15:	1) grt-bt-chl-ms-pl-qtz 2) grt-bt-cal-qtz	ilm, ap
LO-18:	1) grt-bt-chl-ms-qtz	ilm, gr, tur, ap
LO-31c:	1) grt-bt-qtz	tur, chl <sup>1</sup> , ms <sup>1</sup> , ilm
LO-31d:	1) grt-bt-qtz	chl <sup>1</sup> , ms <sup>1</sup> , ilm
TA-11:	1) grt-bt-ms-qtz	
TA-14:	1) grt-bt-chl-ms-pl-qtz	ap
<b>WEDOWEE GROUP</b>		
GG-101:	1) grt-bt-chl-ms-qtz	ilm
<b>EMUCKFAW GROUP</b>		
GG-167:	1) grt-bt-ms-pl-qtz	
NS-4a:	1) grt-bt-hbl-ep-pl-qtz	ms <sup>1</sup> , chl <sup>1</sup>

<sup>1</sup> secondary or retrograde phases

Mineral symbols: ap = apatite, bt = biotite, car = carbonate, chl = chlorite, ep = epidote, gr = graphite, grt = garnet, hbl = hornblende, ilm = ilmenite, ms = muscovite, op = opaque, pl = plagioclase, po = pyrrhotite, py = pyrite, qtz = quartz, ser = sericite, st = staurolite, tur = tourmaline.

Thermometric results range from 480 to 595°C for all of the mineral pairs and average 490±12°C for the district (Table 6). Temperatures estimated from mineral chemistry are less than temperatures estimated from staurolite-biotite stability. This apparent discrepancy may result from  $P_{H_2O} < P_{total}$  (see Stowell et al., in press) or from chemical impurities that stabilized staurolite at temperatures below those obtained in the experimental studies. Temperatures calculated using rim compositions of large, subhedral, zoned garnets and adjacent biotite in the host rocks do not differ significantly from temperatures calculated using rim compositions of small, euhedral, unzoned garnets and adjacent biotite in vein selvages. The single temperature estimate for the Wedowee Group is indistinguishable from these results. This suggests that the rims of all garnet and biotite grains in the district and throughout the Wedowee Group equilibrated at upper greenschist to lower amphibolite facies conditions. Thermometric results clearly indicate higher metamorphic temperatures for the Emuckfaw Group (Table 6).

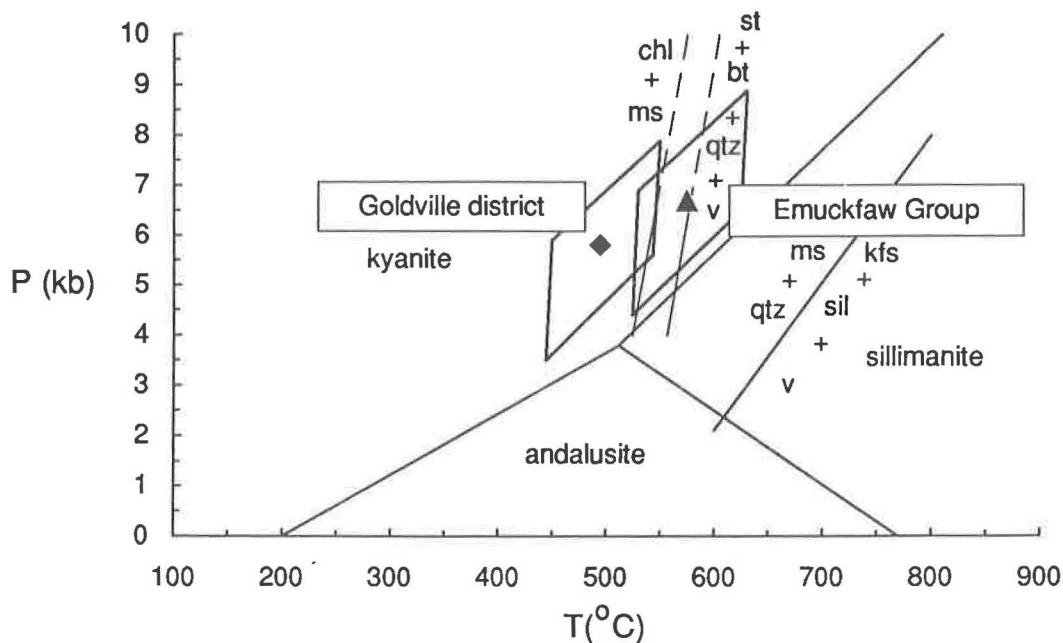


Figure 3. Pressure vs. temperature plot for Goldville district, Wedowee Group, and Emuckfaw Group samples. The rhombic fields show the average pressure and temperature conditions and estimated errors (analytic and thermodynamic) calculated for vein selvage and host rock mineral chemistry from the Goldville district, and for regional metamorphic minerals in the Emuckfaw Group. Muscovite + quartz stability after Chatterjee and Johannes (1974); aluminum silicate phase diagram from Holdaway (1971); chlorite + muscovite = staurolite + biotite + quartz + vapor reaction field from Hoschek (1969); all reaction curves involving vapor are for  $P_{\text{H}_2\text{O}} = P_{\text{total}}$ .

### Plagioclase-Biotite-Garnet-Muscovite Barometry

Metamorphic pressures were calculated for vein selvage and host rock samples using analyzed mineral compositions and Fe-Mg-Ca-K exchange between plagioclase, biotite, muscovite, and garnet (Ghent and Stout, 1981; Hodges and Crowley, 1985). The uncertainty in pressure determinations based on this exchange is greater than  $\pm 1$  kb (Hodges and Crowley, 1985).

Five samples were selected for geobarometry: two from selvages adjacent to quartz-plagioclase-sulfide veins at the Lowe mine, one from quartz-rich phyllitic host rock at the Lowe mine, and one from a vein selvage at the Tallapoosa mine. Mineral compositions from the edges of garnet and plagioclase grains and the centers of phyllosilicate grains were used in the calculations.

Barometric results range from 5.1 to 6.7 kb. No discernible difference was found between barometric results from vein selvages and host rock samples in the district. However, the highest

pressure was calculated for a sample from the Emuckfaw Group, suggesting that rocks within the Alexander City fault zone experienced higher pressures than the Wedowee Group.

**Table 6. Pressures (kb) and temperatures (°C) calculated from elemental exchange equilibria.**

	T-FS <sup>1</sup>	T-GS <sup>2</sup>	T-GU <sup>3</sup>	P-HC <sup>4</sup>
<b>LOWE AND TALLPOOSA MINE</b>				
<b>Veins</b>				
TA-14	485	540	510	6.4
<b>Vein selvages adjacent to quartz and sulfide veins</b>				
LO-2	480	525		5.1
LO-13	515	550		6.4
LO-31	485	539		
<b>Host Rocks</b>				
LO-15	485	535		5.6
LO-18	495	530		
TA-11	500	555		
<b>All Lowe and Tallapoosa mine samples</b>				
<b>Average<sup>5</sup></b>	490±12	540±11	510	5.8±0.6
<b>WEDOWEE GROUP</b>				
GG-101	500	500		
<b>EMUCKFAW GROUP</b>				
GG-167	555	565		
NS-4a	595	615		6.7

Analytical and thermodynamic uncertainties yield errors ca. ±50°C (T-FS, T-GS), ±80°C (T-GU), and ±1 kb (P-HC)

<sup>1</sup> grt-bt temperature: Ferry and Spear (1978) with Hodges and Crowley (1985) garnet activity model

<sup>2</sup> grt-bt temperature: Ganguly and Saxena (1984)

<sup>3</sup> pl-ms temperature: Green and Urdansky (1986)

<sup>4</sup> pl-bt-grt-ms pressure: Hodges and Crowley (1985)

<sup>5</sup> ±1 standard deviation

### Plagioclase-Muscovite Thermometry

The temperature of vein formation at the Tallapoosa mine was calculated using mineral compositions and Na-K exchange between feldspar and muscovite (Green and Urdansky, 1986). Errors for this calculation are ±80°C based on analytical uncertainty alone.

The mineral grains used for this calculation are from within a vein (TA-14), and show no evidence of recrystallization, or disequilibrium. Therefore, this temperature should accurately reflect the conditions of vein formation. The sample contains intergrown coarse muscovite and plagioclase; mineral compositions from directly adjacent to their mutual grain boundaries were utilized to determine the temperature of equilibration.

Thermometric results are  $510 \pm 80^\circ\text{C}$ , consistent with low- to medium-grade (upper greenschist to lower amphibolite facies) metamorphism during vein emplacement.

## DISCUSSION

### Timing of Deformation, Metamorphism, and Mineralization

Mineral textures and structural relationships indicate that  $D_1$  through  $D_3$  structures result from progressive deformation during northwest-southeast oriented shortening (Stowell et al., in press). Garnet and biotite chemistry and textures indicate that peak metamorphic conditions postdate  $D_1$  and predate  $D_3$ . These data and chlorite-muscovite zone assemblages in late shear zones are compatible with a single metamorphic event which peaked between  $D_1$  and  $D_2$ , and included retrograde mineral growth during  $D_3$ .

Paris (1986), Neal (1986), and Neal and Cook (in press) considered the gold deposits to be strata-bound and interpreted the gold-sulfide mineralization as syngenetic with later remobilization of gold into quartz veins during metamorphism. Detailed mapping and petrography indicate that the deposits are transgressive to the stratigraphy (Guthrie and Dean, 1989) and that mineralization appears to postdate the initial stages of metamorphism and deformation (Stowell et al., in press). Some mineralized veins cross-cut  $D_1$  fabrics, others are deformed and bordered by  $D_2$ - $D_3$  shear zones. Mineral assemblages suggest that shearing occurred during and subsequent to peak metamorphism. Peak metamorphic shear zones contain stable biotite and garnet, whereas post metamorphic shear zones contain stable chlorite and muscovite. Preliminary data indicate that retrograde shear zones exhibit variable amounts of alteration (Leshner et al., in press) and gold enrichment (Stowell et al., in press). Stable isotopic data from veins, vein selvages, and an "altered" shear zone (LO-31) suggest that isotopically similar fluids were present during metamorphism, vein emplacement, and post-peak metamorphic shearing (Leshner et al., in press).

### Physical Conditions During Vein Emplacement and Metamorphism

Mineral assemblages, chemistry, and equilibrium relationships for veins, vein selvages, and  $D_2$  mineral fabrics indicate that peak metamorphism and vein emplacement occurred at about  $500^\circ\text{C}$  at 5-6 kb. These results are similar to those determined by stable isotope exchange thermometry for plagioclase-quartz and biotite-quartz pairs in veins and vein selvages at the Lowe mine (Leshner et al., in press). Textures and mineralogy in the Goldville samples suggest that metamorphism never surpassed upper low-grade or lower medium-grade conditions (greenschist or lower amphibolite facies) and that vein emplacement occurred during metamorphism.

Temperatures and pressures estimated for metamorphism and vein emplacement in the Wedowee Group are significantly lower than temperatures and pressures estimated for metamorphism in the Emuckfaw Group. This suggests that the Alexander City fault zone marks an important syn- to post-metamorphic boundary.

Thermobarometric results, the nature of garnet zonation (Stowell et al., in press), the paucity of minerals that define lower medium-grade metamorphism, and absence of minerals that define upper medium-grade metamorphism in the Goldville district indicate that regional metamorphic conditions have been overestimated by previous workers. The peak metamorphic mineral assemblages observed in the Wedowee Group during this study (low- to medium-grade or upper greenschist facies) are similar to previously proposed retrograde assemblages (greenschist facies: Tull, 1975; Steltenpohl and Moore, 1988) and most peak metamorphic mineral assemblages in the district have not been obviously affected by retrograde metamorphism. Therefore, the importance of retrograde metamorphism appears to have been overemphasized for this part of the Piedmont.

## **Genesis of Gold Mineralization**

At present there is no unequivocal evidence for the ultimate source of gold in the Goldville district. However, our data, and the compositions and densities of fluids from primary inclusions in vein quartz (Sha and Leshner, in press) are compatible with gold emplacement in veins along shear zones which were active synchronous with the peak of low- to medium-grade metamorphism.

The presence of vein mineralization in the Goldville district and its apparent absence in the Alexander City fault zone, as defined, suggest that rocks within the Goldville district were more permeable. It is likely that the Alexander City fault zone comprises a wide zone of heterogeneously-sheared rocks exhibiting variable strain, structural style (folding, faulting, ductile shearing), and permeability. This deformation is considered to have accompanied thrusting of the Emuckfaw Group northwestward onto the Wedowee Group (Guthrie and Dean, 1989). Although no strain data are presently available, it is possible that the Goldville district represents a zone of fold-dominated deformation characterized by lower relative strain, dilation, and higher effective permeability, whereas the Alexander City fault zone represents a zone of shear-dominated deformation characterized by higher relative strain, constriction, and lower effective permeability.

## **CONCLUSIONS**

Vein emplacement occurred during  $D_1$ - $D_2$ , synchronous with low- to medium-grade (garnet to staurolite zone) metamorphism. Thermobarometric studies, utilizing a variety of well-constrained elemental exchange equilibria, indicate that vein emplacement initiated during near-peak metamorphic conditions of  $490 \pm 50^\circ\text{C}$  and  $5.8 \pm 1$  kb in the Wedowee Group.

Textures and mineral assemblages indicate that gold-bearing veins were emplaced within shear zones which were active during the peak of metamorphism. Late-stage shear zones adjacent to veins suggest that shearing during low-grade metamorphism (chlorite-muscovite zone) occurred subsequent to mineralization.

Thermobarometric results from the Emuckfaw Group, adjacent to the Goldville district, suggest that metamorphism within the Alexander City fault zone occurred under higher grade conditions ( $575 \pm 50^\circ\text{C}$  and  $6.7 \pm 1$  kb) than mineralization and metamorphism in the Wedowee Group.

## **ACKNOWLEDGEMENTS**

U.S. Borax donated diamond drill core from the Goldville district to the Geological Survey of Alabama and Russell Lands Inc. provided access to mines and prospects in the Goldville district. Greg Guthrie provided two of the samples used for thermobarometry. Jim Saunders kindly reviewed the manuscript. This research was supported by The University of Alabama Research Grants Committee (Grant No. 1340 to C.M.L. and Grant No. 1370 to H.H.S.) and School of Mines and Energy Development (Grant No. 2-29115 to C.M.L. and H.H.S.).

## **REFERENCES**

- Adams, G.I., 1930, Gold deposits of Alabama, and occurrences of copper, pyrite, arsenic and tin: Alabama Geological Survey Bulletin, 40, 91p.
- Bence, A.E., and Albee, A.L., 1968, Empirical correction factors for electron microanalysis of silicates and oxides: Journal of Geology, v. 76, p. 37-67.

- Chatterjee, N.D., and Johannes, W., 1974, Thermal stability and standard thermodynamic properties of synthetic  $2M_1$ -muscovite,  $KAl_2[AlSi_3O_{10}(OH)_2]$ : *Contributions to Mineralogy and Petrology*, v. 48, p. 89-114.
- Drummond, M.S., 1986, Igneous, metamorphic, and structural history of the Alabama Tin Belt, Coosa County, Alabama: Florida State University, unpublished Ph.D. thesis, 411 p.
- Ferry, J.M., and Spear, F.S., 1978, Experimental calibration of the partitioning of Fe and Mg between biotite and garnet: *Contributions to Mineralogy and Petrology*, v. 66, p. 113-117.
- Ganguly, J., and Saxena, S.K., 1984, Mixing properties of aluminosilicate garnets: constraints from natural and experimental data, and applications to geothermo-barometry: *American Mineralogist*, v. 69, p. 88-97.
- Ganguly, J., and Saxena, S.K., 1985, Mixing properties of aluminosilicate garnets: constraints from natural and experimental data, and applications to geothermo-barometry: clarifications: *American Mineralogist*, v. 70, p. 1320.
- Ghent, E.D., and Stout, M.Z., 1981, Geobarometry and geothermometry of plagioclase-biotite-garnet-muscovite assemblages: *Contributions to Mineralogy and Petrology*, v. 76, p. 92-97.
- Green, N.L., and Usdansky, S.I., 1986, Toward a practical plagioclase-muscovite thermometer: *American Mineralogist*, v. 71, p. 1109-1117.
- Guthrie, G.M., and Dean, L.S., 1989, Geology of the New Site 7.5-minute quadrangle, Tallapoosa County, Alabama: Geological Survey of Alabama Quadrangle Series Map 9.
- Guthrie, G.M., and Leshner, C.M., in press, Geologic setting of lode gold deposits in the Northern Piedmont and Brevard Zone, Alabama, in Cook, R.B., Dean, L.S., and Leshner, C.M., eds.: *Gold deposits of Alabama*. Alabama Geological Survey Bulletin 136, p. 11-32.
- Hodges, K.V., and Crowley, P.D., 1985, Error estimation and empirical geobarometry for pelitic systems: *American Mineralogist*, v. 70, p. 702-709.
- Holdaway, M.J., 1971, Stability of andalusite and the aluminum silicate phase diagram: *American Journal of Science*, v. 271, p. 97-131.
- Hoschek, G., 1969, The stability of staurolite and chloritoid and their significance in metamorphism of pelitic rocks: *Contributions to Mineralogy and Petrology*, v. 22, p. 208-232.
- Leshner, C.M., Stowell, H.H., and Green, N.L., in press, Stable isotope geochemistry of lode gold mineralization in the Northern Piedmont, Alabama, in Cook, R.B. ed., *Economic Mineral Deposits of the Southeast*, *Metallic Ore Deposits: Georgia Geological Survey Bulletin 117*, this volume.
- Muangnoicharoen, N., 1975, The geology and structure of a portions of the northern Piedmont, east-central Alabama: University of Alabama, unpublished M.S. thesis, 74 p.
- Neal, W.L., 1986, Geochemical relationships between gold, silver, antimony, arsenic, and bismuth in gold mineralization of the Goldville District, Tallapoosa County, Alabama: Auburn University, unpublished M.S. thesis, 151 p.

- Neal W.L., and Cook, in press, Mineralogy, petrology, and geochemistry of phyllite-hosted gold deposits, Goldville district, Tallapoosa County, Alabama, *in* Cook, R.B., Dean, L.S., and Leshner, C.M., eds.: Gold deposits of Alabama. Alabama Geological Survey Bulletin 136, p. 101-114.
- Neathery, T.L., and Reynolds, J.W., 1973, Stratigraphy and metamorphism of the Wedowee group: a reconnaissance: *American Journal of Science*, v. 273, p. 723-741.
- Pardee, J.T., and Park, C.F., Jr., 1948, Gold deposits of the southern Piedmont: U.S. Geological Survey Professional Paper 213, 156 p.
- Paris, T.A., 1986, The Goldville Project: Results of an exploration project for gold in the northern Alabama Piedmont, *in* Misra, K.C., ed., Volcanogenic sulfide and precious metal mineralization in the southern Appalachians: University of Tennessee, Department of Geological Sciences, Studies in Geology, v. 16, p. 182-205.
- Pouchou, J.L., and Pichoir, F., 1985, "PAP"  $\phi(\rho Z)$  procedure for improved quantitative micro-analysis: *in* Armstrong, J.T., ed.: Microbeam Analysis-1985, p. 104-106.
- Sha, P., and Leshner, C.M., in press, Microthermometry of fluid inclusions in auriferous quartz veins, Goldville district, Northern Piedmont, Alabama, *in* Cook, R.B., ed., Economic Mineral Deposits of the Southeast, Metallic Ore Deposits: Georgia Geological Survey Bulletin 117, this volume.
- Steltenpohl, M.G., and Moore, W.B., 1988, Metamorphism in the Alabama Piedmont: Geological Survey of Alabama Circular 138, 27 p.
- Stowell, H.H., Guthrie, G.M., and Leshner, C.M., in press, Metamorphism and gold mineralization in the Wedowee Group, northern Piedmont, Alabama, *in* Cook, R.B., Dean, L.S., and Leshner, C.M., eds.: Gold deposits of Alabama. Alabama Geological Survey Bulletin 136, p. 133-158.
- Thomas, W.A., Tull, J.F., Bearce, D.N., Russell, G., and Odom, A.L., 1980, Geologic synthesis of the southernmost Appalachians, Alabama and Georgia: *in* Wones, D.R., ed., Proceedings of the International Geological Correlation Program Caledonide Project 27, Department of Geological Sciences, Virginia Polytechnic Institute and State University, Blacksburg, VA, Memoir no. 2, The Caledonides in the U.S.A., ed., p. 91-98.
- Tull, J.F., 1975, Structural and metamorphic features of the northern Alabama Piedmont, *in* Neathery, T.L., and Tull, J.F., eds., Geologic profiles of the northern Alabama Piedmont: Alabama Geological Society, 13th Annual Field Trip Guidebook, p. 63-86.
- Tull, J.F., 1978, Structural development of the northern Alabama Piedmont northwest of the Brevard zone: *American Journal of Science*, v. 278, p. 442-460.

# MICROTHERMOMETRY OF FLUID INCLUSIONS IN AURIFEROUS QUARTZ VEINS, NORTHERN PIEDMONT, ALABAMA

Peng Sha and C. Michael Lesher

Department of Geology, University of Alabama,  
Tuscaloosa, Alabama 35487-0338

## ABSTRACT

Lode gold deposits in the northern Alabama Piedmont are associated exclusively with synkinematic, synmetamorphic quartz veins. Five compositional types of fluids are distinguishable in fluid inclusions in quartz from metapelite-hosted veins in the Goldville district and tonalite-hosted veins at the Hog Mountain mine: **type 1** very high salinity aqueous, **type 2** high salinity CO<sub>2</sub>-bearing aqueous, **type 3** moderate salinity CO<sub>2</sub>-bearing aqueous, **type 4** moderate-low salinity aqueous, and **type 5** CO<sub>2</sub>-rich. Fluid inclusions in the Goldville district formed during four stages: **stage I** minor, isolated, primary, irregularly-shaped types 1, 2, and 3, **stage II** abundant, secondary, elliptically-shaped types 3 and 4 in planar arrays, **stage III** minor, secondary, irregularly-shaped type 4 in linear arrays, and **stage IV** abundant, secondary, irregularly-shaped type 5 in planar arrays. In contrast, fluid inclusions at the Hog Mountain mine formed during two stages, both secondary: **stage I** abundant, irregularly-, elliptically-, or tubularly-shaped types 3 and 4 in planar arrays, and **stage II** rare, irregularly-shaped type 5 in isolation or in linear arrays.

P-V-T-X properties of primary, high salinity (type 1 and 2) aqueous fluids in the Goldville district are not consistent with entrapment at pressures and temperatures determined by independent methods and appear to have been modified subsequent to entrapment. P-V-T-X properties of primary and early secondary, moderate salinity, low-CO<sub>2</sub> (type 3) aqueous fluids are consistent with entrapment during prograde metamorphism and appear to represent the vein-forming metamorphic fluid. Secondary, moderate-low salinity (type 4) aqueous fluids evolved toward higher salinity with decreasing temperature in the Goldville district and lower salinity with decreasing temperature at the Hog Mountain mine, probably reflecting decreasing degrees of interaction with pelitic and tonalitic host rocks, respectively. Late secondary CO<sub>2</sub>-rich (type 5) fluids in both areas were most likely derived by oxidation of graphite in metasedimentary country rocks at low temperatures. The compositional and textural similarities of fluid inclusions in the Goldville district and at the Hog Mountain mine indicate a common metamorphic fluid source and timing of entrapment. Gold precipitation was probably influenced by fluid-rock interactions.

## INTRODUCTION

Lode gold deposits in the northern Alabama Piedmont are hosted by a variety of greenschist-amphibolite facies pelitic metasedimentary, mafic metavolcanic, and felsic intrusive lithologies, but are associated exclusively with synkinematic, synmetamorphic quartz  $\pm$  sulfide  $\pm$  plagioclase  $\pm$  carbonate veins. There is considerable controversy regarding the ultimate source of gold (syngenetic vs. epigenetic) in these deposits (cf. Guthrie and Lesher, in press; Neal and Cook, in press; Paris, 1986; Stowell et al., in press; Lesher et al., this volume), but all workers agree that gold has been remobilized to some degree by vein-forming fluids. The aim of this paper is to define the composition and nature of the vein-forming fluids and to further constrain the physical and chemical conditions of gold mineralization/remobilization in the southern Appalachians.

Materials from three deposits in the northern Piedmont were studied: the Lowe and Tallapoosa mines in the northeastern and southwestern parts of the Goldville district and the Hog Mountain mine 10 km to the northwest (see fig. 1: Stowell and Lesher, this volume). All three deposits have been subjected to recent exploration programs involving diamond core drilling which provided fresh samples of vein quartz for detailed petrographic and microthermometric study. Three types of veins occur in these deposits (Lesher et al., this volume): **type I** barren, deformed monomineralic quartz veins that occur in barren and mineralized lithologies throughout the region, **type II** mineralized quartz-sulfide veins (Hog Mountain) and quartz-plagioclase  $\pm$  sulfide veins (Goldville) that are restricted to mine areas, and **type III** calcite  $\pm$  sulfide  $\pm$  quartz veins that cross-cut other veins. Only type II veins were sampled for this study.

## FLUID INCLUSION PETROGRAPHY

### Goldville District

Two mineral assemblages occur in mineralized (type II) veins in the Goldville district: 1) early, coarse-grained quartz ± plagioclase ± biotite ± garnet ± chlorite, similar to that in the metapelitic host rocks, and 2) late, fine-grained (<0.01 mm) recrystallized quartz ± sericite ± carbonate ± sulfide, generally distributed around early minerals. Free gold is extremely rare except in the weathered zone; sulfides are interpreted to house gold in solid solution or as submicroscopic inclusions. All quartz contains abundant fluid inclusions, both primary and secondary, which vary in size, shape, phase, and distribution (Fig.1). On the basis of cross-cutting relationships, they are grouped into four stages (Table 1).

**Table 1. Petrographic characteristics of fluid inclusions in vein quartz, Goldville district and Hog Mountain mine, northern Alabama Piedmont**

Stage(%)	Size (μm)	Shape	Distribution	Type(%)	Phases	Bubble Volume (%)
<b>GOLDVILLE DISTRICT</b>						
<b>Primary</b>						
I (10)	2-35	irregular	isolated or grouped in centers of grains	3 (55) 2 (35) 1 (10)	CO <sub>2</sub> (v)-H <sub>2</sub> O(l)-CO <sub>2</sub> (l) CO <sub>2</sub> (v)-H <sub>2</sub> O(l)-CO <sub>2</sub> (l)-salts(s) H <sub>2</sub> O(v)-H <sub>2</sub> O(l)-salts(s)	15-60, mostly 20-30
<b>Secondary</b>						
II (60)	0.5-10	spherical, elliptical, tubular	planar arrays along margins of coarse grains	4 (90) 3 (10)	H <sub>2</sub> O(v)-H <sub>2</sub> O(l) CO <sub>2</sub> (v)-H <sub>2</sub> O(l)-CO <sub>2</sub> (l)	10-15
III (5)	0.5-6	irregular	linear arrays along margins of grains	4	H <sub>2</sub> O(v)-H <sub>2</sub> O(l)	1-5
IV (25)	15-40	irregular	planar or linear arrays in fractures cutting all gains	5	CO <sub>2</sub> (l)-CH <sub>4</sub> (l)	0
<b>HOG MOUNTAIN MINE</b>						
<b>Secondary</b>						
I (90)	0.5-30	irregular, elliptical, tubular	planar arrays in fractures	4 (95) 3 (5)	H <sub>2</sub> O(v)-H <sub>2</sub> O(l) CO <sub>2</sub> (v)-H <sub>2</sub> O(l)-CO <sub>2</sub> (l)	5-15
II (10)	15-40	irregular	isolated or linear arrays in fractures	5	CO <sub>2</sub> (l)-CH <sub>4</sub> (l)	0

Abbreviations: v = vapor, l = liquid, s = solid

Primary fluid inclusions, classified as **stage I** in this study, are generally large (5-30 μm) and have irregular shapes or negative crystal forms. At room temperature they contain one H<sub>2</sub>O-rich or CO<sub>2</sub>-rich gas phase + one H<sub>2</sub>O-rich liquid phase ± one CO<sub>2</sub>-rich liquid phase ± multiple solid phases. The daughter minerals are too small to identify (<0.5 μm); most are anisotropic, some have rectangular shapes (gypsum?) and some have rhombic shapes (carbonate?). Vapor bubble volumes range 20-30%, but a few are 50-60%. Most primary fluid inclusions are isolated, but some occur in groups. All are distributed in early quartz, primarily in centers of grains. Along grain boundaries, crushing and recrystallization have overprinted the primary inclusions.

Three stages of secondary fluid inclusions have been recognized: **stage II** ellipsoidal, tubular, or spherical liquid-gas inclusions occurring in planar arrays, **stage III** irregularly-shaped liquid-gas inclusions occurring in linear arrays (healed fractures), and **stage IV** irregularly-shaped liquid inclusions occurring in planar or linear arrays. Their petrographic relationships to stage I inclusions are illustrated in Figure 1. Stage II and III inclusions are much smaller (0.5-8 μm) than stage I, but stage IV inclusions are usually larger (20-40 μm). At room temperature stage II and III

inclusions contain one H<sub>2</sub>O-rich or CO<sub>2</sub>-rich gas phase + one H<sub>2</sub>O-rich liquid phase ± one CO<sub>2</sub>-rich liquid phase, whereas stage IV inclusions contain only a single CO<sub>2</sub>-rich liquid phase. Volumes of vapor bubbles in secondary inclusions are less than those in primary inclusions, 10-15% in stage II and 1-5% in stage III. Stage II and III secondary fluid inclusions occur along the margins of early stage quartz grains; stage IV secondary inclusions occur in arrays along fractures that cross-cut several quartz grains.

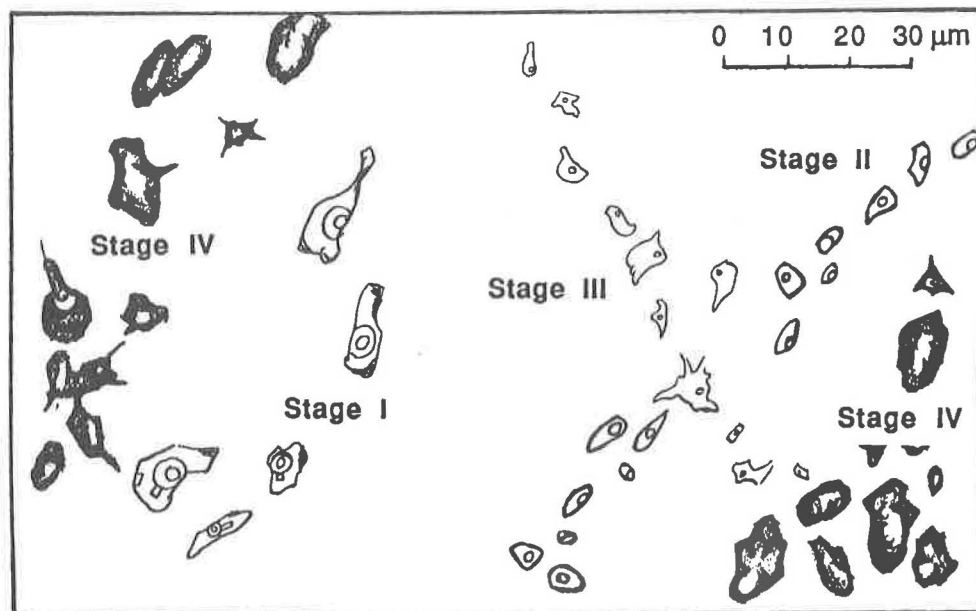


**Figure 1.** Sketch showing petrographic characteristics of different stages of fluid inclusions in vein quartz from the Goldville district.

H<sub>2</sub>O-rich gas, H<sub>2</sub>O-rich liquid, CO<sub>2</sub>-rich liquid, and daughter minerals occur in various proportions in fluid inclusions at room temperature. On the basis of their relative abundance, five types of fluids have been identified: **type 1** very high salinity aqueous fluids, **type 2** high salinity CO<sub>2</sub>-bearing fluids, **type 3** moderate salinity CO<sub>2</sub>-bearing aqueous fluids, **type 4** moderate-low salinity aqueous fluids, and **type 5** CO<sub>2</sub>-rich fluids. Their frequency distributions in the different stages of fluid inclusions are listed in Table 1.

### Hog Mountain

Only secondary fluid inclusions have been identified in mineralized (type II) quartz veins at the Hog Mountain mine. Two stages have been recognized; **stage I** ellipsoidal, tubular, or irregular liquid-gas inclusions occurring in planar arrays, and **stage II** irregular-shaped liquid inclusions occurring in isolation or in planar arrays. Their petrographic characteristics are summarized in Table 1. Stage I inclusions at the Hog Mountain mine are similar to stage II inclusions in the Goldville district, and stage II inclusions at the Hog Mountain mine are similar to stage IV inclusions in the Goldville district, except that they are less abundant.

The apparent absence of primary fluid inclusions in vein quartz at the Hog Mountain mine may indicate that as a population they are too small to characterize with the optical microscope (10% of all detectable inclusions are <5μm) or that they have been destroyed by later deformation (all veins exhibit evidence of post-emplacement deformation).

## FLUID INCLUSION MICROTHERMOMETRY

### Methods

Fluid inclusions were studied using a Fluid Inc.-modified U.S.G.S. gas-flow heating-freezing stage mounted on a Nikon Optiphot-Pol microscope fitted with 15x eyepieces and Leitz EF4x, EF10x, and UT40x objectives. Freezing runs were carried out prior to homogenization runs. Inclusions were quickly frozen to ca. -180°C and warmed slowly to observe the temperatures of phase transitions. Measurements included CO<sub>2</sub> melting temperature ( $T_{mCO_2}$ ), eutectic temperature ( $T_e$ ), ice melting temperature ( $T_{mice}$ ), daughter mineral melting temperature ( $T_{mdm}$ ), clathrate melting temperature ( $T_{mclath}$ ), CO<sub>2</sub> homogenization temperature ( $Th_{CO_2}$ ), and total homogenization temperature ( $Th$ ). The size of the inclusions often precluded determination of  $T_e$ ,  $T_{mdm}$  and  $T_{mclath}$ ; the presence of CO<sub>2</sub> often hampered determination of  $T_{mice}$ .

As the identities of the daughter mineral(s) in the fluid inclusions are not known and little experimental data are available for complex systems, fluid salinities were calculated as NaCl- or MgCl<sub>2</sub>-equivalent depending on eutectic temperature (Roedder, 1984). Salinities of low salinity H<sub>2</sub>O-rich (type 3 and 4) fluids were calculated from measured  $T_{mice}$  using the NaCl solubility equation of Potter et al. (1978) or using an equation ( $wt.\% MgCl_2 = 0.2089 - 1.583 T - 5.044 \times 10^{-2} T^2 - 6.626 \times 10^{-4} T^3$ ,  $r^2 = 0.999$ ) derived by regression of MgCl<sub>2</sub> solubility data given by Linke (1958). Salinities of high salinity H<sub>2</sub>O-rich (type 1 and 2) fluids were calculated from measured  $T_{mdm}$  using an equation ( $wt.\% NaCl = 0.3825 - 1.280 \times 10^{-3} T + 5.585 \times 10^{-6} T^2 - 4.685 \times 10^{-9} T^3$ ,  $r^2 = 0.999$ ) derived by regression of NaCl solubility data given by Keevil (1942). Densities of the CO<sub>2</sub> phase were calculated from measured  $Th_{CO_2}$  using the P-T-density relation of pure CO<sub>2</sub> given by Angus et al. (1976). Densities of H<sub>2</sub>O-rich liquids were calculated assuming unit density for pure H<sub>2</sub>O at room temperature for CO<sub>2</sub>-rich inclusions (Burruss, 1981) or using the equation of Bodnar (1983) for CO<sub>2</sub>-free inclusions. Bulk densities and compositions of fluid inclusions were calculated using bubble volumes estimated at room temperature (Burruss, 1981). As  $T_{mCO_2}$  varies narrowly around -58°C, CH<sub>4</sub> was ignored in most cases (Heyen et al., 1982), except for stage II inclusions at the Hog Mountain mine ( $T_{mCO_2} = ca. -61^\circ C$ ). Measured  $T_{mclath}$  data were not used to calculate fluid compositions (Collins, 1979), because the relative error in measurement ( $\pm 15\%$ ) is larger than for measurement of  $T_{mCO_2}$  ( $\pm 2\%$ ) and  $Th_{CO_2}$  ( $\pm 4\%$ ). Microthermometric data for the Goldville district and Hog Mountain mine are summarized in Table 2.

### Fluid Compositions

Calculated fluid compositions and densities are given in Table 3 and summarized in Table 4. Type 1 and 2 fluids in the Goldville district have anomalously high salinities, whereas stage I and II-type 3 fluids have moderate salinities and CO<sub>2</sub> contents. Stage II-type 4 fluids have low to moderate salinities with negligible CO<sub>2</sub> and have been divided into two subtypes: type 4a fluids are characterized by moderate salinities ( $X_{NaCl(eq.)} = 0.02-0.04$ ) and a relatively narrow range of homogenization temperatures ( $Th = 225-119^\circ C$ ), whereas type 4b fluids are characterized by low salinities ( $X_{NaCl(eq.)} = 0.00-0.02$ ) and a wider range of homogenization temperatures ( $Th = 238-94^\circ C$ ). Stage III-type 4 fluids are moderately saline with negligible CO<sub>2</sub>, similar to stage II-type 4a fluids. Stage IV-type 5 fluids are dominated by CO<sub>2</sub>; CH<sub>4</sub> is only a minor component.

Stage I-type 3 and 4 fluids at the Hog Mountain mine (Table 3) are compositionally similar to stage II-type 3 and 4 fluids in the Goldville district, respectively, except for some with very low eutectic temperatures ( $T_e = -27$  to  $-35^\circ C$ ) and low melting temperatures ( $T_{mice} = -14^\circ C$  to  $-34^\circ C$ ). Available experimental data (summarized by Roedder, 1984) suggest that MgCl<sub>2</sub> is a necessary component in these fluids. On this basis stage I-type 4 fluids have been divided into three subtypes: stage I-type 4a(i) moderate salinity H<sub>2</sub>O-NaCl inclusions ( $X_{NaCl(eq.)} = 0.04-0.07$ ); stage I-type 4a(ii) moderate salinity H<sub>2</sub>O-MgCl<sub>2</sub> inclusions ( $X_{MgCl_2(eq.)} = 0.03-0.05$ ); and stage I-type 4b low salinity NaCl-H<sub>2</sub>O inclusions ( $X_{NaCl(eq.)} = 0.00-0.04$ ). Stage II-type 5 fluids at the Hog Mountain mine are also dominated by CO<sub>2</sub>, similar to stage IV-type 5 fluids in the Goldville district, but appear to contain more CH<sub>4</sub> ( $T_{mCO_2} = ca. -61^\circ C$ ).

**Table 2. Summary of microthermometric data, Goldville district and Hog Mountain mine, northern Alabama Piedmont**

Stage-Type	TmCO <sub>2</sub>	Te	Tmice	Tmclath	ThCO <sub>2</sub>	Tmdm	Th
<b>GOLDVILLE DISTRICT</b>							
<b>Primary</b>							
I-1						300-294 297 (4) 2	345-326 336 (14) 2
I-2	-57.0 to -57.4 -57.2 (0.1) 6				25.4-16.3 21.7 (3.6) 6	198-183 192 (6) 6	353-255 300 (34) 6
I-3	-57.0 to -58.0 56.6 (0.3) 9	-20.8 to -21.3 -21.1 (0.3) 3	-3.9 to -8.5 -5.7 (1.6) 9	7.4-6.0 6.9 (0.8) 3	28.3-15.0 23.0 (3.9) 9		401-242 300 (55) 7
I-?	-56.5 to -57.9 -57.2 (0.4) 23			7.8-6.5 7.1 (0.5) 12	27.5-3.6 18.2 (6.7) 23		370-189 303 (38) 44
<b>Secondary</b>							
II-3	-57.3 -57.3 2		-4.3 to -4.9 -4.6 (0.4) 2		29.7-28.5 29.1 (0.8) 2		278-269 274 (6) 2
II-4a			-4.8 to -7.9 -6.5 (0.7) 28				225-119 158 (42) 17
II-4b		-20.4 to -20.6 -20.5 (0.1) 3	-0.1 to -3.9 -1.8 (0.9) 26				238-94 198 (41) 23
II-?	-57.4 to -58.2 -57.7 (0.3) 5			7.7 1	28.1-19.6 24.9 (3.6) 5		345-126 244 (44) 21
III-4			-7.8 to -10.4 -9.4 (0.8) 18				105-76 89 (11) 5
IV-5					24.6 to -3.5 16.1 (8.2) 12		
<b>HOG MOUNTAIN MINE</b>							
<b>Secondary</b>							
I-3	-57.3 to -59.2 -58.3 (1.3) 2		-8.6 to -19.3 -14.0 (7.6) 2		10.2-9.4 9.8 (0.6) 2		271 1
I-4a(i)			-7.1 to -15.8 -9.9 (1.9) 26				333-92 253 (65) 21
I-4a(ii)		-27.1 to -34.8 -32.8 (2.7) 9	-13.6 to -34.4 -22.5 (4.7) 19				356-104 201 (82) 16
I-4b		-19.7 to -21.3 -20.9 (0.8) 4	-0.1 to -7.1 -4.2(1.5) 33				251-114 165 (35) 27
II-5	-58.0 to -61.8 -60.8 (1.8) 4				7.9 to -13.2 -6.7 (10.0) 4		
?							376-72 237 (67) 65

Temperatures in °C; data given as range (line 1), mean and standard deviation (line 2), and number of measurements (line 3); ? = undifferentiated stage or type

**Table 3. Summary of calculated densities and compositions of inclusion fluids, Goldville district and Hog Mountain mine, northern Alabama Piedmont**

Stage	Type	Density	X <sub>H<sub>2</sub>O</sub>	X <sub>CO<sub>2</sub></sub>	X <sub>NaCl (eq.)</sub>	X <sub>MgCl<sub>2</sub>(eq.)</sub>	X <sub>CH<sub>4</sub></sub>	n
<b>GOLDVILLE DISTRICT</b>								
<b>Primary</b>								
I	1	1.38-1.40 1.39	0.82-0.83 0.83	nil	0.17-0.18 0.17	nil	nil	2
	2	1.16-1.21 1.18 (0.02)	0.79-0.83 0.82 (0.02)	0.05-0.10 0.07 (0.02)	0.10-0.11 0.11 (0.02)	nil	0.001	6
	3	0.93-1.07 1.00 (0.07)	0.81-0.93 0.88 (0.05)	0.04-0.17 0.09 (0.05)	0.02-0.04 0.03 (0.34)	nil	0.002	9
<b>Secondary</b>								
II	3	0.93 0.93	0.85-0.88 0.86	0.10-0.13 0.12	0.02 0.02	nil	0.002	2
	4a	0.89-1.09 1.01 (0.06)	0.96-0.98 0.97 (<0.01)	nil	0.02-0.04 0.03 (0.10)	nil	nil	28
	4b	0.83-1.05 0.90 (0.06)	0.88-1.00 0.99 (0.02)	nil	0.00-0.02 0.01 (0.01)	nil	nil	26
III	4	1.06-1.12 1.09 (0.02)	0.95-0.96 0.96 (<0.01)	nil	0.04-0.05 0.05 (0.07)	nil	nil	18
IV	5	0.77-0.95 0.83 (0.05)	nil	0.95	nil	nil	0.05	12
<b>HOG MOUNTAIN MINE</b>								
<b>Secondary</b>								
I	3	1.00-1.07 1.04	0.77-0.78 0.77	0.16-0.19 0.18	0.03-0.07 0.05	nil	0.005	2
	4a(i)	0.77-1.07 0.91 (0.08)	0.93-0.96 0.95 (0.01)	nil	0.04-0.07 0.05 (0.01)	nil	nil	26
	4a(ii)	n.d.	0.95-0.97 0.96 (0.01)	nil	n.d.	0.03-0.05 0.04 (<0.01)	nil	19
	4b	0.79-1.00 0.95 (0.04)	0.96-1.00 0.98 (0.01)	nil	0.00-0.04 0.02 (0.01)	nil	nil	33
II	5	0.88-0.99 0.96 (0.05)	nil	0.78	nil	nil	0.22	4

Data given as range (line 1) and mean and standard deviation (line 2); n = number of inclusions, n.d. = not determined

## Homogenization Temperatures

The data for 127 stage I through III inclusions in the Goldville district are summarized in Figure 2; stage IV inclusions are homogenous at room temperature. Four hydrothermal events can be recognized with temperature maxima at: 350-230°C, 290-185°C, 170-110°C, and 110-65°C. These data record successive entrapment of stage I-III inclusions with declining temperature, consistent with the relative timing of entrapment based on cross-cutting relationships.

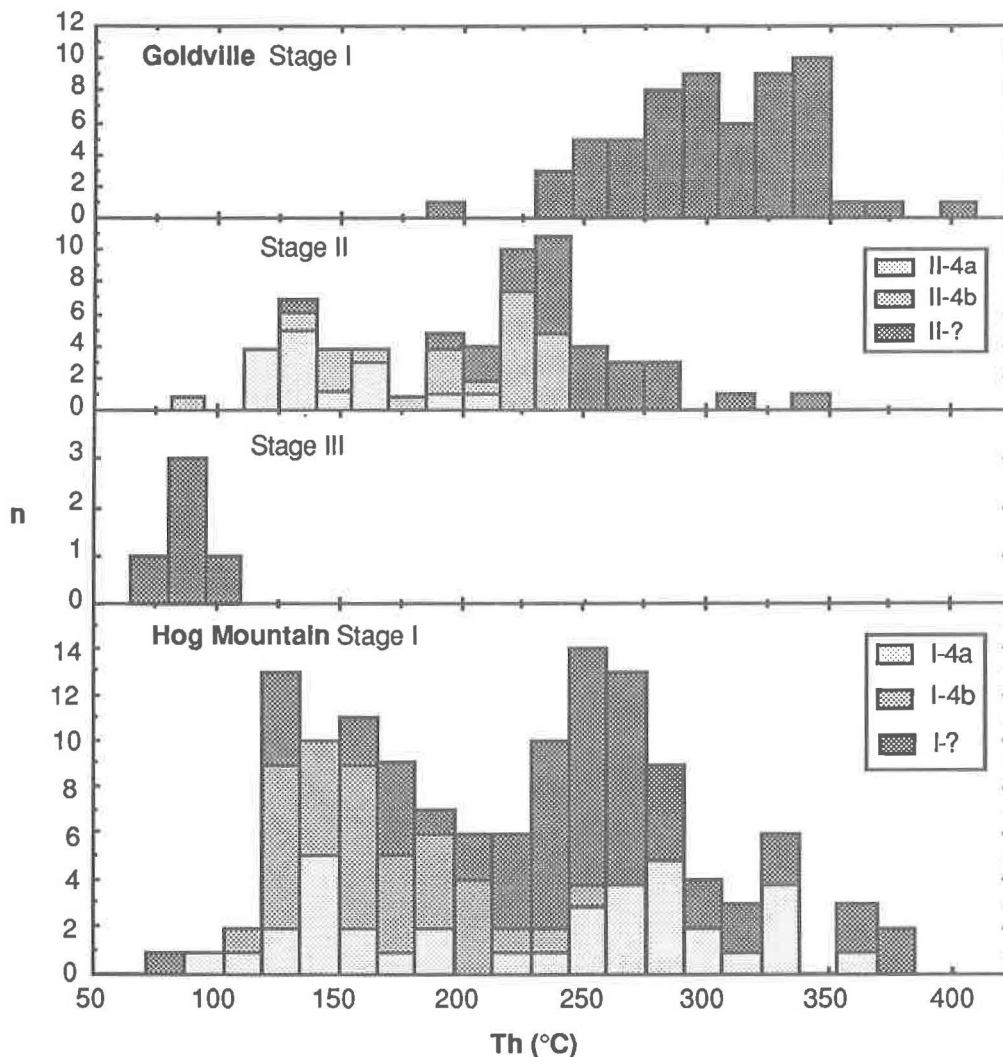


**Figure 2.** Histograms of homogenization temperatures (Th) of fluid inclusions in vein quartz from the Goldville district and the Hog Mountain mine. Inclusion types as defined in text.

Th data for 130 stage I inclusions at the Hog Mountain mine are summarized in Figure 2. Only two hydrothermal events can be recognized with temperature maxima at 340-215°C and 215-120°C. Th of stage I-type 4a(i) and stage I-type 4a(ii) inclusions at the Hog Mountain mine are indistinguishable (Table 2) and span the entire range of Th for stage II-type 4 inclusions in the Goldville district, but stage I-type 4b inclusions at the Hog Mountain mine exhibit a narrower range of lower Th, similar to that of stage II-type 4a inclusions in the Goldville district.

## DISCUSSION

Stage I fluids in the Goldville district are compositionally highly variable, ranging from rare to minor, highly saline fluids (types 1 and 2) to more abundant, moderately saline fluids (type 3). As the different fluids do not occur systematically in close proximity, they could not have formed by necking down and phase segregation of a single precursor fluid. They vary principally in salinity and CO<sub>2</sub> content, and should have been miscible at the inferred conditions of entrapment. Density isochores for type 1 and 2 fluids (Fig. 3), calculated using the computer program FLINCOR (Brown, 1989) and the modified Redlich-Kwong state equation given by Bowers and Helgeson (1983), do not intersect the prograde metamorphic P-T field (495±50°C, 5.8±1 kb) defined by elemental exchange thermobarometry (Stowell and Leshner, this volume) and supported by oxygen isotope thermometry (Leshner et al, this volume), suggesting that type 1 and 2 fluids have been modified subsequent to entrapment.

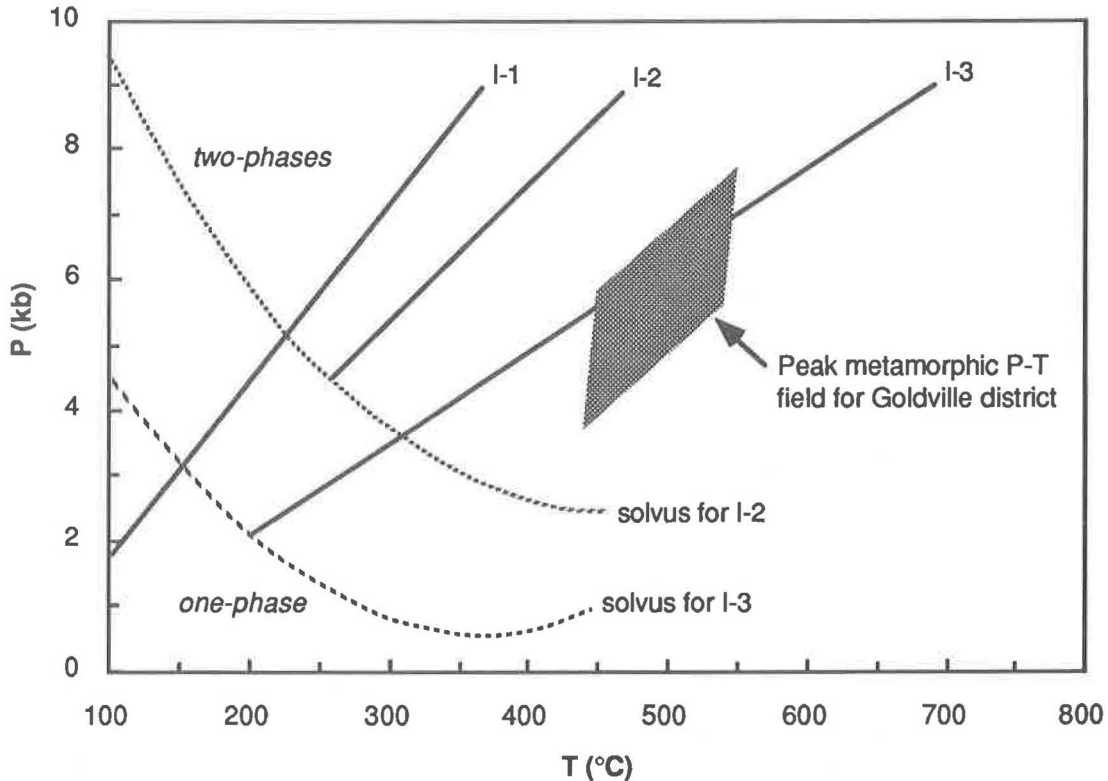


**Figure 3.** P-T diagram showing fluid density isochores for stage I, type 1, 2, and 3 fluids and estimated P-T conditions of vein emplacement for Goldville district (explanation in text). H<sub>2</sub>O-CO<sub>2</sub> solvus calculated using experimental data of Sourlajan and Kennedy (1965).

The P-V-T-X properties of stage I-type 3 fluids in the Goldville district are compatible with entrapment at the P-T conditions of prograde metamorphism (Fig. 3) and most likely represent the vein-forming fluid. Their compositions are similar to those of stage II-type 3 fluids in the Goldville district and stage I-type 3 fluids at the Hog Mountain mine (Table 4), indicating links between primary and secondary fluids in the Goldville district and secondary fluids at the Hog Mountain mine (Table 4) and suggesting derivation from a similar source. Structural, petrographic, and thermobarometric data (Stowell et al., in press) indicate that quartz veins in the Goldville district are synmetamorphic and synkinematic, and stable isotope data (Leshner et al., this volume) suggest that vein-forming fluids were of metamorphic origin. Slightly saline, low-CO<sub>2</sub>, aqueous fluids, such as those of type 3 in these deposits, are typical of metamorphically-generated fluids (Roedder, 1984; Crawford and Hollister, 1986) and may have been derived from adjacent country rocks during metamorphism or from similar rocks deeper in the metamorphic pile. The latter source is more consistent with stable and radiogenic isotopic data (Leshner et al., this volume).

**Table 4. Summary of vein-forming fluid compositions, Goldville district and Hog Mountain mine, northern Alabama Piedmont**

Type	Composition	GOLDVILLE		HOG MOUNTAIN	
		Stage	Th(°C)	Stage	Th(°C)
1	aqueous, very high salinity	I	345-326		
2	aqueous, high salinity, minor CO <sub>2</sub>	I	353-255		
3	aqueous, moderate salinity, minor CO <sub>2</sub>	I	401-242	I	271
		II	278-269		
4	aqueous, moderate-low salinity	II	238-94	I	356-92
		III	105-76		
5	CO <sub>2</sub> -rich, minor-significant CH <sub>4</sub>	IV	n.d.	II	n.d.

n.d. = not determined

Secondary stage II-type 4 fluids in the Goldville district and stage I-type 4 fluids at the Hog Mountain mine have been subdivided into two subtypes, moderate salinity subtype 4a fluids and low salinity subtype 4b fluids. Both exhibit systematic increases in density with decreasing temperature (Figs. 4 and 5). Using the experimental data of Bodnar (1983), these variations can be modeled as cooling trends in the system H<sub>2</sub>O-NaCl, suggesting that two compositionally distinct fluids were present over a wide temperature interval. As the two fluids should have been miscible at the inferred temperatures of entrapment, they could have not had an opportunity to mix, suggesting that the differences were generated locally. Mass balance calculations indicate that fluid-tonalite interactions at the Hog Mountain mine removed Rb, K, Ba, Fe, Co, W, Au, S, and OH from the fluid and added Si, Na, Sr, Ca, Eu, Mg, Mn, and Zn into the fluid (Leshner and Green, 1987), whereas analogous, albeit considerably less extensive, fluid-pelite interactions at the Lowe mine removed Rb, K, Ba, Mo, Au, and OH from the fluid and added Si, Na, Sr, Ca, P, S, and CO<sub>2</sub> into the fluid (C.M.L., unpubl. data). Vein mineralogies indicate that Si, Fe, Au, and S (in quartz-pyrrhotite) precipitated at the Hog Mountain mine, whereas Si, Al, Na, Sr, and Ca (in quartz-albite) precipitated in the Goldville district. The net result is that fluid-wall rock interaction and vein crystallization should have increased fluid salinity at the Hog Mountain mine and decreased fluid salinity in the Goldville district. This is consistent with the somewhat higher salinities of type 3 and 4 fluids at the Hog Mountain mine compared to equivalents in the Goldville district (Table 3).

Secondary fluids in the Goldville district appear to exhibit an overall general trend with decreasing temperature toward greater abundances of *higher* salinity subtypes (II-4b → II-4a → III-4: Fig. 4), whereas secondary fluids at the Hog Mountain mine exhibit an analogous trend toward greater abundances of *lower* salinity subtypes (I-4a → I-4b: Fig. 5). Based on the alteration trends discussed above, these trends probably reflect decreasing degrees of fluid-rock interaction with declining temperature and evolution of fluid compositions towards that of the precursor metamorphic fluid.

Alteration studies at the Hog Mountain mine indicate that fluid-wall rock interactions probably induced gold precipitation (Leshner and Green, 1987). Wall rock alteration is much less pronounced in the Goldville district, but whole-rock geochemical and stable isotopic data define similar alteration trends for the Goldville district and the Hog Mountain mine (C.M.L., unpubl. data; Leshner et al., this volume) and the compositional variations of secondary fluids in both areas are consistent with modification by reaction with wall rocks. Gold precipitation in the Goldville district was probably also influenced by such interactions.

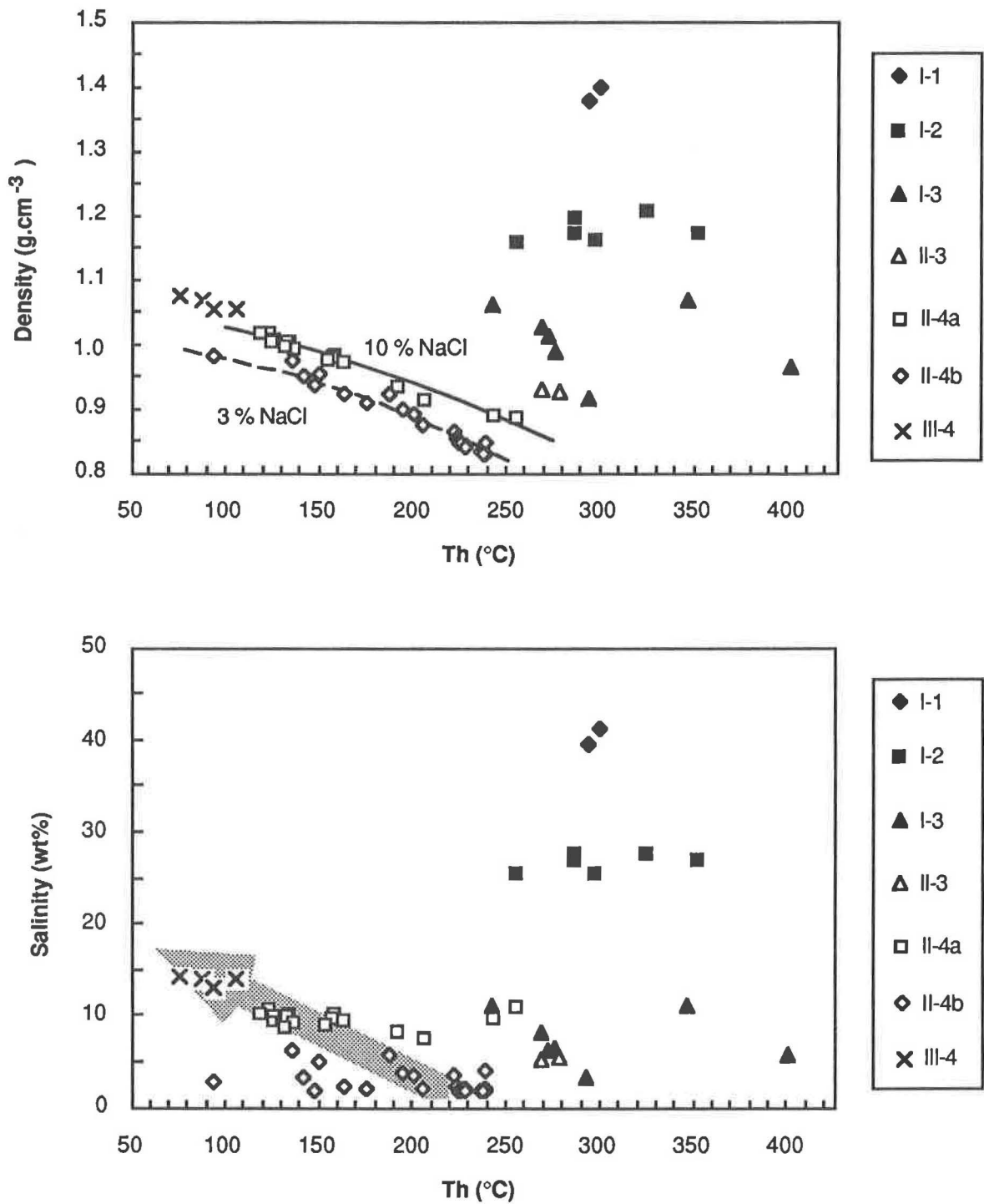


Figure 4. Homogenization temperature (Th) vs. fluid density (top) and salinity (bottom) of fluid inclusions in vein quartz from the Goldville district. Reference curves in top diagram are density evolution trends of fluids in the H<sub>2</sub>O-NaCl system with the indicated salinities (calculation method in text). Salinity trend in bottom diagram reflects decreasing degrees of fluid-wall rock interaction with decreasing temperature.

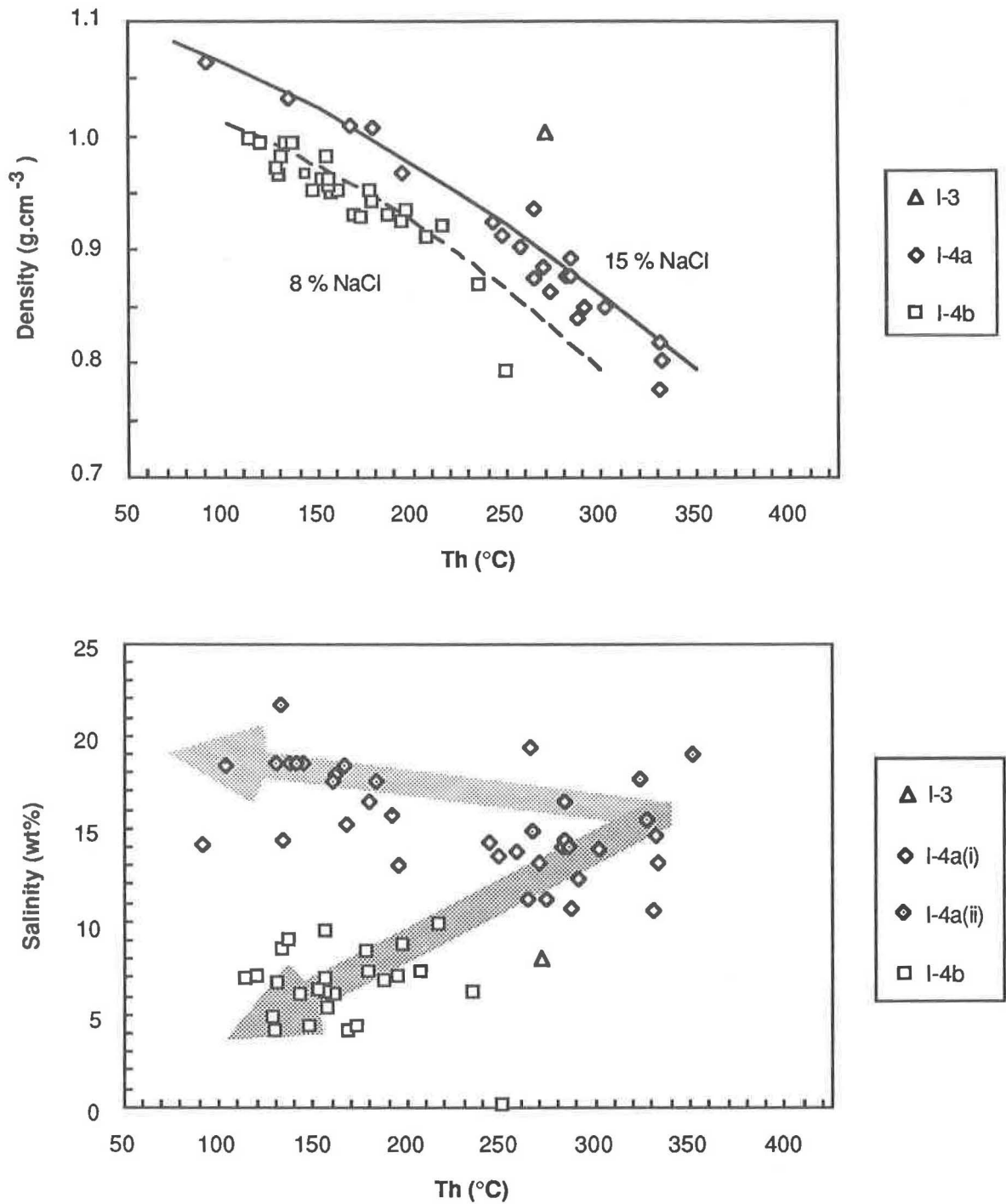


Figure 5. Homogenization temperature (Th) vs. fluid density (top) and salinity (bottom) of fluid inclusions in vein quartz from the Hog Mountain mine. Density evolution curves in top diagram as in Fig. 4. Salinity trends in bottom diagram reflect top cooling (light stipple) and decreasing degrees of fluid-wall rock interaction (heavy stipple).

The final hydrothermal event in the region was dominated by CO<sub>2</sub>-rich fluids (stage IV in the Goldville district and stage II at the Hog Mountain mine). This cannot be attributed to fluid immiscibility in the H<sub>2</sub>O-CO<sub>2</sub> system with declining temperature (Takenouchi and Kennedy, 1964), because there are no conjugate H<sub>2</sub>O-rich fluid inclusions in the same stage. The Wedowee country rocks contain abundant graphite, which is more easily oxidized at lower temperatures (Robie et al., 1978) and CO<sub>2</sub> is considerably more soluble at lower (and higher) temperatures than at moderate (100-250°C) temperatures (Ellis and Golding, 1963), so generation of CO<sub>2</sub>-rich fluids can probably be attributed to oxidation of graphite at low temperatures.

## CONCLUSIONS

- 1) Synkinematic, synmetamorphic auriferous quartz veins at the Hog Mountain, Lowe, and Tallapoosa mines in the northern Alabama Piedmont contain numerous fluid inclusions that can be subdivided into five compositional types depending on salinities and CO<sub>2</sub> contents. Fluid inclusions formed during four recognizable stages at the Lowe and Tallapoosa mines, one primary and three secondary, and two stages at the Hog Mountain mine, both secondary. No primary inclusions have been recognized at the Hog Mountain mine.
- 2) The P-V-T-X properties of rare high salinity "primary" fluids in the Goldville district are not compatible with entrapment at the temperatures and pressures (495±50°C and 5.8±1 kb) determined by independent methods and appear to have been modified subsequent to entrapment.
- 3) Primary and early secondary fluids in the Goldville district and early secondary fluids at the Hog Mountain mine are H<sub>2</sub>O-rich with moderate salinities, minor CO<sub>2</sub>, and only very minor CH<sub>4</sub>. Their P-V-T-X properties are compatible with entrapment at the temperatures and pressures of vein formation. Compositional similarities suggest that they were derived from similar sources, probably by devolatilization of underlying sedimentary lithologies during regional metamorphism.
- 4) Secondary fluids in the Goldville district and at the Hog Mountain mine are H<sub>2</sub>O-rich with moderate-low salinities (predominantly NaCl, some MgCl<sub>2</sub> at Hog Mountain) and negligible CO<sub>2</sub>. Variations in salinity reflect variable degrees of interaction with wall rocks. Deposition of sulfides and gold in the quartz veins and alteration zones was probably influenced by fluid-wall rock interactions.
- 5) Secondary fluids exhibit overall general trends with decreasing temperature toward fluids with higher salinity in the Goldville district and toward fluids with lower salinity in the Hog Mountain district, reflecting decreasing degrees of fluid-wall rock interaction with declining temperature and evolution of the fluid toward that of the metamorphic precursor.
- 6) Late secondary fluids in the Goldville district and at the Hog Mountain mine are CO<sub>2</sub>-rich with minor (Goldville) to significant (Hog Mountain) CH<sub>4</sub>. They were probably derived by oxidation of graphite in carbonaceous country rocks.

## ACKNOWLEDGMENTS

We are very grateful to U.S. Borax and Newmont Exploration Ltd. for donating diamond drill core to the Department of Geology and the Geological Survey of Alabama and for providing copies of unpublished company maps and reports. Harold Stowell kindly provided access to his fluid inclusion stage, helpful advice during data collection and reduction, and insightful comments on the manuscript. Reviews by A.J. Driscoll, Jr. and J.R. Craig resulted in several improvements in the presentation.

This research was supported by the University of Alabama Research Grants Committee (grant nos. 1340 to C.M.L. and 1370 to H.H.S.) and School of Mines and Energy Development (grant nos. 2-29107 and 2-29115 to C.M.L.).

## REFERENCES

- Angus, S., Armstrong, B., deReuck, K.M., Altunin, V.V., Gadetskii, O.G., Chapela, G.A., and Rowlinson, J.S., 1976, International Thermodynamic Tables of the Fluid State. Volume 3. Carbon Dioxide: Pergamon Press, Oxford, 385 p.
- Bodnar, R.J., 1983, A method of calculating fluid inclusion volumes based on vapor bubble diameters and P-V-T-X properties of inclusion fluids: *Economic Geology*, v. 78, p. 535-542.
- Bowers, T.S., and Helgeson, H.C., 1983, Calculation of the thermodynamic and geochemical consequences of nonideal mixing in the system  $H_2O-CO_2-NaCl$  on phase relations in geologic systems: Equation of state for  $H_2O-CO_2-NaCl$  fluids at high pressures and temperatures: *Geochimica et Cosmochimica Acta*, v. 47, p. 1247-1275
- Brown, P.E., 1989, FLINCOR fluid inclusion recalculation program: WISCSWARE, University of Wisconsin, Madison.
- Burruss, R.C., 1981, Analysis of fluid inclusions: Phase equilibria at constant volume: *American Journal of Science*, v. 281, p. 1104-1126.
- Collins, P.L.F., 1979, Gas hydrates in  $CO_2$ -bearing fluid inclusions and the use of freezing data for estimation of salinity: *Economic Geology*, v. 74, p. 1435-1444.
- Crawford, M.L., and Hollister, L.S., 1986, Metamorphic fluids: The evidence from fluid inclusions: in Walther, J.V., and Wood, B.J. (editors), Advances in Physical Geochemistry. Volume 5. Fluid-Rock Interactions During Metamorphism, Springer-Verlag, New York, p. 1-35.
- Ellis, A.J. and Golding, R.M., 1963, The solubility of carbon dioxide above 100°C in water and in sodium chloride solutions: *American Journal of Science*, v. 261, p. 47-60.
- Guthrie, G.M., and Leshner, C.M., in press, Geologic setting of lode gold deposits in the northern piedmont and Brevard zone, Alabama: in Leshner, C.M., Cook, R.B., and Dean, L.S. (editors), Gold Deposits of Alabama, Geological Survey of Alabama Bulletin 136, p. 11-32.
- Heyen, G., Ramboz, C., and Dubessy, J., 1982, Simulation des équilibres de dans le système  $CO_2-CH_4$  en dessous de 50°C et de 100 bar: Application aux inclusions fluides: *Comptes Rendus des Séances de l'Académie des Sciences (Serie II)*, v. 294, p. 203-206.
- Keevil, N.B., 1942, Vapor pressures of aqueous solutions at high temperatures: *Journal of the American Chemical Society*, v. 64, p. 841-850.
- Leshner, C.M., and Green, N.L., 1987, Alteration and gold mineralization, Hog Mountain pluton, northern Alabama Piedmont: in Drummond, M.S., Green, N.L., and Neilson, M.J. (editors), The Granites of Alabama, 24th Annual Field Trip Guidebook, Alabama Geological Society, p. 13-22.
- Leshner, C.M., Stowell, H.H., and Green, N.L., this volume, Stable isotope geochemistry of lode gold mineralization in the northern Piedmont, Alabama: in Cook, R.B. (editor), Economic Mineral Deposits of the Southern Appalachians: Metallic Ore Deposits: Georgia Geologic Survey Bulletin 117.
- Linke, W.F., 1958, Solubilities of Inorganic and Metal-Organic Compounds, v. 1, 4th ed., van Nostrand, Princeton, 1487 p.
- Neal, W.L., and Cook, R.B., in press, Mineralogy, petrology, and geochemistry of phyllite-hosted gold deposits, Goldville District, Tallapoosa county, Alabama: in Leshner, C.M., Cook, R.B., and

- Dean, L.S. (editors), Gold Deposits of Alabama, Geological Survey of Alabama Bulletin 136, p. 173-184.
- Paris, T.A., 1986, The Goldville project: Results of an exploration project for gold in the northern Alabama Piedmont: *in* Misra, K.C. (editor), Volcanogenic Sulfide and Precious Metal Mineralization in the Southern Appalachians: University of Tennessee Department of Geological Sciences Studies in Geology 16, p. 185-205.
- Potter, R.W., Clynne, M.A., and Brown, D.L., 1978, Freezing point depression of aqueous sodium chloride solutions: *Economic Geology*, v. 73, p. 284-285
- Robie, R.A., Hemingway, B.S., and Fisher, J.S., 1978, Thermodynamic properties of Minerals and Related Substances at 298.15 K and 1 Bar ( $10^5$  Pascals) Pressure and at Higher Temperatures: U.S. Geological Survey Bulletin 1452, 456 p.
- Roedder, E., 1984, Fluid Inclusions, Volume 12, Reviews in Mineralogy: Mineralogical Society of America, Washington, 644 p.
- Sourirajan, S. and Kennedy, G.C., 1965, The solubility of carbon dioxide in NaCl solutions at high temperatures and pressures: *American Journal of Science*, v. 263, p. 445-454.
- Stowell, H.H., and Lesher, C.M., this volume, Thermobarometry of synmetamorphic gold deposits, Goldville district, northern Piedmont, Alabama: *in* Cook, R.B. (editor), Economic Mineral Deposits of the Southern Appalachians: Metallic Ore Deposits: Georgia Geologic Survey Bulletin 117.
- Stowell, H.H., Guthrie, G.M., and Lesher, C.M., in press, Metamorphism and Gold mineralization in the Wedowee group, Goldville district, Northern Alabama Piedmont: *in* Lesher, C.M., Cook, R.B., and Dean, L.S. (editors), Gold Deposits of Alabama: Geological Survey of Alabama Bulletin 136, p. 133-158.
- Takenouchi, S. and Kennedy, G.C., 1964, The binary system H<sub>2</sub>O-CO<sub>2</sub> at high temperatures and pressures: *American Journal of Science*, v. 262, p. 1055-1074.

# STABLE ISOTOPE GEOCHEMISTRY OF LODGE GOLD DEPOSITS, NORTHERN PIEDMONT, ALABAMA

C. Michael Lesher, Harold H. Stowell, and Nathan L. Green

Department of Geology, University of Alabama,  
Tuscaloosa, Alabama 35487-0338

## ABSTRACT

Synmetamorphic, synkinematic lode gold mineralization in the central part of the Ashland-Wedowee belt is hosted by Wedowee Group metapelites in the Goldville district and by a tonalite pluton intruded into Wedowee Group metapelites at Hog Mountain. Quartz-plagioclase  $\pm$  pyrrhotite  $\pm$  carbonate veins in the Goldville district were emplaced during progressive D<sub>1</sub>-D<sub>2</sub> deformation and peak metamorphism at  $490 \pm 50^\circ\text{C}$  and  $5.8 \pm 1\text{kb}$  (garnet-biotite-plagioclase-muscovite equilibria); most are bordered by thin chlorite/biotite  $\pm$  garnet selvages and/or narrow Al-Rb-K-Ba-Mg-Fe-Cr-enriched chlorite-muscovite alteration envelopes. Quartz-pyrrhotite  $\pm$  carbonate veins at Hog Mountain were emplaced at  $475\text{-}275^\circ\text{C}$  (plagioclase-muscovite equilibria) during progressive D<sub>2</sub>-D<sub>3</sub> deformation, following peak metamorphism at  $460 \pm 50^\circ\text{C}$  and  $4.5 \pm 1\text{kb}$  (garnet-biotite-plagioclase-muscovite-chlorite equilibria); most exhibit well-defined Rb-K-Ba-Fe-Co-W-S-Au-enriched quartz-muscovite-pyrrhotite alteration envelopes that have been dated at  $294 \pm 15\text{ Ma}$  (K/Ar whole-rock) and  $315 \pm 16\text{ Ma}$  (Rb-Sr whole-rock isochron;  $^{87}\text{Sr}/^{86}\text{Sr}_{\text{initial}} = 0.7061 \pm 0.0012$ ).

H isotopic compositions of tonalites at the Hog Mountain mine vary with degree of alteration (*least-altered tonalites* =  $-78$  to  $-81\text{‰}$   $\delta\text{D}$ , *moderately-altered tonalites* =  $-79$  to  $-74\text{‰}$   $\delta\text{D}$ , *strongly-altered tonalites* =  $-50$  to  $-53\text{‰}$   $\delta\text{D}$ , and *sheared, altered tonalites* =  $-58$  to  $-62\text{‰}$   $\delta\text{D}$ ), reflecting selective incorporation of D into muscovite during alteration and re-equilibration during post-alteration shearing; O isotopic compositions are variable, but nonsystematic ( $9.7$  to  $12.0\text{‰}$   $\delta^{18}\text{O}$ ), reflecting the larger reservoir for O in the rocks and offsetting fractionation between plagioclase, biotite, and muscovite; S isotopic compositions are also variable and nonsystematic ( $9.6$  to  $11.3\text{‰}$   $\delta^{34}\text{S}$ ), probably reflecting mixing of internally-derived magmatic and externally-derived sedimentary S. Analyzed mineral separates yield O isotopic equilibration temperatures and fluid compositions of  $475 \pm 45^\circ\text{C}$  (qtz-ms) and  $335 \pm 40^\circ\text{C}$  (qtz-cal);  $\delta^{18}\text{O}_{\text{fluid}} = 7$  to  $11\text{‰}$ ;  $\delta\text{D}_{\text{fluid}} = -10$  to  $-31\text{‰}$ ;  $\delta^{13}\text{C}_{\text{fluid}} = \text{ca. } -6\text{‰}$ ; and  $\delta^{34}\text{S}_{\text{fluid}} = \text{ca. } 10\text{‰}$ . Discordant O and H isotopic fractionation between quartz, muscovite, and calcite in veins suggests that O in quartz and muscovite records the temperature and fluid composition during initial alteration, whereas H in muscovite and O in calcite record conditions at lower temperatures.

H and O isotopic compositions of metapelites at the Lowe and Jones mines in the Goldville district also vary with degree of alteration (*least-altered metapelites* =  $12.7$  to  $12.9\text{‰}$   $\delta^{18}\text{O}$  and  $-82$  to  $-95\text{‰}$   $\delta\text{D}$ ; *sericitized-chloritized metapelites* =  $11.4$  to  $11.7\text{‰}$   $\delta^{18}\text{O}$  and  $-66$  to  $-69\text{‰}$   $\delta\text{D}$ ) reflecting selective incorporation of D and exclusion of O by muscovite-chlorite during alteration; limited S isotopic data are constant at  $\text{ca. } 19\text{‰}$   $\delta^{34}\text{S}$ . Analyzed mineral separates yield O isotopic equilibration temperatures and fluid compositions of  $550\text{-}340^\circ\text{C}$  (qtz-pl),  $520 \pm 30^\circ\text{C}$  (qtz-bt), and  $350 \pm 15^\circ\text{C}$  (qtz-chl);  $\delta^{18}\text{O}_{\text{fluid}} = 9$  to  $13\text{‰}$ ;  $\delta\text{D}_{\text{fluid}} = -46$  to  $-51\text{‰}$ , and  $\delta^{34}\text{S}_{\text{fluid}} = \text{ca. } 19$ .

The stable isotopic data, together with field, petrographic, microthermometric, and geochemical data, suggest that vein-forming fluids in both areas equilibrated to varying degrees with, and were probably derived from, pelitic metasedimentary rocks, but were not derived from adjacent country rocks. Mineralizing fluids were most likely derived from underlying thrust sheets and/or the underlying North American continental shelf.

## INTRODUCTION

Lode gold mineralization in the northern Piedmont of Alabama is associated with synmetamorphic, synkinematic quartz  $\pm$  sulfide  $\pm$  plagioclase  $\pm$  carbonate veins in a variety of host rocks, predominantly metapelites with lesser mafic metavolcanic rocks and granitoids (Pardee and Park, 1948; Guthrie and Leshner, in press). Some workers have interpreted the deposits as syngenetic and suggested that gold was mobilized into veins during metamorphism (McConnell et al., 1986; Paris, 1986; Neal and Cook, in press), but detailed stratigraphic, structural, metamorphic, and geochemical studies (e.g. Leshner and Green, 1987; Green et al., 1988; Stowell et al., in press) indicate that most of the mineralization is epigenetic.

The aim of this paper is to report the results of a stable isotopic study of the Lowe and Jones mines in the northeastern and southwestern parts of the Goldville district and the Hog Mountain mine 10 km to the northwest (see fig. 1: Stowell and Leshner, this volume). All three deposits have been subjected to recent exploration programs involving diamond core drilling which provided fresh samples of vein minerals, alteration selvages, and alteration envelopes for geochemical analysis. The isotopic data constrain the conditions of vein emplacement and the sources of vein-forming fluids in this part of the southern Appalachians.

Our research indicates that the that the veins were emplaced during prograde metamorphism, that vein minerals and alteration assemblages crystallized from the same fluids, and that vein-forming fluids were derived externally from the zones of mineralization. These data confirm that the gold mineralization in this region is epigenetic.

## GEOLOGIC SETTING

The Hog Mountain deposit and Goldville district occur in the central part of the Ashland-Wedowee belt of the northern Alabama Piedmont (Guthrie and Leshner, in press; see fig. 1: Stowell and Leshner, this volume). Deposits in the Goldville district are hosted by metapelitic phyllite and schist of the Cutnose Gneiss member of the Wedowee Group (Neathery and Reynolds, 1973), whereas the Hog Mountain deposit, 10 km to the northwest, is hosted by a tonalite pluton intruded into the same metasediments. The rocks in this region have experienced polyphase deformation (Guthrie and Dean, 1989) and upper greenschist to lower amphibolite facies metamorphism (Stowell and Leshner, this volume).

Five phases of deformation have been recognized in the area based on local cross-cutting relationships (Guthrie and Dean, 1989):  $D_1$  is characterized by poorly-preserved microscopic to mesoscopic, intrafolial isoclinal, similar folds ( $F_1$ ) and a pervasive axial planar schistosity ( $S_1$ );  $D_2$  is manifested as NE-trending, NW-verging, microscopic to macroscopic, close to isoclinal, quasi-flexural folds ( $F_2$ ), coaxial with  $F_1$ , a discontinuous domainal cleavage to dominant foliation ( $S_2$ ) that transposes  $S_1$ , and NE-striking, ductile to semi-brittle shear zones with northwest-directed transport;  $D_3$  is characterized by NNE-trending, NW-verging, upright to inclined flexural slip folds ( $F_3$ ), a solution crenulation cleavage ( $S_3$ ), and semi-brittle fault zones;  $D_4$  is manifested as SE-plunging, upright open folds ( $F_4$ ) and a localized crenulation or fracture cleavage ( $S_4$ ); and  $D_5$  is characterized by isoclinal to broad, inclined, plunging extensional crenulations ( $S_5$ ) associated with dextral strike-slip faults. These deformational styles correlate in a general manner with regional structures defined by Tull (1978; cf. Guthrie and Leshner, in press).  $D_1$  through  $D_3$  structures are interpreted to result from progressive deformation during northwest-directed shortening. Structural and petrographic studies at Hog Mountain (Leshner and Green, 1987; Guthrie and Leshner, 1988) and Goldville (Stowell et al., in press) indicate that the mineralized veins were emplaced progressively during  $D_1$ - $D_3$ , synchronous with metamorphism.

Petrographic and thermobarometric data indicate that metamorphism in the area peaked between  $D_1$  and  $D_2$  and was followed by retrograde metamorphism during  $D_3$  (Stowell and Leshner, this volume). Metamorphic grade appears to increase southeastward across the area:  $460 \pm 50^\circ\text{C}$  and  $4.5 \pm 1\text{ kb}$  at the Hog Mountain mine (Green and Leshner, 1987),  $490 \pm 50^\circ\text{C}$  and  $5.8 \pm 1\text{ kb}$  at the Lowe mine (Stowell et al., in press), and  $575 \pm 50^\circ\text{C}$  and  $6.7 \pm 1\text{ kb}$  within the Alexander City fault zone (Stowell and Leshner, this volume).

## Hog Mountain Deposit

The geology and gold mineralization at Hog Mountain have been described by Park (1935), Pardee and Park (1948), Green and Leshner (1987, 1988), and Leshner and Green (1987). Hog Mountain is underlain by a small, elongate (1500 m x 400 m), tonalite pluton intruded into interlayered garnet-biotite-chlorite-quartz phyllite, chlorite-sericite phyllite, and graphite phyllite about 20 km northeast of Alexander City, Alabama (see fig. 1 of Stowell and Leshner, this volume). The pluton transgresses  $S_0$  and  $S_1$  in the country rocks, contains inclusions of foliated ( $S_1$ ?) country rocks with prograde mineral assemblages, and is cross-cut by quartz-sulfide veins with foliated alteration envelopes that are deformed, boudinaged, and transposed into the  $S_2$  fabric along the margins of the pluton. As such, the pluton is interpreted to have been emplaced during prograde metamorphism; after  $D_1$ , but prior to or during  $D_2$ . Owing to a narrow range of Rb/Sr ratios, the emplacement age of the Hog Mountain tonalite has been precisely determined, however, vein-related alteration is dated at  $294 \pm 15$  Ma (K/Ar) and  $315 \pm 16$  Ma (Rb/Sr whole-rock isochron,  $^{87}\text{Sr}/^{86}\text{Sr}_{\text{initial}} = 0.7061 \pm 0.0012$ : N.L.G., C.M.L., and A.K. Sinha, unpubl. data).

Three types of veins have been identified at Hog Mountain: I) deformed, milky white quartz veins with small (1-5 mm) lenses of transparent, clear quartz, II) massive, vitreous, grey quartz-sulfide veins, and III) calcite-sulfide  $\pm$  quartz veins. Silica mobility during wall rock alteration has also produced abundant diffuse quartz veins and silicified stockworks in the tonalite. Type I veins are restricted to the penetratively-deformed metasedimentary country rocks, whereas types II and III are restricted to the less-deformed tonalite. Type III veins are paragenetically later and less abundant than type II veins, but some veins are composite and multi-generational.

Type II-III veins are bordered by muscovite-quartz-pyrrhotite alteration envelopes that are systematically enriched in Rb-K-Ba, Fe-Co, W, S, and Au relative to least-altered tonalite (Leshner and Green, 1987). Alteration envelopes range from massive through foliated to sheared, indicating that variable degrees of strain existed during alteration. Some veins are transgressive to the foliation in alteration envelopes, indicating emplacement into pre-existing fractures; others exhibit deformed fabrics, reflecting deformation subsequent to emplacement. Progressive emplacement/deformation is supported by plagioclase-muscovite Na-K exchange thermometry (Leshner and Green, 1987 and unpubl. data) which yields a broad range of temperatures between  $425 \pm 50$  (most type II veins) and  $325 \pm 50^\circ\text{C}$  (most type III veins).

Primary fluid inclusions have not been identified in vein quartz at Hog Mountain, but sparse early secondary inclusions with fluid compositions similar to those in some primary and early secondary inclusions in the Goldville district are  $\text{H}_2\text{O}$ -rich and moderately saline with minor  $\text{CO}_2$  and very minor  $\text{CH}_4$  contents (Sha and Leshner, this volume). Most secondary fluid inclusions are  $\text{H}_2\text{O}$ -rich and slightly-moderately saline with minor  $\text{CO}_2$  contents; anomalously low eutectic temperatures suggest that multiple salts ( $\text{NaCl} \pm \text{MgCl} \pm \text{CaCl} \pm \text{KCl}$ ) are present in some fluids. Late secondary fluid inclusions are  $\text{CO}_2$ -rich with significant  $\text{CH}_4$  contents.

## Goldville District

The Goldville district comprises a 16 km long, northeast-trending group of inactive gold mines and prospects in the central part of the Ashland-Wedowee belt that have been described by Pardee and Park (1948), Neal (1986), Paris (1986), Guthrie and Dean (1989), Neal and Cook (in press), Neal et al. (in press), and Stowell et al. (in press). Host rocks are garnet-biotite-chlorite-sericite-quartz phyllite in the northeast part of the district and graphite phyllite in the southwest part. The phyllites are polydeformed, have been metamorphosed to garnet zone, and sedimentary structures such as thin bedding, cross bedding, and graded bedding are rarely preserved. Gold mines and prospects in the district are associated exclusively with multi-generation quartz  $\pm$  plagioclase  $\pm$  pyrrhotite veins that cross-cut regional stratigraphy, compositional layering, and the earliest recognizable foliation ( $S_1$ ). Veins are variably boudinaged, folded, sheared, and transposed into an  $S_2$  axial planar fabric.

Three types of veins have been identified in the Goldville district: I) monomineralic quartz veins, II) quartz-plagioclase  $\pm$  carbonate  $\pm$  sulfide veins, and III) calcite  $\pm$  quartz  $\pm$  sulfide veins.

Types I and II may be genetically related, as they exhibit similar structural relationships and a continuum of feldspar/quartz ratios. Type I veins are common at the Lowe and Tallapoosa mines and in the host rocks throughout the district. Type II veins appear to be restricted to the mine areas, although their absence in surface exposures could be due to weathering of plagioclase, hindering recognition. Type III veins are relatively rare and cross-cut type I-II veins and S<sub>1</sub>-S<sub>2</sub> fabrics.

Synmetamorphic vein emplacement is confirmed by thermobarometric studies (Stowell et al., in press; Stowell and Lesher, this volume). Fe-Mg exchange between coexisting biotite and garnet from host rocks and biotite-rich selvages adjacent to veins yield indistinguishable equilibration temperatures of  $490 \pm 50^\circ\text{C}$ ; Na-K exchange between coexisting muscovite and plagioclase in veins indicate similar, albeit less precise, equilibration temperatures of  $510 \pm 80^\circ\text{C}$ ; and plagioclase-biotite-muscovite-garnet equilibria indicate pressures of  $5.8 \pm 1$  kb.

Some phyllites adjacent to veins exhibit little or no signs of alteration, however, many are bordered by narrow (<1 cm) selvages of massive chlorite and/or biotite, and some are bordered by narrow (<10 cm) zones of chlorite-muscovite  $\pm$  garnet that locally truncate layering and veins, contain helicitic garnet porphyroblasts which are locally altered to chlorite, and commonly contain significantly smaller grain sizes than host rocks and adjacent vein selvages. These zones are enriched in Rb-K-Ba, Mg-Fe, and Al-Cr relative to least-altered metapelites (C.M.L. and H.H.S., unpubl. data) and appear to represent hydrothermally-altered shear zones.

Primary and early secondary fluid inclusions at the Lowe and Tallapoosa mines in the Goldville district are H<sub>2</sub>O-rich and moderately saline with minor CO<sub>2</sub> and very minor CH<sub>4</sub> contents (Sha and Lesher, this volume). Most secondary fluid inclusions, equivalent to most of those at Hog Mountain, are H<sub>2</sub>O-rich and slightly-moderately saline with minor CO<sub>2</sub> contents. Late secondary fluid inclusions are CO<sub>2</sub>-rich with minor CH<sub>4</sub> contents.

## STABLE ISOTOPE GEOCHEMISTRY

### Sampling and Analytical Methods

All samples for stable isotopic study were taken from diamond drill core beneath the zone of weathering. The suite from Hog Mountain includes whole-rock samples of least-altered tonalite; two profiles across alteration envelopes adjacent to type II veins, one moderately-altered and one strongly altered; and several vein mineral separates from type II (qtz-po) and type III veins (qtz-po-ms-cal). The suite from the Goldville district (Lowe and Jones mines) includes two whole-rock samples of least-altered metapelite and adjacent alteration zones; and several vein mineral separates from type II veins (qtz-pl, qtz-bt, and qtz-chl). Whole-rock samples were crushed in an alumina ceramic jaw crusher and pulverized in an alumina ceramic shatterbox. Mineral separates were hand-picked under a binocular microscope (>99% pure), cleaned ultrasonically in reagent-grade acetone, and pulverized with an agate mortar and pestle.

Stable isotope ratios were determined by mass spectrometry in the Department of Geology at Indiana University under the supervision of Dr. E.M. Ripley, using a 9 cm Finnigan-MAT Delta-E spectrometer for H, C, and O, and a 6" 60°-sector Nuclide spectrometer for S. H was liberated as H<sub>2</sub>O and converted to H<sub>2</sub> with Zn (Kendall and Coplen, 1982), C was liberated as CO<sub>2</sub> with phosphoric acid (Rosenbaum and Sheppard, 1986), O was converted to CO<sub>2</sub> using BrF<sub>5</sub> (Clayton and Mayeda, 1963), and S was combusted with excess CuO to produce SO<sub>2</sub> (Fritz et al., 1974). H and O data are reported as per mil deviations relative to standard mean ocean water (SMOW), C data relative to Pedee Formation belemnite (PDB), and S data relative to Canon Diablo troilite (CDT). Routine analytical precision is  $\pm 0.05\%$  for  $\delta^{13}\text{C}$  and  $\delta^{18}\text{O}$ ,  $\pm 0.1\%$  for  $\delta^{34}\text{S}$ , and  $\pm 1\%$  for  $\delta\text{D}$  (E.M. Ripley, pers.l comm., 1988).

### Results

Stable isotopic data for Hog Mountain and Goldville samples are given in Tables 1 and 2, are illustrated in Figures 1-7, and are summarized below. Corresponding whole-rock major and trace element geochemical data for Hog Mountain are given in Green and Lesher (1988).

**Table 1. Stable Isotope data for least-altered tonalites, altered tonalites, and type II-III vein mineral separates from the Hog Mountain mine, Tallapoosa County, Alabama**

Sample	$\delta D$ (‰)	$\delta^{18}O$ (‰)	$\delta^{34}S$ (‰)	$\delta^{13}C$ (‰)	T (°C)	$\delta D_{fluid}$ (‰)	$\delta^{18}O_{fluid}$ (‰)	$\delta^{34}S_{fluid}$ (‰)	$\delta^{13}C_{fluid}$ (‰)
<b>Least-Altered Tonalites</b>									
HM-2/85.0 I	-81	11.2		10.9					
HM-3/126.0 I	-78	10.9		11.3					
HM-7/281.6 I	-78	9.7		10.2					
<b>Altered Tonalites Adjacent to Type II Vein</b>									
HM-1/234.8 I	-75	11.2		10.3					
HM-1/235.1 m	-69	10.1		10.3					
HM-1/235.3 s	-50	10.4		10.5					
HM-1/235.7 s	-52	10.2		9.6					
HM-1/235.9 s	-53	9.8		10.3					
HM-1/236.1 s-s	-62	10.7		10.5					
HM-1/236.4 s-s	-61	10.8		9.6					
HM-1/236.8 s-s	-58	11.0		10.3					
HM-1/237.0 qv	-88	11.4		9.8					
<b>Altered Tonalites Adjacent to Type II Vein</b>									
HM-2/187.8 I	-77	11.4		11.2					
HM-2/188.1 I	-82	11.2		10.7					
HM-2/188.5 s	-74	11.2		10.7					
HM-2/188.6 s	-75	11.9		10.3					
HM-2/188.7 m	-79	12.0		9.9					
<b>Type II Vein Mineral Separates</b>									
HM-1/235 <i>Muscovite</i>	-49*				425±50 <sup>PM</sup>	-23±8			
HM-1/274 <i>Quartz</i>		13.4			425±50 <sup>PM</sup>		9.9±1.1		
<i>Pyrrhotite</i>			9.9					ca. 10	
<b>Composite Type II-III Vein Mineral Separates</b>									
HM-6/235 <i>Quartz</i>		13.4							
<i>Muscovite</i>		11.1			475±45 <sup>QM</sup>		10.7±0.7		
	-63				335±50 <sup>PM</sup>	-22±9			
<i>Calcite</i>		11.8		-8.21	335±40 <sup>QC</sup>		7.6±1.2		-5.9±1.3
<i>Pyrrhotite</i>			9.0					ca. 9	
HM-2/122 <i>Arsenopyrite</i>			-4.1						

Notes: analytical methods, conventions, and calculation methods given in text; errors based on analytical uncertainties; alteration intensity (as defined by Leshner and Green, 1987): I = incipient, I = slight, m = moderate, s = strong, s-s = strong with shearing, qv = quartz vein; \* $\delta D$  value for muscovite in HM1/235 calculated by extrapolation of whole-rock  $\delta D$ -K<sub>2</sub>O data (Fig. 1); geothermometers: PM = pl-ms Na-K exchange, QM = qtz-ms O isotope exchange, QC = qtz-cal O isotope exchange; .

**Table 2. Stable isotope data for metapelites, alteration zones, and type II vein mineral separates from the Lowe mine and Jones vein, Tallapoosa County, Alabama**

Sample	Type	$\delta D$ (‰)	$\delta^{18}O$ (‰)	$\delta^{34}S$ (‰)	Temp. (°C)	$\delta^{18}O_{fluid}$ (‰)	$\delta D_{fluid}$ (‰)	$\delta^{34}S_{fluid}$ (‰)
<b>Metapelites</b>								
LO-23C	country rock	-82	12.7					
LO-23A	alteration zone	-69	11.7					
LO-31A	country rock	-95	12.9	18.6				ca. 19
LO-31B	alteration zone	-79	13.2	18.8				ca. 19
LO-31C	alteration zone	-66	11.4					
<b>Type II Vein Mineral Separates</b>								
JO-5	quartz plagioclase		15.2 13.4		385±45	10.9±0.7		
LO-26	quartz biotite	-85	14.5 9.9		520±30	12.4±0.2	-48±2	
LO-30	quartz plagioclase		15.2 13.9		475±45	12.5±0.7		
LO-31	quartz plagioclase		14.5 13.0		435±40	11.2±0.7		
LO-32	quartz chlorite	-78	14.7 8.7		350±15	9.4±0.4	-50±1	

Notes: analytical methods, conventions, and calculation methods given in text; errors based on analytical uncertainties; LO = Lowe mine, JO = Jones mine.

Three *least-altered tonalites* at Hog Mountain with 1.7-1.9% K<sub>2</sub>O and 0.05-0.93% S range between 9.7 and 11.2‰  $\delta^{18}O$ , between -78 and -81‰  $\delta D$ , and between 10.2 and 11.3‰  $\delta^{34}S$ . These ranges exceed analytical uncertainties and reflect a combination of original compositional inhomogeneity in the pluton (66-72% SiO<sub>2</sub>, 0.2-0.6% TiO<sub>2</sub>, 16-18% Al<sub>2</sub>O<sub>3</sub>) and pervasive incipient alteration (Green and Leshner, 1987; Leshner and Green, 1987). H isotopic compositions of altered rocks vary systematically with degree of alteration and deformation, whereas O and S are more uniform. Four *moderately-sericitized tonalites* with 2.0-3.9% K<sub>2</sub>O and 0.24-0.69% S range between 11.2 and 12.0‰  $\delta^{18}O$ , between -79 and -74‰  $\delta D$ , and between 9.9 and 11.2‰  $\delta^{34}S$ ; three *decussate-textured, strongly sericitized-sulfidated tonalites* with 6.3-6.8% K<sub>2</sub>O and 1.8-3.0% S range between 9.8 and 10.4‰  $\delta^{18}O$ , between -50 and -53‰  $\delta D$ , and between 9.6 and 10.5‰  $\delta^{34}S$ ; and two *strongly foliated, sericitized-sulfidated tonalites* with 5.9-8.8% K<sub>2</sub>O and 2.2-3.0% S range between 10.7 and 11.0‰  $\delta^{18}O$ , between -58 and -62‰  $\delta D$ , and between 10.3 and 10.5‰  $\delta^{34}S$ . An *impure quartz vein* with 87% SiO<sub>2</sub> contains 11.4‰  $\delta^{18}O$ , -88‰  $\delta D$ , and 9.8‰  $\delta^{34}S$ . Linear regression of samples from a single vein alteration envelope (Fig. 1), confirms that muscovite is the principal host for D and K, and yields a  $\delta D$  value of -49‰ at 7.1% K<sub>2</sub>O (the average composition of muscovite determined by electron probe microanalysis; Green and Leshner, 1988). Mineral separates from a type II vein yield  $\delta^{18}O_{qtz} = 13.4$  and  $\delta^{34}S_{sp} = 9.9$ . Mineral separates from a type III vein and alteration selvage yield  $\delta^{18}O_{qtz} = 13.4$ ,  $\delta^{18}O_{ms} = 11.1$ ,  $\delta^{18}O_{cal} = 11.77$ ,  $\delta D_{ms} = -63$ ,  $\delta^{13}C_{cal} = -8.21$ , and  $\delta^{34}S_{sp} = 9.0$ .

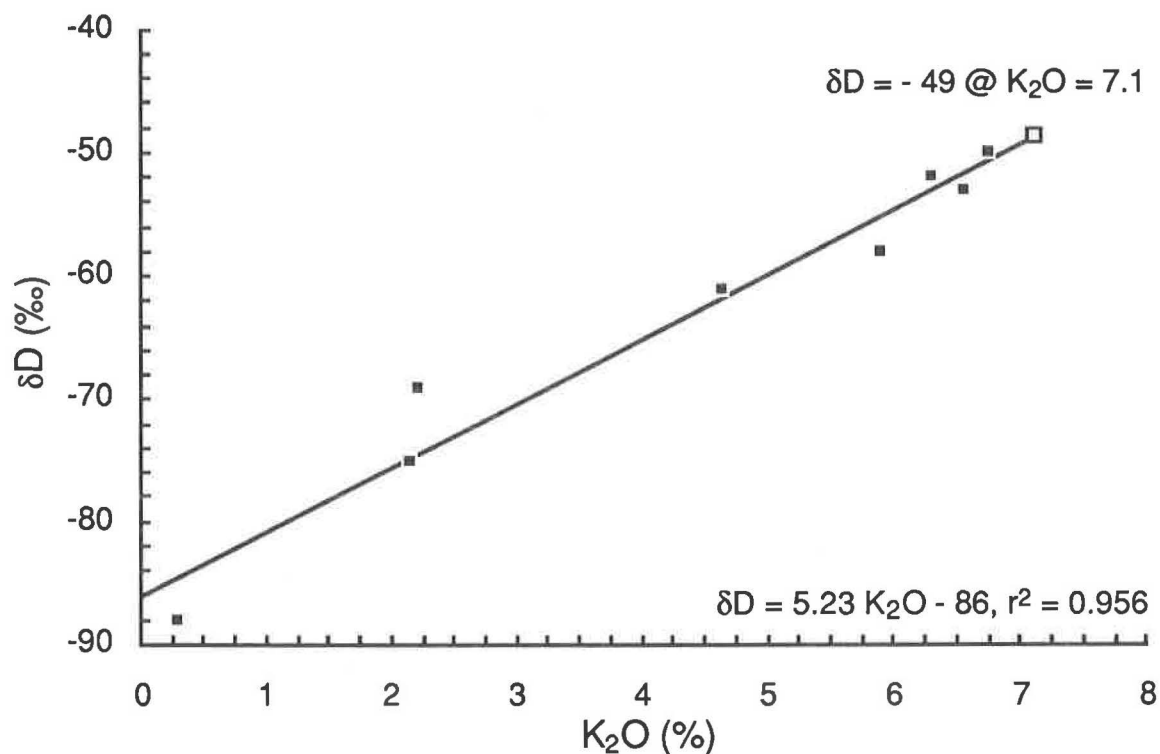


Figure 1. Plot of  $\delta D$  vs.  $K_2O$  for altered tonalites in HM-1/234-237m at Hog Mountain; regression excludes sample 236.1 (Table 1). H isotopic composition of average muscovite with 7.1%  $K_2O$  (determined by electron probe microanalysis) is  $-49\%$   $\delta D$ .

Two *least-altered metapelites* at Goldville exhibit 12.7 and 12.9%  $\delta^{18}O$ ,  $-82$  and  $-95\%$   $\delta D$  and 18.6%  $\delta^{34}S$ . H and O isotopic compositions of altered rocks vary systematically with degree of alteration, whereas S appears to be more uniform. Three *altered metapelites* range between 11.4 and 13.4%  $\delta^{18}O$  and between  $-79$  and  $-66\%$   $\delta D$ , and exhibit 18.8%  $\delta^{34}S$ . Mineral separates yield  $\delta^{18}O_{qtz} = 14.5-15.2\%$ ,  $\delta^{18}O_{pl} = 13.0-13.9\%$ ,  $\delta^{18}O_{bt} = 9.9\%$ , and  $\delta^{18}O_{chl} = 8.7\%$ .

### Stable Isotope Geothermometry

Samples utilized for stable isotope thermometry comprise coexisting mineral pairs which are inferred to be in equilibrium, however, different pairs have been sampled from different veins and are not necessarily cogenetic. Plagioclase and quartz are intimately intergrown within the veins at Goldville and are most likely to be in equilibrium. Coarse-grained muscovite, biotite, and chlorite are uncommon within quartz veins at Goldville or Hog Mountain and were separated (with difficulty) from vein selvages; elemental exchange thermometry suggests that muscovite/biotite selvages and veins equilibrated at the same temperatures (Stowell et al., in press; Stowell and Leshner, this volume). Local replacement of biotite by chlorite in other samples suggests that some chlorite postdates other minerals.

Temperatures of equilibration may be calculated using coexisting minerals and experimentally-determined or theoretically/empirically-derived O isotopic exchange equilibria. There are substantial discrepancies between experimentally- and theoretically- or empirically-determined fractionation factors (see reviews by O'Neil, 1986, and Kyser, 1987). Experimentally-determined values were used wherever possible; they are considered to be more applicable and appear to give results more consistent with our elemental exchange thermometry.

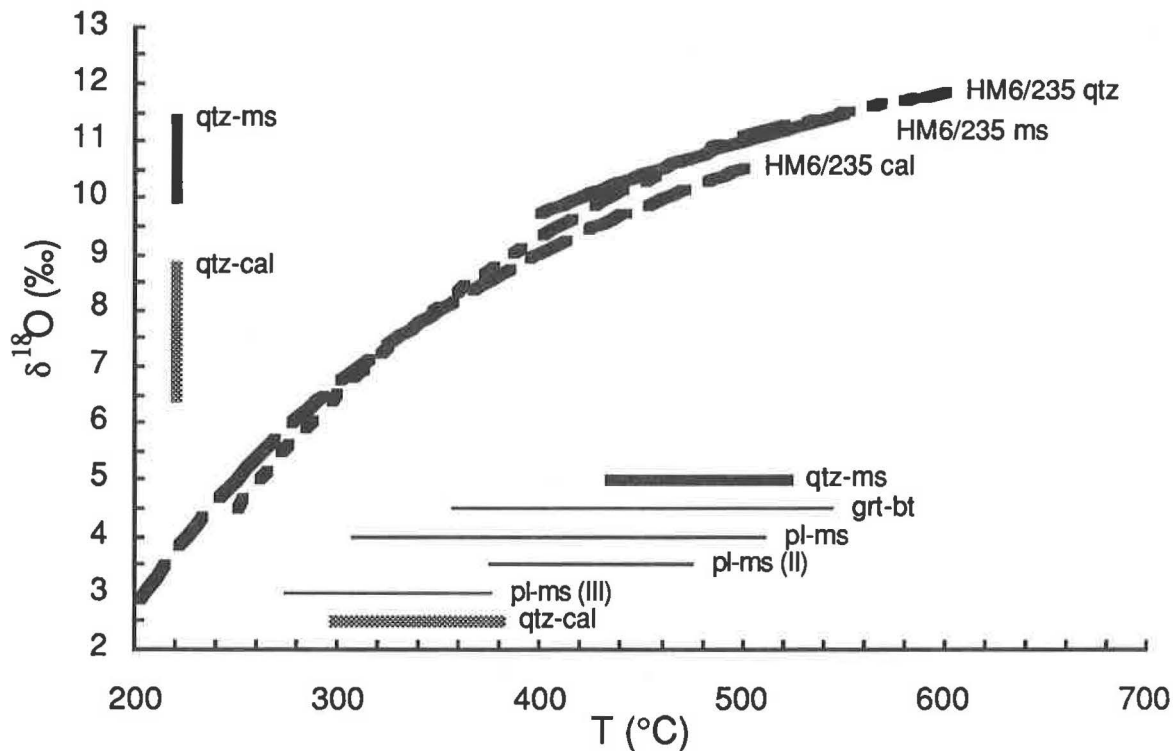


Figure 2. Calculated  $\delta^{18}\text{O}$  values of aqueous fluids in equilibrium with quartz (short dashed line), muscovite (solid line), and calcite (long dashed line) mineral separates from the Hog Mountain mine (Table 1). Also shown are temperature ranges calculated from quartz-muscovite and quartz-calcite O isotope fractionation, garnet-biotite Fe-Mg exchange thermometry, and plagioclase-muscovite Na-K exchange thermometry for stage II (qtz-po±cal) and stage III (cal-po±qtz) veins.

O isotopic fractionation factors are taken from Matsuhisa et al. (1979: quartz-water and plagioclase-water), O'Neil and Taylor (1969: muscovite-water), Bottinga and Javoy (1975: biotite-water), Wenner and Taylor (1971: chlorite-water), and O'Neil et al. (1969: calcite-water); H isotopic fractionation factors are taken from Suzuoki and Epstein (1976: muscovite-water and biotite-water), Graham et al. (1987: chlorite-water); and C isotopic fractionation factors are taken from Bottinga (1969: calcite- $\text{CO}_2$  and graphite- $\text{CO}_2$ ). Simultaneous solutions of mineral-water equations for coexisting phases yield temperatures of equilibration and isotopic compositions of aqueous fluids (Tables 1 and 2; Figs. 2 and 5). Based on the reduced sulfide assemblages (po ± cpy ± sph ± mo), calculated low oxidation states of fluid inclusions (P. Sha and C.M.L., unpubl. data), and relatively high temperatures of equilibration calculated below, the oxidation state of the hydrothermal fluid is assumed to have been below the  $\text{SO}_2/\text{H}_2\text{S}$  boundary and isotopic fractionation between  $\text{H}_2\text{S}-\text{S}^{-2}$  or  $\text{HS}^{-}-\text{S}^{-2}$  is inferred to have been negligible (see Ohmoto, 1986).

Temperatures of equilibration of veins and selvages at Hog Mountain (Table 1; Fig. 2) are  $475 \pm 45^\circ\text{C}$  calculated from quartz-muscovite O isotope fractionation and  $335 \pm 40^\circ\text{C}$  calculated from quartz-calcite O isotope fractionation. These temperatures correspond closely to the  $425 \pm 50^\circ\text{C}$  and  $325 \pm 50^\circ\text{C}$  values calculated by Green and Leshar (1988) for early (type II qtz-po±cal) and late (type III cal-po±qtz) stage veins using plagioclase-muscovite Na-K exchange thermometry.

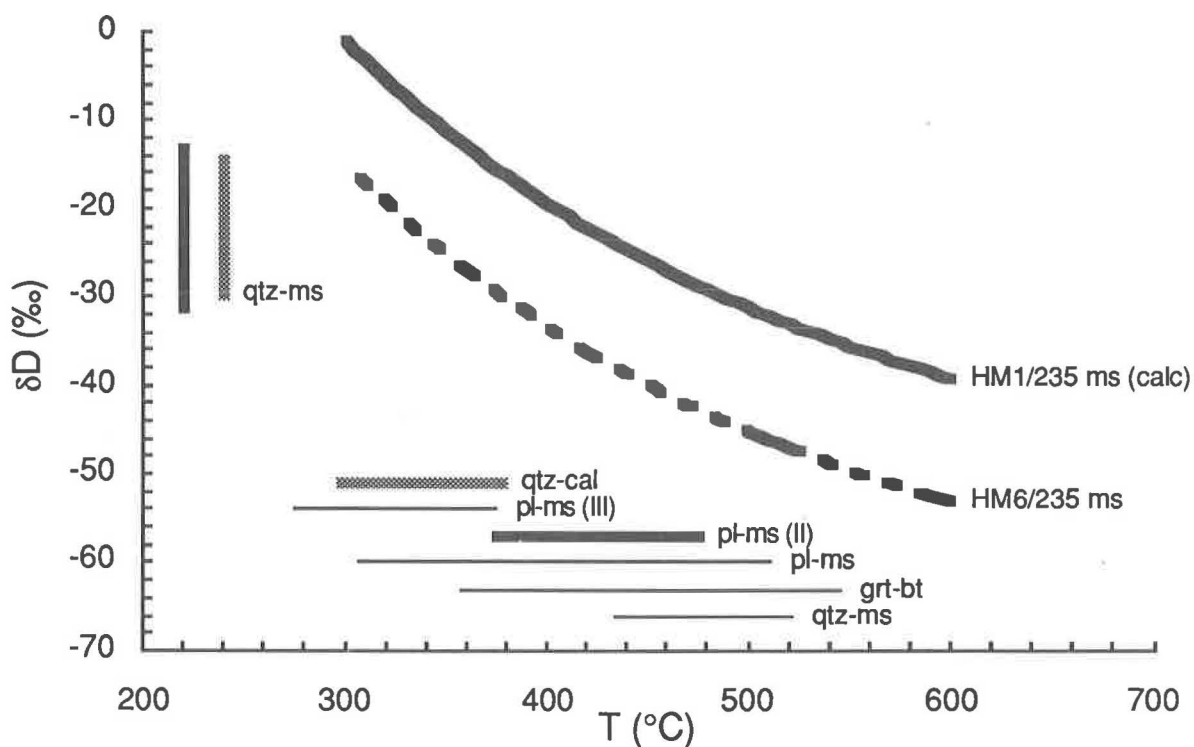


Figure 3. Calculated  $\delta D$  values of aqueous fluids in equilibrium with early muscovite (solid line: composition calculated in Fig. 1) and late muscovite (dashed line: mineral separate) from the Hog Mountain mine. Temperature ranges as in Figure 2.

Temperatures of equilibration of veins and selvages at Goldville (Table 2; Fig. 5) are 550-340°C calculated from quartz-plagioclase O isotope fractionation (3 pairs; low precision attributable to similar slopes of quartz and plagioclase fractionation curves: Fig. 5),  $520 \pm 30^\circ\text{C}$  calculated from quartz-biotite O isotope fractionation, and  $350 \pm 15^\circ\text{C}$  calculated from quartz-chlorite O isotope fractionation. Isotopic re-equilibration by self-diffusion is not considered to have affected the results, as diffusion calculations (Cole and Ohmoto, 1986) suggest that re-equilibration would be insignificant for plagioclase, mica, and quartz. Unfortunately, no diffusion data are available for chlorite.

### Fluid Compositions

The isotopic composition of the early (stage II) vein-forming fluid at the Hog Mountain deposit (Table 1; Figs. 2-4) is  $9.9 \pm 1.1\%$   $\delta^{18}\text{O}$  calculated from quartz-water O isotope fractionation at the plagioclase-muscovite Na-K exchange temperature,  $10.7 \pm 0.7\%$   $\delta^{18}\text{O}$  calculated from quartz-muscovite O isotope fractionation,  $-23 \pm 8\%$   $\delta D$  calculated from muscovite-water H isotope fractionation at the plagioclase-muscovite Na-K exchange temperature, and ca.  $10\%$   $\delta^{34}\text{S}$  assuming negligible pyrrhotite-water S isotope fractionation. The isotopic composition of the late (stage III) vein-forming fluid at Hog Mountain (Table 1; Figs. 2-4) is  $7.6 \pm 1.2\%$   $\delta^{18}\text{O}$  calculated from quartz-calcite O isotope fractionation,  $-22 \pm 9\%$   $\delta D$  calculated from muscovite-water H isotope fractionation at the plagioclase-muscovite Na-K exchange temperature,  $-5.9 \pm 1.3\%$   $\delta^{13}\text{C}$  calculated from calcite-water C isotope fractionation at the quartz-calcite O temperature, and ca.  $9\%$   $\delta^{34}\text{S}$  assuming negligible pyrrhotite-water S isotope fractionation.

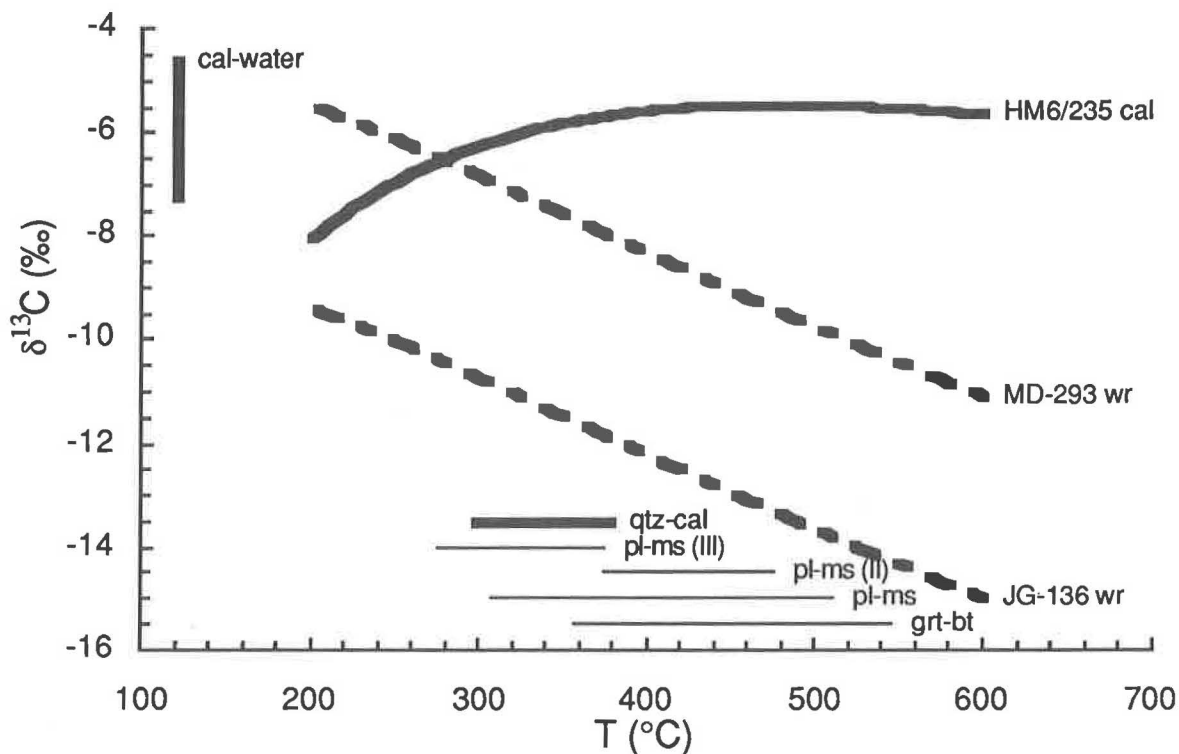


Figure 4. Calculated  $\delta^{13}\text{C}$  value of aqueous fluid in equilibrium with a calcite (solid line) mineral separate from the Hog Mountain mine (Table 1). Also shown is the graphite- $\text{CO}_2$  fractionation curve for graphite-rich (MD-293: 9.1% C, -19.9‰  $\delta^{13}\text{C}$ ) and normal graphitic phyllite (JG-136: 0.8% C, -23.8‰  $\delta^{13}\text{C}$ ) from the Wedowee Group (Wesolowski et al., 1987). Temperature ranges as in Figure 2.

The isotopic composition of the vein-forming fluid in the Goldville district (Table 2; Figs. 5-6) is 10.2-13.2‰  $\delta^{18}\text{O}$  calculated from quartz-plagioclase (3 pairs) and quartz-biotite O isotope fractionation,  $-48 \pm 2\%$   $\delta\text{D}$  calculated from biotite-water H isotope fractionation at the quartz-biotite O temperature,  $-50 \pm 1\%$   $\delta\text{D}$  calculated from chlorite-water H isotope fractionation at the quartz-chlorite O temperature, and ca. 19‰  $\delta^{34}\text{S}$  assuming negligible pyrrhotite-water S isotope fractionation. The isotopic composition of the late-stage fluid (Table 2; Figs. 5-6), calculated from quartz-chlorite O isotope fractionation is  $9.4 \pm 0.4\%$   $\delta^{18}\text{O}$ .

## DISCUSSION

### Hog Mountain Tonalite

All tonalites exhibit incipient alteration: sericitization of plagioclase and introduction of hydrothermal quartz. As quartz is markedly enriched in  $^{18}\text{O}$  relative to most other rock-forming silicates (see summaries by O'Neil, 1986 and Kyser, 1987), silicification would systematically increase  $\delta^{18}\text{O}$  values of altered tonalites. Thus, unaltered tonalites were probably characterized by slightly lower values, of the order of 9-10‰  $\delta^{18}\text{O}$ , similar to those of other pre- and syn-kinematic granitoids in the northern Alabama Piedmont (Wesolowski et al., 1987).

The strongly positive S isotopic values of least-altered tonalites (10-11‰  $\delta^{34}\text{S}$ ) are clearly non-mantle ( $0 \pm 1\%$ ; Ohmoto, 1986) and may reflect incorporation of sedimentary S during generation and/or emplacement, but pervasive incipient alteration of the tonalite and the low abundance of S in the least-altered rocks (<0.3%; Green and Lesher, 1988) preclude a unique interpretation.

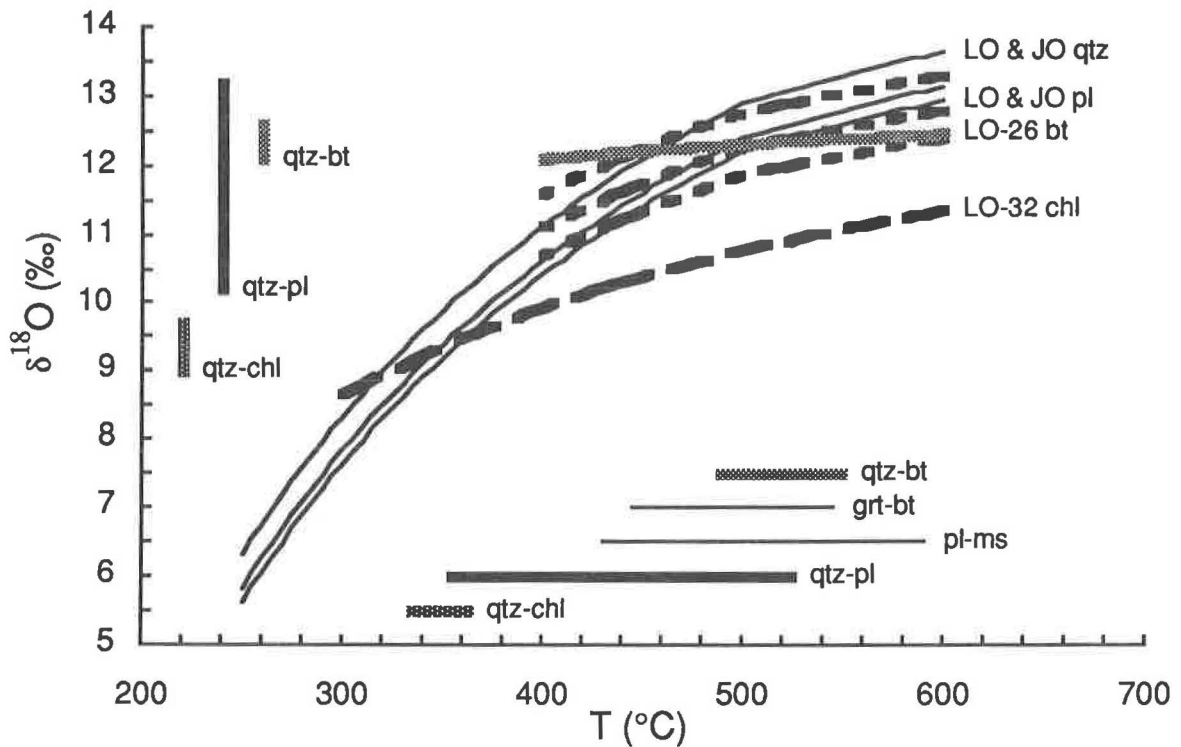


Figure 5. Calculated  $\delta^{18}\text{O}$  values of aqueous fluids in equilibrium with quartz (thin solid lines), plagioclase (dashed lines), biotite (stippled line), and chlorite (thick solid line) mineral separates from the Lowe mine and Jones vein (Table 1). Also shown are temperature ranges calculated from quartz-plagioclase, quartz-biotite, and quartz-chlorite O isotope fractionation, garnet-biotite Fe-Mg exchange thermometry, and plagioclase-muscovite Na-K exchange thermometry.

### Vein Emplacement

The restrictive association of gold mineralization with structurally-controlled veins, their transgressive relationship to stratigraphy, and thermobarometric data all indicate that the present distribution of gold is a result of metamorphism during progressive D<sub>1</sub>-D<sub>2</sub> deformation. Temperatures of O isotopic equilibration in veins and alteration selvages at Hog Mountain ( $475 \pm 45^\circ\text{C}$  for qtz-ms and  $335 \pm 40^\circ\text{C}$  for qtz-cal) correspond very closely to temperatures calculated using plagioclase-muscovite Na-K exchange thermometry (Leshner and Green, 1987 and unpubl. data) and to maximum inferred trapping temperatures of fluid inclusions in vein quartz (Sha and Leshner, this volume). These temperatures are similar to slightly lower than estimates of peak metamorphism in the pluton ( $460 \pm 50^\circ\text{C}$  and  $4.5 \pm 1\text{kb}$ ; Leshner and Green, 1987 and unpubl. data), indicating that vein emplacement occurred during or slightly after the metamorphic peak, consistent with observed field relationships. The discordant D and O isotopic fractionation between quartz, muscovite, and calcite at Hog Mountain (Table 1) suggests that O in quartz and muscovite records the temperature (and fluid composition) during initial alteration, whereas H in muscovite and O in calcite record conditions at lower temperatures.

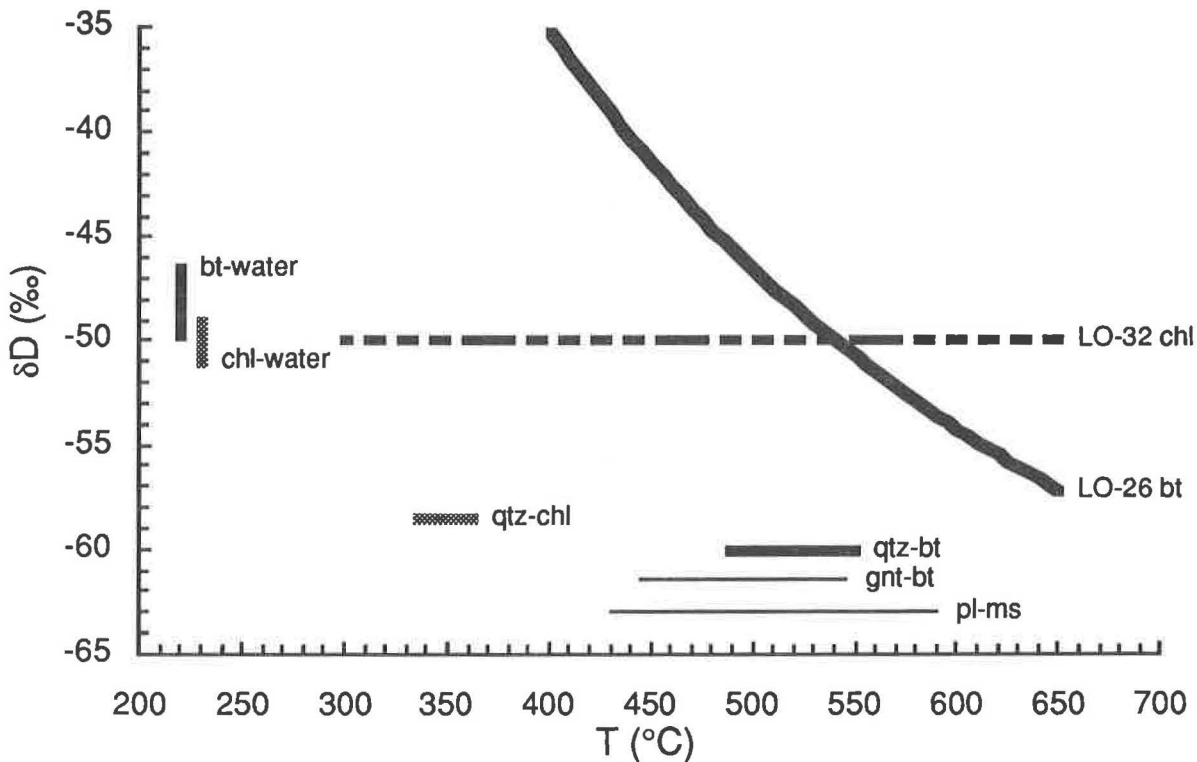
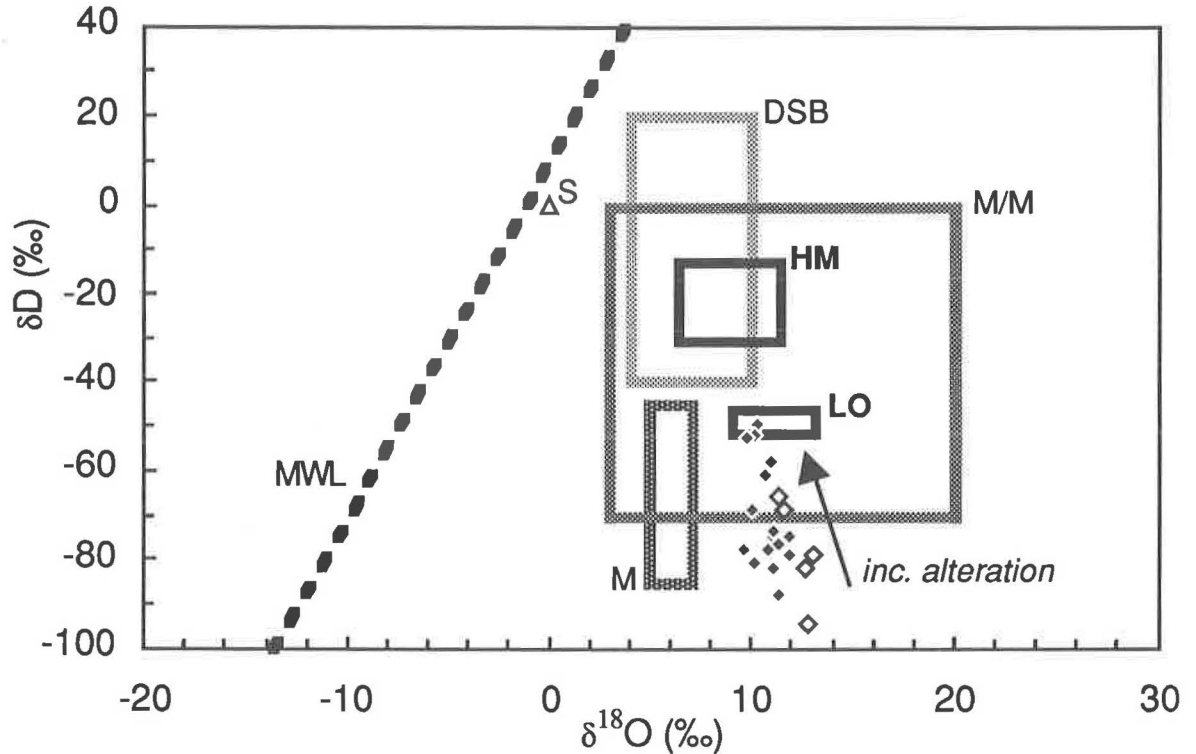


Figure 6. Calculated  $\delta D$  values of aqueous fluids in equilibrium with biotite (solid line) and chlorite (dashed line) mineral separates from the Lowe mine. Temperature ranges as in Figure 5.

Temperatures of O isotopic equilibration at Goldville (550-340°C for qtz-pl,  $520 \pm 30^\circ\text{C}$  for qtz-bt, and  $350 \pm 15^\circ\text{C}$  for qtz-chl) overlap the  $490 \pm 50^\circ\text{C}$  and  $510 \pm 80^\circ\text{C}$  temperatures calculated by Stowell et al. (in press) and Stowell and Lesher (this volume) using garnet-biotite Fe-Mg and plagioclase-muscovite Na-K exchange thermometry, respectively, and are consistent with the P-V-T-X properties of fluid inclusions in vein quartz (Sha and Lesher, this volume). The garnet-biotite, quartz-biotite, and quartz-plagioclase temperatures calculated from vein minerals and vein selvages are identical, within errors, to prograde metamorphic temperatures determined in the country rocks. These data and prograde zoning of garnet grains indicates that the veins were emplaced during peak metamorphism. The quartz-chlorite temperatures probably reflect retrograde metamorphic conditions; the differences (plagioclase  $\approx$  biotite  $>$  chlorite) are consistent with observed paragenetic relationships.

### Hydrothermal Alteration

The systematic enrichment of D in altered tonalites at Hog Mountain and altered pelites at Goldville reflects selective incorporation of D into phyllosilicates during alteration. At the calculated temperatures of vein formation, muscovite is enriched in D relative to biotite by ca. 20‰ (relatively temperature independent) and chlorite is enriched in D relative to biotite by ca. 15-30‰ (strongly temperature dependent) (Suzuoki and Epstein, 1976; Graham et al., 1987). These enrichments are consistent both in sense and magnitude with the observed positive H isotopic shifts in the altered rocks. At Hog Mountain,  $\delta D$  values of strongly-altered decussate-textured tonalites (-50 and -53‰) and the corresponding calculated muscovite (-49‰) are higher than those of strongly-altered foliated rocks (-58 and -62‰) and a corresponding muscovite separate (-63‰), suggesting that the latter re-equilibrated with the fluid at lower temperatures during post-emplacement deformation.



**Figure 7.** Plot of  $\delta D$  vs.  $\delta^{18}O$  showing whole-rock isotopic compositions of least-altered and altered Hog Mountain tonalites (solid diamonds) and Wedowee metapelites (open diamonds) and calculated compositional fields of veins-forming fluids at the Hog Mountain mine (HM) and the Lowe mine (LO), compared to calculated compositional fields of deep sedimentary brines (DSB), metamorphic fluids (M/M), magmatic fluids (M), meteoric waters (MWL), and standard mean ocean water (S) (Sheppard, 1986).

As noted above, incipient sericitization and silicification are probably responsible for the minor dispersion in  $\delta^{18}O$  values of least-altered tonalites (Fig. 7). At the calculated temperatures of vein formation, muscovite is depleted in  $^{18}O$  relative to quartz by 2-3‰, depleted relative to plagioclase by 1-2‰, and enriched relative to biotite by 3-4‰ (O'Neil and Taylor, 1969; Matsuhisa et al., 1979; Bottinga and Javoy, 1975). The trend of slightly decreasing  $\delta^{18}O$  with increasing intensity of alteration is consistent with the original proportions of quartz, plagioclase, and biotite in the tonalite ( $pl > qtz > bt$ ), the small magnitudes of fractionation involved, and the offsetting directions of  $^{18}O$  enrichment ( $qtz > pl > ms > bt$ ) relative to alteration trends ( $pl \rightarrow ms + qtz$ ,  $bt \rightarrow ms$ ).

Although there are insufficient data to quantitatively model fluid-rock isotopic fractionation during alteration, the trends of D enrichment and  $^{18}O$  depletion with increasing degree of alteration of tonalites at the Hog Mountain mine and metapelites at the Lowe mine are similar and are consistent with alteration by fluids of compositions calculated independently from the isotopic compositions of mineral separates (Fig. 7). For example, least-altered tonalites (solid diamonds: ca. -80‰  $\delta D$  and 10‰  $\delta^{18}O$ ) would be in H and O isotopic equilibrium with magmatic fluids (ca. -50‰  $\delta D$  and 8‰  $\delta^{18}O$ ) at granite solidus temperatures, whereas strongly-altered tonalites (solid diamonds: ca. -50‰  $\delta D$  and 10‰  $\delta^{18}O$ ) would be in isotopic equilibrium with calculated vein-forming fluids (HM) at metamorphic temperatures. At the same temperatures, least-altered

metapelites (open diamonds: ca. -90‰  $\delta D$  and 13‰  $\delta^{18}O$ ) would be in H and O isotopic equilibrium with metamorphic fluids (M/M: ca. -70‰  $\delta D$  and 11‰  $\delta^{18}O$ ), whereas strongly-altered metapelites (open diamonds: ca. -70‰  $\delta D$  and 11‰  $\delta^{18}O$ ) would be in isotopic equilibrium with calculated vein-forming fluids (LO). At lower (diagenetic) temperatures, the metapelites would be in isotopic equilibrium with deep sedimentary brines (DSB).

The correspondence between rock alteration trends and fluid compositions calculated from vein mineral separates indicates that the same fluids from which vein minerals crystallized were also responsible for alteration of the country rocks and introduction of gold.

### Fluid Source

The presence of vein-associated alteration at Hog Mountain and Goldville indicates that the vein-forming fluids were not in chemical or isotopic equilibrium with the country rocks and could not have been derived locally by "lateral secretion." This is supported by Sr isotopic data at Hog Mountain which preclude derivation from Wedowee metapelites. Strontium isotopes do not fractionate, so the  $^{87}Sr/^{86}Sr$  ratio of the fluid will be equal to that of the  $0.7061 \pm 0.0012$  initial  $^{87}Sr/^{86}Sr$  ratio of the hydrothermal alteration zone (Green et al., 1988). This value is significantly less radiogenic than average Wedowee Group metapelites which exhibit initial  $^{87}Sr/^{86}Sr =$  ca. 0.715 (Russell, 1978), but more radiogenic than the least-altered tonalites ( $^{87}Sr/^{86}Sr_{initial} =$  0.7050: N.L.G., C.M.L., and A.K. Sinha, unpubl. data).

The limited C isotopic data are equivocal. Although the calcite at Hog Mountain could have been in C isotopic equilibrium with the most C-rich graphitic phyllonite analyzed by Wesolowski et al. (1987), most Wedowee metapelites exhibit more negative  $\delta^{13}C$  values (down to -26.5‰) and could not have been in equilibrium with the fluids that equilibrated with the calcite.

The vein-forming fluid at Hog Mountain was characterized by 7 to 11‰  $\delta^{18}O$ , -15 to -31‰  $\delta D$ , -5 to -7‰  $\delta^{13}C$ , and ca. 9‰  $\delta^{34}S$ , whereas the vein-forming fluid at Goldville was characterized by 9 to 13‰  $\delta^{18}O$ , -44 to -48‰  $\delta D$ , ca. 19‰  $\delta^{34}S$ . The H and O isotopic composition of the Hog Mountain fluid is similar to that of deep sedimentary brines or metamorphic fluids, but is markedly different from seawater, meteoric waters, or magmatic fluids (Fig. 7). The Goldville fluid is also within the field of metamorphic fluids, but is significantly depleted in D and enriched in  $^{34}S$  relative to the Hog Mountain vein-forming fluid. Although these fluids fall within the range that might form by mixing of metamorphic fluids and meteoric waters, the alteration trends do not define mixing lines between such fluids. The positive S isotopic signatures of the fluids are also consistent with an oxidized, nonmagmatic, probable metasedimentary source for the S (see Ohmoto, 1986).

The vein-forming fluid at Hog Mountain was enriched in D, Rb, K, Ba, Fe, W, S, and Au, and the vein-forming fluid at Goldville was enriched in D, Rb, K, Ba, Mg, Fe, Al, and Au. All these elements are enriched in pelitic sedimentary rocks and could be mobilized during metamorphism. As such, vein-forming fluids were most likely derived from deeper parts of the metamorphic pile, metasediments of the Ashland-Wedowee belt underlying the Goldville-Hog Mountain area, metasediments of underlying thrust sheets, and/or metasediments of the underlying North American continental shelf (Green et al., 1988), and ascended along permeable zones that developed during deformation.

### CONCLUSIONS

Auriferous quartz veins in the central part of the Ashland-Wedowee belt were emplaced after the initiation of deformation and during to slightly after peak metamorphism. Temperatures of O isotopic equilibration at Hog Mountain are  $475 \pm 45^\circ C$  for quartz-muscovite and  $335 \pm 40^\circ C$  for quartz-calcite, consistent with  $425 \pm 50$  and  $325 \pm 50^\circ C$  temperatures obtained by plagioclase-muscovite Na-K exchange thermometry for type II and type III veins, respectively. Temperatures of O isotopic equilibration at Goldville are  $550-340^\circ C$  for quartz-plagioclase,  $520 \pm 30^\circ C$  for quartz-biotite, and  $350 \pm 15^\circ C$  for quartz-chlorite, consistent with  $490 \pm 50^\circ C$  temperatures obtained by garnet-biotite Mg-Fe exchange thermometry and  $510 \pm 80^\circ C$  temperature obtained by plagioclase-muscovite Na-K exchange thermometry. Discordant D and O isotopic fractionation between

quartz, muscovite, and calcite at Hog Mountain suggests that O in quartz and muscovite records the temperature (and fluid composition) during initial alteration, whereas H in muscovite and O in calcite record conditions at lower temperatures.

The presence of alteration envelopes adjacent to mineralized veins at the Hog Mountain deposit and at deposits in the Goldville district indicates that the country rocks in both areas were not in equilibrium with vein-forming fluids and could not have been derived locally, negating models involving local mobilization ("lateral secretion") of syngenetic gold into quartz veins during metamorphism. Altered tonalites at Hog Mountain and altered metapelites at Goldville are markedly enriched in D relative to least-altered equivalents, reflecting selective incorporation of D in phyllosilicates. Altered metapelites at Goldville are also depleted in  $^{18}\text{O}$ , reflecting exclusion by phyllosilicates.

The vein-forming fluid at Hog Mountain was characterized by 7 to 11‰  $\delta^{18}\text{O}$ , -15 to -31‰  $\delta\text{D}$ , -5 to -7‰  $\delta^{13}\text{C}$ , and ca. 9‰  $\delta^{34}\text{S}$ , whereas the vein-forming fluid at Goldville was characterized by 9 to 13‰  $\delta^{18}\text{O}$ , -46 to -51‰  $\delta\text{D}$ , and ca. 19‰  $\delta^{34}\text{S}$ . The H and O isotopic compositions of such fluids are similar to those of basinal brines or metamorphic fluids, but are markedly different from seawater, meteoric waters, or magmatic fluids. The stable isotopic data, together with field, petrographic, microthermometric, and geochemical data, suggest that vein-forming fluids in both areas equilibrated to varying degrees with, and were probably derived from, pelitic metasedimentary rocks, but were not derived from adjacent country rocks. Mineralizing fluids were most likely derived from underlying thrust sheets and/or the underlying North American continental shelf.

#### ACKNOWLEDGEMENTS

We are grateful to Newmont Exploration Ltd. and U.S. Borax for donating diamond drill core to the University of Alabama and the Geological Survey of Alabama and for providing copies of unpublished drill logs, maps, and reports; to Russell Lands Inc. for access to the deposits; to Joe Thacker and Peng Sha for performing mineral separations; to Ed Ripley for performing the stable isotope analyses; and to Mark Drummond for his insightful comments on the manuscript.

We have benefitted greatly from discussions with many colleagues, especially Bob Cook and Greg Guthrie. Our research on gold deposits in Alabama has been supported by the University of Alabama Research Grants Committee (grant nos. 1340 to C.M.L., 1345 to N.L.G., and 1370 to H.H.S.) and School of Mines and Energy Development (grant nos. 2-29107 to N.L.G. and C.M.L., and 2-29115 to C.M.L., N.L.G., and H.H.S.).

#### REFERENCES

- Bottinga, Y., 1969, Calculated fractionation factors for carbon and hydrogen isotope exchange in the system calcite-carbon dioxide-graphite-methane-hydrogen-water vapor: *Geochimica et Cosmochimica Acta*, v. 33, p. 49-64.
- Bottinga, Y., and Javoy, M., 1975, Oxygen isotope partitioning among the minerals in igneous and metamorphic rocks: *Reviews in Geophysics and Space Physics*, v. 13, p. 401-418.
- Clayton, R.N., and Mayeda, T.K., 1963, The use of bromine pentafluoride in the extraction of oxygen from oxides and silicates for isotopic analysis: *Geochimica et Cosmochimica Acta*, v. 27, p. 43-52.
- Cole, D.R., and Ohmoto, H., 1986, Kinetics of isotopic exchange at elevated temperatures and pressures, in Valley, J.W., Taylor, H.P., and O'Neil, J.R. (editors), Stable Isotopes in High Temperature Geological Processes: Mineralogical Society of America, *Reviews in Mineralogy*, v. 16, p. 41-87.
- Fritz, P., Drimmie, R.J., and Nowickie, V.K., 1974, Preparation of sulfur dioxide for mass spectrometer analysis by combustion of sulfides with copper oxide: *Analytical Chemistry*, v. 76, p. 164.

- Graham, C.M., Viglino, J., and Harmon, R.S., 1987, Experimental study of hydrogen isotope exchange between aluminous chlorite and water and of hydrogen diffusion in chlorite: *American Mineralogist*, v. 72, p. 566-579.
- Green, N.L., and Leshner, C.M., 1987, Mineralogy and geochemistry of the Hog Mountain pluton, Northern Alabama Piedmont, in M.S. Drummond, N.L. Green, and M.J. Neilson (editors), The Granites of Alabama: Alabama Geological Society, 24th Annual Field Trip Guidebook, p. 1-12.
- Green, N.L., and Leshner, C.M., 1988, Geology of the Hog Mountain tonalite and associated lode gold deposits, northern Alabama Piedmont: University of Alabama School of Mines and Energy Development Faculty Research Report 88, 42 p.
- Green, N.L., Sinha, A.K., and Leshner, C.M., 1988, Gold associated with retrograded shear zones: An Alleghanian episode of mineralization in the southern Appalachians: Geological Society of America, Annual Meeting, Abstracts with Programs, v. 21, no. 7, p. A277.
- Guthrie, G.M., and Dean, L.S., 1989, Geology of the New Site 7.5-Minute Quadrangle, Tallapoosa and Clay Counties, Alabama: Alabama Geological Survey Quadrangle Map 9, 41 p.
- Guthrie, G.M., and Leshner, C.M., 1988, Structural and metamorphic controls on lode gold mineralization, Tallapoosa County, Alabama: Geological Society of America, Southeastern Section Meeting, Abstracts with Programs, v. 20, no. 4, p. 268.
- Guthrie, G.M., and Leshner, C.M., in press, Stratigraphic, metamorphic, and structural settings of lode gold deposits in the northern Alabama Piedmont, in Leshner, C.M., Cook, R.B., and Dean, L.S. (editors), Gold Deposits of Alabama: Geological Survey of Alabama Bulletin 136, p. 11-32.
- Kendall, C., and Coplen, T.B., 1982, Multisample conversion of water to hydrogen by Zn for stable isotope determination: *Analytical Chemistry*, v. 57, p. 1437-1440.
- Kyser, T.K., 1987, Equilibrium fractionation factors for stable isotopes, in Kyser, T.K. (editor), Stable Isotope Geochemistry of Low Temperature Fluids: Mineralogical Association of Canada, Short Course, v. 13, p. 1-84.
- Leshner, C.M., and Green, N.L., 1988, Syn-metamorphic hydrothermal alteration, Hog Mountain gold deposit, Northern Alabama Piedmont. Geological Society of America, Southeastern Section Meeting, Abstracts with Programs, v. 20, no. 4, p. 277.
- Leshner, C.M., and Green, N.L., 1987, Alteration and gold mineralization, Hog Mountain pluton, Northern Alabama Piedmont, in M.S. Drummond, N.L. Green, and M.J. Neilson (editors), The Granites of Alabama, 24th Annual Field Trip Guidebook, Alabama Geological Society, p. 13-22.
- Matsuhisa, Y., Goldsmith, J.R., and Clayton, R.N., 1979, Oxygen isotope fractionation in the system quartz-albite-anorthite-water: *Geochimica et Cosmochimica Acta*, v. 43, p. 1131-1140.
- McConnell, K.I., Abrams, C.E., and German, J.M., 1986, Gold deposits in the Northern Piedmont of Georgia and Alabama and their relationship to lithostratigraphic units, in Misra, K.C. (editor), Volcanogenic Sulfide and Precious Metal Mineralization in the Southern Appalachians: University of Tennessee, Department of Geological Sciences, Studies in Geology 16, p. 164-181.
- Neal, W.L., 1986, Geochemical relationships between gold, silver, antimony, arsenic, and bismuth in gold mineralization of the Goldville District, Tallapoosa County, Alabama: Auburn University, unpublished M.S. thesis, 151 p.

- Neal, W.L., and Cook, R.B., in press, Mineralogy, petrology, and geochemistry of phyllite-hosted gold deposits, Goldville district, Tallapoosa, Alabama, *in* Leshner, C.M., Cook, R.B., and Dean, L.S. (editors), Gold Deposits of Alabama: Geological Survey of Alabama Bulletin 136, p. 101-114.
- Neal, W.L., Cook, R.B., and Paris, T.A., in press, Gold and related trace metal geochemistry at the Tallapoosa and Lowe mines, Goldville district, Tallapoosa County, Alabama, *in* Leshner, C.M., Cook, R.B., and Dean, L.S. (editors), Gold Deposits of Alabama: Geological Survey of Alabama Bulletin 136, p. 115-132.
- Neathery, T.L., and Reynolds, J.W., 1973, Stratigraphy and metamorphism of the Wedowee group: a reconnaissance: *American Journal of Science*, v. 273, p. 723-741.
- Ohmoto, H., 1986, Stable isotope geochemistry of ore deposits, *in* Valley, J.W., Taylor, H.P., Jr., and O'Neil, J.R. (editors), Stable Isotopes in High Temperature Geological Processes: Mineralogical Society of America, Reviews in Mineralogy, v. 16, p. 491-559.
- O'Neil, J.R., 1986, Theoretical and experimental aspects of isotope fractionation, *in* Valley, J.W., Taylor, H.P., Jr., and O'Neil, J.R. (editors), Stable Isotopes in High Temperature Geological Processes: Mineralogical Society of America, Reviews in Mineralogy, v. 16, p.1-40.
- O'Neil, J.R., and Taylor, H.P., Jr., 1969, Oxygen isotope equilibrium between muscovite and water: *Journal of Geophysical Research*, v. 74, p. 6012-6022.
- O'Neil, J.R., Clayton, R.N., and Mayeda, T.K., 1969, Oxygen isotope fractionation in divalent metal carbonates: *Journal of Chemical Physics*, v. 51, p. 5547-5558.
- Pardee, J.T., and Park, C.F., Jr., 1948, Gold deposits of the southern Piedmont: U.S. Geological Survey Professional Paper 213, 156 p.
- Paris, T.A., 1986, The Goldville project: Results of an exploration project for gold in the northern Alabama Piedmont, *in* Misra, K.C. (editor), Volcanogenic Sulfide and Precious Metal Mineralization in the Southern Appalachians: University of Tennessee, Department of Geological Sciences, Studies in Geology 16, p. 185-205.
- Park, C.F., Jr., 1935, Hog mountain gold district, Alabama: American Institute of Mining and Metallurgical Engineers Transactions, Mining Geology, v. 115, p. 209-228.
- Rosenbaum, J. and Sheppard, S.M.S., 1986, An isotopic study of siderites, dolomites, and ankerites at high temperatures. *Geochimica et Cosmochimica Acta*, v. 50, p. 1147-1150.
- Russell, G.S., 1978, U-Pb, Rb-Sr, and K-Ar isotope studies bearing on the tectonic development of the southernmost Appalachian orogen, Alabama: Florida State University, unpublished Ph.D. dissertation, 197 p.
- Sha, P., and Leshner, C.M., this volume, Microthermometry of fluid inclusions in auriferous quartz veins, Hog Mountain-Goldville district, northern Alabama Piedmont, *in* Cook, R.B. (editor), Economic Mineral Deposits of the Southern Appalachians: Metallic Ore Deposits: Georgia Geologic Survey Bulletin 117.
- Sheppard, S.M.F., 1986, Characterization and isotopic variation in natural waters, *in* Valley, J.W., Taylor, H.P., Jr., and O'Neil, J.R. (editors), Stable isotopes in High Temperature Geological Processes: Mineralogical Society of America, Reviews in Mineralogy, v. 16, p. 165-183.
- Stowell, H.H., and Leshner, C.M., this volume, Thermobarometry of synmetamorphic gold deposits, Goldville district, Northern Piedmont, Alabama, *in* Cook, R.B. (editor), Economic

Mineral Deposits of the Southern Appalachians: Metallic Ore Deposits: Georgia Geologic Survey Bulletin 117.

- Stowell, H.H., Guthrie, G.M., and Leshner, C.M., 1989, Metamorphism and gold mineralization in the Wedowee Group, Goldville district, Northern Alabama Piedmont, *in* Leshner, C.M., Cook, R.B., and Dean, L.S. (editors), Gold Deposits of Alabama: Geological Survey of Alabama Bulletin 136, p. 133-158.
- Suzuoki, T., and Epstein, S., 1976, Hydrogen isotope fractionation between OH-bearing minerals and water: *Geochimica et Cosmochimica Acta*, v. 40, p. 1229-1240.
- Tull, J.F., 1978, Structural development of the Alabama Piedmont northwest of the Brevard zone: *American Journal of Science*, v. 278, p. 442-460.
- Wenner, D.B., and Taylor, H.P., Jr., 1971, Temperatures of serpentinization of ultramafic rocks based on  $^{18}\text{O}/^{16}\text{O}$  fractionation between co-existing serpentine and magnetite: *Contributions to Mineralogy and Petrology*, v. 32, p. 165-185.
- Wesolowski, D., Drummond, M.S., and Gomolka, J., 1987, Oxygen and carbon isotope distributions in granitoids and metasediments of the Rockford district and adjacent portions of the northern Alabama Piedmont and Inner Piedmont, *in* Drummond, M.S., and Green, N.L. (editors), Granites of Alabama: Geological Survey of Alabama, p. 221-238.

THE ROYAL VINDICATOR GOLD DEPOSIT, HARALSON COUNTY, GEORGIA:  
A METAMORPHOSED EPITHERMAL HOT-SPRINGS TYPE GOLD DEPOSIT

Travis A. Paris  
Consulting Geologist  
5604 Malmsbury Road, Knoxville, TN 37921-3827

ABSTRACT

The Royal Vindicator gold deposit occurs in the northern Piedmont of western Georgia near the boundary between the Talladega Group and the Wedowee Group. The deposit is hosted in the lower part of an alternating sequence of felsic and mafic metavolcanics interpreted to be equivalent to the Hillabee Greenstone. Regional strike of foliation/bedding at the deposit is approximately east-west, dipping  $15^{\circ}$ - $20^{\circ}$  to the south. The overlying Wedowee Group is in gradational contact with the underlying Hillabee metavolcanics, not in fault contact as is common in Alabama and as suggested by Heuler and Tull (1989).

The gold ores consist of strata-bound pyritic, siliceous bodies hosted in altered felsic metavolcanics. Gold particles observed in reflected light microscopy range from 0.0005 mm to 2.0 mm in longest dimension; and occur in four different habits: (1) discrete ovoid to ragged particles of native gold; (2) ovoid to ragged gold grains within and on pyrite grains; (3) composite grains of gold associated with highly reflective, silvery white and duller gray, unidentified minerals; and (4) subhedral grains intergrown with magnetite or hematite. Geochemical analyses of the ore bodies reveal a strong positive correlation of gold with silver and molybdenum and a subtle correlation with mercury, arsenic, copper, and lead.

The gold mineralization is interpreted to have been deposited synchronously with felsic tuffs along the flanks of shallow, elongate basins by a volcanic hot springs system. The hot springs solutions formed siliceous sinters, altering and replacing tuffs as they were being deposited. During the Devonian-aged Acadian(?) orogeny the deposit was metamorphosed to the biotite zone and possibly the garnet zone of the greenschist facies and deformed. Altered tuffs are now siliceous, auriferous, pyritic magnetite-sericite-quartz schists. The metasinters are now fine-grained, alternating layers of auriferous quartz and pyrite, oriented parallel to bedding/foliation. These auriferous horizons contrast with barren milky quartz veins which both parallel and cut across bedding/foliation.

## INTRODUCTION

This paper describes the geology of the Royal Vindicator gold deposit and presents data on the geologic setting, geochemistry of ore and country rocks, modes of gold occurrence and distribution, and interpretation of the origin of the deposit.

## LOCATION

The Royal Vindicator gold mine is a former gold producer currently being reevaluated by industry concerns. It is located in southwestern Haralson County, Georgia, approximately 5 km east of the Georgia-Alabama state line, and 4.8 km south of the town of Tallapoosa (fig. 1). The countryside surrounding the site is comprised of small farms and timberlands.

## PRODUCTION HISTORY

The exact point in time at which gold was discovered at the Royal Vindicator deposit is obscure. Yeates and others (1896) reported that gold was originally discovered at the site by a farmer named Owens around 1840. More recently, however, Reeves (1975) reported that gold may have been discovered at the site as early as 1829. Shearer (1917) noted that the deposit was being operated as the Hollins (Holland) mine in 1834. The deposit was operated as a successful placer and saprolite mine with minor production from shallow shafts from the time of its discovery until the Civil War (Yeates and others, 1896; Shearer, 1917). Production after the war was sporadic with various operators depleting the surface deposits and switching to underground methods. These later mining attempts lasted for only a few years at a time because of poor economics resulting from the low recovery of gold from increasingly sulfidic ores. During one such period, beginning in 1887, the deposit was known as the Camille mine (Yeates and others, 1896; Shearer, 1917). In 1896 the deposit was purchased by the Royal Gold Mining Company which erected a concentrating mill, roasting furnace, and chlorination (modified Thies) plant for treating the sulfidic ores (Yeates and others, 1896; Lane, 1900; Jones, 1909). This milling operation was also unsuccessful in obtaining an economic recovery of gold from the ores.

Underground mining prior to 1900 was through inclined shafts, but by 1910 a vertical shaft had been sunk to 155 feet (47.2 m). The mine was last worked through this shaft from 1914 to 1917 by the Royal Vindicator Mines Company before finally closing permanently (Shearer, 1917; Ruhl, 1917; Reeves, 1975). The mine was dewatered, sampled, and evaluated with two core holes in the mid-1930's. This effort resulted in no renewed production (Maillot, 1940).

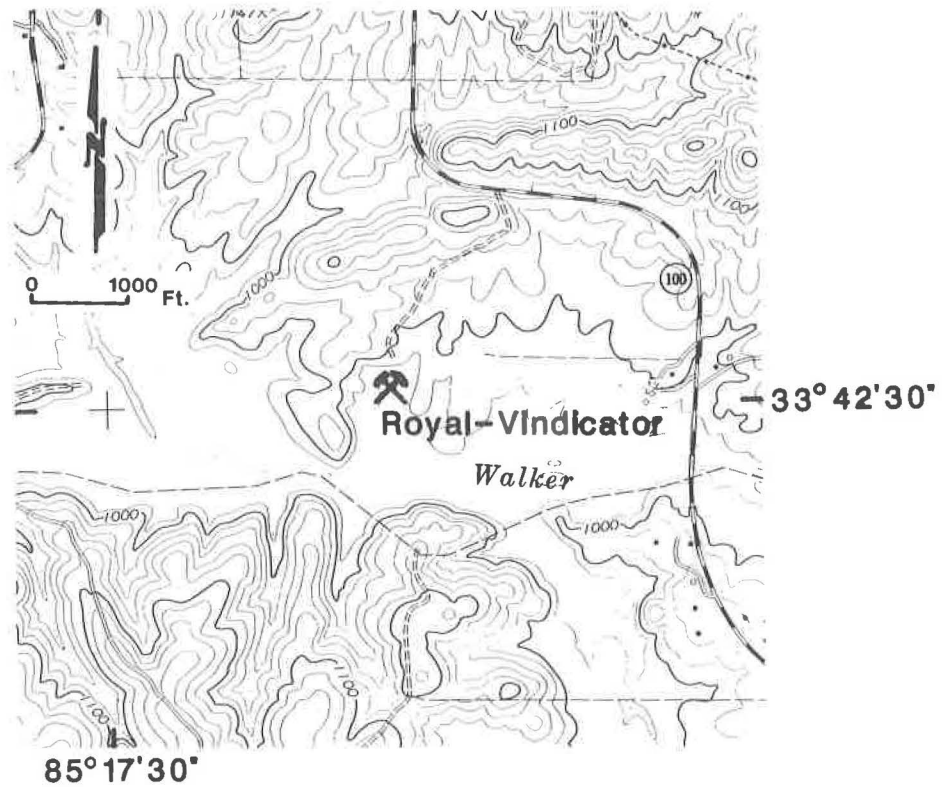


Figure 1. Location of the Royal Vindicator gold deposit, Tallapoosa County, Georgia. Map base taken from the Tallapoosa, Georgia, 7.5-minute quadrangle. Contour interval is 20 feet.

The most recent exploration of the deposit began in late 1979. U.S. Borax conducted regional reconnaissance and detailed geologic mapping of the mine region followed by soil and stream sediment geochemistry, ground magnetic and VLF-EM surveys, and core and reverse circulation drilling. In 1987 the prospect was acquired by a joint venture between Atlantic Goldfields, Inc., and Jascan Resources, Inc., who conducted further core and shallow auger drilling. The main shaft was also dewatered and reconditioned to allow mapping and channel sampling of the 105 foot (32 m) level workings. Exploration to the end of 1988 has identified approximately 75,000 tons of old tailings averaging 0.045 oz/tn gold and outlined south-southeast trending mineralized bodies containing approximately 350,000 tons grading 0.145 oz/tn gold.

Yeates and others (1896) and Jones (1909) reported that the Royal mine yielded approximately 5,000 ounces of gold from surficial and shallow underground workings. More recent studies, however, indicate as much as 40,000 ounces of gold with minor silver credits were produced from an estimated 250,000 tons of ore. This conclusion is based on the extent of surficial and underground workings, mine assays, and the volume and grade of tailings (West Georgia College, unpublished reports; Ruhl, 1917; Maillot, 1940).

#### PREVIOUS INVESTIGATIONS

The Royal Vindicator gold mine occurs in one of a group of greenstone and felsic gneiss units containing gold and copper mineralization which has historically been called the Dahlonga gold belt (Yeates and others, 1896; Jones, 1909). The structural and stratigraphic setting of the Royal Vindicator mine area has only recently been examined in greater detail and is still not well defined.

Hurst and Crawford (1969) located the Royal mine in an arcuate-shaped unit of chlorite schist and amphibolite flanked to the north by quartzite and phyllite of the Talladega Group and to the south by garnetiferous, graphitic mica schists of the Wedowee Group. They interpreted the gold bearing quartz and sulfide mineralization as the product of hydrothermal alteration along a shear zone.

Cressler (1970) indicated the greenstone outcrops along Georgia Highway 100 immediately east of the mine and in the Walker Creek valley are Hillabee Chlorite Schist (Hillabee Greenstone). The quartzite ridge 1 km north of the mine and forming Tally Mountain to the northeast was correlated with the Cheaha Sandstone Member of the Talladega Slate.

Neathery and Hollister (1984) show the Royal deposit is hosted in chlorite schist associated with other mineralized mafic units of the western Georgia Piedmont associated with

the Wedowee Group.

Geologists of the Georgia Geologic Survey have recently placed the Royal Vindicator deposit in various geologic units. While the majority of gold production in the Dahlonega gold belt occurred in the New Georgia Group (Abrams and McConnell, 1984; McConnell and Abrams, 1982, 1984; McConnell and others, 1986; and German, 1985), the Royal Vindicator and a number of other west Georgia gold deposits fall outside of this stratigraphic unit. Abrams and McConnell (1984), McConnell and Abrams (1984), and McConnell and others (1986) placed the Royal Vindicator in the stratigraphically younger Dog River Formation of the western Sandy Springs Group, which structurally overlies rocks of the Talladega Group to the northwest, and is separated from them by the Allatoona Fault.

More recently, German (1988) assigned the Royal-Vindicator deposit to an unnamed greenstone and quartzofeldspathic gneiss unit flanked to the north by the Talladega Group and to the south by the Andy Mountain Formation of the Sandy Springs Group (western belt). The presence of a fault separating the various units is not indicated, and German (1988; in press) correlates the greenstone unit with the Hillabee Greenstone, which is in gradational contact with underlying Talladega Group metasediments.

Heuler and Tull (1989) have extended the Hillabee Greenstone into Georgia. They conclude the arcuate chlorite schist unit in the deposit vicinity, as well as a linear chlorite schist unit between Tallapoosa and Buchanan, Georgia, is Hillabee Greenstone. The Jemison Chert and Butting Ram Sandstones of the Talladega Group metasediments are extended by Heuler and Tull (1989) into the mine area as the quartzite and phyllite units which underlie the prominent ridge north of the mine site and Tally Mountain to the northeast. Wedowee Group metasediments structurally overlie the Hillabee Greenstone and are separated from it by the Hollins Line Fault. However, Heuler and Tull (1989) place the Royal Vindicator gold deposit within a felsic schist unit contained in the Wedowee Group, not in the Hillabee Greenstone.

Paris (1986, 1989a) has recognized that the Royal Vindicator gold deposit is hosted by siliceous schist in a felsic metavolcanic unit interbedded with mafic and felsic metavolcanics which correlate stratigraphically and geochemically with the Hillabee Greenstone. This metavolcanic sequence is stratigraphically underlain by metasediments of the Talladega Group and stratigraphically overlain by metasediments of the Wedowee Group (Paris, 1986).

## STRATIGRAPHY

### Introduction

The Royal Vindicator mine area occupies predominantly forested uplands and some swamp areas which are deeply weathered and contain only scattered, small rock outcrops. Three major lithostratigraphic units crop out in the mine area - the Talladega Group, the Hillabee Greenstone, and the Wedowee Group. Gold mineralization of potential economic grade occurs within the upper part of a silicified, pyritized felsic unit in the lower part of the Hillabee Greenstone sequence.

### Talladega Group

The oldest lithostratigraphic unit in the mine area is the Talladega Group. Muscovite-quartz schist and phyllite intercalated with thin quartzite beds underlie the prominent ridge approximately 350 m north of the mine (fig. 2). These rocks are suggested to be correlative with the Jemison Chert and Butting Ram Sandstone sequence of the Talladega Group, in agreement with Heuler and Tull (1989).

Exploration drilling approached to within 5- to 10-m of the Hillabee Greenstone-Talladega Group contact but did not cut it. More recently, however, this stratigraphic contact has been penetrated by core drilling at the mine site by the Georgia Geologic Survey (German, in press), and confirms that mafic metavolcanics are in gradational contact with siliceous and calcareous metasediments of the Talladega Group. Similar contact relationships have been recognized in Alabama by Tull and others (1978), Tull and Stow (1980, 1982), and Paris (1989b).

### Wedowee Group

Bluffs and uplands south of the mine area and Walker Creek are underlain by rocks correlated with the Wedowee Group which structurally and stratigraphically (?) overlies the Hillabee Greenstone (fig. 2). In Georgia, rocks of the Wedowee Group are known as the Andy Mountain Formation of the Sandy Springs Group, western belt (Abrams and McConnell, 1981).

The Wedowee Group, as seen in both core and outcrop at the Royal Vindicator deposit, is comprised mainly of graphitic phyllite, sulfide-bearing chlorite-garnet-biotite-muscovite+graphite phyllite, and massive to locally micaceous quartzite. Also present are lesser amounts of biotite-chlorite+amphibole schist, garnetiferous quartzite, and milky quartz veins. These lithologies are similar to those reported for the Cragford Phyllite of the Wedowee Group in Alabama by Neathery and Reynolds (1975).

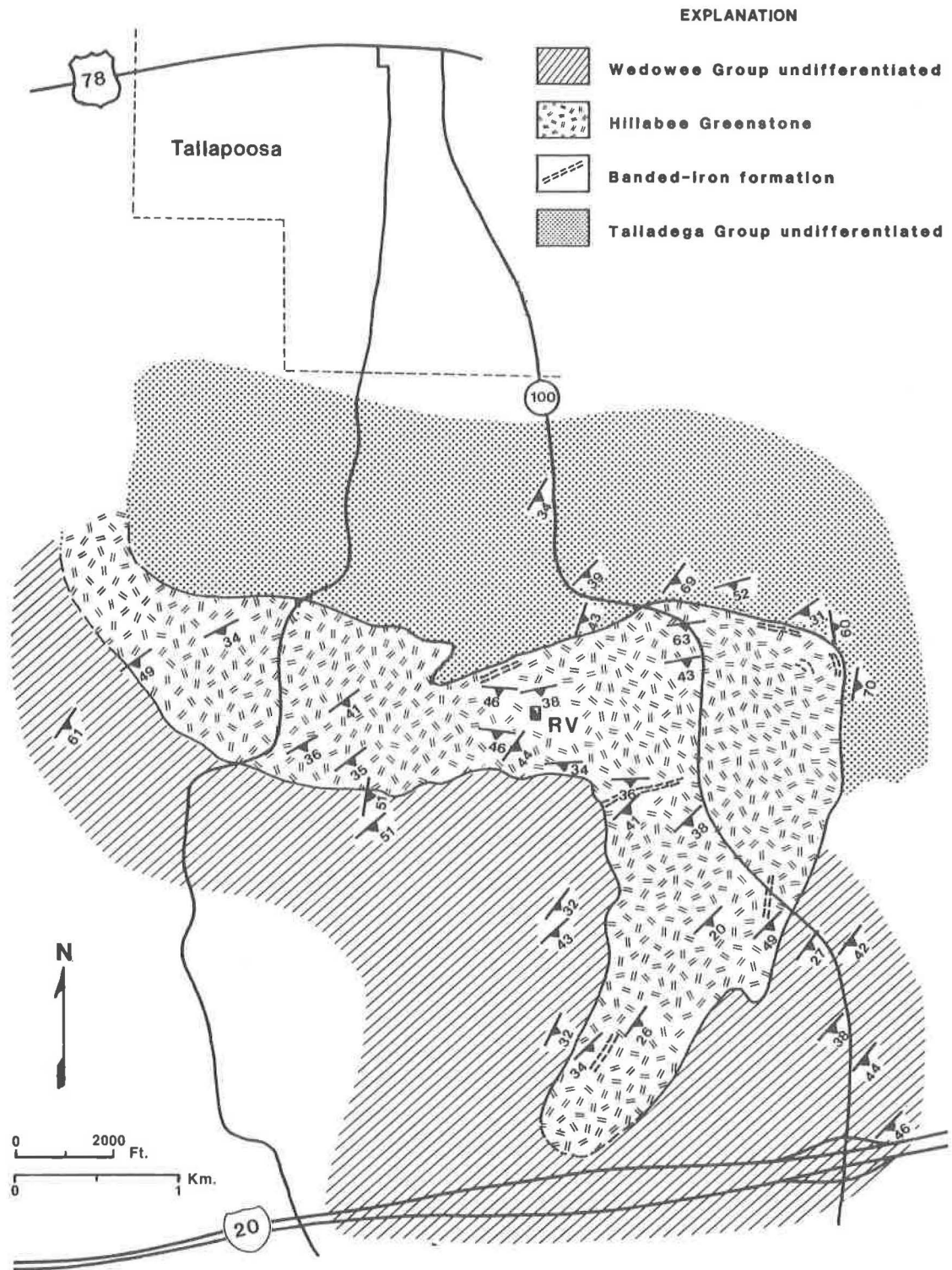


Figure 2. General geology of the Royal Vindicator gold deposit (RV) area, Tallapoosa County, Georgia.

Twelve core holes penetrate the contact of the Wedowee Group metasediments with the underlying Hillabee Greenstone metavolcanic sequence. No fault contact or shear zone appears to be present. The contact appears to be a gradational zone with Wedowee lithologies interbedded with those of the Hillabee. Additionally, a graphitic phyllite and quartzite unit up to 45 m thick which correlates well with the Wedowee Group lies roughly 70 m below the contact of and within the Hillabee Greenstone.

Sparse mineralization was also encountered in core which penetrated the Wedowee Group. Base-metal mineralization, comprised of 1- to 2-mm grains of galena and red-brown sphalerite,, occurs in 1- to 3-cm thick massive to banded quartzite horizons hosted in garnet-chlorite-biotite-muscovite phyllite and graphitic phyllite. Also present, disseminated within the phyllites and spatially associated with the base-metal mineralization, are 2- to 3-mm long arsenopyrite crystals. This mineral assemblage is similar to that seen in the Tallapoosa mine, Tallapoosa County, Alabama, a deposit which also occurs in the Wedowee Group (Paris, 1985).

#### Hillabee Greenstone

A unit of white, laminated to banded, quartz-sericite schist, striking approximately east-west and dipping at 15 to 50 southeast, was mapped in saprolite exposed in the walls of the old mine cuts. Foliation/bedding is locally modified by chevron folding. Thin glassy quartz lenses and bands locally occur parallel to foliation/bedding; major quartz veining is absent. Weathering of pyrite in the schist leaves cubic- to ragged-shaped, iron-oxide filled voids and stains the saprolite to a tan to red-orange color. No readily identifiable shear zone or other potential control of the gold mineralization is apparent in outcrop.

The quartz-sericite schist unit is underlain by weathered chlorite schist in two mine cuts. Weathered epidote-quartz-feldspar+chlorite gneiss and schist overlies the quartz-sericite schist in the southern part of the mine cut and in drainage trenches.

Rock types found in outcrops away from the mine workings are predominantly chlorite schist and minor chlorite-epidote-feldspar gneiss, felsic schist, and banded iron formation. All of these rocks, based on lithologies, metamorphic grade, stratigraphic position, and lithogeochemical analyses of drill core, are correlated with the Hillabee Greenstone (Paris, 1986, 1989a).

Core drilling to delineate the extent and tenor of gold mineralization also allowed the development of a mine area stratigraphy (Table 1). To date, 51 NX/NQ (51-mm diameter) core holes (totaling approximately 7153.2 m) and five 133-mm

Table 1. Stratigraphic/Lithologic Column Based on Core Drilling, Royal Vindicator Gold Deposit, Haralson County, Georgia

Name	Lithology	Thickness (meters)
Cragford Phyllite (after Neathery and Reynolds, 1975)	graphitic phyllite; chlorite-garnet-graphite-phyllite; chlorite schist; $\pm$ garnet quartzite	>110
Upper Volcanic Sequence	chlorite schist; sericite-quartz schist; biotite-quartz-feldspar gneiss; chlorite-epidote-quartz-feldspar $\pm$ garnet gneiss	50-71
Upper Sedimentary Sequence	graphite phyllite; chlorite-graphite-mica schist; mica schist; quartzite	0-45
Mixed Chlorite and Sericite Schist Zone	chlorite schist; sericite-quartz $\pm$ chlorite schist	7-10
Upper Greenstone II	chlorite schist	7-15
Upper Gneiss II	biotite-quartz-feldspar $\pm$ garnet gneiss	4-23
Upper Greenstone	chlorite schist with cpy and po bearing epidote-quartz granofels (lapilli or amygdules); minor banded iron-formation at top	9-19
Upper Gneiss	chlorite-epidote-quartz-feldspar $\pm$ garnet $\pm$ biotite gneiss	10-26
Hanging Wall Greenstone	chlorite schist; epidote-chlorite schist	0-9
Siliceous Zone	pyrite-magnetite-quartz-sericite schist; quartzite; quartz; sericite-feldspar-quartz $\pm$ epidote $\pm$ garnet schist; pyrite bands	2-34
Footwall Greenstone	chlorite schist; epidosite	2-5
Lower Gneiss	biotite-muscovite-quartz feldspar $\pm$ garnet gneiss	11-17
Lower Greenstone	chlorite schist; banded iron-formation near base	16-17

Wedowee--  
Group

Hillabee Greenstone

diameter, reverse circulation holes (totaling approximately 359.4 m) have been drilled at the Royal Vindicator in order to outline the gold-bearing zones.

Rocks of the Hillabee Greenstone in the mine area appear to have been deposited as an alternating felsic-mafic metavolcanic sequence approximately 250-m thick, overlain by graphitic metasediments. At least one hiatus in volcanism is indicated by a wedge of graphitic phyllite and quartzite in the middle of the volcanic section. The Hillabee stratigraphy in the upper parts of the drill holes is variable from hole to hole, probably representing rapid facies changes in the volcanic environment, possibly tied to waning volcanism. The stratigraphy in the lower portions of the holes is much more consistent and appears to represent more stable, cyclic volcanism. The major mafic and felsic cycles are informally named in the order of their occurrence above or below the main gold-bearing unit (Table 1).

#### Mafic Units

The mafic metavolcanic units are comprised predominantly of biotite-chlorite schist, chlorite+amphibole schist, and epidote-biotite-chlorite+garnet schist. These units vary from individual beds a few centimeters to several meters thick. Units comprised of different or similar mafic lithologies vary from 9- to 20-m thick. Possible relict volcanic features include 2- to 5-mm blocky, saussuritized feldspar megacrysts interpreted as relict phenocrysts, elliptical epidote-quartz clasts (0.5- to 4-cm long) thought to represent compacted lapilli, and rounded calcite-quartz and epidote-quartz structures 2 to 10 mm in diameter which may be filled vesicles or amygdules. Individual mafic metavolcanic units are not traceable in outcrop due to poor exposure and similar gross lithologies.

#### Upper greenstone

At least one mafic metavolcanic unit is distinctive and is identifiable and correlatable in core, based on trace mineral content. This unit, the Upper greenstone, contains scattered elliptical epidote-quartz clasts (0.5- to 4-cm long) which contain traces of pyrrhotite, chalcopyrite, and local pyrite in minute fractures in the clast boundaries and interiors. The clasts are interpreted to be deformed lapilli, possibly compressed pumice fragments.

#### Banded Iron Formation

Associated with some mafic units are thin (7- to 15-cm thick), banded magnetite-quartz+pyrite granofels units interpreted to be Algoma-type banded iron formation (BIF: Gross, 1980). These banded iron formations crop out in the area and have been intersected by core drilling in two different mafic units at the mine. In core, a highly

discontinuous BIF occurs at the top of the Upper greenstone associated with an equally discontinuous felsic lapilli tuff with a chloritic matrix. It has not been identified in outcrop. A second BIF located just above the base of the lower greenstone can be traced discontinuously in outcrop for several kilometers to the east and southeast of the mine area, roughly marking the Hillabee Greenstone-Talladega Group contact. The BIF which occurs at the top of the upper greenstone has not been identified in outcrop. At least two other BIF's are known in the Royal Vindicator mine area (fig. 2). Highly deformed BIF crops out on a low knoll approximately 1.6 km east-northeast of the mine site at what is thought to be the same stratigraphic level as the gold-mineralized zone, but contains no gold. Another BIF can be traced discontinuously for approximately 100 m in the vicinity of old prospect workings 0.9 km southeast of the major Royal Vindicator mine workings.

### Felsic Units

Felsic lithologies cored at the Royal Vindicator mine include, sericite-quartz+pyrite schist, sericite-quartz-feldspar+pyrite schist, muscovite-biotite-quartz-feldspar+garnet gneiss, and chlorite-epidote-quartz-feldspar+pyrite+garnet+biotite gneiss. These units also cannot be traced for any distance beyond or correlated outside of the mine area due to weathering and poor exposure. In the upper portion of the core holes the felsic schistose units are intercalated with chloritic schist. The gneissic units occur in the lower parts of the holes as thin-bedded to massive-bedded horizons 4- to 30-m thick.

The dominant minerals of the felsic lithologies are sericite, chlorite, quartz and feldspar. Biotite, epidote, garnet, pyrite, and calcite are accessory minerals. Quartz occurs as fine-grained material of the groundmass, in veinlets of gray, glassy quartz and milky white quartz, and locally as rounded to elliptical (2- to 6-mm across), bluish quartz "eyes" which are interpreted as relict phenocrysts. Feldspar (plagioclase) is commonly fine-grained or forms blocky shaped grains (2- to 4-mm across) which are variably saussuritized. Individual blocky grains in the fine-grained groundmass are interpreted as relict phenocrysts. Epidote occurs as fine-grained material in the well foliated to massive groundmass with fine-grained sericite and chlorite, as round radiating crystal masses interpreted as filled amygdules, and as elliptical quartz-epidote masses to 4 cm in length interpreted as altered lapilli. Biotite forms 1- to 4-mm brown laths oriented parallel to foliation. Garnet occurs as single, scattered, red to red-purple, subhedral grains 0.5- to 3-mm in diameter, and in bands of grains one or two grains thick. Pyrite varies widely in abundance throughout the metavolcanic section, occurring as anhedral grains (<0.5- to 3-mm), rounded grains or equant to flattened cubes up to 10 mm across, and as bands of subhedral grains

parallel to foliation/bedding. Calcite is found as 0.5- to 3-mm disseminated grains in the groundmass and as 0.5- to 1-mm thick bands parallel to foliation.

The most distinctive felsic units are the Upper gneiss and the Siliceous zone.

#### Upper Gneiss

The Upper gneiss is a distinctive marker unit 10- to 26-m thick. It is comprised predominantly of chlorite-epidote-quartz-feldspar+pyrite+garnet+biotite gneiss which occurs immediately above the Siliceous zone or is separated from it by a chlorite schist unit as much as 10-m thick (the Hanging wall greenstone). The greatest abundance of epidote and chlorite occurs structurally above and laterally displaced to the east of the greatest underlying gold concentrations. Epidote abundance decreases rapidly away from the gold mineralization. The lack of facing criteria allows two interpretations: (1) the epidote and chlorite concentration in the Upper gneiss unit represents an alteration product formed originally beneath the gold horizon, or (2) it represents a volcanic unit above the gold horizon that was altered by mineralizing solutions during and after gold deposition.

#### Siliceous Zone

The Siliceous zone is a variably altered, laminated, siliceous, felsic metavolcanic unit. The most intense alteration and gold mineralization are contained in the uppermost 5- to 15-m of the unit. Core drilling indicates that the overall thickness of the Siliceous zone varies from 2.1 to 32.8 meters. The variations in thickness of the Siliceous zone are believed to define two depositional basins with an hourglass shape in plan. The axes of these basins now trend down-dip approximately S80 E.

In underground workings and drill core, the unit is represented by intercalated, banded white, gray, and tan feldspathic schist, quartz-sericite schist, and fine-grained silica bands with disseminated and banded pyrite. Gold occurs with strongly altered, siliceous rock containing a distinctive pyrite and iron-oxide assemblage. Silicification occurs as fine-grained quartz permeating the original tuff (alteration), as micro-crystalline bands interpreted to be metachert, and as milky quartz vein segregations oriented parallel to bedding/foliation.

The protolith of the Siliceous zone has been logged in drill core away from the altered, gold-bearing zone. There, the rock is an unaltered muscovite-biotite-quartz-feldspar+garnet+chlorite+epidote schistose gneiss (rhyodacitic meta-volcanic). Blocky 1- to 2-mm feldspar grains and 2- to 3-mm rounded blue quartz grains are scattered through the rock,

giving it a similar appearance to that of the felsic metavolcanics in other parts of the section.

#### Footwall greenstone

A thin (0.6- to 2.4-m thick) chlorite schist occurs at the base of the Siliceous zone and is known as the Footwall greenstone. This unit forms a distinctive marker bed within which drilling was usually terminated.

#### STRUCTURE

Abrams and McConnell (1984) and McConnell and Abrams (1984) define  $S_1$  as the dominant foliation in rocks of the "Greater Atlanta Area", and this fabric is related to  $F_1$  isoclinal, recumbent folding. They indicate that major outcrop patterns, however, are the expression of  $F_2$  isoclinal to open folds.

German (1988) recognizes  $S_2$  as the dominant S surface. This fabric is related to  $F_2$  isoclinal to open folds which are responsible for most outcrop patterns in the west Georgia area.

The predominant foliation in the prospect area is a schistosity defined by preferably oriented platy minerals (micas and chlorite). The fabric parallels compositional layering (bedding) and is termed  $S_1$ . Weaker, poorly developed fabrics include minor axial planar foliation in some isoclinal fold noses and minor chevron folds whose axial surfaces intersect  $S_1$  at a low angle. The strike of foliation/bedding varies widely from west-northwest to east-northeast. Dips are almost exclusively to the south at  $10^\circ$  to  $50^\circ$ . Rare dip reversals to  $15^\circ$  northwest were noted in underground workings.

The rocks in the mine area have been multiply deformed, and although a rigorous examination of structures has not been made, certain observations can be described. The major outcrop trend in the mine area defines a zigzag fold (fig. 2), represented by an  $F_1$  overturned synform-antiform pair plunging southeast which has in turn been deformed by  $F_2$  folds which locally transpose  $S_1$  into the  $F_2$  intrafolial folds. The synform portion of the  $F_1$  fold is represented by the deflection of the east-northeast-trending ridge just north of the mine to a south-southwest direction at Tally Mountain. The trend of this fold can also be traced by discontinuous outcrops of a banded iron formation adjacent to the Talladega Group-Hillabee Greenstone contact. The Royal Vindicator mine occurs in the upright limb of the synform. Broad north-northeast-trending  $F_3$  warps and northwest-trending  $F_4$  warps are easily seen in the underground mine workings, and are probably the cause of some of the northwest to northerly strikes of foliation seen in surface outcrops.

F<sub>3</sub> and F<sub>4</sub> are similar to those recorded by German (1988).

Faulting is comprised mainly of post-metamorphic, brittle, high-angle reverse faults trending north-northwest. These are best exposed in underground mine workings. No evidence is seen for the presence of the Hollins Line thrust fault as mapped in the vicinity by Heuler and Tull (1989). Core drilling through the Wedowee Group-Hillabee Greenstone contact and limited exposures of the contact in outcrop do not appear to support the presence of this fault in the Royal Vindicator mine area.

#### METAMORPHISM

Paris (1986) recognized that the Royal Vindicator gold deposit lithologies lie in the biotite zone of the greenschist facies, while German (1988) indicated that the general metamorphic grade may be as high as the staurolite grade of the amphibolite facies. However, German (1988) indicates that the metamorphic grade at the Royal Vindicator mine is no higher than garnet grade.

Metamorphic grade in the immediate mine area appears to be the garnet grade of the greenschist facies. Epidote, biotite, and chlorite characterize mafic and felsic rocks of the Hillabee Greenstone sequence, and red garnets 0.1- to 2-mm in diameter are common in the felsic units but are rare in the chlorite schists. Amphiboles are rarely observed, and these appear to be actinolite. Although a local mineral collector has reported staurolite in the vicinity of the Royal Vindicator mine, none was observed during this study.

The overlying Wedowee Group lithologies also contain abundant biotite, chlorite, and garnet. Although no kyanite or staurolite is seen in the immediate Royal Vindicator mine area, German (1988) reports their presence in the overlying Andy Mountain Formation (Wedowee Group) rocks in other areas.

Mafic units in the Hillabee Greenstone and Wedowee Group in the vicinity of the Royal Vindicator mine are predominantly chloritic schists that are locally actinolitic; rocks dominated by amphiboles are very rare. The absence of abundant amphiboles may be attributed to intense magnesian alteration of the rocks, which allowed certain chlorite species to be stable into the lower amphibolite facies.

#### GEOCHEMISTRY

##### Geochemistry of the Metavolcanics

The metavolcanic sequence hosting the Royal Vindicator mine correlates well with the Hillabee Greenstone based on its stratigraphic position in relation to the Talladega group

lithologies. In addition, major element whole rock geochemical analyses of this and other studies (McConnell and Abrams, 1984; German, 1988) are very similar to those of the Hillabee Greenstone reported by Tull and others (1978) in Alabama.

Lithologies seen in mine cuts and core indicate a strong bimodal distribution of mafic to felsic rock types, and a standard AFM plot (fig. 3) of 30 core analyses (Appendix 1) confirms this distribution. The chlorite schists (mafic metavolcanics) are all basaltic in composition with tholeiitic affinities, and felsic metavolcanics (quartz-sericite schist and gneiss) are dacitic to rhyolitic in composition with both tholeiitic and calc-alkaline affinities. Although alteration is definitely present in portions of the stratigraphic section (Siliceous zone and Upper gneiss) and is probably pervasive throughout the section, the AFM plot of Royal Vindicator samples shows a similar distribution for gross lithologic types as that found by Tull and others (1978) for unaltered lithologies of the Hillabee Greenstone in Alabama. This would indicate that major remobilization of most elements has either not taken place or is pervasive in all samples.

#### Exploration Geochemistry

Surficial exploration for gold in the area of the old mine and the surrounding area was conducted using soil geochemistry. Samples were collected from the B-horizon at 15.3 m intervals on north-south oriented grid lines spaced 61 m part. Samples were analyzed for Au by fire assay-atomic absorption methods and Ag, Cu, Pb, Zn, As, Mo, and Ba were analyzed by atomic absorption techniques. This sampling revealed only a localized gold anomaly in soils in the immediate pit area and two weak coincident Au-Mo+Cu anomalies to the east of the mine.

In comparison, analyses of 30 selected core samples for Au, Ag, Cu, Pb, Zn, As, Mo, and Ba (Appendix 1) revealed a distinctive correlation of Au with Ag and Mo (Table 2). A subtle, but recognizable correlation of Au with Hg, As, Cu, and Pb is also present.

#### ALTERATION AND MINERALIZATION PATTERNS

Yeates and others (1896) and Jones (1909) report the gold mineralization occurs in intercalated quartz veins and schist dipping steeply to the south. Descriptions obtained from old reports and maps of companies that had worked and sampled the mine, along with unpublished notes from the Georgia Geologic Survey (Shearer, 1917) indicates that the gold mineralization is associated with a zone of shallow dipping siliceous schist with quartz veining, possibly a shear zone. Current work confirms the association of gold

TABLE 2

Correlation coefficients for trace metals in 30 selected core samples from the Royal Vindicator gold deposit, Haralson County, Georgia.

	Au	Ag	As	Ba	Cu	Cr	Hg	Li	Mo	Pb	Zn
Au	---										
Ag	0.669	---									
As	0.193	0.285	---								
Ba	-0.061	0.137	-0.054	---							
Cu	0.164	0.213	0.208	-0.141	---						
Cr	-0.136	-0.118	0.471	-0.085	0.029	---					
Hg	0.337	0.243	-0.047	0.133	-0.094	-0.231	---				
Li	-0.083	0.538	0.069	0.550	0.194	0.087	-0.032	---			
Mo	0.885	0.521	0.056	-0.002	-0.170	-0.001	0.210	-0.129	---		
Pb	0.349	0.766	0.397	0.329	0.356	0.040	0.265	0.660	0.256	---	
Zn	-0.213	0.186	-0.038	-0.225	0.666	-0.045	-0.143	0.304	-0.223	0.362	---

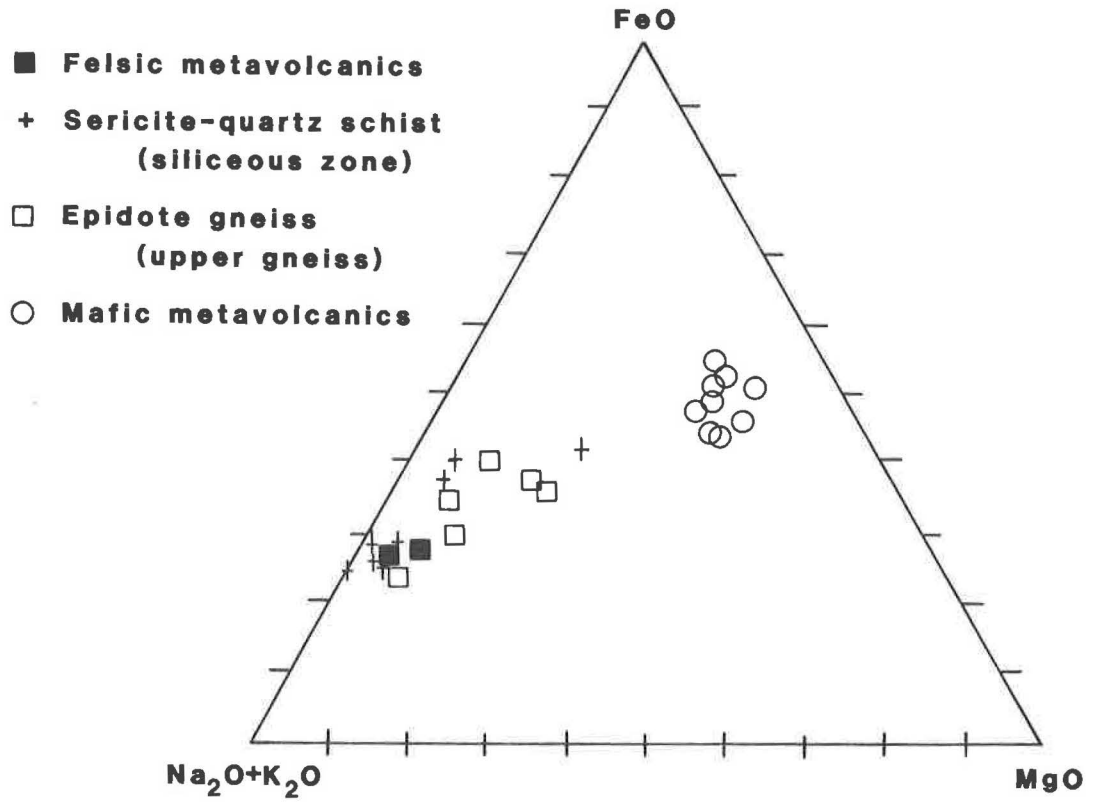


Figure 3. AFM plot of selected Royal Vindicator gold deposit lithologies.

mineralization with a siliceous felsic schist dipping to the south at a shallow angle but casts doubt on the role of shearing and quartz veining.

Assays from core and reverse circulation drilling show that gold mineralization occurs predominantly in strata-bound, altered and silicified felsic metavolcanics of the Siliceous zone; however, trace amounts of gold do occur at other points in the stratigraphic section. The upper limit of the altered, gold-mineralized sequence begins at the basal contact of the Upper gneiss or Hanging wall greenstone with the Siliceous zone. Below this contact, mineralized, altered portions of the Siliceous zone felsic volcanics are generally 3- to 15-m thick. The base of the gold mineralized section is marked by a thin (2- to 10-mm thick) zone containing pyrrhotite and black-green chlorite intergrown with iron-carbonate (siderite?) lenses. Below this horizon, gold and magnetite are not present, pyrite is rare, and the degree of silicification rapidly diminishes.

Gold values appear to be directly proportional to the abundance of silica, pyrite, and iron oxides. These mineral phases form the alteration pattern which distinguishes the Siliceous zone from other felsic metavolcanic units in the section. Gold values of milky quartz veins, the classic or typical ore at many gold deposits and which cross cut the Siliceous zone at various places, are only trace to non-detectable.

Secondary silicification and quartz banding parallel to bedding/foliation is the major alteration effect which blurs primary volcanic textures. Accompanying the widespread alteration but less obvious is an iron enrichment consisting of iron oxides and iron sulfides. Disseminated to weakly banded zones of magnetite and hematite grains (0.5- to 2.0-mm in diameter) constitute up to 5 percent of the rock in areas of strongest silicification and gold mineralization. Pyrite is also present as equant to distorted cubes 0.5- to 20.0-mm across; as 0.5- to 20-mm thick bands of subhedral to euhedral crystals (fig. 4); as 30-cm long pods associated with silica bands (fig. 5); and as disseminated, anhedral grains 0.5- to 2.0-mm across. Pyrite content in altered areas varies from 1 to 20 percent and averages 5 to 7 percent. Based on euhedral shape and pressure shadows, much of the pyrite associated with the gold was probably recrystallized during metamorphism.

Examination of polished sections of "ore" and sulfide concentrates has identified chalcopyrite, galena, sphalerite, arsenopyrite, stibnite, covellite, and chalcocite as trace minerals within the Siliceous zone. Molybdenum is present at elevated concentrations associated with higher gold assays, but no molybdenite has been identified. The highly reflective phase associated with gold in composite grains may be a bismuth or telluride mineral.

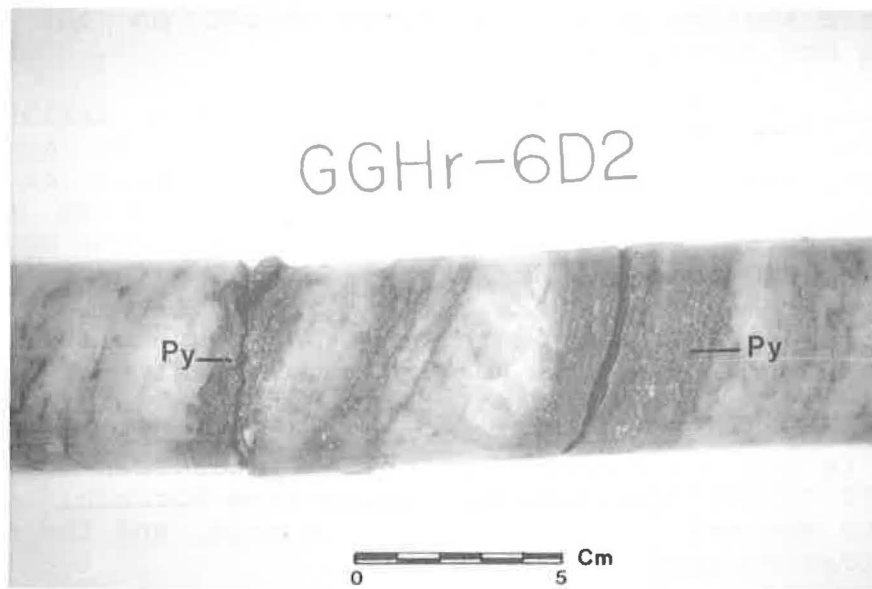


Figure 4. Photograph of prominent pyrite bands (Py) in core from the Siliceous zone; sample is from drill hole GGHR-6D2.

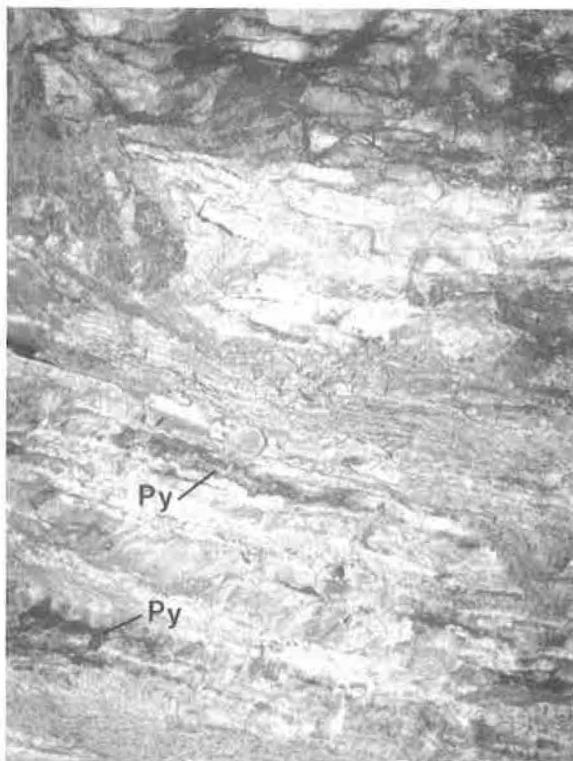


Figure 5. Photograph of pyrite pods (Py) in banded ore of the Siliceous zone on the 105-foot (32-meter) mine level. Quarter (24 mm) for scale.

Gold and silver are the only precious metals identified at the Royal Vindicator mine. No attempt has been made to assay for platinum group metals. Native gold is the only precious metal mineral identified to date. Silver assays appear directly related to those of gold. The silver is probably alloyed with the gold, but it may also occur in the lattice of other minerals such as galena or as a separate, unidentified mineral phase.

Shearer (1917) and Maillot (1940) stated that in unoxidized ores, free milling gold comprised approximately 20 to 30 percent of the gold recovered, with the rest being contained in heavy mineral concentrates (predominantly pyrite).

Gold occurs in a number of different habits at the Royal Vindicator mine: (1) native gold in quartz (fig. 6); (2) gold grains within or attached to pyrite grains (fig. 7); (3) subhedral crystals associated with magnetite and hematite (fig. 8); and (4) composite grains composed of gold, a highly reflective, silvery colored metallic mineral, and a pinkish colored metallic mineral in quartz and pyrite.

Gold particles have variable shapes, occurring as ragged flakes, spindles, rounded or ovoid forms, and as blocky, subhedral crystals. Grain sizes (longest dimension) vary from 0.0005- to 2.0-mm with an average length to width ratio of 2:1. Visible gold particles in core and non-oxidized samples of the Siliceous Zone are rare. Measurement of 12 gold grains viewed in polished ore samples yield an average grain length of 0.028 mm. Measurements of a population of gold grains obtained from a heavy mineral separate and a sulfide concentrate by Cuesta Research Ltd. emphasized that gold grains 0.004- to 0.0005-mm in length, and averaging 0.001 mm in length, dominated the samples.

The variety of forms of gold mineralization suggests the metal has been preserved in part, in its original habits. While there may have been some remobilization and recrystallization due to metamorphism and deformation, the distribution of gold based on core assays is restricted to a maximum of four enriched zones separated by zones of low grade. These zones maintain their equivalent stratigraphic positions regardless of the overall tenor of the deposit (fig. 9). This distribution suggests either a strata-bound, syngenetic or stratiform epigenetic origin for the gold-bearing portions of the Siliceous zone.

In addition to the strata-bound appearance of the gold mineralization, a further control on its localization is indicated by the distribution of gold mineralization grade to thickness of the Siliceous zone. Utilizing an isopach map of the Siliceous zone (fig. 10), ore grade mineralization

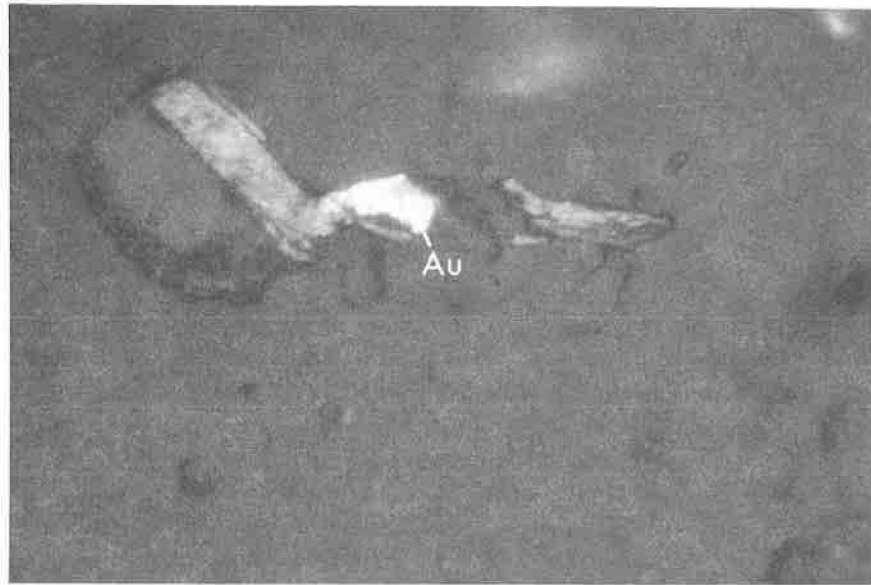


Figure 6. Photomicrograph of a 0.02-mm long anhedral gold grain (Au) in quartz; plane-polarized light. Sample is from a depth of 86 meters (283 feet) in drill hole GGHR-6D5.

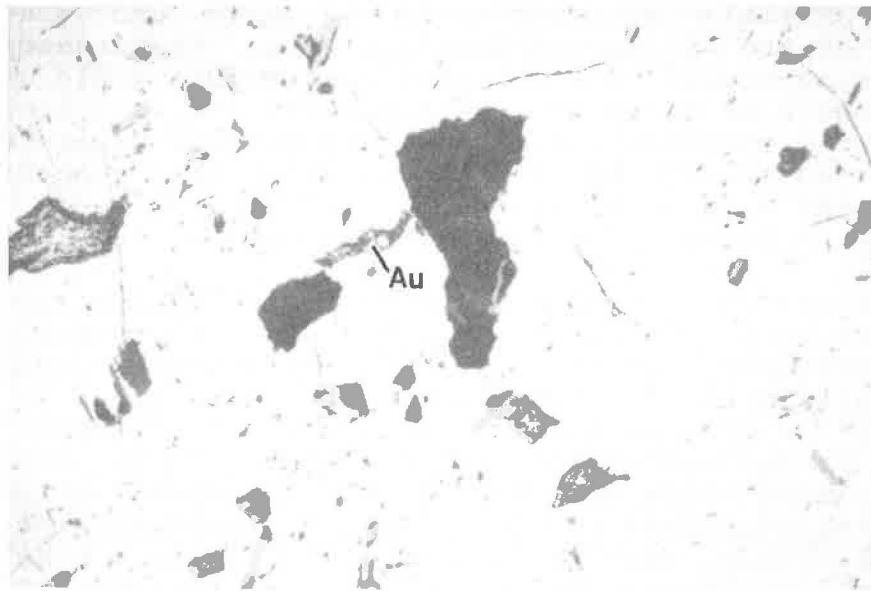


Figure 7. Photomicrograph of 0.05-mm long spindle-shaped gold grain (Au) in pyrite (Py); plane-polarized reflected light. Sample is from a depth of 86 meters (283 feet) in drill hole GGHR-6D5.

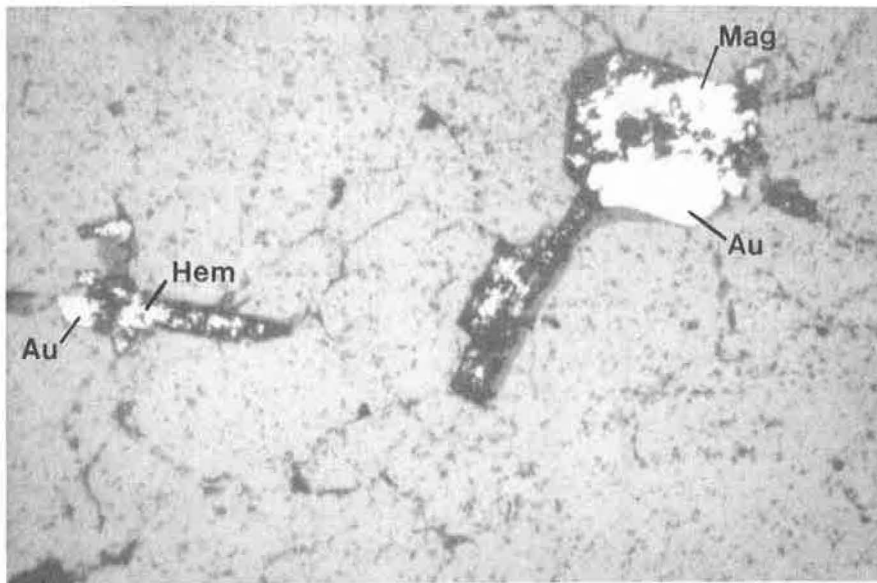


Figure 8. Photomicrograph of subhedral gold grains (Au) in contact with magnetite (Mag) and hematite (Hem) in quartz matrix. The larger gold grain is 0.2-mm long; plane-polarized reflected light. Sample is from a depth of 85 meters (281 feet) in drill hole GGHR-6D5.

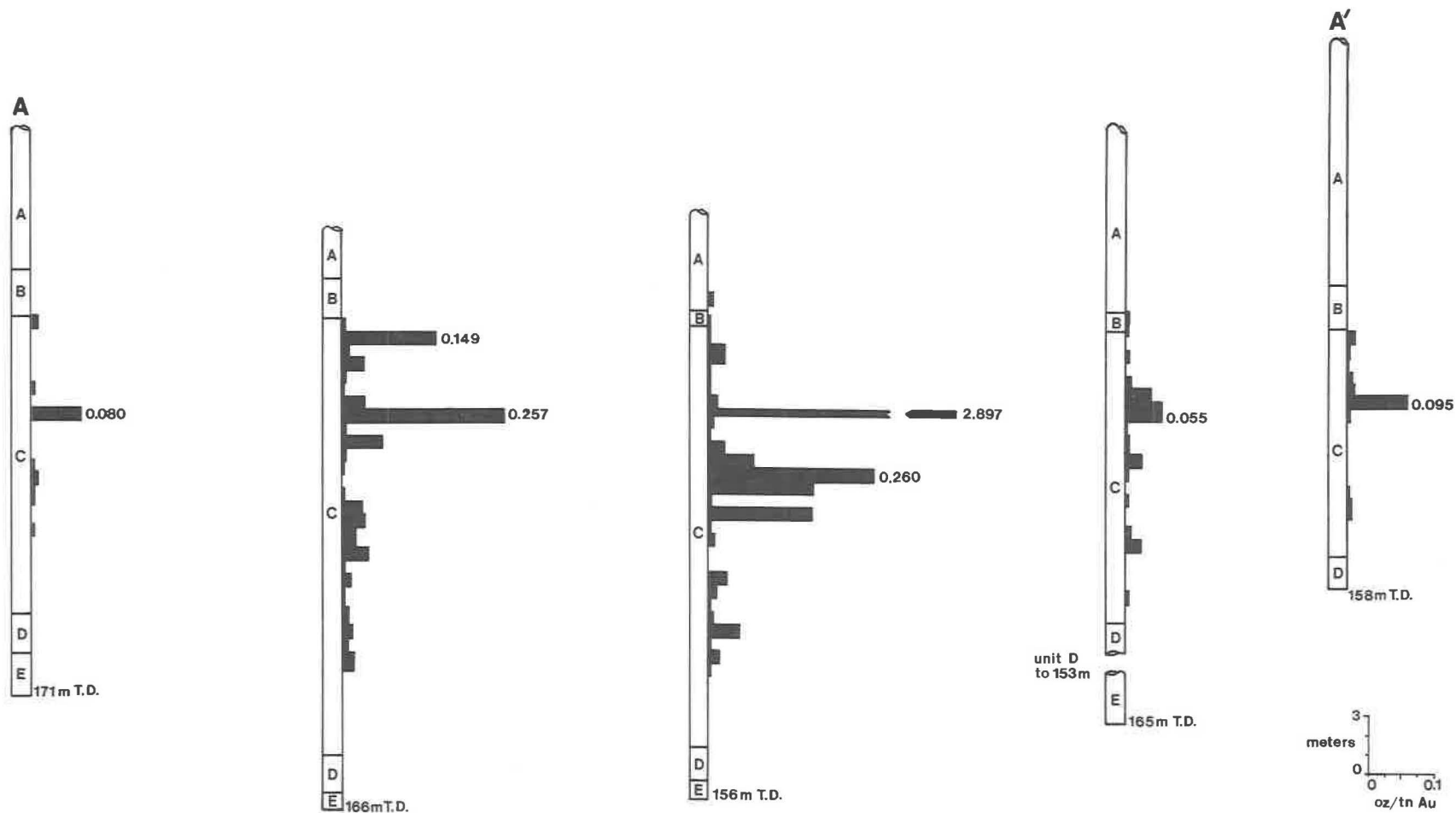


Figure 9. Assay sections of core holes showing gold horizon distribution in the Siliceous zone (unit C) and correlation of the gold-bearing zones between drill holes. The base of the Hanging wall greenstone (unit B) is used as the reference datum plane. Other lithologies are Upper gneiss (A), Footwall greenstone (D), and Lower gneiss (E). See figure 10 for drill hole locations.

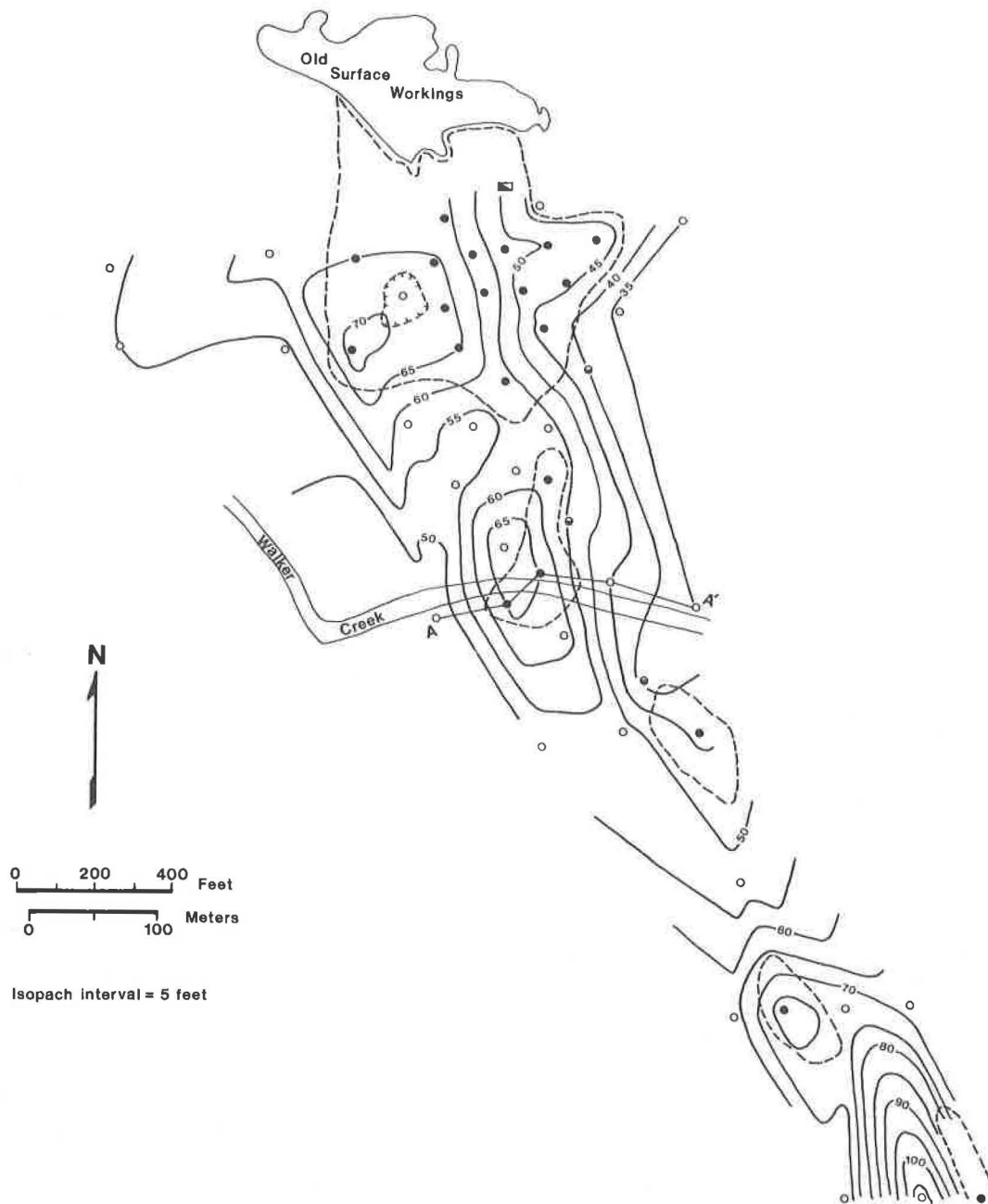


Figure 10. Isopach map of the Siliceous zone. Contour interval is 5 feet. Areas bounded by dashed lines represent zones of rock at least 8-foot (2.4-meters) thick containing at least 0.08 oz/ton gold. Solid circles are locations of drill holes intersecting the above grades and thicknesses. Half-solid circles are locations of drill holes intersecting at least 8 feet (2.4 meters) of mineralized rock containing between 0.04 oz/ton gold and 0.08 oz/ton gold. Open circles are the locations of drill holes that failed to intersect significant mineralization.

(>2.4 m @ 0.08 oz/tn Au) can be shown to occur along the eastern flank of a south-southeast plunging basin. This concentration of gold mineralization also corresponds with the greatest thickness of the overlying Upper gneiss unit which is considered to be an alteration zone spatially related to the gold mineralization.

## CONCLUSIONS

The metavolcanic sequence hosting the Royal Vindicator gold deposit is correlated both stratigraphically and geochemically with the Hillabee Greenstone. In Alabama, the Hillabee Greenstone and its associated mineralization, and the underlying Talladega Group metasediments form a distinctive stratigraphic succession and topographic expression. Prominent base-metal sulfide deposits, and to a lesser extent gold deposits, occur low in the Hillabee Greenstone section. The Pyriton sulfide deposits in Clay County, Alabama occur in Hillabee Greenstone approximately 40 m above the contact with the Jemison Chert (Stow and Tull, 1979). The Crutchfield and Anna-Howe gold deposits in Cleburne County and the Dempsey gold-pyrite prospect of Clay County are both hosted in Hillabee Greenstone and are approximately 40- to 50-m above the Hillabee Greenstone-Talladega Group contact (Paris 1989b, 1989c). Gold prospects such as the Stewart, Jemison, and B. T. Childers and sulfide prospects such as the Garrett (fig. 11) are noted to occur low in the Hillabee section, near the contact with the Talladega Group (Paris and Cook, 1989). Many of these deposits contain significant felsic or siliceous units and are spatially associated with banded iron formation. The Talladega Group near the contact usually underlies a subdued to pronounced ridge. The Royal Vindicator deposit exhibits a similar overall stratigraphic and topographic section. The major element chemistry of the greenstones and felsic metavolcanics of the Hillabee, as analyzed by Tull and others (1978) is also similar to that of the mafic and felsic metavolcanics examined in this study at the Royal Vindicator.

Tull and Stow (1982) suggest that the sulfide deposits of the Hillabee Greenstone formed in a continental margin-arc environment. An alternative interpretation suggested by this study is that the volcanic sequence formed in a failed rift near the continental margin of a back-arc basin. A similar model is proposed by German (1988). The abundance of apparent pyroclastic textures indicates the rocks were deposited in shallow marine to slightly emergent subaerial conditions. An alternative interpretation of the pyroclastic textures is that they were related to highly gas-charged submarine domes and flows; however, no discrete domes have been identified to date.

It is proposed that gold mineralization at the Royal Vindicator deposit is the result of deposition of gold by

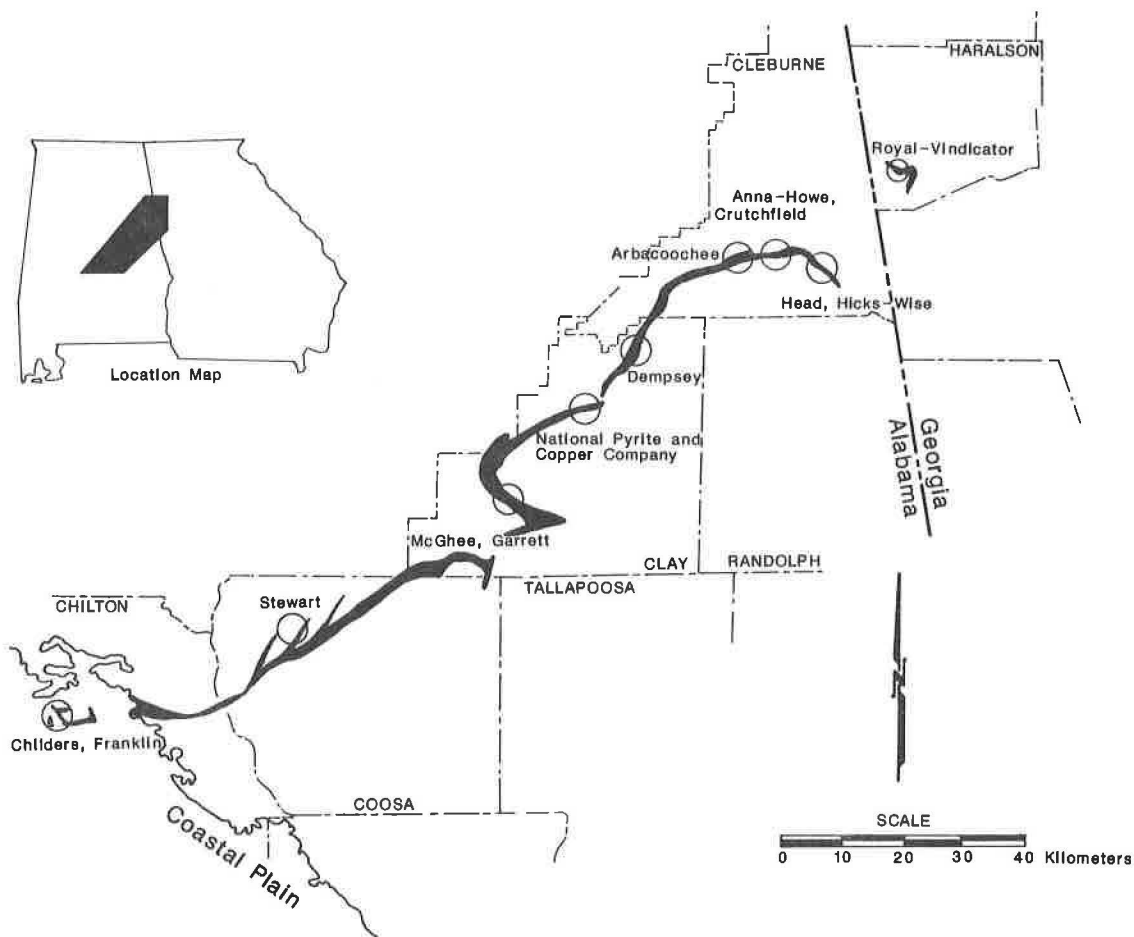


Figure 11. Location of base- and precious-metal occurrences hosted by Hillabee Greenstone or correlative units, Alabama and western Georgia.

hot-springs fluids along an irregular, west-facing slope on the eastern edge of what is now a narrow, south-southeast-trending basin. Deposition took place during a period of felsic volcanism in an alternating mafic-felsic volcanic sequence. Gold mineralization appears to have been deposited in three or more pulses in hot springs terraces, or in hot springs terraces and more permeable zones in immediately underlying or contemporaneously deposited felsic pyroclastics. Precious-and base-metal mineralization and associated volcanism probably took place over a relatively short time span.

Following deposition of the gold-bearing horizons the deposits were buried by further volcanism which was in turn finally overwhelmed by sedimentation which formed the Wedowee Group. The deposits and enclosing rocks were subsequently multiply deformed and metamorphosed to the upper greenschist facies during the Acadian orogeny (Tull, 1982).

#### ACKNOWLEDGEMENTS

The author served as project geologist at the Royal Vindicator project for U.S. Borax from 1979 to 1987 and for the Atlantic Goldfields and Jascan Resources joint venture from 1987 to 1989. I would like to thank U.S. Borax, Atlantic Goldfields, Inc., and Jascan Resources, Inc. for permission to publish information about the deposit derived from their exploration. Gratitude is also expressed to Jerry German, Keith McConnell, Charlotte Abrams, Jim Tull, Robert B. Cook, and George Heuler for their insights into the geology of the western Georgia and eastern Alabama Piedmont and lively discussions of the geologic setting of the mine area and deposit genesis. Special appreciation is expressed to Ken Gillon for his critical review and editing which markedly improved the paper. Final interpretations are the author's responsibility.

#### REFERENCES CITED

- Abrams, C.E. and McConnell, K.I., 1981, Stratigraphy of the area around the Austell-Frolona antiform, west-central Georgia, in Wigley, P.B., ed., Latest thinking on the stratigraphy of selected areas in Georgia: Georgia Geologic Survey Information Circular 54-A, p. 55-67.
- \_\_\_\_\_, 1984, Geologic setting of volcanogenic base and precious metals deposits of the west Georgia Piedmont: A multiply deformed metavolcanic terrain: Economic Geology, Vol. 70, no. 7, pp. 1521-1539.
- Cressler, C.W., 1970, Geology and ground-water resources of Floyd and Polk Counties, Georgia: The Geological Survey of Georgia, Information Circular 39, 95 p.
- Cuesta Research Limited, 1988, Mineralogy, gold ore concentrates: Atlantic Goldfields, Inc. and Jascan Resources, Inc. - Royal Vindicator Gold Mine:

- unpublished report for A.C.A. Howe International, Ltd., 17 p.
- German, J.M., 1985, The geology of the northeastern portion of the Dahlonega gold belt: Georgia Geologic Survey Bulletin 100, 41 p.
- \_\_\_\_\_, 1988, The geology of gold occurrences in the west-central Georgia Piedmont: The Carroll County gold belt and the southwestern portion of the Dahlonega gold belt: Georgia Geologic Survey Bulletin 107, 47 p., maps in pocket.
- \_\_\_\_\_, Stratigraphic implications from core drilling in the vicinity of the Royal-Vindicator gold mine, Haralson County, Georgia: Georgia Geologic Survey Information Circular 84, in press.
- Gross, G.A., 1980, A classification of iron formations based on depositional environments: Canadian Mineralogist, Vol. 18, p. 215-222.
- Heuler, G.F., and Tull, J.F., 1989, Geologic mapping of the Talladega belt of Haralson County, Georgia [abs.]: Geological Society of America Abstracts with Programs, Vol. 21, no. 3, p. 22.
- Hurst, V.J. and Crawford, T.J., 1969, Sulfide Deposits, Coosa Valley Area, Georgia: Economic Development Administration, U.S. Department of Commerce, 190 p.
- Jones, S.P., 1909, Second report on the gold deposits of Georgia: Geological Survey of Georgia Bulletin 19, 283 p.
- Lane, C., 1900, Royal Vindicator Mines: unpublished report for the Royal Vindicator Mines Company, 3 p.
- Maillot, E.E., 1940, Royal Vindicator Mine, Georgia: unpublished prospectus, assay map, 14 p.
- McConnell, K.I., and Abrams, C.E., 1982, Geology of the New Georgia Group and associated massive sulfide and gold deposits: West-central Georgia: Guidebook in Exploration for metallic resources in the southeast symposium, University of Georgia Center for Continuing Education, Athens Georgia, p. 143-170.
- \_\_\_\_\_, 1984, The geology of the Greater Atlanta Region: Georgia Geologic Survey Bulletin 96, 127 p.
- McConnell, K.I., Abrams, C.E., and German, J.M., 1986, Gold deposits in the northern Piedmont of Georgia and Alabama and their relationship to lithostratigraphic units, in Misra, K.C. (ed.), Volcanogenic Sulfide and Precious Metal Mineralization in the Southern Appalachians: University of Tennessee Department of Geological Sciences Studies in Geology 16, p. 164-181.
- Neathery, T.L., and Hollister, V.F., 1984, Volcanogenic sulfide deposits in the southernmost Appalachians: Economic Geology, Vol. 79, p. 1540-1560.
- Neathery, T.L., and Reynolds, J.W., 1975, Geology of the Lineville East, Ofelia, Wadley North, and Mellow Valley Quadrangles, Alabama: Geological Survey of Alabama Bulletin 109, 120 p., maps.
- Paris, T.A., 1985, The Goldville project: Results of an exploration project for gold in the northern Alabama

- Piedmont, in Misra, K.C. (ed.), Volcanogenic Sulfide and Precious Metal Mineralization in the Southern Appalachians: University of Tennessee Department of Geological Sciences Studies in Geology 16, p. 182-205.
- \_\_\_\_\_, 1986, Geology of the Royal-Vindicator gold deposit, Haralson County, Georgia [abs.]: Geological Society of America Abstracts with Programs, Vol. 18, no. 1, p. 60.
- \_\_\_\_\_, 1989a, The Royal Vindicator gold deposit: A metamorphosed epithermal hot springs type gold deposit [abs.]: Geological Society of America Abstracts with Programs, Vol. 21, no. 3, p. 53.
- \_\_\_\_\_, 1989b, Geology of the Crutchfield and Anna-Howe gold mines, Cleburne County, Alabama, in Gold Deposits of Alabama: Geological Survey of Alabama Bulletin 136, in press.
- \_\_\_\_\_, 1989c, Geology of the Dempsey gold-pyrite prospect, Clay County, Alabama, in Gold Deposits of Alabama: Geological Survey of Alabama Bulletin 136, in press.
- Paris, T.A., and Cook, R.B., 1989, Exploration geology of selected gold prospects traditionally related to the Hillabee Greenstone, Alabama and Georgia, in Geological Survey of Alabama Bulletin 136, in press.
- Reeves, M., 1975, Tallapoosa Gold Mine, in The History of Mining in Haralson County, Georgia: unpublished manuscript, West Georgia College Library Special Collections, 4 p., map.
- Ruhl, O., 1917, Royal Vindicator Mine: unpublished consultants report for the Royal Vindicator Mines Company, 6 p., assay map.
- Shearer, H.K., 1917, Old Royal Gold Mine: unpublished field notes, Georgia Geologic Survey, 8 p.
- Stow, S.H. and Tull, J.F., 1979, Sulfide mineralization in Tull, J.F. and Stow, S.H., eds., The Hillabee meta-volcanic complex and associated rock sequences: Alabama Geological Society, 17th Annual Field Trip Guidebook, p. 33-36.
- Tull, J.F., 1982, Stratigraphic framework of the Talladega slate belt, Alabama Appalachians, in Bearce, D.N., Black, W.W., Kish, S.A., and Tull, J.F., eds., Tectonic Studies in the Talladega and Carolina Slate Belts, Southern Appalachian Orogen: Geological Society of America, Special Paper 191, p. 3-18.
- Tull, J.F., and Stow, S.H., 1980, Structural and stratigraphic setting of arc volcanism in the Talladega slate belt of Alabama, in Frey, R.W., ed., Excursions in Southeastern Geology, Vol. 2: American Geological Institute, p. 545-581.
- \_\_\_\_\_, 1982, Geologic setting of the Hillabee meta-volcanics and associated strata-bound sulfide in the Appalachian Piedmont of Alabama: Economic Geology, Vol. 77, no. 2, p. 312-321.
- Tull, J.F., Stow, S.H., Long, L., and Hayes-Davis, B., 1978, The Hillabee Greenstone: Geochemistry, structure,

mineralization and theories of origin: University of Alabama Mineral Resources Institute, Research Report Number 1, 100 p.

West Georgia College Library, Royal Gold Mine File: a collection of letters and an unsigned report from the period 1909-1911 relating to the Royal Gold Mine, obtained by West Georgia from the University of Missouri Western Historical Manuscript Collection--Rolla, 10 p.

Yeates, W.S., McCallie, S.W., and King, F.P., 1896, A preliminary report on a part of the gold deposits of Georgia: Geological Survey of Georgia, Bulletin 4-A, 542 p.

Appendix 1

Analyses of metavolcanic (Hillabee Greenstone) lithologies at the Royal Vindicator gold deposit. Major element data in percent; trace element data in ppm. Total iron as  $\text{Fe}_2\text{O}_3$ . Sample numbers should be prefixed GGHR-6D. All analyses by U.S. Borax Research Corporation, Anaheim, California.

Sample No.	7-160	16-100	18-150	19-90	22-255	18-265
$\text{SiO}_2$	68.60	75.20	71.00	76.10	71.70	72.10
$\text{TiO}_2$	0.37	0.23	0.33	0.25	0.33	0.25
$\text{Al}_2\text{O}_3$	13.40	11.70	12.70	12.10	12.70	13.20
$\text{Fe}_2\text{O}_3$	5.10	3.70	5.10	3.40	5.10	3.10
$\text{FeO}$	--	--	--	--	--	--
$\text{MnO}$	0.14	0.06	0.13	0.07	0.14	0.07
$\text{MgO}$	2.50	0.81	2.10	1.20	1.20	0.83
$\text{CaO}$	1.37	1.44	1.74	0.96	1.50	2.30
$\text{Na}_2\text{O}$	5.20	5.40	5.50	5.80	5.40	4.60
$\text{K}_2\text{O}$	0.43	0.18	0.17	0.36	0.24	2.00
$\text{P}_2\text{O}_5$	--	--	--	--	--	--
L.O.I.	1.89	0.82	1.79	1.34	1.18	1.36
TOTAL	99.00	99.54	100.56	101.58	99.49	99.81
Au	<0.02	<0.02	<0.02	<0.02	<0.02	<0.02
Ag	0.7	0.5	0.7	0.5	0.5	0.5
As	<2.0	<2.0	<2.0	<2.0	<2.0	<2.0
Ba	22.0	4.0	22.0	19.0	26.0	223.0
Cu	7.0	7.0	25.0	4.0	39.0	4.0
Cr	<136.0	<136.0	<136.0	<136.0	<136.0	<136.0
Hg	0.06	<0.05	0.10	<0.05	<0.05	<0.05
Li	<5.0	<5.0	<5.0	<5.0	<5.0	<5.0
Mo	<5.0	<5.0	5.0	<5.0	<5.0	<5.0
Rb	<9.0	<9.0	<9.0	9.0	<9.0	82.0
Pb	10.0	<5.0	10.0	<5.0	7.0	10.0
Sr	14.0	29.0	29.0	<10.0	29.0	34.0
Zn	118.0	33.0	76.0	41.0	102.0	31.0
Rock Type	EFG	EFG	EFG	EFG	EFG	LG

EFG = chlorite-epidote-quartz-feldspar gneiss (Upper gneiss unit);

LG = biotite-muscovite-quartz-feldspar gneiss (Lower gneiss unit).

Appendix 1 (contd.)

Sample No.	22-20	22-140	7-115	18-95	22-60	22-170
SiO <sub>2</sub>	92.50	71.90	50.20	48.20	53.40	48.40
TiO <sub>2</sub>	0.03	0.25	1.00	1.00	0.87	1.60
Al <sub>2</sub> O <sub>3</sub>	3.30	13.40	14.50	13.60	13.80	12.70
Fe <sub>2</sub> O <sub>3</sub>	1.65	2.60	10.90	12.30	10.30	13.90
FeO	--	--	--	--	--	--
MnO	0.02	0.04	0.28	0.28	0.16	0.24
MgO	0.73	0.68	8.30	8.30	5.80	7.10
CaO	0.04	2.40	8.00	11.00	8.00	10.60
Na <sub>2</sub> O	1.18	4.20	3.90	1.97	2.50	2.80
K <sub>2</sub> O	0.15	2.50	0.20	0.36	0.31	0.34
P <sub>2</sub> O <sub>5</sub>	--	--	--	--	--	--
L.O.I.	0.69	1.22	2.35	2.18	4.69	1.40
TOTAL	100.29	99.19	99.63	99.19	99.83	99.08
Au	<0.02	<0.02	<0.02	<0.02	<0.02	<0.02
Ag	0.2	0.2	0.7	1.0	1.0	0.7
As	<2.0	<2.0	<2.0	<2.0	7.0	<2.0
Ba	10.0	156.0	7.0	38.0	67.0	24.0
Cu	21.0	26.0	7.0	12.0	92.0	139.0
Cr	205.0	<136.0	136.0	136.0	273.0	136.0
Hg	<0.05	<0.05	<0.05	0.09	0.05	0.09
Li	<5.0	<5.0	<5.0	<5.0	10.0	<5.0
Mo	8.0	<5.0	<5.0	<5.0	<5.0	<5.0
Rb	<9.0	82.0	<9.0	9.0	18.0	<9.0
Pb	<5.0	10.0	10.0	12.0	17.0	12.0
Sr	<10.0	62.0	19.0	58.0	67.0	62.0
Zn	12.0	19.0	71.0	60.0	68.0	55.0
Rock Type	UGII	UGII	UGST	UGST	UGSTII	UGST

UG = chlorite schist with chalcopyrite and pyrrhotite bearing epidosite clasts (Upper greenstone unit); UGSTII = chlorite schist (Upper greenstone II unit); FWG = chlorite schist (Footwall greenstone unit); HWG = chlorite schist (Hanging wall greenstone unit).

## Appendix 1 (contd.)

Sample No.	7-280	16-120	16-175	18-255	19-180	22-335
SiO <sub>2</sub>	48.20	45.10	47.40	50.50	47.30	49.10
TiO <sub>2</sub>	1.60	1.00	1.30	0.85	1.70	1.20
Al <sub>2</sub> O <sub>3</sub>	13.80	14.90	14.70	13.80	13.60	14.20
Fe <sub>2</sub> O <sub>3</sub>	13.20	12.40	12.90	10.00	13.70	11.60
FeO	--	--	--	--	--	--
MnO	0.27	0.14	0.21	0.17	0.28	0.24
MgO	7.60	7.60	8.10	7.30	8.00	9.00
CaO	9.10	6.30	7.40	8.40	9.40	8.70
Na <sub>2</sub> O	3.40	3.00	3.50	3.90	2.80	3.20
K <sub>2</sub> O	0.26	1.64	0.58	0.11	0.37	0.16
P <sub>2</sub> O <sub>5</sub>	--	--	--	--	--	--
L.O.I.	2.03	6.53	3.18	3.57	2.31	2.94
TOTAL	99.46	98.61	99.27	98.60	99.46	100.34
Au	<0.02	<0.02	<0.02	<0.02	<0.02	<0.02
Ag	1.0	1.9	1.4	1.0	1.0	0.7
As	<2.0	<2.0	<2.0	<2.0	<2.0	<2.0
Ba	14.0	355.0	110.0	12.0	19.0	12.0
Cu	133.0	23.0	132.0	17.0	162.0	6.0
Cr	<136.0	136.0	<136.0	136.0	<136.0	273.0
Hg	<0.05	0.07	<0.05	<0.05	0.06	<0.05
Li	10.0	48.0	14.0	10.0	14.0	14.0
Mo	<5.0	<5.0	5.0	<5.0	<5.0	<5.0
Rb	<9.0	73.0	18.0	<9.0	9.0	<9.0
Pb	14.0	24.0	12.0	14.0	17.0	10.0
Sr	38.0	96.0	29.0	58.0	43.0	53.0
Zn	240.0	92.0	58.0	63.0	359.0	76.0
Rock Type	FWG	HWG	FWG	FWG	FWG	FWG

FWG = chlorite schist (Footwall greenstone unit); HWG = chlorite schist (Hanging wall greenstone unit).

## Appendix 1 (contd.)

Sample No.	7-1A	7-16	16-1	16-12	18-2	18-12
SiO <sub>2</sub>	77.20	73.40	70.50	74.00	82.30	82.10
TiO <sub>2</sub>	0.15	0.18	0.20	0.17	0.17	0.08
Al <sub>2</sub> O <sub>3</sub>	10.20	12.30	11.70	12.10	7.70	8.30
Fe <sub>2</sub> O <sub>3</sub>	2.50	2.50	5.70	2.60	2.20	2.10
FeO	--	--	--	--	--	--
MnO	0.37	0.03	0.02	0.03	0.03	0.02
MgO	0.38	0.43	0.76	0.39	0.34	0.10
CaO	1.45	3.10	0.82	1.69	1.04	0.99
Na <sub>2</sub> O	5.50	4.40	6.10	4.40	4.40	4.70
K <sub>2</sub> O	0.37	1.18	0.75	1.75	0.28	0.05
P <sub>2</sub> O <sub>5</sub>	--	--	--	--	--	--
L.O.I.	1.22	2.61	2.08	2.09	0.87	1.14
TOTAL	99.34	100.13	98.63	99.22	99.33	99.58
Au	1.95	<0.02	2.31	<0.02	1.19	7.86
Ag	1.0	0.2	1.4	0.5	0.7	2.4
As	<2.0	<2.0	5.0	<2.0	<2.0	2.0
Ba	50.0	65.0	53.0	127.0	36.0	53.0
Cu	8.0	6.0	48.0	54.0	12.0	7.0
Cr	<136.0	<136.0	<136.0	<136.0	<136.0	<136.0
Hg	0.09	0.06	0.06	0.05	0.09	0.09
Li	<5.0	<5.0	10.0	<5.0	<5.0	<5.0
Mo	13.0	<5.0	5.0	<5.0	<5.0	59.0
Rb	<9.0	27.0	27.0	64.0	9.0	9.0
Pb	11.0	12.0	17.0	7.0	10.0	19.0
Sr	29.0	43.0	29.0	48.0	24.0	24.0
Zn	18.0	19.0	36.0	24.0	18.0	6.0
Rock Type	SZ	SZ	SZ	SZ	SZ	SZ

SZ = sericite-quartz+pyrite+feldspar schist (Siliceous zone unit).

Appendix 1 (contd.)

Sample No.	18-26	19-2	19-13	19-24	22-5	22-20
SiO <sub>2</sub>	73.50	73.70	77.50	74.50	79.10	94.20
TiO <sub>2</sub>	0.17	0.30	0.12	0.17	0.08	0.02
Al <sub>2</sub> O <sub>3</sub>	11.90	11.30	11.50	12.30	9.60	2.80
Fe <sub>2</sub> O <sub>3</sub>	2.40	4.90	2.50	2.50	2.10	1.65
FeO	--	--	--	--	--	--
MnO	0.03	0.06	0.04	0.03	0.04	0.02
MgO	0.44	0.69	0.26	0.44	0.03	0.74
CaO	2.50	1.26	1.36	2.40	1.52	0.04
Na <sub>2</sub> O	4.40	5.80	4.60	4.70	5.20	1.17
K <sub>2</sub> O	1.25	0.82	1.64	1.46	0.60	0.16
P <sub>2</sub> O <sub>5</sub>	--	--	--	--	--	--
L.O.I	2.49	--	0.79	2.41	1.48	0.49
TOTAL	99.08	98.83	100.31	100.91	99.75	101.29
Au	<0.02	1.71	0.16	<0.02	1.17	<0.02
Ag	0.4	1.0	0.5	0.5	0.7	0.2
As	<2.0	<2.0	<2.0	<2.0	<2.0	<2.0
Ba	85.0	110.0	204.0	77.0	86.0	173.0
Cu	6.0	17.0	9.0	6.0	6.0	16.0
Cr	<136.0	<136.0	<136.0	<136.0	<136.0	205.0
Hg	0.09	0.09	0.11	<0.05	<0.05	0.06
Li	<5.0	10.0	<5.0	<5.0	<5.0	<5.0
Mo	<5.0	<5.0	<5.0	<5.0	17.0	20.0
Rb	36.0	27.0	36.0	36.0	18.0	<9.0
Pb	8.0	10.0	10.0	<5.0	7.0	10.0
Sr	34.0	24.0	34.0	29.0	29.0	38.0
Zn	19.0	48.0	8.0	13.0	14.0	8.0
Rock Type	SZ	SZ	SZ	SZ	SZ	SZ

SZ = sericite-quartz+pyrite+feldspar schist (Siliceous zone unit).

## GOLD DEPOSITS OF THE DAHLONEGA BELT, NORTHEAST GEORGIA:

George V. Albino\*  
Department of Geology, Bryn Mawr College  
Bryn Mawr, PA, 19010

Gold deposits of the Dahlonega Belt occur in a one to two km wide zone marked by retrograde metamorphism and well-developed near-vertical foliation and sub-horizontal stretching lineation. A number of features indicate that the gold belt is a zone of high shear strain. These include ribbon mylonites, development of S-C and C-C' fabrics, parallelism between fold axes and stretching lineations, and rare sheath folds. Kinematic indicators including S-C and C-C' relationships and asymmetric quartz c-axis patterns suggest movement along the Dahlonega Belt shear zone was dextral. Southwest of Dahlonega there is evidence for a later phase of cratonward reverse faulting. Retrogressive alteration along the Dahlonega Belt resulted in formation of kyanite and staurolite at the expense of early sillimanite-bearing assemblages. Elongate, pre-kinematic and syn-kinematic plutons of granitic to tonalitic composition occur within the belt and along its southeast margin.

Gold deposits of the Dahlonega Belt include well-defined quartz veins, zones of sheeted quartz veins, and broad zones containing lenticular quartz-carbonate-sulfide pods. Many of the auriferous zones are spatially associated with pre and syn-kinematic felsic intrusive rocks. Auriferous veins consist dominantly of quartz, with lesser calcite or dolomite, tourmaline, muscovite, biotite, hornblende, garnet and chlorite. Pyrrhotite and pyrite are both common and are accompanied by minor magnetite, chalcopyrite, galena, sphalerite, and gahnite. Gold occurs both as the native metal and in the tellurides petzite, calaverite, and sylvanite. In addition to gold and silver the ores contain low but locally anomalous concentrations of arsenic, antimony, tungsten, molybdenum, and mercury.

Alteration assemblages vary with host rock lithology, with carbonatization and biotitization dominant in metabasites, and base leaching in quartzofeldspathic rocks. Mineral assemblages and compositions indicate alteration at temperatures  $>500^{\circ}\text{C}$  and at pressures of  $>4.5$  to  $5\text{ kb}$  accompanying infiltration of a fluid with  $X_{\text{CO}_2}$  of  $\geq 0.2$ .

### INTRODUCTION

The Dahlonega Gold Belt in the Eastern Blue Ridge of northeast Georgia (Figure 1) has been one of the most important gold-producing areas of the southeastern U.S.. It probably accounted for the bulk of Georgia's production of more than 870,000 ounces, from first discovery of gold in 1829 until production essentially ceased in the late 1930's

---

\* - Present address, Corona Gold Inc., 940 Matley Lane, #15, Reno, NV, 89502

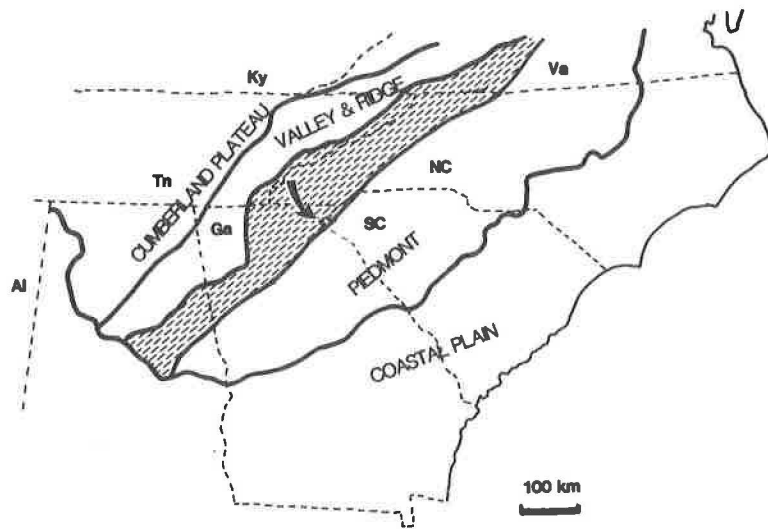


**Figure 1. Location map, showing subdivisions of the Southern Appalachians (Blue Ridge in dash pattern). Approximate location of Dahlonega Belt indicated by arrow.**

(Koschmann and Bergendahl, 1968). Most gold produced from the Dahlenega Belt has come from placers and hydraulic mining of saprolite (Pardee and Park, 1948), with little gold recovered from primary unoxidized ores. Although its total production is not large by world standards, the Dahlenega Belt is of considerable scientific interest as a nearly unique example of a significant gold belt hosted by high grade metamorphic rocks.

The purpose of the present paper is to describe the geological setting of the gold occurrences of the Dahlenega Belt and the nature of the auriferous zones and their associated alteration assemblages, and to discuss the conditions under which mineralization occurred and the nature of the ore-forming process. The genetic relationship between the Dahlenega Belt occurrences and the more important group of deposits hosted by greenschist facies metamorphic rocks (e.g. Kerrich, 1983, Phillips, 1985, Weir and Kerrick, 1987) will also be discussed.

## REGIONAL GEOLOGY

The Dahlenega Belt is in the Eastern Blue Ridge of the Appalachian Orogen. The Eastern Blue Ridge is separated from the Piedmont Province to the east by the Brevard Zone, and from the Western Blue Ridge, which consists mainly of the Late Precambrian to Cambrian Ocoee and Great Smoky Groups, by the Hayesville Thrust (Figure 2). The Eastern Blue Ridge is dominantly a region of high grade metamorphic rocks, probably mostly of Late Precambrian to Early Paleozoic age, which were metamorphosed and thrust eastward over the North American Craton during the Taconic Orogeny (Hatcher, 1978, 1987).

In northeast Georgia the Eastern Blue Ridge is divided into three belts, from southeast to northwest, the Tallulah Falls, Dahlenega, and Richard Russell Belts (Figure 2). The Tallulah Falls and Richard Russell Belts are very similar in terms of rock types present, their relative proportions, metamorphic grade, and structural style. They probably at one time were parts of a single continuous thrust sheet (the Hayesville Thrust Sheet) consisting mainly of coarse-grained, weakly foliated, banded psammitic gneiss with lesser amounts of pelitic schist and gneiss, amphibolite, and minor ultramafic rocks and aluminous schist. Psammitic and pelitic rocks are migmatitic (Figure 3A), and contain granitic (K-feldspar rich) and trondhjemitoid (plagioclase-rich) leucosome. Dioritic to granitic intrusive rocks are common in the Tallulah Falls Belt along its contact with the Dahlenega Belt, but are largely absent in the Richard Russell Belt. Mafic rocks are minor in the Richard Russell and Tallulah Falls Belts, except for the mafic to ultramafic Lake Burton Complex, consisting mainly of amphibolite and metagabbro (Hopson, 1988), which partly rings the Tallulah Falls Dome in the Tallulah Falls Belt. Its position flanking the core of the dome indicates it is structurally lower than most of the exposed metasediments.

Metamorphic grade in the Tallulah Falls and Richard Russell Belts is upper amphibolite (Bryant and Reed, 1979; Carpenter, 1970). Migmatitic metasediments contain assemblages diagnostic of the upper kyanite or sillimanite zone with either aluminosilicate+melt or aluminosilicate+K-feldspar in both belts. Along strike to the northeast, in rocks equivalent to the Richard Russell Belt, granulite facies assemblages occur suggesting peak metamorphic temperatures of at least 750°, and pressures

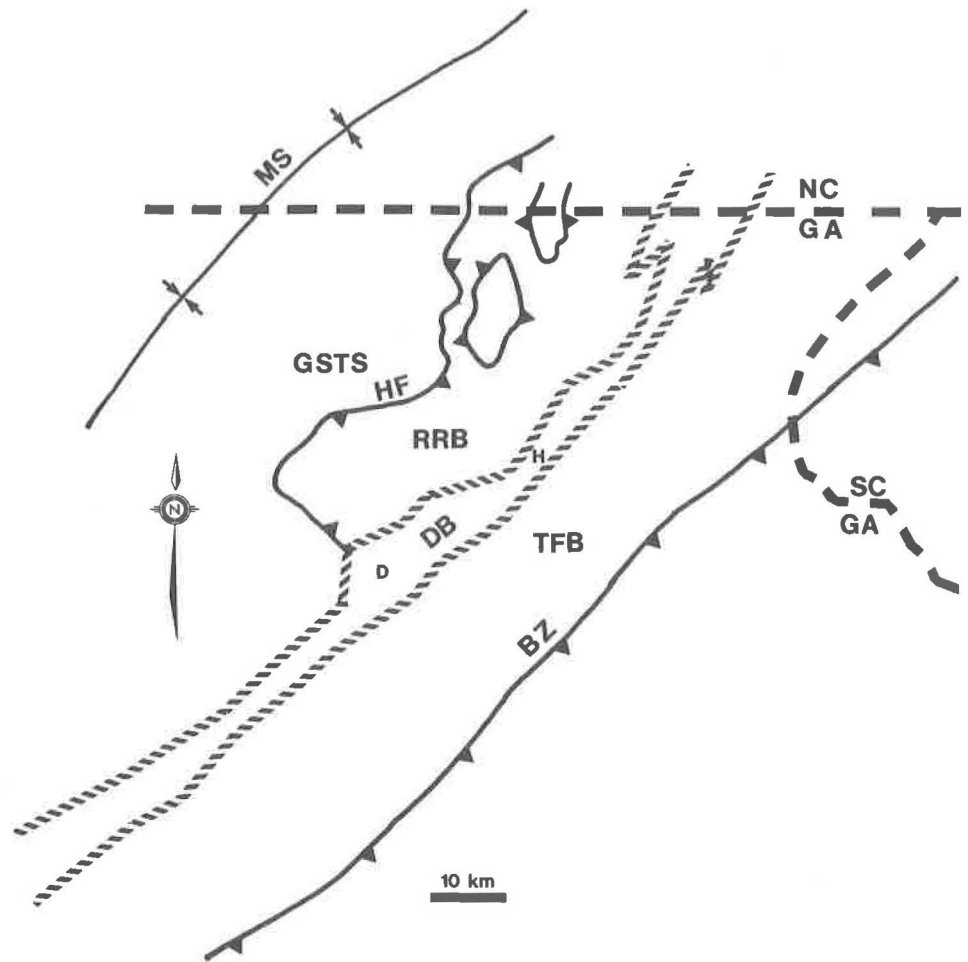


**Figure 2. General geologic map of the Eastern Blue Ridge in northeast Georgia. DB = Dahlongea Belt; RRB = Richard Russell Belt; TFB = Tallulah Falls Belt; GSTS = Great Smoky Thrust Sheet; HF = Hayesville Fault; BZ = Brevard Zone, and; MS = Murphy Syncline. Also shown for reference are the towns of Dahlongea (D) and Helen (H). Modified after Nelson (1985).**

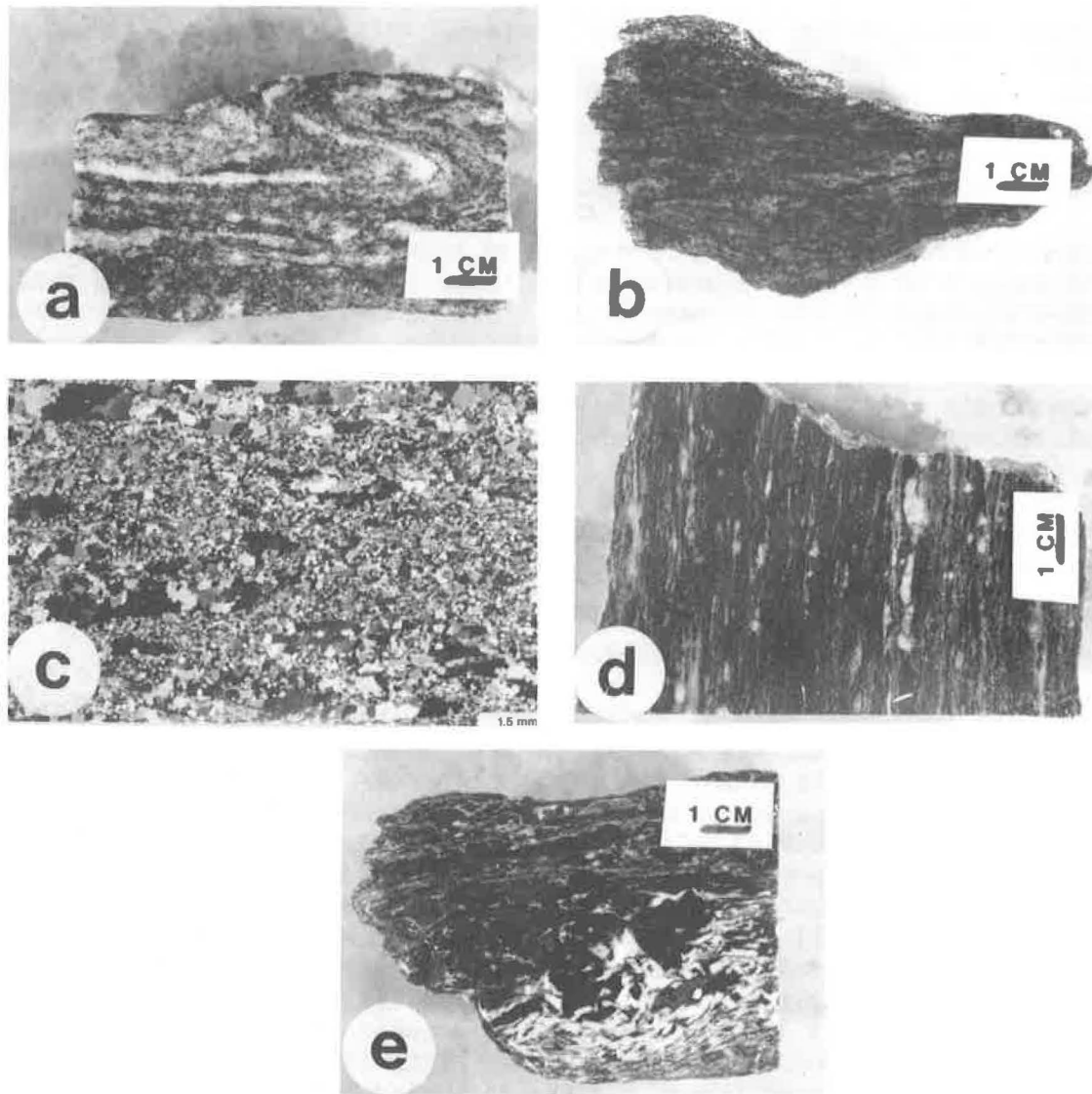


**Figure 3. Rocks of the Dahlongega Belt and flanking belts. A, Coarse-grained migmatitic quartz-biotite-plagioclase gneiss from the Tallulah Falls Belt. B, Psammitic schist from DB near Helen showing "pinstripe" texture defined by biotite laminae. C, Quartz-ribbon textures in psammitic schist from DB east of Helen. Rock consists of polycrystalline quartz ribbons in a much finer-grained quartz-plagioclase-biotite matrix. D, Medium-grained, well-foliated banded amphibolite from Creighton-Franklin Mine. Hornblende occurs as oriented needle-like grains in dark, amphibole-rich layers. E, Amphibolite from southeast margin of Dahlongega Belt near Lake Allatoona. Reduction of grain size and production of a penetrative schistosity is apparent.**

of 6.5 to 7.0 kb (Absher and McSween, 1985).

The entire sequence of rocks of the Eastern Blue Ridge has been thrust over autochthonous Precambrian strata of the North American miogeocline, as evidenced by the presence of windows through the high grade crystalline rocks of the Hayesville thrust sheet, in which Great Smoky Group strata are exposed (Nelson, 1985). Movement along the Hayesville Thrust is generally considered to have been pre-metamorphic, but there must have been some later displacement either along the Hayesville Fault or some unrecognized parallel structure (see below). This movement probably occurred during Alleghanian thrusting (Albino, 1987; Vauchez and Dallmeyer, 1989).

In northeast Georgia the Hayesville Thrust Sheet appears to be a composite nappe consisting of a stack of thinner thrust sheets. Evidence in support of this interpretation includes inverted thermal gradients in several areas in the Richard Russell Belt and its extension into North Carolina (Albino, 1987; Tso, 1987; Kittelson and McSween, 1987) and the occurrence of thin fault-bounded slivers of basement gneiss exposed around the margin of the Tallulah Falls Dome (Stieve et al., 1988). The pattern of metamorphic isograds around the Tallulah Falls Dome, with lower kyanite zone succeeded outward by upper kyanite and upper sillimanite zones (Hatcher, 1973), is indicative of an inverted metamorphic gradient, providing another piece of evidence supporting correlation of the Richard Russell and Tallulah Falls Belts.

#### THE DAHLONEGA BELT

The Dahlonega Belt is defined by: 1) its straight trend, and the parallelism between its boundaries and orientation of foliation and lithologic contacts within the belt; 2) better developed foliation and lineation, as compared to the flanking rocks; 3) low metamorphic grade compared to the flanking belts; 4) occurrence of felsic plutons and dikes, as well as felsic gneisses within the belt and along its southeast margin; 5) occurrence of abundant amphibolite, and; 6) occurrence of numerous gold deposits and a small number of massive sulfide bodies. The Dahlonega Belt was considered a zone of shearing by early workers in the area (Jones, 1909; Crickmay, 1952; Furcron and Teague, 1945), but has more recently been described as a largely intact stratigraphic sequence (Hatcher, 1979; McConnell, 1980; McConnell and Abrams, 1983, 1984, 1988; German, 1985, 1988), or as a pile of thrust sheets, including melange units (Higgins et al., 1984, 1988).

#### Rock Types

Rock types in the Dahlonega Belt are similar to those in flanking areas, dominantly psammitic gneiss, micaceous schist and gneiss, amphibolite, and lesser amounts of ultramafic rock. The greater proportion of amphibolite in the Dahlonega Belt, as well as the occurrence of felsic igneous rocks are points of dissimilarity. Small amounts of Fe- and Mn-rich metasediments are also locally abundant in the Dahlonega Belt (McConnell and Abrams, 1983, 1984; German, 1985, 1988).

Psammitic gneiss or semi-schist is the most abundant rock type. It is generally fine- to medium-grained and consists mainly of quartz,

plagioclase ( $An_{20}$ ), and biotite, with variable amounts of muscovite, garnet, clinozoisite, ilmenite, and locally magnetite or pyrrhotite. It has a well-developed foliation defined by the orientation of biotite flakes, thin mica seams, and millimeter- to centimeter-scale compositional banding (Figure 3B). Folding of this fabric is common on scales ranging from a few centimeters to several tens of centimeters. The folds are typically isoclinal, and some 'eye' patterns typical of sheath folds have been observed. Muscovite is quite variable in abundance, with more muscovite in gneisses from the southeastern part of the Dahlongega Belt (note that muscovite also increases along strike to the southeast as will be discussed below). In many samples muscovite is obviously late-formed, as it is partly pseudomorphous after biotite or occurs as unoriented poikiloblastic flakes in strongly foliated gneiss. Quartz occurs both as small xenoblastic grains and as large ribbon-like aggregates in a finer-grained quartz-plagioclase-biotite matrix (Figure 3C). The polycrystalline ribbons correspond to Type 2A of Bouiller and Boucher (1978). Garnets are typically well-formed, and are euhedral against biotite; unusual discoidal garnets, which are much thinner perpendicular to foliation than they are wide, are locally common. Garnets of the Dahlongega Belt are richer in CaO and MnO than those in the flanking belts (Albino, unpub. data).

Mica schist is coarser-grained than psammitic rocks, and is essentially a quartz-biotite rock with minor plagioclase and muscovite. Locally muscovite is dominant, and garnet, staurolite and/or kyanite may be present. Muscovite occurs mostly as thin blades later than, and partly replacing biotite laths. Aluminosilicate minerals occur as porphyroblasts or poikiloblasts, and locally reach sizes of up to 3-4 cm. Rocks with abundant aluminosilicates in some instances contain small amounts of dark blue-green hornblende as ragged, diffuse poikiloblasts. The mica schists are well-foliated with fabric defined by orientation of the mica sheets and locally by fine-scale compositional banding. Folding and crumpling of the main fabric is common, as are shear bands. Garnet, and less commonly staurolite, poikiloblasts commonly have internal inclusions in trails discordant to the foliation external to the porphyroblasts suggesting syn-metamorphic deformation as described elsewhere by Bell et al. (1986).

Amphibolites are abundant in the Dahlongega Belt. They occur as persistent units hundreds of metres thick, as pods with strike lengths of metres to a few hundred metres, or as bands, as thin as a few cm, in micaceous or psammitic metasediments (McConnell, 1980; Gillon, 1982). Amphibolites are locally banded, and consist of plagioclase ( $An_{20-35}$ ), dark green to blue-green hornblende, and variable amounts of quartz, ilmenite and clinozoisite. They are typically well foliated, and possess a strong lineation defined by long axes of hornblende prisms (Figure 3D). Polycrystalline quartz ribbons with strong crystallographic preferred orientations are common in quartz-rich varieties. Coarse-grained granoblastic amphibolite occurs in small pods throughout the belt, and locally the more typical, medium-grained foliated amphibolite may be seen to have formed through shearing of these rocks (Figure 3E).

Small bodies of metamorphosed ultramafic rock occur adjacent to some amphibolites (e.g. Gillon, 1982), and locally with aluminous schist zones in the metasedimentary sequence. These are either olivine- or anthophyllite- and chlorite-rich. The different mineral assemblages probably represent primary chemical differences, with anthophyllite-rich

rocks derived from pyroxenites.

Felsic to intermediate igneous rocks are an important component of the Dahlongega Belt, and plutonic rocks identical to those in the Dahlongega Belt occur in the Tallulah Falls Belt along its boundary with the Dahlongega Belt. There are two general types of felsic rocks in the Dahlongega Belt, felsic gneisses and massive to foliated cross-cutting intrusive bodies. Felsic gneisses are pervasively foliated, strongly recrystallized and contain metamorphic minerals such as garnet and hornblende similar to those found in adjacent rocks; such minerals are absent in the cross-cutting intrusive rocks, which, although commonly foliated, are mineralogically similar to typical plutonic rocks.

Felsic gneiss occurs mostly as discontinuous lenses along linear belts as much as 20 km in length, with individual lenses from a few metres to > 100m thick, and with strike lengths of tens of metres to a few kilometres. The Barlow Gneiss (German, 1988) occurs principally near Dahlongega, and contains ovoid, 3-6 mm long blue quartz 'eyes' and plagioclase porphyroclasts in a matrix of quartz, plagioclase, biotite, and minor clinozoisite and sphene or ilmenite (Figure 4A). Similar rocks with blue quartz eyes occur at the Charles Mine in Forsyth County.

The Galt's Ferry Gneiss (McConnell, 1980; McConnell and Abrams, 1984), occurs in the southwest part of the Dahlongega Belt. Quartz eyes are not common, and the rocks consist of granoblastic plagioclase and quartz, with euhedral garnet crystals and radiating sheaf-like aggregates of hornblende along foliation planes (Figure 4B). Clinozoisite is locally abundant, and occurs as monominerallic patches as large as 10 cm, as well as disseminated throughout the rock. The Galt's Ferry Gneiss also differs from the generally homogeneous Barlow Gneiss in the common presence of compositional banding, defined by variation in hornblende content.

Both the Barlow and Galt's Ferry Gneisses are well-foliated to locally mylonitic in appearance. Where probable primary igneous textures are preserved, the felsic gneisses are typically medium to coarse-grained hypidiomorphic-granular rocks, similar to typical granitic intrusive rocks. The strong foliation in the felsic gneisses, combined with the abundance of typical metamorphic minerals in the Galt's Ferry Gneiss indicates that these rocks were part of the Dahlongega Belt during deformation and metamorphism. This has led McConnell and Abrams (1983, 1984) and German (1988a, 1988b) to suggest that they are of felsic flows or sub-volcanic intrusions. On the other hand, the petrographic and geochemical similarity between the Galt's Ferry Gneiss and the Cavender Creek Pluton (Cook et al., 1984) near Dahlongega (Albino, unpub. data), which, although recrystallized and containing metamorphic hornblende and garnet, clearly truncates foliation at its contact with the Dahlongega Belt metasediments, argues for a syn-tectonic intrusive origin for the Galt's Ferry Gneiss. As well, the Barlow Gneiss at the Barlow Mine, its type locality, truncates foliation in amphibolite (Pardee and Park, 1948), demonstrating the intrusive origin of this unit.

In addition to the felsic gneisses there are several varieties of intrusive rocks in the Dahlongega Belt. The least felsic variety is diorite to granodiorite which occurs along the southeast margin of the Dahlongega Belt in close association with two-mica granite containing sparse magmatic garnet. It is medium-grained, generally weakly foliated, and consists of 2 to 3 mm subhedral to euhedral plagioclase in a matrix of biotite, quartz, plagioclase ± orthoclase and minor sphene, apatite and zircon. Associated granites are white, very leucocratic and range from

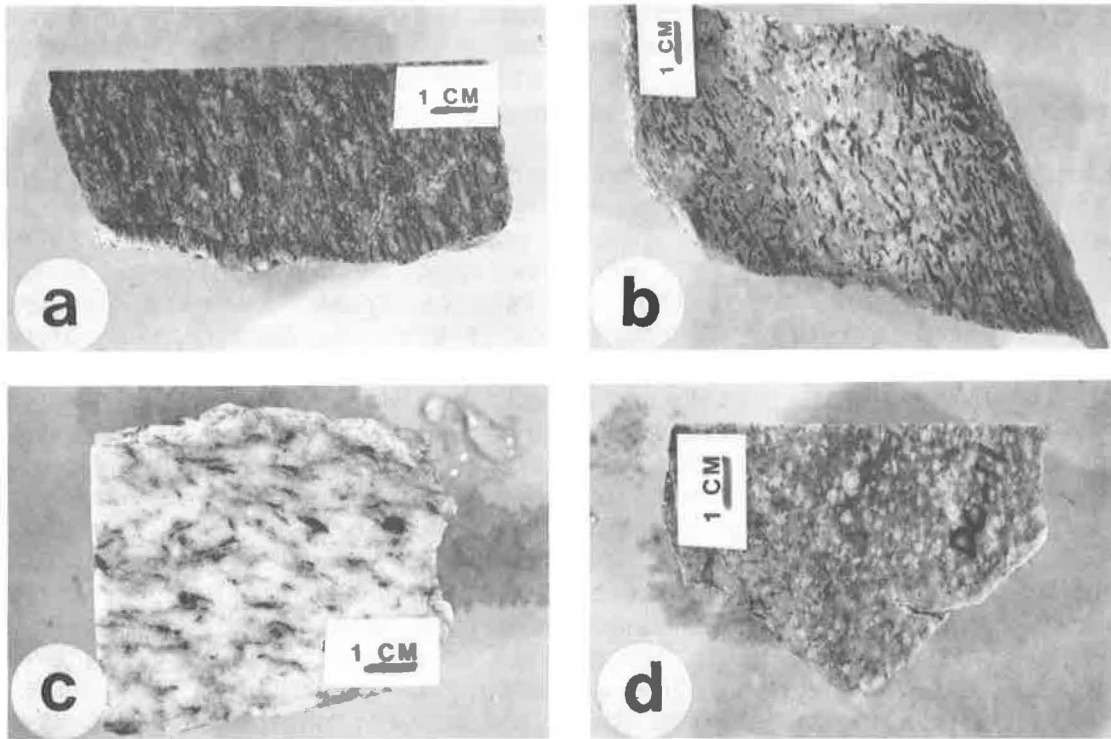


**Figure 4. Igneous rocks of the Dahlenega Belt. A. Barlow Gneiss from small branch off Cane Creek southwest of Dahlenega. Blue quartz eyes are in plagioclase-quartz-biotite groundmass. B. Galt's Ferry Gneiss, Lake Allatoona. Rock consists of dark grey ribbon-like quartz grains in pale grey to white plagioclase-quartz groundmass. Abundant coarse-grained black hornblende occurs in sprays and rosettes oriented parallel to foliation. C. Coarse-grained, weakly foliated trondhjemite from Yahooola Creek near Dahlenega Consolidated Mine. D. Albite and biotite-porphyritic trondhjemite from dike at Dahlenega Consolidated Mine. Sample is slightly deformed.**

weakly foliated, southeast of the Dahlongega Belt, to quartz ribbon mylonite within the belt. Granite consists of quartz, 1 to 2 cm microcline phenocrysts, plagioclase and muscovite. Biotite occurs locally, and pink to red garnet is present in trace amounts. Southeast of the Dahlongega Belt the granite is in very elongate bodies as much as 20 to 30 km in length, oriented parallel to the Dahlongega Belt-Tallulah Falls belt contact. These bodies are variably referred to as Hightower Granite (Crickmay, 1952), Rabun Gneiss (Hatcher, 1974), or Yonah Gneiss (Gillon, 1982). Within the Dahlongega Belt granite is as thin, discontinuous bands of strongly deformed to mylonitic granite near the SE margin of the belt, and as irregular pods of weakly-deformed, coarse-grained to pegmatitic granite throughout the Dahlongega Belt. As a result of its coarse-grained nature and the abundant microcline phenocrysts, kinematic indicators such as S/C relationships and asymmetric tails like those described elsewhere by Simpson and Schmid (1983 and Passchier and Simpson (1986) are well-developed in the more deformed bodies. Chemically, these rocks are characterized by only moderate  $\text{SiO}_2$  ( $\leq 70\%$ ), high  $\text{K}_2\text{O}$  and  $\text{K/Na}$ , and low to very low contents of high field strength elements such as zirconium, niobium and yttrium (Albino, unpub. data).

The third variety of intrusive rock in the Dahlongega Belt was observed only in the valley of Yahoola Creek near the Dahlongega-Consolidated property. It is a coarse-grained, equigranular biotite-muscovite trondhjemite to granodiorite. It consists of abundant sodic plagioclase, quartz, biotite and muscovite. Microcline is present locally (Figure 4C). The muscovite is at least partly secondary, as it partially pseudomorphs biotite. Trondhjemite crops out in two irregular oval bodies which are not elongate parallel to the Dahlongega Belt trend. This, combined with the generally weakly foliated nature of the rocks, suggests that it was intruded fairly late in the deformational history of the Dahlongega Belt. Locally, however, it is intensely foliated, and grades into fine-grained quartz-muscovite-pyrite schist. Chemically the trondhjemite is similar to the granite described above in terms of  $\text{SiO}_2$  content and abundance of HFS elements, but has much higher  $\text{Na/K}$  and contains less barium and rubidium, and more strontium than the granite (Albino, unpub. data).

The fourth variety of intrusive rock in the Dahlongega Belt is fine-grained plagioclase porphyritic trondhjemite, chemically similar to coarse-grained trondhjemite (Figure 4D). Porphyritic trondhjemite occurs as dikes ranging from tens of cm's to 2-3 metres in width, mostly at the Dahlongega Consolidated property along Yahoola Creek, but also in a single undeformed dike a few metres wide in Rabun County at the northeast end of the gold belt (Hatcher, 1974). Where unaltered this rock consists of albite to oligoclase phenocrysts in a fine-grained felsitic groundmass of quartz, albite, biotite, and minor sphene. The dikes at the Dahlongega-Consolidated Mine have been folded, are foliated, and locally grade into fine-grained muscovite-albite-quartz+pyrite phyllonite. Compositionally the porphyritic trondhjemite is similar to coarse-grained trondhjemite, differing mainly in higher  $\text{SiO}_2$ , suggesting that they may be a more differentiated equivalent of the coarse-grained rock. Titanium, zirconium and yttrium are low in both varieties of trondhjemite, while rubidium, barium, and strontium are also present in slightly greater amounts. The combination of spatial relationship, similar timing with respect to gold mineralization, and their similar compositions suggest that the fine-

grained porphyritic and coarse-grained equigranular trondhjemites are part of the same igneous suite.

### Structural Geology of the Dahlongega Belt

The Dahlongega Belt has a well-developed foliation and lineation, and the linear trend of this fabric (Figure 5) is very different from the situation in flanking belts, in which foliation trends are very variable, and complex interference patterns occur on both outcrop and regional scales (Figure 5). The planar fabric within the Dahlongega Belt is defined by compositional banding on a fine (mm) to megascopic (map unit) scale and by the preferred orientation of micas and amphiboles. The sub-horizontal lineation typical of the belt is defined by the long axes of prismatic hornblende in amphibolite, shapes of elongate mica aggregates in metasediments, and orientations of fold axes. The foliation trends northeast along the belt, and northeast of Dahlongega dips very steeply to the NW or is sub-vertical. In the area around and southwest of Dahlongega the dip of the fabric changes to moderate (to steep) to the southeast. In the same area marked by the change in attitude of foliation there is a distinct widening of the belt, there is considerable folding of flexural-slip type of the Dahlongega Belt fabric, and there are more numerous zones of very fine-grained mica-rich phyllonite. This change in attitude of foliation corresponds to a change in strike of the Hayesville Fault and where the trace of the Hayesville Fault merges with that of the Dahlongega Belt (Figure 2).

The distinctive fabric of the Dahlongega Belt formed through rotation of pre-existing fabrics and pressure solution of quartz and feldspar in the northwest part of the belt, and by recrystallization during ductile shearing, particularly in the southeast part of the belt. This last mechanism was responsible for mylonitic textures, including spectacular coarse ribbons in quartz-rich amphibolites (Figure 6A). The occurrence of parallel stretching lineations and fold axes, as well as rare sheath folds (Figure 6B) are interpreted as evidence of high shear strain (Bell, 1978; Escher and Watterson, 1974; Cobbold and Quinquis, 1980), with the sub-horizontal orientation of lineations suggesting movement was essentially strike-slip in nature. There are several types of features which give an indication of the sense of shearing across the Dahlongega Belt, including S/C fabrics in granitic rocks, asymmetric quartz c-axis patterns in ribbon mylonites, 'snowball'-type garnets (Figure 7A), and local shear bands in micaceous schists (Figure 7B). All indicators suggest movement along the Dahlongega Belt was dextral.

The large size and lack of subgrains or other evidence of incomplete recovery in quartz ribbons indicate that mylonitization took place under relatively high grade metamorphic conditions (Bouchez, 1987). This conclusion is supported by the occurrence of small grains of other minerals in the ribbons, indicating grain growth and the occurrence of maxima in the quartz c-axis patterns attributable to prism slip (Bouiller and Bouchez, 1978). Well-preserved quartz c-axis patterns suggest shearing was syn- or post-peak metamorphic, as the patterns would not likely have survived prograde metamorphism.

Evidence of flattening across the belt includes widespread foliation boudinage (Platt and Vissers, 1980), common 'discoidal' garnets with short dimensions perpendicular to foliation (Figure 7C), and abundant mica

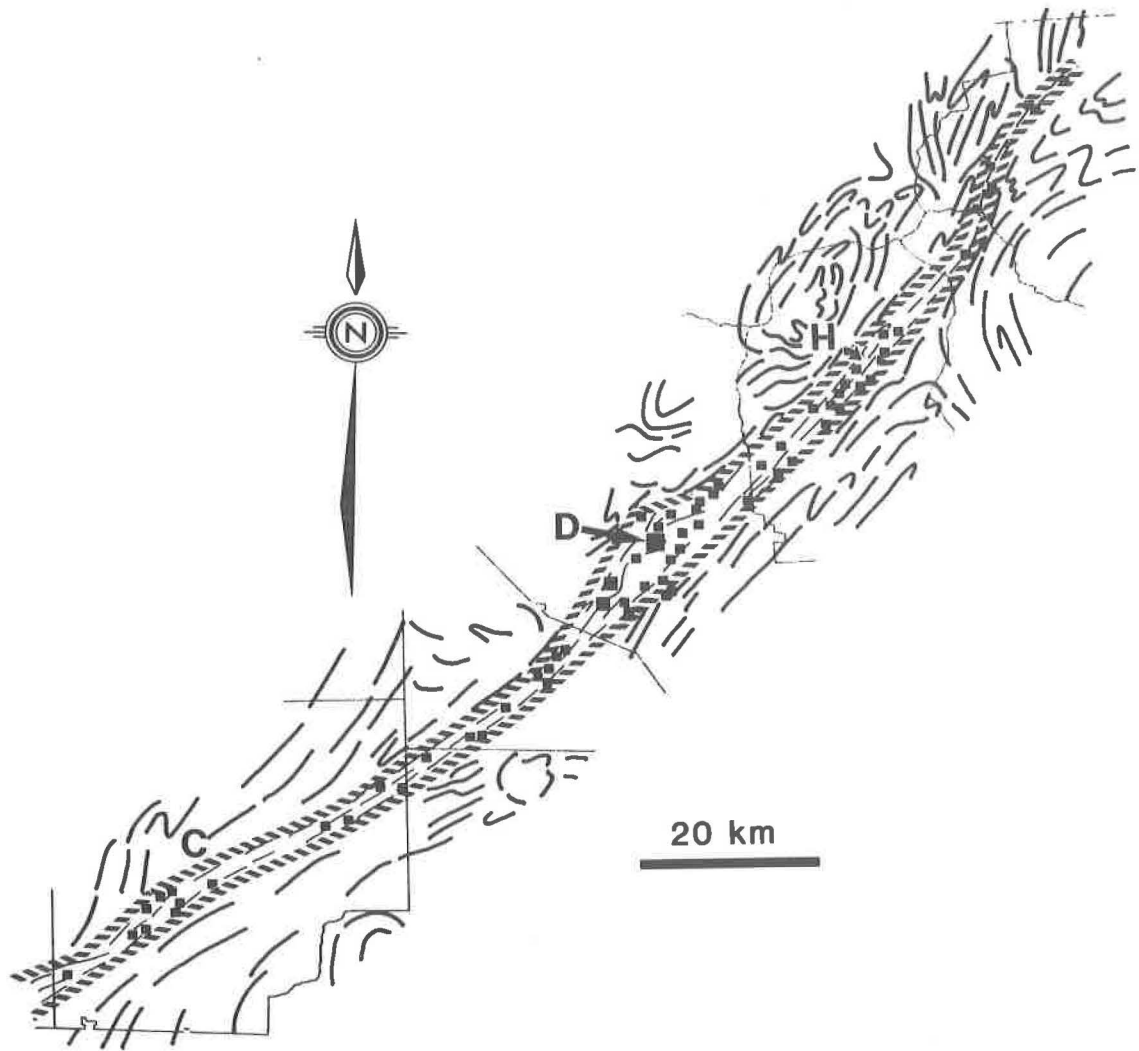


**Figure 5. Trend-surface map of the Dahlongega Belt and flanking belts. The Dahlongega Belt is outlined by the striped line; curving lines represent strike of dominant planar fabric. Solid squares indicate location of gold deposits and occurrences; locations of Canton (C), Dahlongega (D), and Helen (H) are shown for reference. Structural data compiled from numerous sources, locations of gold deposits from German (1985).**

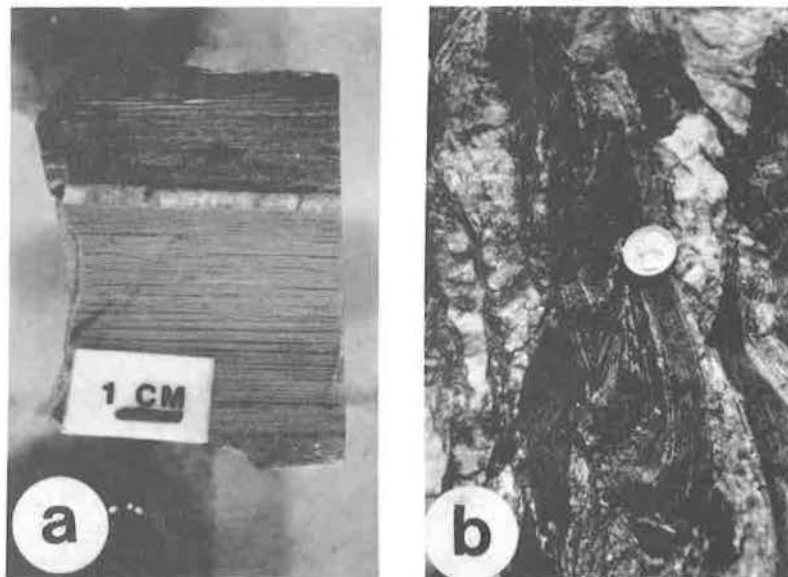


**Figure 6. Features indicative of shearing in the Dahlongega Belt. A, Ribbon mylonite, southwest of Lake Burton. Very large, continuous planar quartz ribbons are in matrix of fine-grained clinzoisite and quartz. B, Sheath fold in quartz veined amphibolite near Canton. Axis of fold is sub-horizontal, suggesting strike-slip movement along DB.**

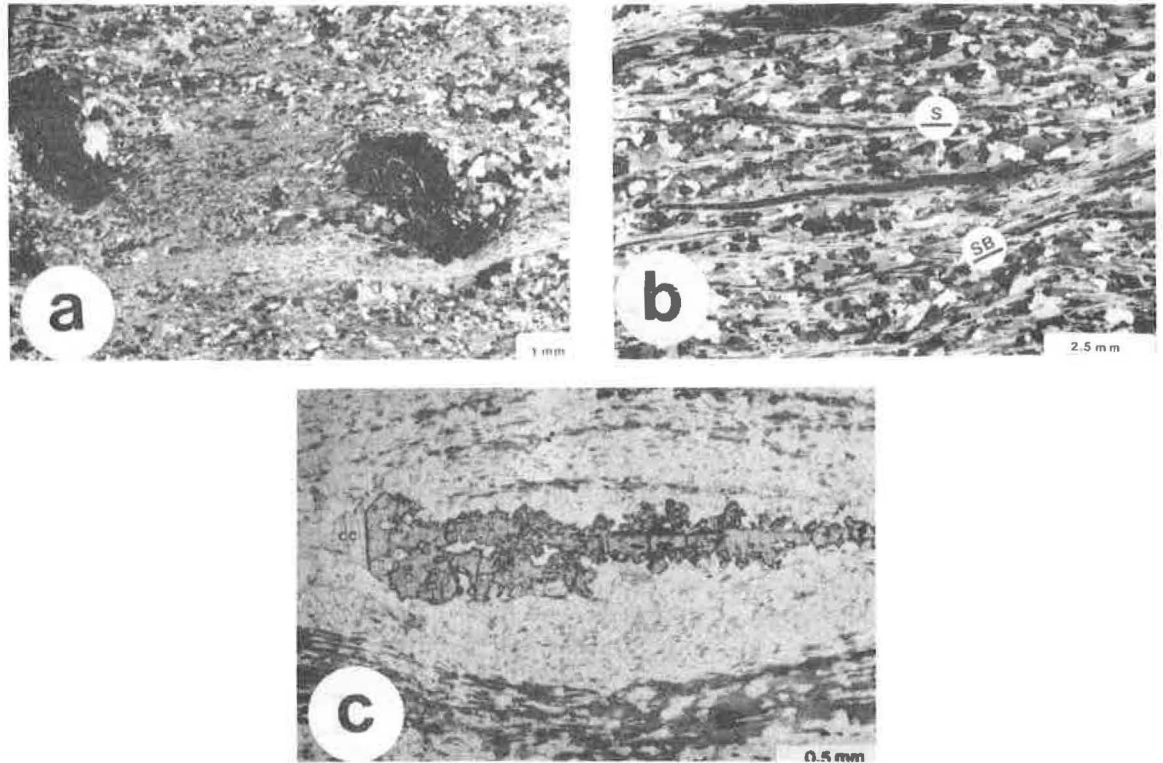


**Figure 7. Deformational features of the Dahlongega Belt. A, Rotated garnets in fine-grained psammitic gneiss, Turkey Hill Mine. Nature of inclusion trails in garnets and asymmetry of quartz pressure shadows indicate dextral shear. B, Psammitic schist, Wildcat Creek near Lake Burton. Shear bands (SB) are well-developed (Note slide is reversed from orientation in field, so actual sense of shearing is dextral). C, Discoidal garnet typical of psammitic gneisses of Dahlongega Belt, Turkey Hill Mine. Such textures are the result of shortening across the belt.**

seams, formed by pressure solution of quartz and feldspar, giving rise to the common pinstripe nature of the psammitic metasediments. This combination of shearing parallel to, and shortening across the Dahlenega Belt indicates that deformation probably occurred in a transpressive environment as defined by Sanderson and Marchini (1984).

### Metamorphism of the Dahlenega Belt

The Dahlenega Belt has traditionally been regarded as a belt of relatively low grade metamorphism (kyanite or staurolite zone) surrounded by rocks of the higher grade (sillimanite zone) Tallullah Falls and Richard Russell Belts. Sillimanite does, however, occur in incompletely retrogressed pelitic schist from several localities in the Dahlenega Belt (Gillon, 1982, this study) with muscovite and quartz and in the assemblage sillimanite-almantine-biotite, which suggests a temperature of 525° to 550° (Figure 8). This early, highest temperature assemblage was succeeded by kyanite-almantine-biotite and staurolite-garnet-biotite. This sequence of assemblages suggests that the retrograde P-T path was either isobaric or followed a cooling path more or less parallel to a normal orogenic geothermal gradient (Figure 8), indicating retrogression was not related to uplift and decompression. In the latest stages of retrograde metamorphism, staurolite was partly replaced by muscovite, and locally abundant pale green chlorite crystallized in the pressure shadows around garnets. Pressure and temperature during early stages of retrograde alteration were more than 5 kb and 500° to >550°C based on the garnet-biotite thermometer of Thompson (1976) and Ghent's (1976) garnet-plagioclase geobarometer (Albino, unpub. data). This pressure represents conditions during the early stages of retrogression when kyanite+garnet were stable.

Retrograde alteration in rocks flanking the Dahlenega Belt is manifested by the appearance of muscovite, which was not part of the stable assemblage during peak metamorphism. Muscovite growth was in part at the expense of garnet, and garnets in the Richard Russell Belt are commonly partly surrounded by symplectic muscovite-biotite-quartz intergrowths. Retrograde temperatures of 525°-575°C have been obtained for these samples (Albino, unpub. data) using the garnet-biotite geothermometer of Thompson (1976).

Retrograde alteration of amphibolites is pervasive, and resulted in the formation of clinozoisite-bearing assemblages, in contrast to the upper amphibolite grade metabasites of the flanking belts which contain very calcic plagioclase (up to An<sub>70+</sub>) and no epidote-group minerals. Later stages of retrogression are commonly associated with formation of carbonate-rich assemblages, and is largely the result of infiltration of CO<sub>2</sub>-rich fluids.

The rare ultramafic rocks of the Dahlenega Belt also provide some important data on the temperature history of the area. The occurrence of anthophyllite in these rocks indicates that they were at one time subjected to temperatures of 600°-650° or higher (Evans and Trommsdorff 1970). The anthophyllite has been largely replaced by mixtures of talc, serpentine after metamorphic olivine, and calcic amphibole. The existence of the early anthophyllite, and the high temperatures it implies, are important evidence of an early stage of high grade metamorphism in the Dahlenega Belt. In the part of the Dahlenega Belt southwest of

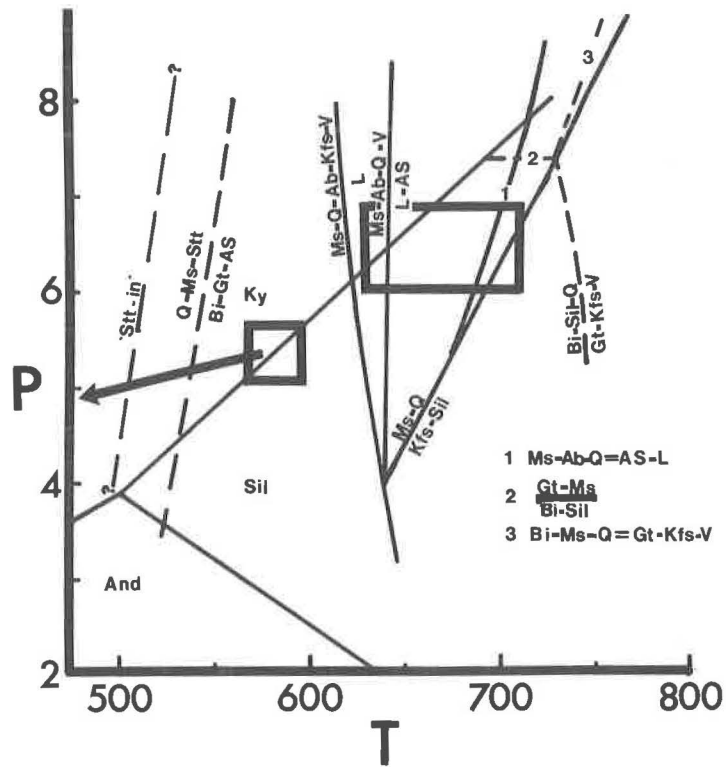


Figure 8. Pressure-temperature grid showing locations of reactions relevant to prograde and retrograde metamorphism in the Dahlenega Belt and flanking belts. Boxes indicate peak and retrograde metamorphic conditions in the Richard Russell and Tallulah Falls Belts calculated from mineral compositions and inferred from assemblages; arrow represents inferred path of retrogression in the Dahlenega Belt based on mineral compositions and assemblages.

Dahlonaga the degree of retrograde metamorphism increases, and there are zones of very fine-grained, intensely foliated phyllonite, which have mineral assemblages typical of greenschist to lowest amphibolite grade metamorphism, such as muscovite-chlorite-biotite and hornblende-epidote-albite. The phyllonitic rocks with these low grade assemblages sometimes contain shear sense indicators demonstrating northwest-directed thrusting, contemporaneous with retrogression. This low grade metamorphic event may be Alleghanian, and based on field relationships is later than most or all of the gold deposits of the Dahlonaga Belt.

#### GOLD DEPOSITS OF THE DAHLONEGA BELT

Gold deposits of the Dahlonaga Belt include: 1) broad zones of very low-grade ore; 2) medium to narrow, generally tabular pyritic quartz veins or sets of sheeted veins; 3) sets of thin sheeted quartz veins in trondhjemite dikes, and; 4) narrow high grade quartz veins containing abundant visible gold. Detailed descriptions of many individual properties are given by Pardee and Park (1948), Jones (1909), and Yeates et al. (1896).

Deposit of the first type could generally be mined only where deep weathering had resulted in formation of thick saprolite horizons amenable to hydraulic mining. These deposits have, however, been a significant source of gold in the Dahlonaga Belt, as they include the deposits of Findley Ridge and the Barlow Cut near Dahlonaga. Gold occurs in generally tabular zones containing abundant pod-like quartz veins (Figure 9A), containing a few percent pyrite and traces of other sulfides, in a wide zone of mica-, pyrite/pyrrhotite-, and locally carbonate-rich (altered) rocks. Gold content of unweathered rocks are low, typically less than 100 ppb. This low primary grade argues that supergene migration of gold, as well as freeing of refractory gold during sulfide breakdown, contributed to the formation of these deposits (Lesure, 1971).

The second type of deposit, in which gold occurs in tabular quartz veins (Figure 9B) or zones of tabular sheeted veins containing considerable pyrite or arsenopyrite, has also been a major source of gold in the Dahlonaga Belt, as it includes the Creighton-Franklin, Cherokee and several other important producers in the area. Ore shoots within these veins tend to be steeply plunging rods with plunge length much greater than strike length, in which the veins are thicker and richer than average (Pardee and Park, 1948). Gold grades in these veins are moderate, ranging from a few ppm to as much as 30-40 ppm, greater abundances occurring in sulfide-rich parts of veins. In some deposits, notably the Creighton-Franklin Mine, sulfide-bearing wallrock adjacent to the veins contains gold in possibly economic amounts, 2-5 ppm (Table 1).

The third type of deposit, thin sheeted quartz veins in dikes, is at the Dahlonaga-Consolidated Mine, where the Knight 'Vein', an important source of ore from both surface and underground workings, is actually an intensely foliated, 2-3 m wide albite porphyritic dike, which contains abundant 3 mm to 2 cm wide glassy quartz veins parallel to the dike contact. The veins contain a few percent 1-2 mm pyrite cubes (Figure 9C) which are closely associated with gold and precious metal tellurides. Auriferous quartz veins occur in coarse-grained and fine-grained porphyritic trondhjemite at the Dahlonaga Consolidated Mine (Lindgren, 1906), flanked by zones in which biotite has been replaced by muscovite.

**Table 1. Abundances of selected ore metals in altered and mineralized samples from the Dahlongega Belt.**

SAMPLE	Au	Ag	As	Sb	Hg	W	Mo
BB-4	0.035	<5	<2	0.2	0.018	<4	12
BB-5	<0.06	<5	<2	0.3	--	<4	<5
BB-9	0.021	<5	<2	<0.2	--	<4	<5
BY-7	17.000	10	<2	<0.2	0.007	<4	<5
CF-2	7.500	<5	<2	<0.2	0.007	16	<5
CF-3	0.270	<5	<2	<0.2	--	<4	<5
CF-6	0.022	<5	<2	0.2	--	<4	<5
CF-12	1.100	<5	7	<0.2	0.005	<4	<5
CF-16	0.089	<5	<2	<0.2	--	<4	<5
CF-20	0.010	<5	<2	<0.2	--	<4	<5
CF-23	0.720	<5	<2	<0.2	--	5	5
CF-24	0.012	<5	<2	<0.2	--	<4	<5
CH-1	0.060	14	9200	3.8	0.028	<4	<5
CH-2-109	0.037	<5	410	0.3	--	<4	11
CH-2-123	<0.005	<5	33	<0.2	--	<4	<5
CH-2-130	<0.005	<5	7	0.2	--	<4	<5
CH-2-153	0.021	<5	8	<0.2	--	<4	<5
CH-2-169	<0.006	<5	310	0.3	--	<4	<5
CH-2-225	0.029	26	9300	2.9	0.007	<4	<5
CH-3-83	0.008	<5	65	0.5	--	<4	6
CH-3-120	0.041	63	34	1.1	0.021	<4	<5
CH-3-155	0.012	<5	12	<0.2	--	<4	5
CH-3-174	0.007	<5	21	<0.2	--	<4	<5
CH-3-182	0.022	<5	1400	0.5	<0.005	<4	7
CH-3-281	<0.008	<5	2600	1	0.005	5	<5
DC-1A	11.000	7	2	0.2	<0.005	<4	<5
DC-2	0.420	<5	<2	0.2	--	<4	<5
DC-3	1.900	<5	<2	0.2	0.006	<4	<5
DC-4	4.100	<5	<2	0.2	--	<4	<5
DC-10	0.200	<5	<2	<0.2	--	<4	<5
DC-11	0.810	<5	<2	0.3	--	<4	<5
DC-105	0.016	<5	<2	0.2	0.005	<4	<5
DC-108	0.025	<5	<2	0.3	0.005	<4	<5
JMV-1	0.410	<5	<2	<0.2	<0.005	<4	<5
JSV-5	0.008	<5	<2	0.3	--	<4	<5
JSV-7	<0.005	<5	2	0.2	--	<4	<5
JSV-8	<0.005	<5	<2	0.2	--	<4	<5
JSV-9	<0.005	<5	<2	0.2	--	<4	<5
RBT-2	<0.005	<5	<2	0.2	--	<4	<5
TH-2	<0.005	<5	5	<0.2	--	<4	<5
TH-4	6.400	<5	170	<0.2	0.050	<4	6
WC-3	<0.005	<5	<2	0.2	--	<4	<5
WC-9	<0.005	<5	<2	0.3	--	<4	<5
WC-14	0.005	<5	<2	0.3	<0.005	<4	<5
WC-16	<0.005	<5	<2	<0.2	--	<4	<5

All abundances reported in parts per million. Analyses by X-ray Assay Laboratories, Don Mills, Ontario. Au, Ag, As, Sb, W, and Mo analysed by INAA; Te determined by flameless AAS, and Hg by graphite furnace AAS (--- not analyzed).

BB = Battle Branch, CF = Creighton-Franklin, CH = Charles, DC = Dahlongega-Consolidated, JMV and JSV = Jones Vein/Lot 10, RBT = outcrops outside Robertstown, TH = Turkey Hill, WC = Wildcat Creek

Thin tongues of intrusive rock cut auriferous quartz veins at the White County (Pardee and Park, 1948) and the Dahlonega-Consolidated Mines, suggesting mineralization occurred essentially synchronous with plutonism.

The fourth deposit type consists of thin, high grade quartz veins containing considerable visible gold, sometimes as the only ore mineral, but also commonly with abundant galena or arsenopyrite; they commonly cross-cut schistosity of enclosing rocks. They are mostly in the vicinity of Dahlonega and include some veins of the Calhoun, Turkey Hill, and Battle Branch Mines and the Loud Mine in White County. These veins commonly are close to deposits of the first three types.

Auriferous veins of the Dahlonega belt are mostly quartz, commonly with lesser amounts of plagioclase ( $An_{20-30}$ ), calcite or dolomite, apatite, muscovite, and biotite. Hornblende, zoisite/clinozoisite, and tourmaline are common in veins hosted by amphibolite, whereas garnet is a common constituent of metasediment-hosted deposits; kyanite has been observed in gold-bearing veins at the Battle Branch (Pardee and Park, 1948) and Charles Mines (this study). The quartz ranges from white to dark grey, and is glassy to sugary. It typically shows considerable evidence of recrystallization, and in places it occurs as elongate ribbons similar to those in mylonites. Accessory vein minerals occur either along vein margins (especially apatite which occurs as pale green stubby prisms to  $>1$  cm), or along partings in the central parts of veins, commonly associated with pyrite and pyrrhotite (Figure 9B). Banding is fairly common in the larger veins, where thick pyrite-rich or garnet bands occur.

Opaque mineral assemblages are typically simple, with pyrite, pyrrhotite or arsenopyrite dominant. Where pyrite or arsenopyrite coexist with pyrrhotite, textural relationships indicate that pyrrhotite deposition was late (Figure 9D, 9E), although composite pyrrhotite-chalcopyrite blebs do occur as inclusions in gold-bearing pyrite. The common occurrence of pyrrhotite in pressure shadows (Figure 9E) is one manifestation of the paragenetic relationships among the Fe sulfides, as is the occurrence of pyrrhotite in small, discontinuous veinlets which sharply cross-cut foliation. Pyrrhotite is most common in amphibolite-hosted deposits, where it occurs in wall rock adjacent to veins, without accompanying pyrite, as well as in the veins themselves. In felsic and metasedimentary rocks pyrite is always dominant, both in the veins, where it occurs with pyrrhotite, and in the wall rocks.

Chalcopyrite is common in small amounts in the Dahlonega Belt, although rarely visible in hand specimen. It occurs entirely in close association with pyrrhotite, commonly as composite grains associated with pyrite, some of which have well-developed crystal forms (Figure 9F). This probably indicates these composite grains formed initially as intermediate solid solution ( $iss - (CuFe)_{1+x}S$ ), and that pyrite and iss were deposited contemporaneously. This assemblage is stable only at temperatures of  $>450^{\circ}C$  (Barton and Skinner, 1979).

Minor galena occurs at a number of properties (Pardee and Park), and is commonly associated with high grade ore shoots. Galena does not universally indicate high gold contents, however, as galena-bearing samples from the Battle Branch and Charles Mines, are not all enriched in gold (samples BB-4 and CH-3-120, Table 1).

Oxide minerals occur in small amounts in many Dahlonega Belt quartz veins. Ilmenite, as thin, sometimes curved plates is most common. Magnetite, as isolated euhedra and locally as masses a few cm in size, is

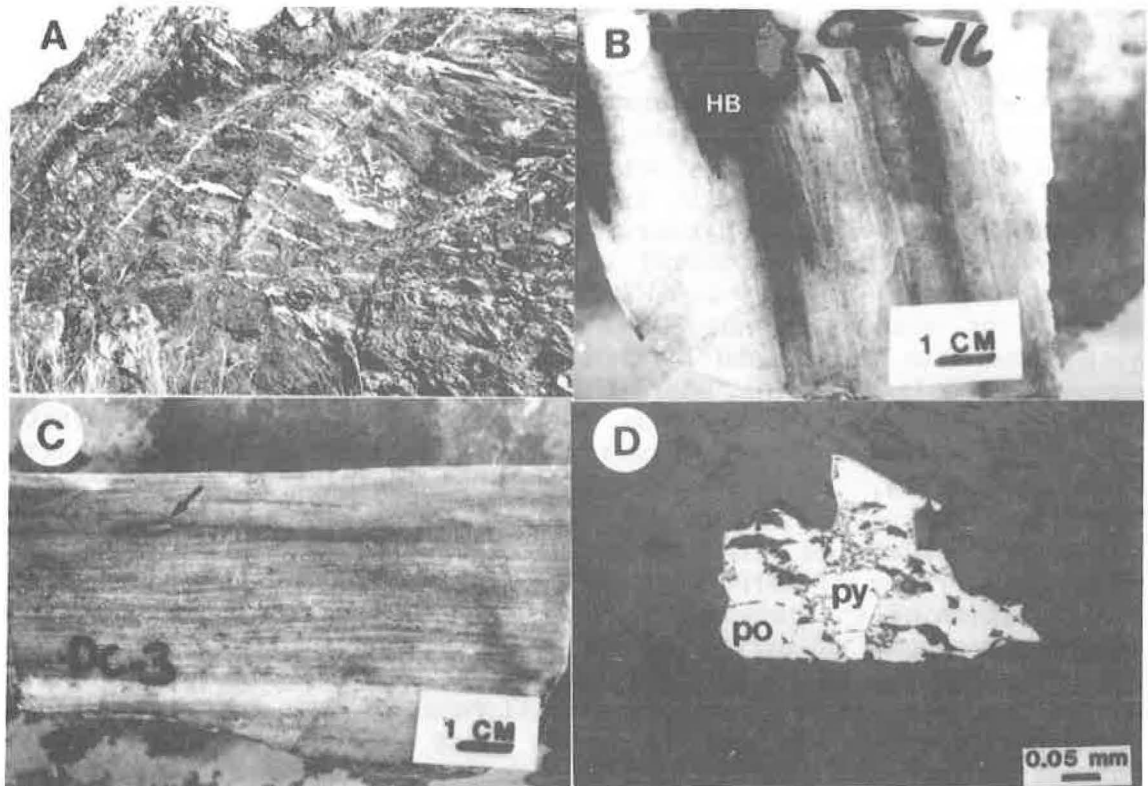


**Figure 9. Veins, ore textures and ore mineralogy of DB gold deposits.**  
**A,** Tabular zone of pod-like quartz veins in sheared and carbonatized amphibolite, near Canton. **B,** Banded quartz vein from Creighton-Franklin Mine. Vein is mainly white quartz, with dark bands of hornblende (hb), and coarse pyrite euhedra with pyrrhotite pressure shadow (arrow). **C,** Mylonitized porphyritic trondhjemite, Dahlonega-Consolidated Mine. Gold is in thin veinlets parallel to dike contacts or in euhedral pyrite grains occurring along foliation (arrow). **D,** Pyrite (py) surrounded and partly replaced by later pyrrhotite (po) in quartz vein, Creighton-Franklin Mine. (Continued on next page.)

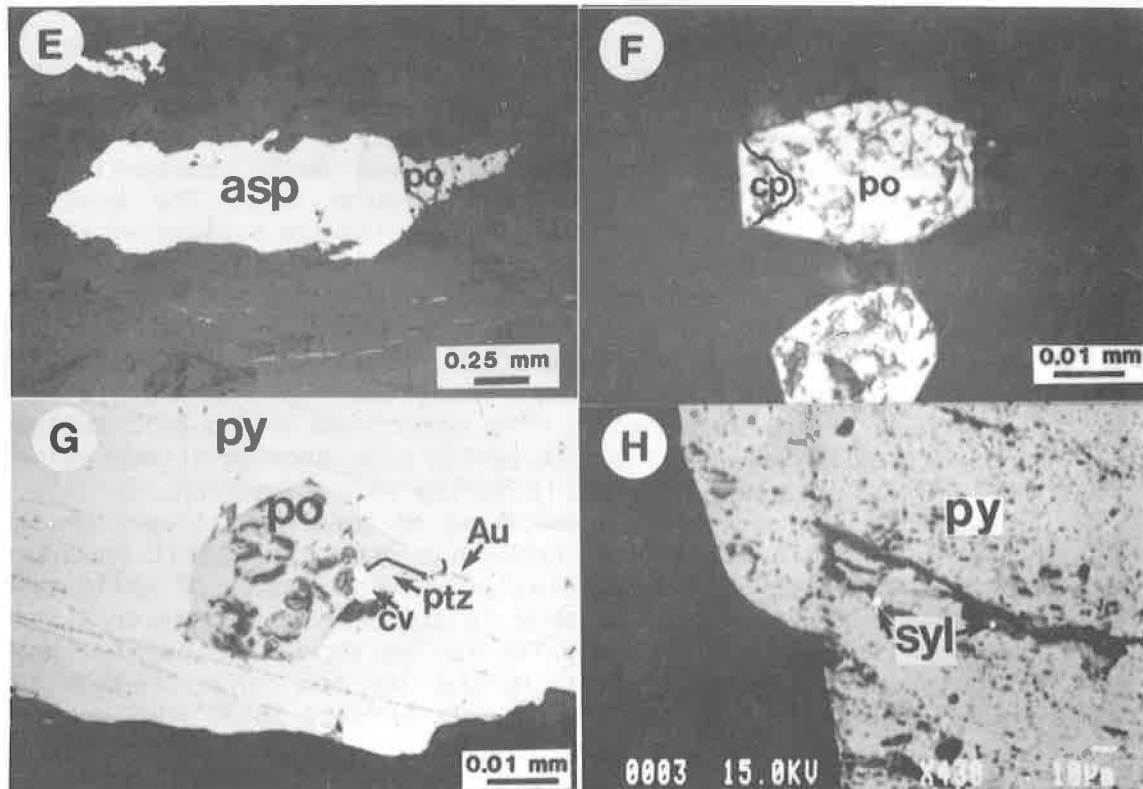


**Figure 9 (Cont.). E, Coarse subhedral arsenopyrite (asp) with pyrrhotite (po) in pressure shadow. F, Composite chalcopyrite (cp) -pyrrhotite (po) grain in quartz vein, showing apparent crystal outline, Creighton-Franklin Mine. G, Composite pyrite-chalcopyrite grain in pyrite occurring with calaverite (cv), petzite (ptz), and native gold (Au) in ore from Dahlonega-Consolidated Mine. H, Sylvanite (sylv) in fractures in pyrite, Dahlonega- Consolidated Mine. Back-scattered electron image.**

fairly widespread. Gahnite, the Zn spinel was noted by Lindgren (1906) at the Standard Mine near Dahlonega.

Gold- and gold-silver tellurides occur in most unweathered samples containing more than 1 ppm gold. These minerals are all extremely fine-grained, ranging from 1 to a maximum of 10 to 20 microns in size. In many cases they were only noted optically after they had been detected by EDS analysis. The tellurides found include petzite, calaverite, and rare sylvanite. Sylvanite was observed in a single sample in fractures in pyrite (Figure 9H), in contrast to petzite and calaverite which occur in a large number of samples. These two phases (petzite > calaverite) are typically found in composite grains with small amounts of native gold (Figure 9G). These composite grains are closely associated with pyrite, and occur either as inclusions in pyrite or along pyrite-gangue grain boundaries. Where included in pyrite the gold-bearing phases are commonly accompanied by pyrrhotite-chalcopyrite composite grains. Assay data on a limited number of samples from the Dahlonega Belt substantiate the correlation between gold and tellurium (Figure 10F). The consistent association of native gold, petzite and calaverite are suggestive that the three minerals represent the breakdown products of some mineral which has decomposed, probably on cooling. The data of Cabri (1965) suggest that the original gold-silver-tellurium phase was gold-rich petzite-hessite<sub>ss</sub>, which is likely stable only at temperatures above approximately 400°C at pressures of 4.5 to 5 kb, further confirming the high temperature origin of the Dahlonega Belt gold deposits. The occurrence of the gold-telluride mineral intergrowths as inclusions in pyrite also provide strong evidence that gold deposition was fairly early during vein formation.

In addition to recoverable quantities of gold and silver, the ores of the Dahlonega Belt contain variable but generally small amounts of arsenic, tungsten, molybdenum, and tellurium, and traces of antimony and mercury (Figure 10; Table 1). Arsenic is abundant (up to percent level) in a few localities where arsenopyrite is the main iron sulfide phase, but in most occurrences is present in the low ppm range (Figure 10B). Antimony is present in much smaller amounts (Figure 10C), and in general is strongly correlated with arsenic (Figure 10H), suggesting that it also occurs in arsenopyrite. A similar relationship is observed for mercury, which is present in even lesser quantities (Figure 10D).

There are at least two, and possibly three, distinct populations with respect to gold content (Figure 10A, E). The larger group contains gold in the range of <5 to approximately 60-100 ppb, and may itself be divisible into two sub-groups, one with gold <10 ppb, and the second containing 10 to 100 ppb gold. These groups appear to correspond to the two populations noted by Cook and Burnell (1985), with the higher grade population ecorresponding to their 'chemical sedimentary' unit. The second major group consists of 'ore' samples with gold content close to or greater than 1 ppm (Table 1, Figure 10E). The two populations which contain anomalous amounts of gold may reflect different mechanisms of gold deposition, with gold-silver telluride deposition playing an important role in the higher grade group, and gold concentration controlled by non-equilibrium processes, possibly co-precipitation with pyrite or arsenopyrite, in the low-grade group (see, for instance, Romberger, 1986). There is no correlation between gold and arsenic abundances in the sample population as a whole (Figure 10G), but if only data from gold-poor rocks is included there is a general association of gold with arsenic.

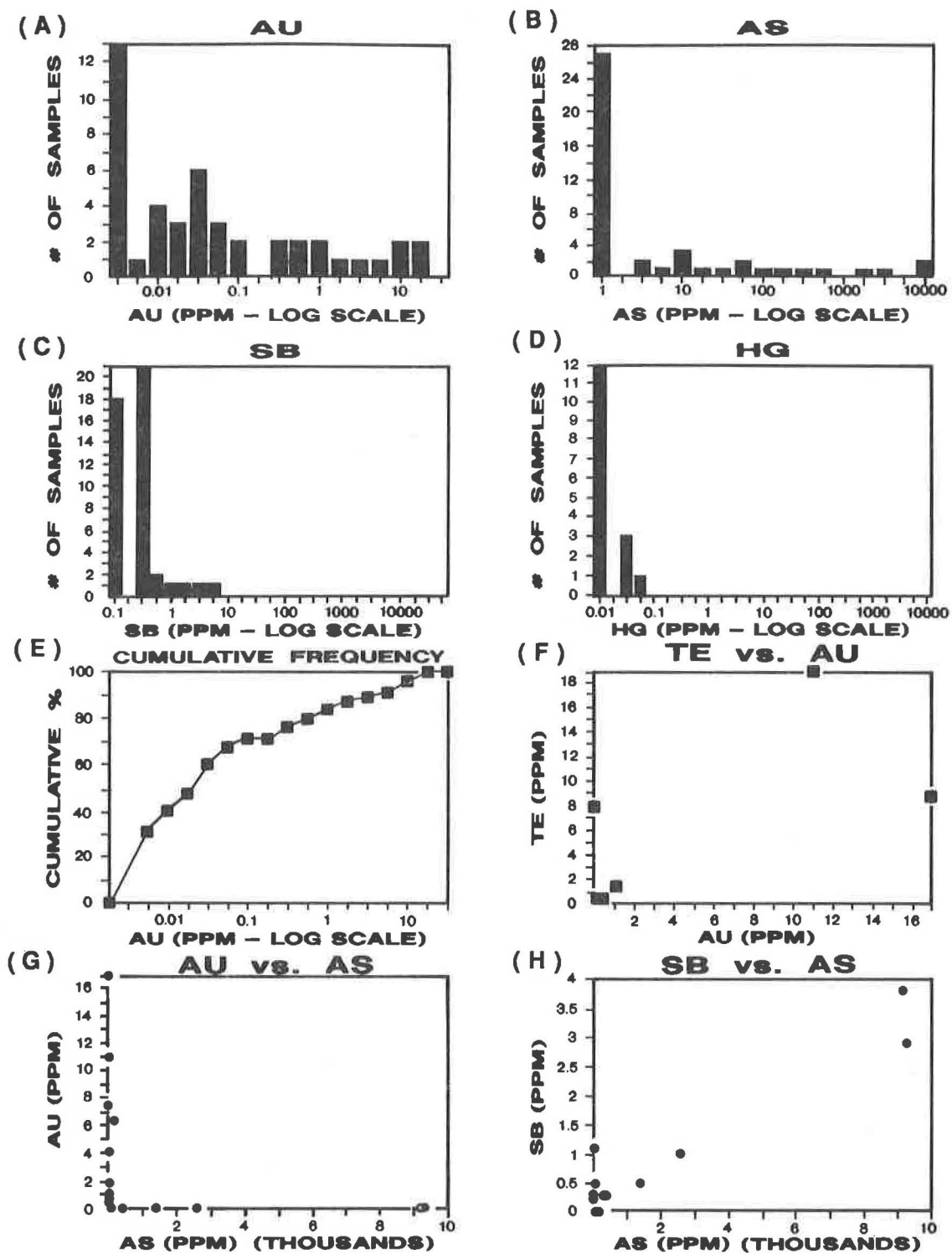


Figure 10. Metal abundances and correlations in altered and mineralized samples from the Dahlonega Belt. Data from Table 1.

## HYDROTHERMAL ALTERATION

### Mineral Assemblages and Textures

Mineralogical changes accompanying gold mineralization are greatest in amphibolites, and are much less obvious in granitic rocks and metasediments, where alteration is commonly expressed only by modal changes without appearance or disappearance of phases. Alteration was synchronous with to slightly later than retrograde metamorphism and shearing, based on the sequence of alteration assemblages in pelitic rocks, from kyanite-garnet to kyanite-staurolite to staurolite-muscovite, and on the occurrence of alteration minerals both with preferred orientations and as decussate aggregates. In selvages flanking late-formed brittle quartz-tourmaline-pyrite+pyrrhotite veins, well-developed quartz ribbons are preserved, but the matrix has been altered to biotite, muscovite, calcite and pyrrhotite and locally tourmaline, indicating that alteration outlasted mylonitization.

Alteration in amphibolites is of two types involving either CO<sub>2</sub> addition or Fe-Mg depletion. The first type (CO<sub>2</sub> addition) is restricted to the immediate vicinity of quartz veins, and is more closely related to significant gold deposits such as the Creighton-Franklin Mine. The main mineralogical changes in this type of alteration include: 1) decrease or total destruction of plagioclase; 2) increase in modal quartz; 3) increase in clinozoisite-zoisite abundance, and; 4) the appearance of biotite, calcite and/or dolomite, and pyrrhotite (Figure 11A). More locally chlorite, muscovite and tourmaline are present in altered amphibolite (Figure 11B). Textures of the altered rocks are variable, they range from well-foliated and lineated to very coarse-grained decussate, with very large sprays (>1 cm) of prismatic hornblende and clinozoisite. In a few zones carbonatization is accompanied by iron metasomatism, which has led to development of abundant Fe-silicates such as almandine and grunerite, accompanied locally by significant amounts of magnetite and/or iron sulfides.

Iron and magnesium-depleted zones are either thin zones flanking quartz veins, or broad (metres wide) zones associated with intense shearing along lithologic contacts; locally sulfide-bearing irregular quartz-clinozoisite-hornblende-magnetite veins occur in some of these zones. Although no major gold deposits appear to be related to these zones, there are small hydraulic pits in saprolite where sulfidic quartz veins occur with the altered amphibolites. The altered zones are mainly fine-grained granular quartz and plagioclase (An<sub>30-40</sub>), with variable amounts of clinozoisite (often quite abundant) and small amounts of magnetite, garnet, and hornblende. Compositions of plagioclase and hornblende are very similar to those in unaltered rocks. The main mineralogical changes are an increase in modal quartz and plagioclase, and a large decrease in modal hornblende.

Altered intrusive rocks occur at the Dahlenega-Consolidated, Barclay, and Charles Mines. At the Dahlenega-Consolidated mine auriferous quartz veins occur in both coarse-grained and fine-grained porphyritic trondhjemite. Biotite in coarse-grained trondhjemite flanking veins is partly replaced by both coarse and shreddy muscovite. Albite and muscovite are more abundant, and biotite much less abundant, in porphyritic trondhjemite near veins (Figure 11C). Locally thin biotite-hornblende-apatite veinlets cut otherwise fresh trondhjemite, but these

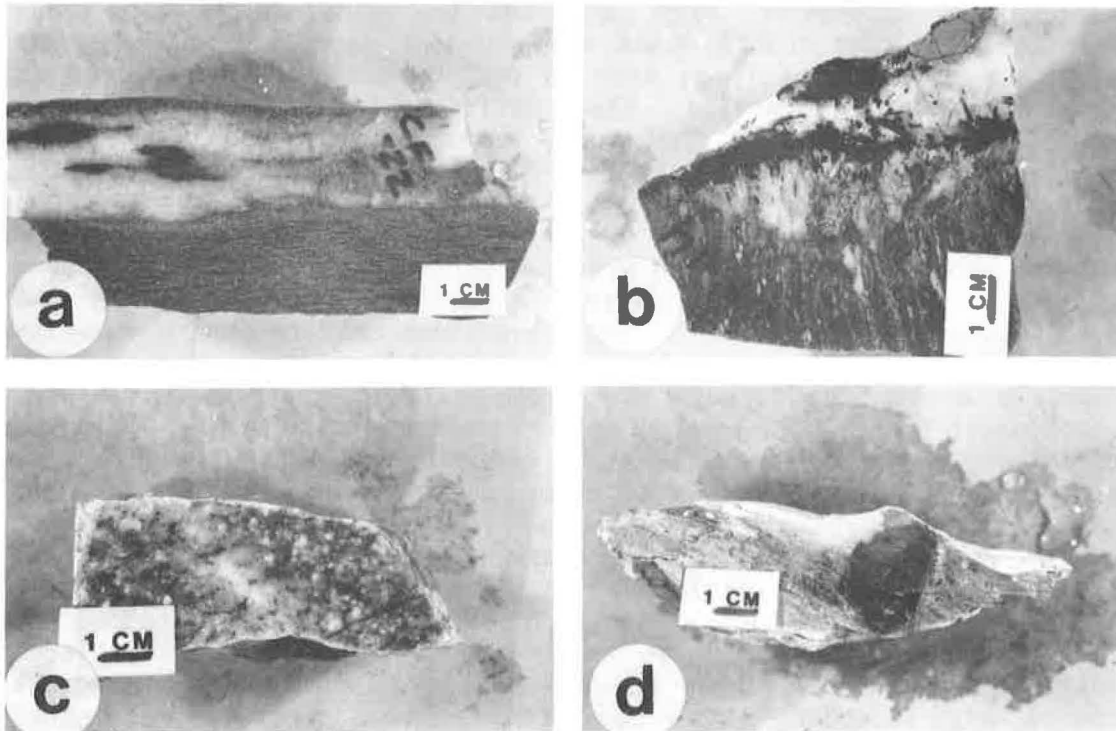


**Figure 11. Hydrothermal alteration in gold deposits of the Dahlonega Belt.**

**A, Biotite-hornblende-clinozoisite-calcite zone flanking pyritic and auriferous quartz vein with central hornblende parting, Creighton-Franklin Mine. B, Altered selvage around late, cross-cutting quartz-pyrite-pyrrhotite-tourmaline (T) vein in amphibolite, Creighton-Franklin Mine. Bleaching around vein is result of muscovite-dolomite replacement of amphibolite assemblage of hornblende and plagioclase. C, Porphyritic trondhjemite, Dahlonega Consolidated Mine, showing bleaching from an increase in albite and muscovite, and loss of biotite. Similar features also occur on larger scales. D, Coarse-grained garnet (GT) in muscovite schist, Battle Branch Mine. Garnet shows evidence of rotation, but kyanite and staurolite in fine-grained muscovite schist are randomly oriented.**

do not appear to be associated with gold-bearing quartz. Thin quartz-calcite-pyrite veinlets occur near the auriferous zones. Disseminated pyrite appears to be rare, with the exception of zones of strongly foliated quartz-muscovite-pyrite schist traceable into coarse-grained trondhjemite at the Consolidated property.

At the Barclay Mine the main auriferous quartz vein cuts the Persimmon Creek Gneiss, a recrystallized and foliated tonalite of uncertain age (Hatcher, 1974). Alteration around the vein has resulted in muscovite replacement of biotite. In the 'Quarry' Zone at the same mine gold occurs in deformed pegmatitic stringers in a gneissic tonalite matrix with no obvious mineralogical effects.

Two types of alteration occur in metasediments along the Dahlonga Belt, discrete alteration zones adjacent to veins, and broad zones containing auriferous quartz veins and abundant garnet, staurolite and kyanite, which occur mostly as syn- to post-tectonic porphyroblasts as large as 3 to 4 cm (Figure 11D). Aluminosilicate-rich zones are commonly poorly foliated, suggesting that these assemblages formed late in the deformation of the Dahlonga Belt. These rocks consist of quartz, biotite, ilmenite and garnet with or without staurolite or kyanite; plagioclase is generally absent. Quartz veins, commonly containing large garnet and locally staurolite and kyanite, occur in some aluminosilicate-rich zones. Gold is locally closely associated with the garnet and kyanite (Pardee and Park, 1948). Coarse-grained apatite occurs in veins and aluminosilicate-rich vein selvages at several localities, particularly the Battle Branch and Jones-Lot 10 Mines. Coarse-grained, highly poikiloblastic hornblende, rare in metasedimentary rocks of the Dahlonga Belt, is present locally. Late-formed chlorite and muscovite occurs in pressure shadows around porphyroblasts and as partial replacement of aluminosilicate minerals; replacement of foliation-parallel biotite by unoriented muscovite blades is also common. Quartz, calcite and pyrite are mainly restricted to veinlets, with the exception of a broad altered and slightly auriferous zone at the Charles Mine, where calcite-quartz-biotite-garnet-hornblende-plagioclase+Fe sulfide is the common assemblage.

Altered selvages flanking quartz veins are characterized abundant muscovite, with secondary muscovite as fine-grained, generally unoriented scaley aggregates, commonly with associated tourmaline. Biotite is minor in these zones, reflecting the growth of muscovite at its expense; garnet, too, commonly is corroded in appearance, apparently as a result of muscovite replacement. Minor calcite and pyrite are common and locally abundant. These zones of muscovite- and pyrite-rich schist have themselves been important sources of gold in some of the saprolite 'belts', for instance those around Helen (Jones, 1909; Yeates et al., 1896). Assays from unweathered pyritic muscovite-rich schist, however, indicate that the gold content of unweathered rock is low (Table 1).

#### Conditions of Mineralization and Composition of the Ore-Forming Fluid

Garnet-biotite geothermometry (Thompson, 1976) and garnet-plagioclase (+quartz and  $Al_2SiO_5$ ) geobarometry (Ghent, 1976) indicate that retrograde metamorphism and alteration took place at temperatures of  $>500^\circ C$  and pressures of 5kb. The common occurrence of pyrite or arsenopyrite with pyrrhotite, iss, ilmenite and magnetite indicate that the mineralizing fluids had moderate values of  $f_{O_2}$  and  $f_{S_2}$  (Barton and Skinner, 1979). The

presumed occurrence of  $\text{iss}+\text{pyrite}$ , and gold-rich  $\text{petzite-hessite}_{\text{ss}}$ , also support a high temperature origin for the sulfides and gold mineralization (see above).

The mineral assemblages in altered amphibolites suggest that the ore-forming fluid was  $\text{CO}_2$ -rich. Calculations based on a temperature of  $550^\circ\text{C}$  and a pressure of 5 kb indicate that the fluids has an  $X_{\text{CO}_2}$  as high as 0.25 (Hoschek, 1980) in order to form the dominant  $\text{biotite-hornblende-calcite-quartz}$  assemblage (Figure 12). The later and less abundant  $\text{muscovite-chlorite-dolomite-quartz}$  zones reflect alteration either by more  $\text{CO}_2$ -rich fluids or at a lower temperature (Figure 12). The low abundance of carbonate in altered zones in other rock types reflects the role of bulk composition in governing alteration mineralogy; only calcium-rich rocks like the amphibolites will tend to be carbonatized at the temperatures prevalent in this area. Alteration of  $\text{quartzofeldspathic}$  rocks such as  $\text{trondhjemite}$  or  $\text{tonalite}$  and  $\text{psammitic}$  metasediments consisted of  $\text{H}^+$  metasomatism, expressed by the formation of  $\text{muscovite}$ , with attendant loss of potassium and possibly some sodium. The potassium gained by  $\text{biotite}$  formation in some amphibolites may have been derived from the metasedimentary rocks in this way. The prevalence of  $\text{H}^+$  metasomatism as an important form of alteration in the Dahlonaga Belt gold deposits is a result of the temperature dependence of reactions between white micas ( $\text{muscovite}$  or  $\text{paragonite}$ ) and feldspars (Meyer and Hemley, 1967), because, at a constant  $\text{K}^+/\text{H}^+$  (or  $\text{Na}^+/\text{H}^+$ ), formation of micas will be favored over feldspars with decreasing temperature. That is, if a fluid in equilibrium with  $\text{muscovite}$  and  $\text{albite}$  at a given temperature is allowed to react with a rock at a lower temperature (but with  $\text{K}^+/\text{H}^+$  held constant), the result will be  $\text{muscovite}$  replacement of  $\text{feldspar}$  (or  $\text{biotite}$ ), such as is seen in the Dahlonaga Belt and other gold deposits in metamorphic belts (Weir and Kerrick, 1987). The occurrence of  $\text{muscovite}+\text{feldspar}$  as the common assemblage in these rocks indicates that the mineralizing fluid was likely slightly acid to neutral (Meyer and Hemley, 1967).

The lesser abundance of carbonate in altered rocks of the Dahlonaga Belt, as compared to  $\text{greenschist-hosted}$  Mother Lode-type deposits, is explained by the relationship between temperature and equilibrium  $X_{\text{CO}_2}$  for mixed volatile reactions on isobaric  $\text{T}-X_{\text{CO}_2}$  sections (Figure 12). At higher temperatures carbonatization equilibria are displaced to higher values of  $X_{\text{CO}_2}$ , and therefore  $\text{calcite-bearing}$ , rather than  $\text{dolomite-bearing}$  assemblages will be formed in mafic rocks, resulting in lower  $\text{CO}_2$  contents in altered rocks. As well, in  $\text{Ca-poor}$  lithologies such as  $\text{quartzofeldspathic}$  metasediments and felsic igneous rocks, even  $\text{calcite}$  will not typically form from fluids with  $X_{\text{CO}_2}$  in the range calculated for the Dahlonaga Belt fluids. Similar arguments can be applied to sulfidation reactions which would tend to produce  $\text{pyrrhotite}$  or  $\text{pyrite}$  in altered wall rocks. Because of the positive slope of sulfidation equilibria on  $\text{T}-f_{\text{S}_2}$  diagrams, formation of sulfide minerals from  $\text{Fe-oxides}$  or  $\text{silicates}$  is less likely to occur at high than low temperatures, which explains why rocks with more than a few percent sulfide are absent in the Dahlonaga Belt, in contrast to the more abundant  $\text{Fe-sulfides}$  in alteration zone of deposits formed at lower temperatures (e.g. Phillips, 1985).

The very close association between gold and tellurides in most deposits examined is also an unusual feature compared to  $\text{greenschist-hosted}$  Mother Lode ores, where a gold-tellurium association is usually part of a late stage of ore formation (Weir and Kerrick; Phillips, 1985). This relationship in the Dahlonaga Belt ores may indicate that Au

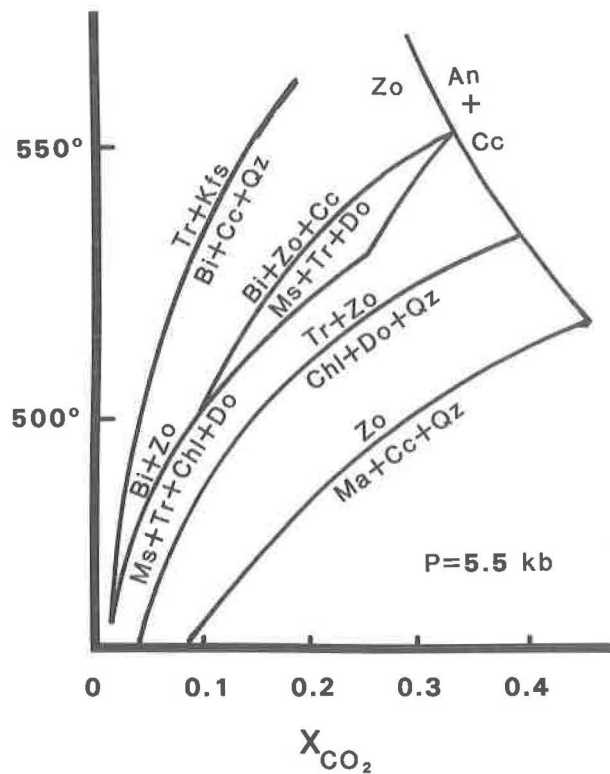


**Figure 12.** T- $X_{\text{CO}_2}$  section showing stability fields for assemblages in altered amphibolites of the Dahlongea Belt. Note that early assemblages such as biotite-clinzoisite formed at higher  $X_{\text{CO}_2}$  or lower temperature than later chlorite- or muscovite-bearing assemblages.

saturation is not normally reached at the high temperatures at which the Dahlonega Belt ores were deposited, and that the presence of sufficient aqueous tellurium to cause saturation and precipitation of gold-rich petzite-hessite<sub>ss</sub> was a prerequisite for gold deposition. Precipitation of gold-silver telluride may have been caused by cooling, as the change in Au solubility as a function of temperature is much greater for tellurides than for the equilibrium involving Au<sup>0</sup> (using data for the Au telluride, calverite, as no data exist for the high temperature phase which probably was deposited in the Dahlonega Belt mineralized zones). Deposition of the gold-silver telluride may have resulted in depletion of tellurium in the fluid, explaining why gold tellurides are not abundant in the main stage mineralization in most Mother Lode-type deposits. The occurrence of very small amounts of gold (<100 ppb) in a number of samples lacking tellurides may be the result of gold incorporation in the lattice of common sulfide minerals, probably arsenopyrite or pyrite. Incorporation of gold in sulfide lattices has long been a hotly debated topic, but the recent data of Cathelineau et al. (1988) provides firm evidence that gold does occur in the lattice of arsenopyrite up to several thousand ppm. Mining of such low grade deposits was probably only possible where intense weathering over along period of time produced thick saprolite zones, which were enriched by accumulation of gold from an overlying 'collapsed' zone of weathered rock.

#### Tectonic Setting and Timing of Events in the Dahlonega Belt

There are few published radiometric age determinations for the Eastern Blue Ridge, so timing of events along the Dahlonega Belt must be inferred indirectly. Peak metamorphism in the area is temporally related to nappe emplacement, based on the evidence of inverted metamorphic gradients. This deformation is generally considered to be Taconic in age (e.g. Glover et al., 1983).

The Dahlonega Belt shearing is associated with retrogression of the peak assemblages, and thus is probably post-Taconic. The association of greenschist facies retrogression with westward-directed thrusting in the southwestern part of the Dahlonega Belt indicates that there was a later, lower-grade retrogression-thrusting event, probably Alleghanian in age by analogy with the Brevard Zone (Edelman et al., 1987). The single hornblende <sup>39</sup>Ar-<sup>40</sup>Ar age determination from the Dahlonega Belt (Dallmeyer, 1988) of 331 Ma probably records cooling through 450-500°C, which, based on temperatures of retrogression and mineralization, may have been later than Dahlonega Belt metamorphism and mineralization. This date, does however, provide a lower limit for the age of the belt. The synchronous nature of at least some plutonism, deformation and gold deposition, however, suggests an Acadian age (360-380 Ma) for the belt, based on: 1) probable Acadian ages for syn-kinematic granitic rocks southeast of the Dahlonega Belt (Fullagar and Goldberg, 1988) and similar plutons in Alabama (Drummond et al., 1988); 2) evidence of Acadian transpression in the sedimentary record of the southern and central Appalachian (Ferrill and Thomas, 1988), and; 3) the occurrence of a number of major Acadian dextral strike-slip faults in the northern Appalachians (Williams and Leger, 1988). A younger, early Alleghanian age, as suggested by Leshner and Green (1988) for gold deposits at Hog Mountain, Talapoosa County, Alabama, is also consistent with available data.

Whether gold deposits of the Dahlongega Belt are Acadian or Alleghanian in age, the structural evidence indicates that deformation took place in a transpressive setting, which may have been due to non-orthogonal plate convergence. Where plate convergence is significantly oblique ( $\geq 22^\circ$ ) the orogen-parallel component of plate motion is typically partitioned into strike-slip faults (trench-linked strike-slip faults of Woodcock, 1986). In a transpressional regime these strike-slip faults may be accompanied by 'flower structures', which are zones in which shortening across a fault is accommodated by vertical extrusion of material to higher structural levels. The combination of shear parallel to the belt and flattening across it is consistent with the Dahlongega Belt being the deep level equivalent of a flower structure. The greater abundance of amphibolite in the Dahlongega Belt relative to the flanking areas may also be attributable to upward movement of the structurally lower mafic/ultramafic Lake Burton Complex as a result of shortening across the belt.

The Dahlongega Belt has been affected by post-mineralization retrograde metamorphism associated with continentward thrusting of the crystalline rocks of the Blue Ridge. The effects of this superposed deformation are only evident southwest of Dahlongega, where published regional maps (e.g. Nelson, 1985) show the Hayesville Thrust curving sharply southward, and joining the Dahlongega Belt. These features suggest that the Hayesville Thrust, or some closely related structure, have undergone reactivation during Alleghanian thrusting (Vauchez and Dallmeyer, 1989).

## CONCLUSIONS

In brief, the Dahlongega Belt is interpreted as a 1-2 km wide ductile shear zone which underwent shortening and right-lateral displacement in a transpressive regime during the accretion of the Avalon Terrane to North America in the Acadian Orogeny. Shearing was contemporaneous with retrograde metamorphism at temperatures of  $500^\circ$ - $550^\circ\text{C}$  and pressures of ca. 5 kb. Emplacement of felsic plutonic rocks, including both K- and Na-rich varieties, and formation of auriferous quartz veins also occurred during shearing. Formerly exploited gold deposits are of several types, all of which are characterized by an abundance of vein quartz. The mineralizing fluid was  $\text{CO}_2$ -rich, and interaction with amphibolites resulted in formation of calcite-, clinozoisite, and biotite-bearing assemblages. Alteration in quartzofeldspathic by the same fluids rocks consisted mainly of muscovite formation at the expense of feldspars and biotite. High gold abundances are accompanied by tellurium enrichment in most deposits examined, and the ubiquitous association of gold, petzite, and calaverite is consistent with gold precipitation in the form of gold-rich petzite-hessite<sub>ss</sub>, a phase stable only at high temperature. The occurrence of widespread, very low-grade gold mineralization may be the result of incorporation of gold in the lattice of arsenopyrite or pyrite. Other elements slightly enriched in Dahlongega Belt occurrences are arsenic, antimony, mercury, tungsten, and molybdenum. Similarities between the deposits of the Dahlongega Belt and the classical greenschist-hosted Mother Lode-type deposits suggests that the Dahlongega Belt ores are the mid-crustal equivalent of Mother Lode-type deposits such as those in the Sierra Nevada of California, the Abitibi Greenstone Belt of the Canadian

Shield, and the Eastern Goldfields province of the Yilgarn Block in Western Australia.

#### ACKNOWLEDGEMENTS

A large number of people and organizations have contributed to this study. These include BP Minerals, which funded the work reported here, as well as the property holders in the Dahlongega Belt who allowed me access to their properties and core. Discussions with workers in the area, including Bob Cook, Jerry German, Janet Hopson, Travis Paris, and in particular Ken Gillon, whose 1986 thesis provided an extremely important geologic base in the Helen area, were also very helpful. Reviews of various incarnations of this paper by Bob Hodder, Bob Cook, and Jerry German led to substantial improvements. I must emphasize, however, that the conclusions of this paper are my own, and that many of them are not shared by the geologists mentioned above.

#### REFERENCES

- Absher, B.S. and McSween, H.Y., Jr., 1985, Granulites at Winding Stair Gap, North Carolina: the thermal axis of Paleozoic metamorphism in the southern Appalachians: *Geol. Soc. America Bull.*, v. 96, p. 588-599.
- Albino, G.V., 1987, The Dahlongega Belt, southeast Georgia Blue Ridge. I) Deformation textures and history: *Geological Society of America Abstracts with Programs*, v. 19, p. 73.
- Barton, P.B., Jr. and Skinner, B.J., 1979, Sulfide mineral stabilities: in Barnes, H.L. (ed.), *Geochemistry of Hydrothermal Ore Deposits* (2nd edition), New York, John Wiley & Sons, p. 278-403.
- Bayley, W.S., 1928, *Geology of the Tate quadrangle, Georgia*: Georgia Geol. Survey Bull. 43, 170 p.
- Becker, G.F., 1894, Reconnaissance of the gold fields of the southern Appalachians: *U.S. Geol. Surv. 16th Annual Report, Part 3*, p. 251-319.
- Bell, T.H., 1978, Progressive deformation and reorientation of fold axes in a ductile mylonite zone: the Woodroffe Thrust: *Tectonophysics*, v. 44, p. 285-320.
- , Rubenach, M.J., and Fleming, P.D., 1986, Porphyroblast nucleation, growth and dissolution in regional metamorphic rocks as a function of deformation partitioning and foliation development: *Jour. Met. Geol.*, v. 4, p. 37-67.

- Bouiller, A-M. and Bouchez, J-L., 1978, Le quartz en rubans dans les mylonites: Bull. Soc. Geol. Fr., vol. 22, p. 253-262.
- Bryant, B. and Reed, J.C., Jr., 1970, Structural and metamorphic history of the southern Blue Ridge: in Fisher, G.W. et al. (eds.), Studies of Appalachian geology-central and southern: New York, Interscience Publishers, p. 213-225.
- Cabri, L.J., 1965, Phase relations in the Ag-Au-Te system and their mineralogical significance: Econ. Geol., v. 60, p. 1569-1606.
- Carpenter, R.H., 1970, Metamorphic history of the Blue Ridge province of Tennessee and North Carolina: Geol. Soc. America Bull. v. 81, p. 749-762.
- Cathelineau, M, Boiron, M.C., Holliger, Ph., and Marion, Ph., 1988, Gold-rich arsenopyrites: crystal-chemistry, gold location and state, physical and chemical conditions of crystallization: in Goode, A.D.T. and Bosma, L.I. (compilers), Bicentennial Gold 88, Extended Abstracts Oral Program, Geol. Soc. Australia Inc., Abstracts No. 22, p. 235-240.
- Cobbold, P.R. and Quinquis, H., 1980, Development of sheath folds in shear regimes: Jour. Struct. Geol., v. 2, p. 119-126.
- Cook, R.B. and Burnell, J.R., Jr., 1985, Trace metal signature of major lithologic units, Dahlonega District, Lumpkin County, Georgia: Geol. Soc. America Abstracts with Programs, v. 17, p. 85.
- and -----, 1983, Geology of the Dahlonega district, Georgia: Geol. Soc. America Abstracts with Programs, v. 15, p. 109.
- , -----, and Sibley, D.E., 1984, Preliminary geologic map of the Dahlonega district, Georgia: Georgia Geol. Surv., Open-File Report 85-3.
- Crickmay, G.W., 1952, Geology of the crystalline rocks of Georgia: Georgia Geol. Surv. Bulletin 58, 54 p.
- Dallmeyer, R.D., 1988, Late Paleozoic evolution of the western Piedmont and eastern Blue Ridge, Georgia: Controls on the chronology of terrane accretion and transport in the southern Appalachian orogen: Geol. Soc. America Bull., v. 100, p. 702-713.
- Drummond, M.S., Wesolowski, D., and Allison, D.T., 1988, Generation, diversification, and emplacement of the Rockford Granite, Alabama Appalachians: Mineralogic, petrologic, isotopic (C & O), and P-T constraints: Jour. Petrol., v. 29, p. 869-898.
- Edelman, S.H., Liu, A., and Hatcher, R.D., Jr., 1987, The Brevard Zone in South Carolina and adjacent areas: An Alleghanian orogen-scale dextral shear zone reactivated as a thrust fault: Jour. Geology, v. 95, p. 793-806.

- Escher, A. and Watterson, J., 1974, Stretching fabrics, folds and crustal shortening: *Tectonophysics*, vol. 22, p. 223-231.
- Evans, B.W. and Trommsdorff, V., 1970, Regional metamorphism of ultramafic rocks in the central Alps: Parageneses in the system CaO-MgO-SiO<sub>2</sub>-H<sub>2</sub>O: *Schweiz. Mineral. Petrog. Mitt.*, v. 50, p. 481-492.
- Ferrill, B.A. and Thomas, W.A., 1988, Acadian dextral transpression and synorogenic sedimentary successions in the Appalachians: *Geology*, v. 16, p. 604-608.
- Fullagar, P.D. and Goldberg, S.A., 1988, Rb-Sr and U-Pb geochronological investigations in the ADCOH site area, southern Appalachians: *Geol. Soc. America Abstracts with Programs*, v. 20, p. 264.
- Furcron, A.S. and Teague, K.H., 1945, Sillimanite and massive kyanite in Georgia: *Georgia Geol. Surv. Bulletin* 51, 76 p.
- German, J.M., 1988a, The geology of gold occurrences in the west-central Georgia Piedmont: *Georgia Geol. Surv. Bull.* 107, 48 p.
- , 1988b, Geology of the Dahlonega and Carroll County gold belts, Georgia: *Geol. Soc. America Abstracts with Programs*, v. 20, p. 266.
- , 1985, The geology of the northeastern portion of the Dahlonega gold belt: *Georgia Geol. Surv. Bull.* 100, 41 p.
- Ghent, E.D., 1976, Plagioclase-garnet-Al<sub>2</sub>Si<sub>2</sub>O<sub>5</sub>-quartz: a potential geothermometer-geobarometer: *Am. Mineral.*, v. 61, p. 710-714.
- Gillon, K.A., 1982, Stratigraphic, structural, and metamorphic geology of portions of the Cowrock and Helen, Georgia, 71/2° quadrangles: unpublished M.S. thesis, University of Georgia, Athens, Georgia, 236 p.
- Glover, L., Speer, J.A., Russell, G.S., and Farrar, S.S., 1983, Ages of regional metamorphism and ductile deformation in the central and southern Appalachians: *Lithos*, v. 16, p. 223-245.
- Guthrie, G.M. and Leshner, C.M., 1988, Structural and metamorphic controls on lode gold mineralization, Talapoosa County, Alabama: *Geol. Soc. America Abstracts with Programs*, v. 20, p. 268.
- Hatcher, R.D., Jr., 1987, Tectonics of the southern and central Appalachian internides: *Ann. Rev. Earth Plan. Sci.*, v. 15, p. 337-362.
- , 1978, Tectonics of the western Piedmont and blue Ridge, southern Appalachians: review and speculations: *Am. Jour. Sci.*, v. 278, p. 276-304.
- , 1979, The Coweeta Group and Coweeta Syncline: major features of the North Carolina-Georgia Blue Ridge: *Southeastern Geol.*, v. 21, no. 1, p. 17-29.

- , 1974, An introduction to the Blue ridge tectonic history of northeast Georgia: Georgia Geol. Soc. Guidebook, 60 p.
- , 1973, Basement versus cover rocks in the Blue Ridge of northeast Georgia, northwestern South Carolina, and adjacent and adjacent North Carolina: Am. Jour. Sci., v. 273, p. 671-685.
- , 1971, The geology of Rabun and Habersham Counties: Georgia Geol. Surv. Bull. 83, 48 p.
- Higgins, M.W., Atkins, R.L., Crawford, T.L., Crawford, R.F., III, and Cook, R.B., 1984, A brief excursion through two thrust stacks that comprise most of the crystalline terrane of Georgia and Alabama: Georgia Geol. Soc. Guidebook, 19th Annual Field Trip, 67 p.
- , -----, Nelson, A.E., and Crawford, T.J., 1988, The Talking Rock Complex: an ancient accretionary complex, northern Georgia and southern North Carolina: Geol. Soc. America Abstracts with Programs, v. 20, p. 270.
- Hopson, J.L., 1988, Petrogenesis of the Lake Burton mafic-ultramafic complex: Geol. Soc. America Abstracts with Programs, v. 20, p. 271.
- Hoschek, G., 1980, Phase relations of a simplified marly rock system with applications to the western Hohe Tauern (Austria): Contrib. Mineral. Petrol., v. 73, p. 53-68.
- Jones, S.P., 1909, Second report on the gold deposits of Georgia: Geol. Surv. Georgia Bull. 19, 283 p.
- Kerrich, R., 1983, Geochemistry of gold deposits in the Abitibi greenstone belt: Can. Inst. Mining Metal. Special Paper 27, 75 pp.
- Kittelson, R.C. and McSween, H.Y., Jr., 1987, The amphibolite to granulite facies transition in the Blue Ridge, Macon County, NC: Geol. Soc. America Abstracts with Programs, v. 19, p. 93.
- Koschmann, A.H. and Bergendahl, M.H., 1968, Principal gold-producing districts of the United States: U.S. Geol. Surv. Prof. Paper 610, 283 pp.
- Leshner, C.M. and Green N.L., 1988, Syn-metamorphic hydrothermal alteration, Hog Mountain gold deposit, northern Alabama Piedmont: Geol. Soc. America Abstracts with Programs, v. 20, p. 277.
- Lesure, F.G., 1971, Residual enrichment and supergene transport of gold, Calhoun Mine, Lumpkin County, Georgia: Econ. Geol., v. 66, p. 178-186.
- Lindgren, W., 1906, The gold deposits of Dahlonega, Georgia: U.S. Geol. Surv. Bull. 293, p. 119-128.

- McConnell, K.I., 1980, Origin and correlation of the Pumpkinvine Creek Formation: a new unit in the Piedmont of northern Georgia: Georgia Geol. Surv. Info. Circ. 52, 19 p.
- and Abrams, C.E., 1988, Metamorphosed felsic to intermediate volcanic rocks and their association with volcanogenic gold deposits in the northern Piedmont of Georgia: Geol. Soc. America Abstracts with Programs, v. 20, p. 279.
- and -----, 1984, Geology of the Greater Atlanta Region: Georgia Geol. Surv. Bull. 96, 127 p.
- and -----, 1983, Geology of the New Georgia group and associated sulfide and gold deposits: west-central Georgia: Society of Economic Geologists, Field Trip Guidebook, Atlanta, Georgia, 27 p.
- Meyer, C. and Hemley, J.J., 1967, Wallrock alteration: in Barnes, H.L. (ed.) Geochemistry of hydrothermal ore deposits, New York, Holt Rinehart and Winston, p. 166-245.
- Murray, J.B., 1973, Geologic map of Forsyth, and north Fulton Counties, Georgia: Georgia Geol. Surv. Bull. 88 (map only).
- Nelson, A.D., 1985, Major tectonic features and structural elements in the northwest part of the Greenville Quadrangle, Georgia: U.S. Geol. Surv. Bull. 1643., 22 p.
- and Gillon, K.A., 1985, Stratigraphic nomenclature in the Richard Russell and Helen thrust sheets, Georgia and North Carolina: U.S. Geol. Surv. Bull. 1605-A, p. A59-A62.
- Pardee, J.T. and Park, C.F., Jr., 1948, Gold deposits of the southern Piedmont: U.S. Geol. Surv. Prof. Pap. 213, 156 p.
- Passchier, C.W. and Simpson, C., Porphyroclast systems as kinematic indicators: Jour. Struct. Geol., v. 8, p. 831-843.
- Phillips, G.N., 1985, Archean gold deposits of Australia: University of the Witwatersrand Economic Geology Research Unit Information Circular 175, 40 pp.
- Platt, J.P. and Vissers, R.L.M., 1980, Extensional structures in anisotropic rocks: Jour. Struct. Geol., v. 2, p. 397-410.
- Romberger, S.B., 1986, The solution chemistry of gold applied to the origin of hydrothermal deposits: in: Clark, L.D. (ed.), Gold Deposits of the Western Shield, Canadian Institute of Mining and Metallurgy Special Volume 38, p. 168-186.
- Sanderson, D.J. and Marchini, W.R.D., 1984, Transpression: Jour. Struct. Geol., v. 6, p. 449-458.
- Simpson, C. and Schmid, S.M., 1983, An evaluation of criteria to deduce the sense of movement in sheared rocks: Geol. Soc. America Bull.,

v. 94, p. 1281-1288.

- Stieve, A.L., Sinha, A.K., and Hatcher, R.D., Jr., 1988, Rb/Sr whole rock Grenville age for the basement gneisses of Tallulah Falls Dome, northeastern Georgia: Geol. Soc. America Abstracts with Programs, v. 20, p. 318.
- Thompson, A.B., 1976, Mineral reactions in pelitic rocks: I. Prediction of P-T- $X_{(Fe-Mg)}$  phase relations: Am. Jour. Sci., v. 276, p. 401-424.
- Tso, J.L., 1987, Evidence of inverted metamorphic isograds between Fries and Galax, SW Virginia Blue Ridge: Geol. Soc. America Abstracts with Programs, v. 19, p. 133.
- Vauchez, A.R., and Dallmeyer, R.D., 1989, Polyphase tectonic history of the Hayesville Fault, Georgia-North Carolina: Geol. Soc. America Abstracts with Programs, v. 21, no. 3, p. 63.
- Weir, R.H., Jr. and Kerrick, D.M., 1987, Mineralogic, fluid inclusion, and stable isotope studies of several gold mines in the Mother Lode, Tuolumne and Mariposa Counties, California: Econ. Geol., v. 82, p. 328-344.
- Woodcock, N.H., 1986, The role of strike-slip faults at plate boundaries: Phil. Trans. Royal Soc. London, vol. 317, p. 13-29.
- Yeates, W.S., McCallie, S.W., and King, F.P., 1896, A preliminary report on a part of the gold deposits of Georgia: Georgia Geol. Surv. Bull. 4-A, 542 p.

# PALEOPLACER GOLD IN THE LILESVILLE SAND AND GRAVEL DEPOSITS, NORTH CAROLINA

James R. Craig  
Department of Geological Sciences  
Virginia Polytechnic Institute and State University  
Blacksburg, VA 24060

and

John E. Callahan  
Department of Geology  
Appalachian State University  
Boone, North Carolina 28608

## ABSTRACT

Paleoplacer gold has been found in Eocene(?) lag gravel deposits of the Citronelle Formation in the Lilesville Area of Anson County, North Carolina. The processing of the sand-, gravel- and cobble-rich beds for commercial construction grade sand and gravel at rates of up to 10,000 tons per day has resulted in concentration of heavy minerals, including gold. The heavy minerals are dominantly ilmenite with minor kyanite-sillimanite, zircon, rutile, magnetite, hornblende, staurolite, epidote and monazite, with traces of cassiterite and gold. The gold grains were apparently derived from gold deposits exposed to the north and west.

The gold, present in grains dominantly less than 1 mm but ranging upward to 5 mm in maximum dimension, occurs generally as irregular to flattened nuggets typical of fluvial transport. The presence of several small euhedral gold crystals, however, may indicate some secondary mobilization and recrystallization. The silver contents of the gold grains range from 0% to 24% (fineness 1000 to 760), and approximately one-third of the grains analyzed by electron microprobe exhibit the development of partial to complete gold-rich rims with finenesses of 990-1000.

## INTRODUCTION

Placer deposits of gold are widespread, geographically occurring throughout geologic time along rivers and streams draining areas where lode gold deposits have cropped out. Recent placer occurrences are well known in many parts of the southern and central Appalachians and are especially well documented in the Charlotte 1° x 2° quadrangle (e.g., D'Agostino and Rowe, 1986; D'Agostino et al., 1987, 1989). Although they served as the initial discovery sites and major early producers in many of the states, few have been worked or considered economic in recent years.

Paleoplacer deposits, including the world's largest reserves (the Witwatersrand deposits in South Africa; Pretorius, 1981), are much less common because they are so often either deeply buried or re-eroded and dispersed. Nevertheless, D'Agostino and Rowe (1986) and D'Agostino and Whitlow (1989) report the occurrence of placer gold within Cretaceous gravels and in fossil stream channels cut into the Triassic rocks in the Charlotte 1° x 2° quadrangle of North Carolina. Cook and Nelen (1989) have described paleoplacers in the Cretaceous sediments of the Alabama coastal plain, and Sharp (1988) reports gold in the Cretaceous of the South Carolina coastal plain. The present paper

presents new information on paleoplacer gold found within Eocene(?) gravel deposits of the Citronelle Formation that is presently being exploited for sand and gravel. These heretofore undescribed gold occurrences that contain small quantities of gold (Callahan and Craig, 1989) are important because: (1) they, or others like them, may have economic potential; (2) they may provide information on the past erosional history of the mid-Atlantic region; and (3) they may provide information on the nature of placer gold in general.

#### LOCATION, GENERAL GEOLOGY OF THE DEPOSITS, AND SAMPLING

Paleoplacer gold has been found in the gravels of the Citronelle Formation approximately 5 km east of the town of Lilesville in the Piedmont region of Anson County, North Carolina (79°55'W Long.; 34°55'N Lat.; Fig. 1). The Citronelle Formation named by Matson (1916) has been mapped by Cooley (1970) in this area as a series of isolated patches with a total aerial extent of about 64 km<sup>2</sup> adjacent to the present valley of the Pee Dee River. Cooley (1970) has interpreted these beds as a channel-bar complex of a slowly degrading, laterally migrating stream with a current direction roughly parallel to the present valley trend (i.e., north to south). Similar terrace deposits occur, as shown in Figure 1, along many parts of the eastern Piedmont of North Carolina. The age of the deposits is not known with certainty but has been interpreted as late Pliocene (Berry, 1916) and as middle Eocene and late Eocene (Cooley, 1970).

The Citronelle beds are up to 10 m in thickness and unconformably overlie sands and clays of the Cretaceous age Middendorf Formation which in turn lies unconformably on the Carboniferous age Lilesville granite (Butler and Fullagar, 1975; Cooley, 1970). The layers are distinct, continuous at least for tens to hundreds of meters, and the contact with underlying beds is sharp. The Citronelle Formation is composed of cross-stratified sands with included stringers of gravel. The basal gravel, often the most visible unit because of its resistance to erosion, consists of moderately to well sorted sand and coarse gravels. Abundant white cobbles, commonly in the range of 5-10 cm, are composed of 75-91% metaquartzite with the remainder vein quartz (Cooley, 1970). The nearly spherical nature of many of the cobbles and pebbles suggests a significant distance of transport in high energy fluvial environment. Gravel, cobble and sand beds are poorly consolidated and quite friable and hence have proven to be easily exploitable sources of sand and gravel for construction purposes.

The source area(s) of the metaquartzite pebbles and the heavy minerals in the sand fraction associated with them has not been documented. The vein quartz pebbles could be from any of the numerous quartz veins in the Piedmont. One possible source for the metaquartzite is the Pilot Mountain, North Carolina, region where similar lithologies are found. The heavy minerals could be derived from lithologies in the Charlotte, Kings Mountain, or Inner Piedmont belts.

The samples described in this study were obtained primarily from the Hedrick Industries sand and gravel operation that is about 5 km east of Lilesville along U.S. Route 74. This operation currently processes approximately 6000 tons per day of sediment that is washed and sized into a variety of sand and gravel products. The initial step in processing is the disaggregation of the poorly indurated material by means of a rotating washing trommel equipped with high pressure hoses. The slurry is discharged over a riffle of heavy steel bars and then carried by conveyor belt to a series of screens for sizing. The approximately 10 cm deep riffle tends to collect tramp iron scrap and heavy minerals as well as some cobbles and sand, all of which becomes tightly packed. Samples of this sediment were extracted using picks and small trowels and were crudely panned on the spot to eliminate the tramp iron and other assorted scrap metal, coins, and lead hunting shot..

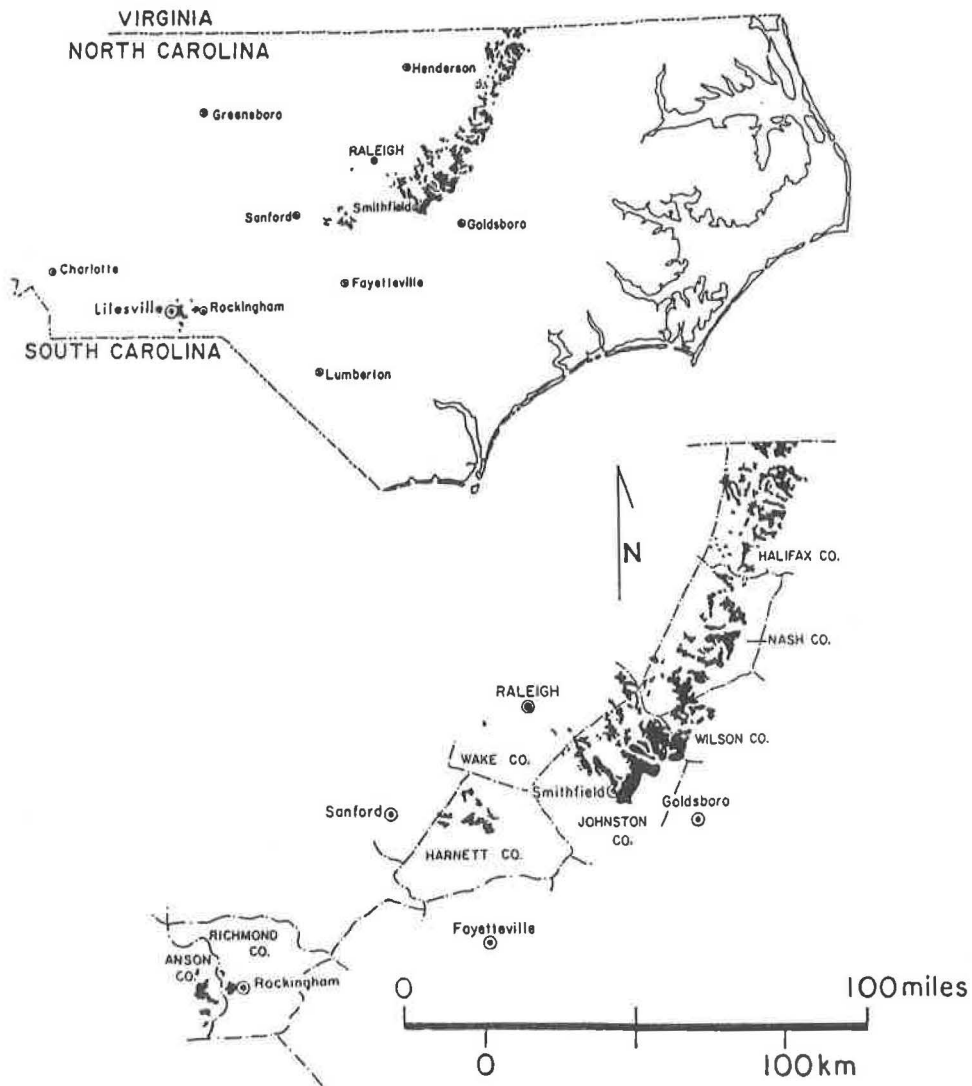


Figure 1. Sketch map of North Carolina showing the location of Lilesville and the distribution of terrace deposits (in black) on the eastern portion of the Piedmont. The insert at the lower right provides greater detail; the Lilesville deposits are shown in the eastern edge of Anson County. From Callahan and Craig (1989) after Brown et al. (1985).

The remaining sediment was washed into buckets and returned to the laboratory for careful panning, sampling, and analysis. Repeated hand panning in the laboratory yielded more than 9000 grains of gold ranging from less than 0.1 mm to a maximum of 5 mm (Fig. 2). Representative grains of gold and the associated minerals were selected and mounted in cold setting epoxy for electron microprobe analysis. After grinding and polishing by standard techniques (Craig and Vaughan, 1981), grains were analyzed using an ARL-SEM-Q employing pure gold, silver, copper, National Bureau of Standards gold-silver wires and livingstonite ( $\text{HgSb}_4\text{S}_8$ ) as standards. Analysis was carried out using a beam current of 20 nanoamps at 20 kV, and the data were reduced using the Bence-Albee program.

## THE PALEOPLACER GOLD AND ASSOCIATED HEAVY MINERALS

The Citronelle Formation where exposed and mined for sand and gravel east of Lilesville, North Carolina, is dominantly composed of quartz as cobbles, gravel, and sand. The heavy mineral content averages 0.3 % of the total, two-thirds of which is composed of ilmenite and its alteration products (Callahan and Craig, 1989). Also present are two populations of zircon, kyanite, magnetite, hornblende, staurolite, epidote, monazite, rutile, and traces of cassiterite and gold (Table 1). Most of these minerals are present as roughly equant 0.1-1.0 mm grains, although larger grains occur. Ilmenite, the most abundant of the heavy minerals, typically occurs as somewhat rounded grains that contain numerous exsolution lamellae of hematite. Near the margins of the grains, the hematite has weathered out, leaving empty voids as shown in Figure 3A. One of the zircon populations consisted of pinkish euhedral crystals (Fig. 3B) with length-to-width ratios in the range 2:1 to 3:1; these had hafnium contents of 1.0-1.3 wt %  $\text{HfO}_2$ . The other zircons are colorless, have length-to-width ratios in the range 3:1 to 4:1, and have hafnium contents of 0.75-0.90 wt %  $\text{HfO}_2$ . The two populations of zircons as well as the monazite grains are generally euhedral, commonly display growth zoning, and commonly contain small liquid and solid inclusions. The kyanite occur as thin bluish rectangular plate-like fragments up to 5 mm in length that commonly contain inclusions of rutile, ilmenite, and possibly magnetite (Fig. 3C). Magnetite is present only in trace quantities but has been observed in the form of a 1 mm long, doubly terminated octahedron. Much of the magnetic fraction consists of small, hollow spheres of unknown origin (Fig. 3D). As these consist of iron and iron oxide in a somewhat eutectic-like intergrowth, we suspect that they may be a by-product of an iron refining or foundry operation. Furthermore, these appear very similar to the steel shot particles that are attributed to metal refining and processing plants in The Particle Atlas (McCrone et al., 1969). A few 1-2 mm grains of cassiterite were observed and confirmed by means of the electron microprobe. These are very similar in appearance to the much more common yellow-brown, roughly equant grains of staurolite.

Small numbers of approximately 0.1 mm gold grains were recovered during the processing of approximately one ton of the average, in-place, Citronelle beds at the Bonsal and Hedrick sand and gravel operations. On the basis of these samples, the average gold content appears to be approximately 0.00247 gm/ton (or 0.000079 troy oz per ton) = 0.003 mg per kilogram (Callahan and Craig, 1989). In contrast, the sampling of the riffles at the washer of the Hedrick operation has yielded over 9000 gold grains. The quantity of raw sand and gravel from which these were concentrated is unknown and could easily exceed one million short tons. The 20 kg of concentrate (after removal of scrap iron and pebbles greater than one-fourth inch (6.5 mm) yielded approximately six grams of gold; this corresponds to a grade of approximately 9.6 troy oz/ton in this concentrate). Although not intended to be statistically rigorous because many of the very smallest gold grains were not recovered, an approximate distribution of gold grains is given in Table 2. The largest single gold nugget recovered was very irregular and measured  $3 \times 5$  mm and weighed 0.408 gm. This nugget contained about 25% by volume quartz; hence, the gold portion

**Table 1.** Approximate weight percentages of heavy minerals from the minus 40-mesh fraction, in the Citronelle Formation in the area of study. From Callahan and Craig (1989).

Mineral	Weight Percentage
Ilmenite	50
Altered ilmenite	17
Kyanite	11
Zircon	5
Rutile	5
Magnetic (mt + iron spheres)	4
Hornblende	3
Staurolite	2
Epidote	1
Monazite	0.5
Other (including cassiterite and gold)	1.5

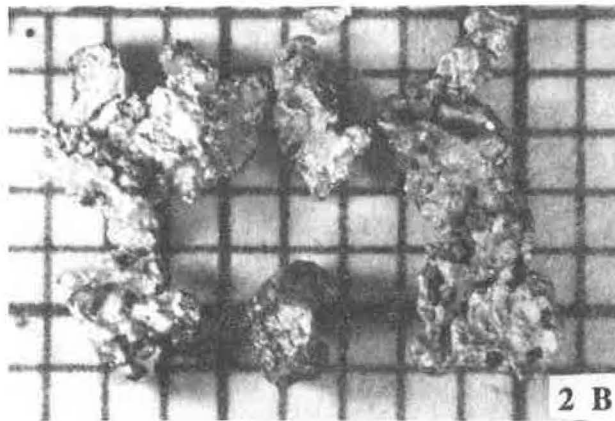
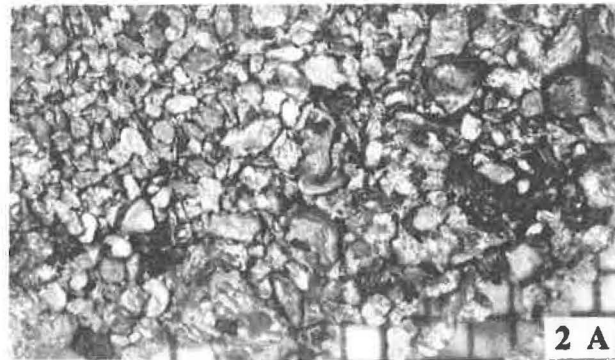


Figure 2. Examples of paleoplacer gold from the Lilesville, NC, deposits. (A) Typical example of fine-grained gold containing an assortment of irregular and flattened grains. (B) Highly irregularly-shaped, large gold grain. The grid scale visible is in millimeters.

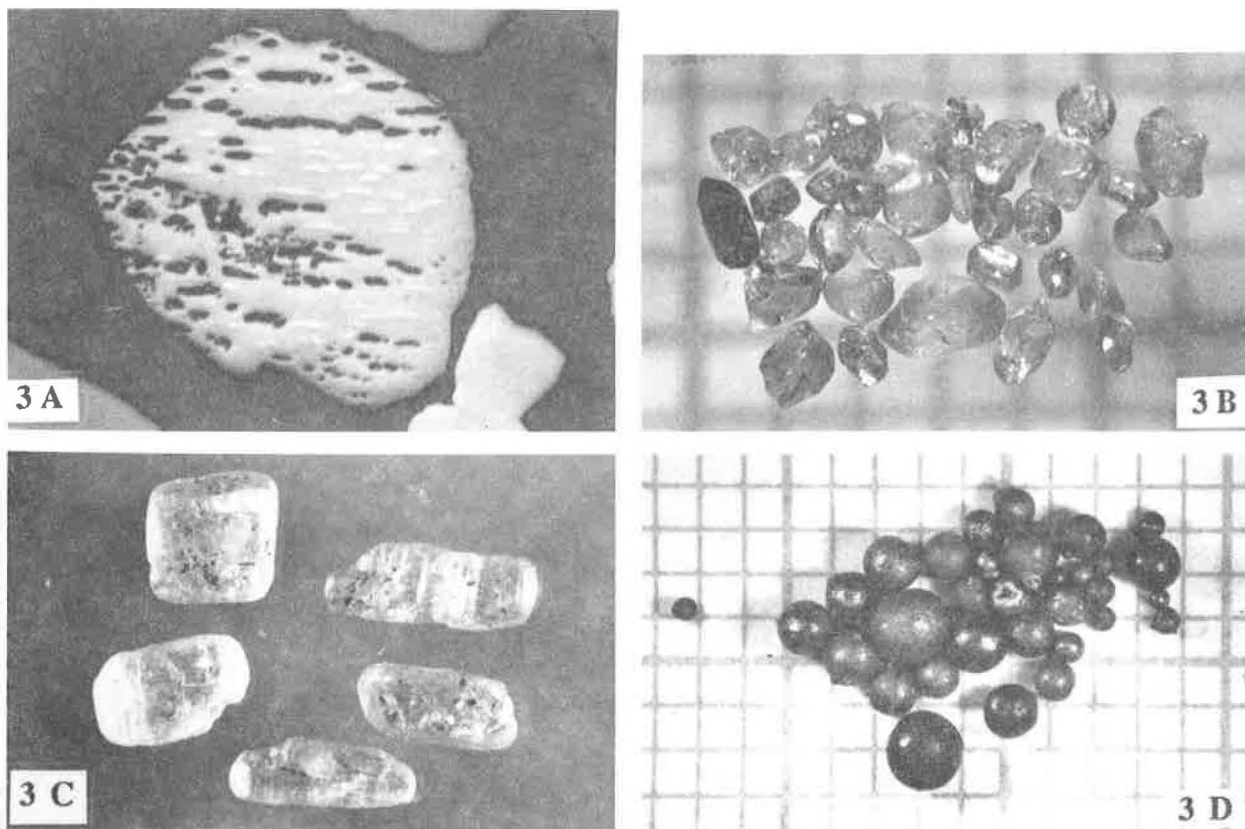


Figure 3. Heavy mineral components from the Lilesville, NC, paleoplacer deposits. (A) Photomicrograph of ilmenite from the Lilesville deposits. Note that the exsolved hematite lamellae (white) have been weathered out near the margins of the ilmenite grains. Width of field of view is 0.6 mm. (B) Typical examples of the "pink" zircons, the more common of the two zircon populations. (C) The kyanite laths typically contain small inclusions of ilmenite and rutile. (D) Magnetic metallic spheres believed to represent contaminants from iron refining operations or from steel bird shot. The grid visible in each photograph is in millimeters.

Table 2. Approximate size distribution of gold grains recovered from the Citronelle Formation gravels in this study; based on representative sample of 2726 grains.

Size Range	No. Grains	Percentage
<0.1 mm	1240	45.5
0.1-0.5 mm	885	32.5
0.5-1.0 mm	508	18.6
1.0-2.00 mm	75	2.8
2.0-5.0 mm	15	0.7
>5.0 mm	3	0.1

was estimated to be approximately 0.39 gm. The second largest gold nugget was 0.148 gm. Several hundred grains weighed 4-5 mg, but the average grain weight was probably only about 0.6 mg.

The gold grains display a wide variety of shapes and a moderate range of colors independent of their sizes. Most grains are crudely equant to very slightly flattened as is characteristic of placer gold grains that have been transported considerable distances in streams. There are also numerous gold grains in the form of thin disks that might be evidence of intense pounding during transport. In contrast, a moderate number of grains (generally larger than 1 mm) display angular to sharp and delicate points and irregular projections that display little or no sign of sedimentary abrasion or pounding. One to 2% of the grains that are greater than 0.5 mm display crystal faces or face-like surfaces; it is not clear if these represent gold crystal faces or are the imprints of previously adjacent minerals.

The most surprising observation was the discovery of approximately 20 completely to nearly completely terminated gold crystals, all in the size range of <0.5 mm (Fig. 4). Most of these crystals are dodecahedrons that are very well developed and are nearly equant. Very few display any evidences of abrasion or distortion.

### GOLD COMPOSITIONAL AND TEXTURAL DATA

In order to carry out ore microscopic examination of the grains and to conduct electron microprobe analysis, randomly selected gold grains were mounted using cold setting epoxy and polished using conventional techniques (Craig and Vaughan, 1981). The individual gold grains were mounted in small custom-cut cavities carved into a blank epoxy section. After grains were placed in their respective holes, a thin coating of fresh epoxy was placed over the grains to cement them into the section for polishing. This technique allowed the mounting of large and small grains so that all would be exposed simultaneously during grinding and polishing.

The compositions of the grains were determined using point or small area raster (5  $\mu\text{m}^2$  to 10  $\mu\text{m}^2$ ) analysis. One hundred individual analyses were carried out on 62 grains from two operating sand and gravel pits; Table 3 presents 65 analyses of 47 representative grains from the Hedrick mining operation after discarding obviously faulty analyses and duplicates; Table 4 contains 17 analyses of 15 randomly picked grains from the Bonsal mining operation. The analyses have been tabulated in order of descending fineness of the grain or, if rimmed, the core of the grain. Copper was analyzed in all grains and mercury in most grains. Both copper and mercury contents are generally very low and show no discernible correlation with gold fineness. Copper was found to be anomalously high in grains no. 20 (0.66%), no. 15 (1.19%), and extraordinarily high in grain no. 11 (13.09%) in Table 3 and in grains no. 2 (3.81%) and no. 7 (1.44%) in Table 4. Many mercury analyses were 0.10% or less, but five values exceed 0.20%; the highest from the Hedrick deposit was 0.52% (no. 46), and the highest from the Bonsal deposit was 0.92% (no. 10).

Optical examination using reflected light revealed that all grains were not internally homogeneous, but that many possessed "rims" or regions that displayed different colors than the interior. These rims varied from nearly continuous to very discontinuous and from only a few microns to nearly 100 microns in thickness. Although the colors of the rims were sometimes only subtly different from the cores, it was evident that the boundaries between the rims and cores were extremely sharp, although very irregular, as is shown in Figures 5 and 6. The rim compositions (Tables 3 and 4) ranged compositionally from 836 fine (No. 46 in Table 3) to 999 fine (Nos. 31, 33, 33 in Table 3) with many rims exceeding 990 fine. The high fineness rims exhibit a relatively high degree of porosity, whereas the

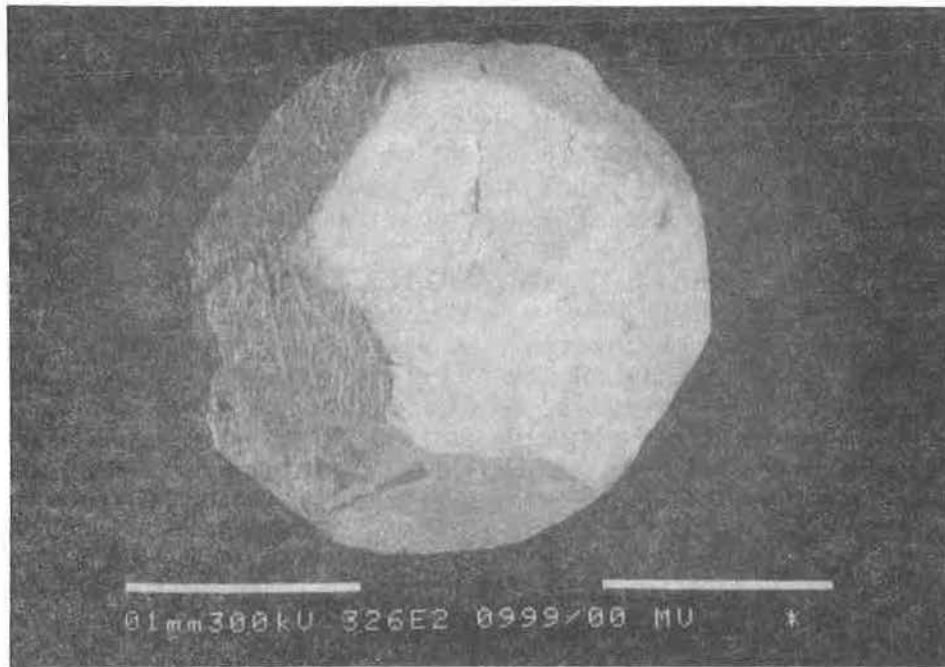


Figure 4. Gold crystals, many completely euhedral, are found disseminated among the paleoplacer gold grains. The absence of erosion or impact textures on these crystals indicates that either they must be very close to their source area or that they formed or were recrystallized after deposition in the paleoplacer. The largest crystal face visible in this figure is 0.5 mm in its largest dimension.

Table 3. Electron microprobe analyses of gold grains from the Hedrick Mine in the Citronelle Formation near Lilesville, North Carolina. Analyses arranged in descending order of fineness of grain cores; all data in weight percent.

Grain No.		Au	Ag	Cu	Hg	Total	Fineness
1 <sup>a</sup>	core	100.12	0.00	0.04	-	100.16	1000
2 <sup>b</sup>	core	97.99	0.00	0.00	-	97.99	1000
3 <sup>a</sup>	core	99.51	0.05	0.01	-	99.57	999
4 <sup>c</sup>	core	99.73	0.07	0.00	-	99.80	999
5	core	101.24	0.28	0.06	-	101.58	997
6 <sup>c</sup>	core	102.18	0.36	0.25	-	102.79	997
7 <sup>c</sup>	core	101.28	0.45	0.06	-	101.79	996
8 <sup>c</sup>	core	100.23	0.53	0.08	-	100.84	995
9 <sup>d</sup>	core	98.38	0.55	0.00	-	98.93	994
10	core	101.13	0.59	0.22	0.11	102.05	994
11	core	88.33	0.87	13.09	-	102.28	990
12	core	99.03	1.75	0.23	-	101.01	983
13	core	98.60	2.22	0.08	-	100.89	978
14	core	101.29	2.40	0.17	0.01	103.87	977
15	core	95.33	2.46	1.19	-	98.98	975
16	core	98.59	2.83	0.10	0.38	101.90	972
17	core	96.46	3.00	0.01	-	99.47	970
18	core	98.18	3.24	0.14	-	101.57	968
19	core	93.58	3.31	0.10	0.10	97.09	966
20	core	96.45	3.86	0.66	-	100.98	962
21	core	96.36	3.96	0.05	0.27	100.64	961
22	core	98.42	4.41	0.05	0.00	102.88	957
23	core	99.94	4.44	0.07	0.11	99.55	955
24	core	97.53	5.35	0.09	0.01	102.98	948
25	core	94.78	5.26	0.08	0.17	100.29	947
26	core	96.21	5.42	0.26	0.16	102.05	947
27	core	94.25	5.53	0.11	0.00	99.89	944
28	core	97.00	5.90	0.08	0.08	103.06	943
29 <sup>d</sup>	core	91.85	7.54	0.07	-	99.46	924
30	core	91.19	9.02	0.03	-	100.24	910
	rim	91.64	6.97	0.13	-	98.74	929
31	core	89.97	10.62	0.09	-	100.68	894
	rim	102.52	0.07	0.00	-	102.59	999
32	core	89.73	10.63	0.02	-	100.38	894
	rim	102.49	0.08	0.10	-	102.67	999
33	core	89.06	11.93	0.40	-	101.39	882
	rim	100.37	0.08	0.00	-	100.45	999
34	core	89.67	12.06	0.03	0.03	101.79	881
	rim	102.77	0.32	0.03	0.14	103.26	997

<sup>a</sup> Surface of flattened gold disk.

<sup>b</sup> Surface of gold sphere.

<sup>c</sup> Interior of flattened gold disk.

<sup>d</sup> Surface of gold crystal.

- Not analyzed for

Table 3 (continued).

Grain No.		Au	Ag	Cu	Hg	Total	Fineness
35	core	89.33	12.10	0.08	0.00	101.51	881
	rim	97.62	1.53	0.06	-	99.20	985
36	core	84.81	12.23	0.08	0.10	97.22	874
	rim	99.51	0.79	0.03	0.12	100.45	992
37	core	88.04	13.29	0.05	0.01	101.39	869
	rim	102.07	0.97	0.02	0.17	103.23	991
38	core	84.34	13.07	0.02	0.01	97.44	865
	rim	99.35	0.49	0.04	0.14	100.02	995
39	core	86.29	13.46	0.10	-	99.85	865
	rim	87.53	13.24	0.02	-	100.79	869
40	core	86.62	13.49	0.13	-	100.23	865
	rim	97.80	3.75	0.09	-	100.65	963
41	core	85.20	13.60	0.03	0.01	98.84	862
	rim	98.39	0.78	0.02	0.06	99.25	992
42	core	87.58	14.19	0.04	-	101.81	861
	rim	100.76	1.67	0.00	-	102.43	983
43	core	86.24	14.13	0.11	-	100.48	859
	rim	92.77	8.09	0.23	-	101.08	920
44	core	86.13	15.60	0.07	-	101.80	847
	rim	102.69	0.90	0.12	-	103.71	991
45	core	84.22	16.48	0.10	-	100.80	836
	rim	98.50	1.94	0.11	-	100.55	981
46	core	80.35	19.50	0.03	0.52	100.40	805
	rim	84.45	16.61	0.05	0.17	101.28	836
47	core	77.76	22.42	0.00	-	100.04	776
	rim	98.89	0.15	0.14	-	99.18	999

Table 4. Electron microprobe analyses of gold grains from the W.R. Bonsal Mine in the Citronelle Formation near Lilesville, North Carolina. Analyses arranged in descending order of fineness of grain cores; all data in weight percent.

Grain No.		Au	Ag	Cu	Hg	Total	Fineness
1	core	97.61	0.64	0.13	0.31	98.68	994
2	core	94.15	0.81	3.81	0.01	99.15	992
3	core	97.51	2.66	0.11	0.00	100.27	973
4	core	96.33	3.10	0.10	0.00	99.53	969
5	core	94.36	3.44	0.13	0.00	97.92	965
6	core	92.15	4.76	0.09	0.00	96.99	951
7	core	91.73	5.67	1.44	0.17	99.01	942
8	core	92.53	5.68	0.10	0.00	98.31	942
9	core	89.26	6.17	0.12	0.04	97.91	936
10	core	87.63	8.27	0.07	0.92	96.90	914
11	core	89.68	9.78	0.02	0.00	99.48	902
12	core	81.76	15.58	0.03	0.00	97.38	840
13	core	80.06	16.06	0.03	0.04	96.19	833
	rim	97.99	0.64	0.00	0.20	98.83	994
14	core	75.57	22.65	0.03	0.08	98.33	769
15	core	75.69	23.86	0.02	0.00	99.57	760
	rim	98.04	0.17	0.05	0.00	98.27	998

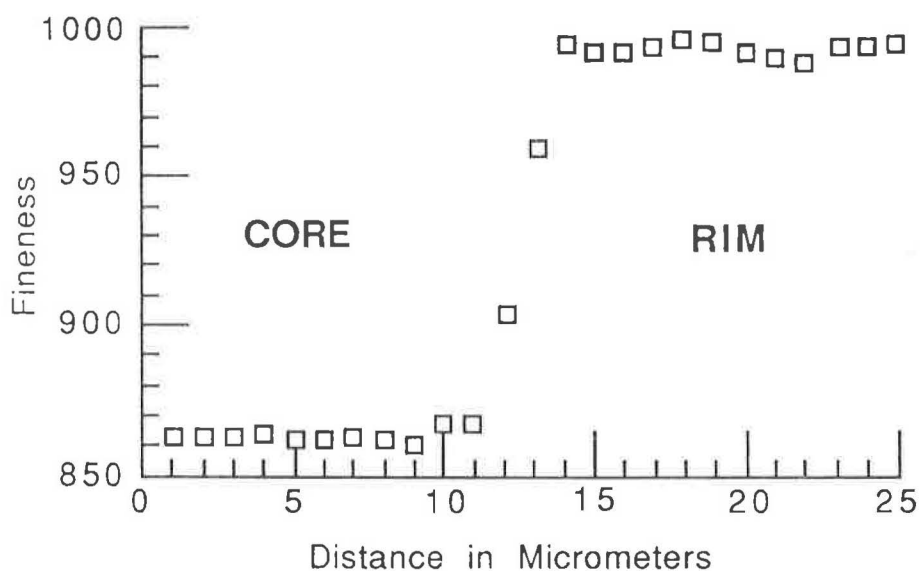
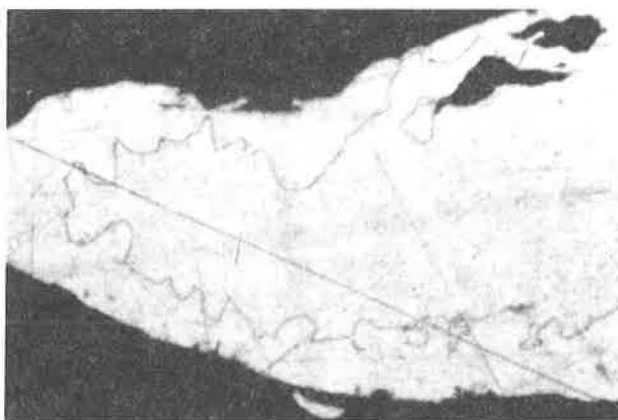


Figure 5. Many of the gold grains exhibit development of partial to complete rims of higher purity gold at the margins of grains. (A) A reflected light photomicrograph showing the presence of a higher-purity rim (991 fine) on an homogeneous grain with a fineness of 869. The width of the field of view is 0.6 mm. (B) A plot of the fineness from a grain interior through a higher-purity rim (grain no. 37 in Table 3) as determined by electron microprobe analyses along a traverse. The analytical spot size was approximately 1  $\mu\text{m}$  across, and the steps were 1.0  $\mu\text{m}$  apart.

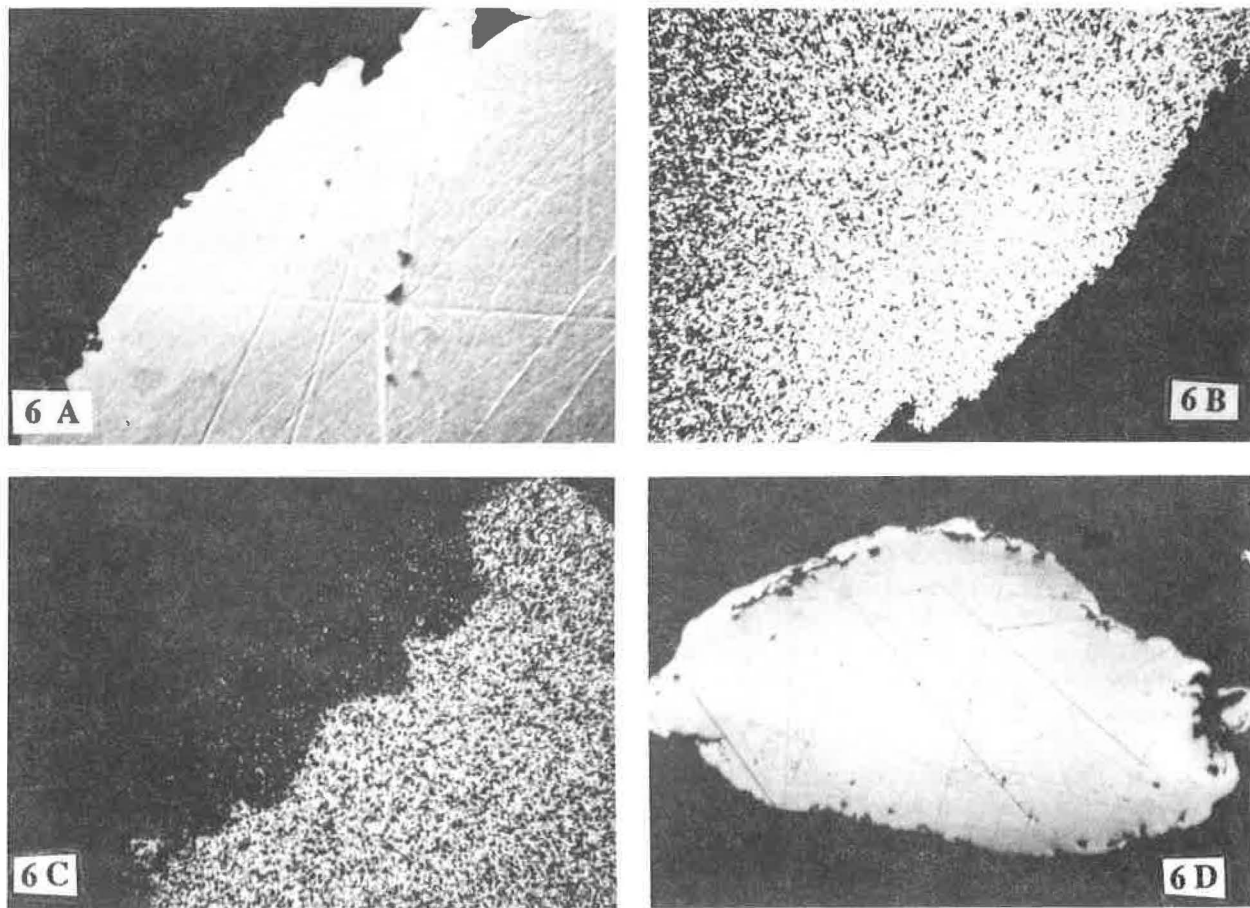


Figure 6. The nature of the gold enrichment in the rims of grains is evident in images of grain no. 37 of Table 3 on which the rim averages approximately  $40\ \mu\text{m}$  in thickness. (A) Backscattered electron image; the slightly lighter area is the gold-enriched margin. (B) The X-ray map showing the distribution of gold. (C) The X-ray image showing the distribution of silver. The width of the field of view is  $0.2\ \text{mm}$ . (D) The marginal areas of this grain exhibit a high degree of porosity where the gold-enriched rims are developed. The width of the field of view is  $1.1\ \text{mm}$ .

marginal areas where rims are not developed exhibit little or no porosity. This porosity is evident by examining the rim areas in the grain (shown in Fig. 6D).

The presence of higher purity gold rims on cores of lower fineness was first reported by Porcher (1882) who observed them on placer grains from the Brush Creek locality in Montgomery and Floyd Counties, Virginia. Porcher (p. 3) states, "The metal is in small rounded grains, which have almost exactly the color of fine gold and full metallic luster; but specific gravity is low (15.46), and on cutting the grains, or scraping them with a knife, it becomes apparent that the color first observed is superficial only, the metal in the interior being almost white." [The analysis gave gold -65.31, silver 34.01, copper 0.14, iron -0.20 and quartz 0.34.] This phenomenon has subsequently been noted by several authors, including Johnson and Uglow (1924), M.S. Fisher (1935), N.H. Fisher (1945), Stumpfl and Clark (1965), Ramdohr (1965, 1969), Desborough et al. (1970a,b), and Knight and McTaggart (1986), and Cook and Nelen (1989) and has been found to be present in many localities in the southeastern United States (Groen, 1987)

Examination of Figure 7, a plot of the data in Table 3, demonstrates that rims were recognized on 17 (or 38%) of the 47 representative and randomly selected grains chosen for analysis from those recovered at the B.V. Hedrick operation. Although there is no correlation of rim fineness with the composition of the underlying core of the grain on which it has developed, it appears that a composition of about 920 fine may represent a general threshold for rim development. Every grain with a core fineness of lower than 920 exhibited some degree of rim development, whereas no grain with a core fineness above this level displayed any rim. Most rim compositions (see Table 3 and note the filled black squares on Fig. 7) have been verified by duplicate analyses. However, some of the true compositions of the thinnest rims may be higher than the analyses indicated, because the analytical volume of the electron spot may be larger than the thickness of the rim. Such analyses would report as a mixture of the compositions of the high purity rim and the lower fineness core.

The gold grains from the Bonsal deposit (Table 4 and Fig. 8) reveal a somewhat different pattern in terms of rim development. Although the grains display a compositional range similar to that of the Hedrick deposit, only two grains were found to exhibit the development of rims. It is not known if this reflects differences in the site of recovery (the steel grate of the trommel at the Hedrick versus the accumulated heavies at the bottom of the sand screws at the Bonsal) or differences in the transportation or sites of deposition.

Traverses of closely spaced (1-3 micrometers) analyses by electron microprobe, as well as randomly spaced spot analyses, have revealed that the interiors of grains are quite homogeneous. Most grains varied by less than 10 fineness units (1 wt % Au); the maximum variation observed was less than 20 fineness units (2 wt % Au).

## DISCUSSION

The origin of the gold recovered from the gravel and sand deposits near Lilesville, NC, is not presently known. Most of the grains display rounded and flattened morphologies indicative of long distances of fluvial transport. Other grains, however, retain many sharp and delicate edges that do not appear to have suffered any abrasion or pounding as would be expected from significant transport. Furthermore, the several subhedral and euhedral gold crystals show no evidence of abrasion. Such crystals certainly could not have experienced any appreciable transport. Accordingly, it appears that the crystals and perhaps some of the irregular grains with sharp margins have either undergone little transport or have been recrystallized or precipitated *in situ*.

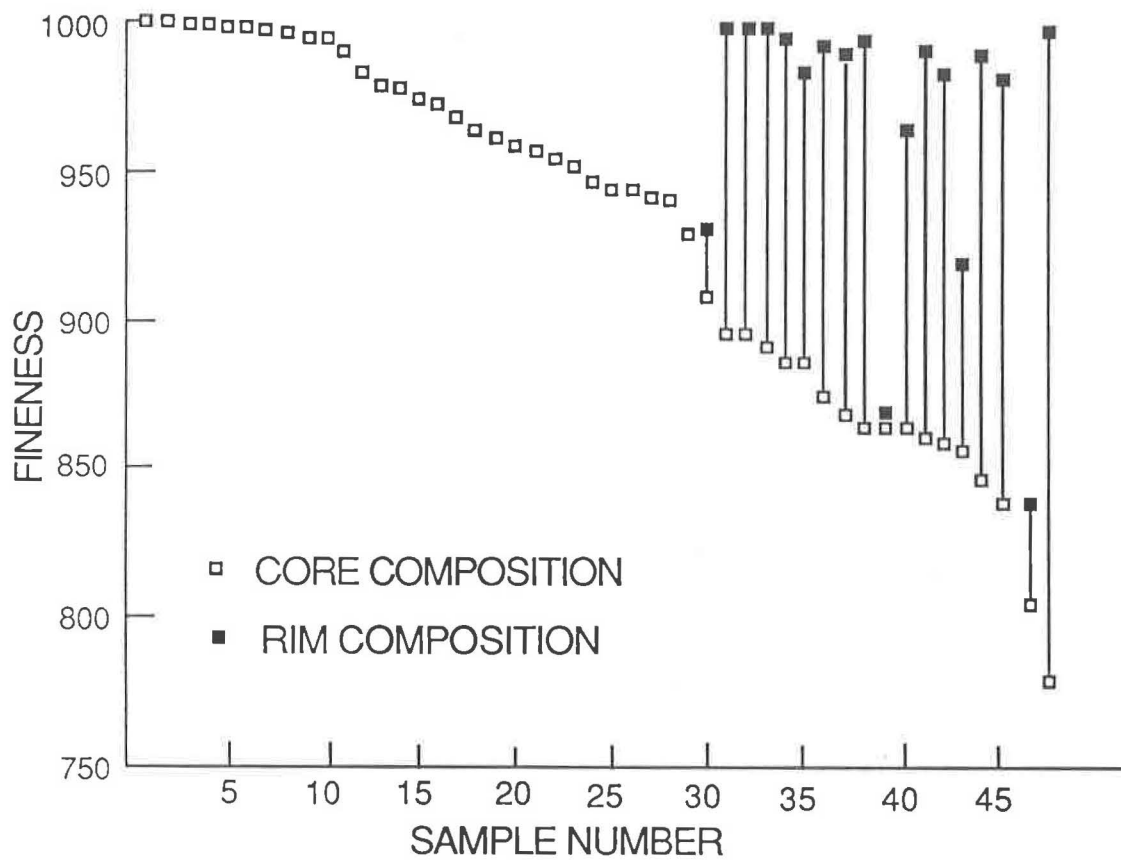


Figure 7. Plot of the fineness of 47 randomly selected and representative gold grains from the Hedrick deposit. The compositions of the cores of the grains (numbered as in Table 3) are shown by the open boxes in order of descending fineness. The compositions of the corresponding rims on the grains are plotted in filled boxes.

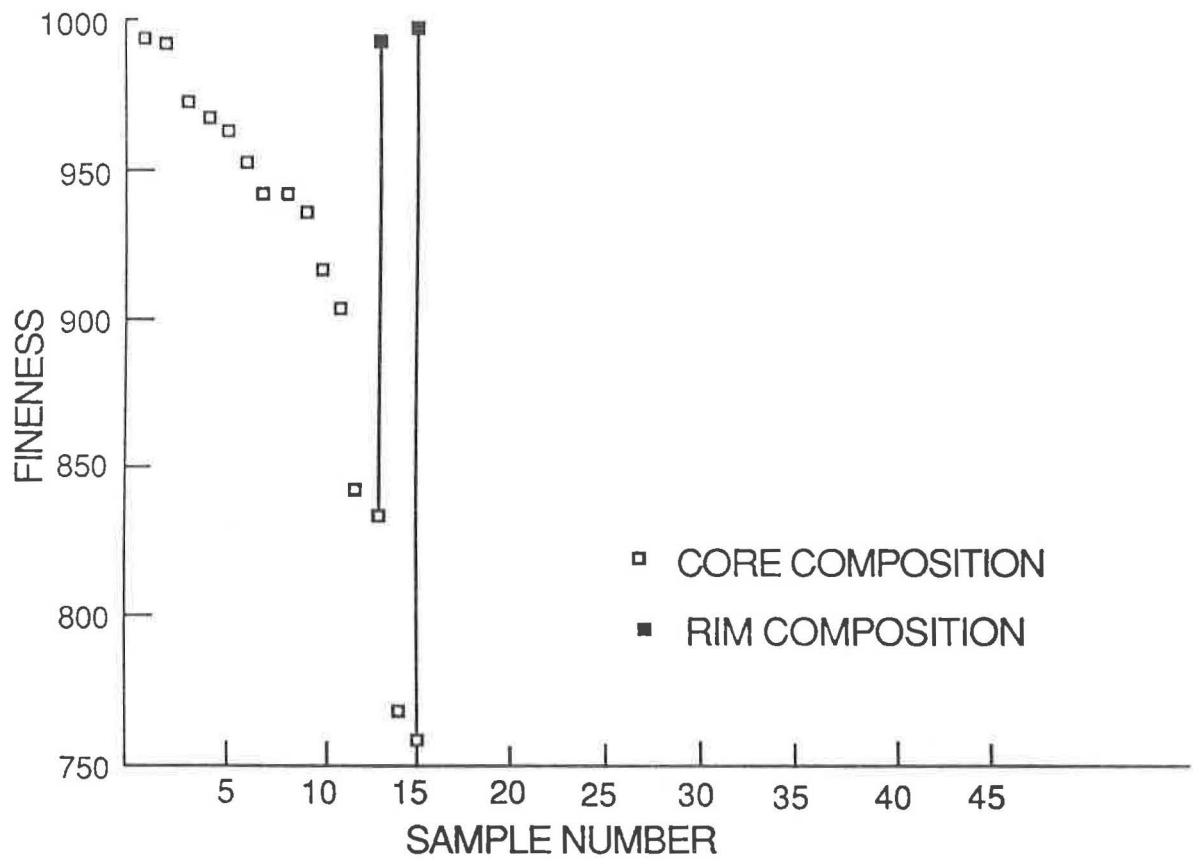


Figure 8. Plot of the fineness of 15 randomly selected and representative gold grains from the Bonsal deposit. The compositions of the cores of the grains (numbered as in Table 4) are shown by the open boxes in order of descending fineness. The compositions of the corresponding rims on the grains are plotted in filled boxes.

Many workers have noted the tendency for the grains size of placer gold grains to decrease downstream from the source area and for grains to become more flattened with distance of transport. Other workers (e.g., Smith, 1913; Ferguson, 1924; Fisher, 1945) have also reported that the fineness of placer gold grains increases with transport.

The distance of transport experienced by the gold grains in the Lilesville deposits is unknown, but the highest fineness measured in grain interiors are, in general, found in the grains whose morphologies (i.e., thin, flattened disks) are most consistent with significant fluvial transport.

The mechanism by which high purity rims develop on placer gold grains is unknown. Desborough (1970) and Knight and McTaggart (1986) speculated that the rims formed through a leaching mechanism whereby the silver is selectively dissolved, leaving a residual gold-enriched zone.

Such a mechanism presumably requires diffusion of silver through the gold-silver alloy to the metal-solution interface where the selective solution could occur. Groen (1987), however, has calculated the profile that would be expected to develop as a result of such diffusion and found that the boundary should be a relatively smooth transition from the internal core composition to the pure rim. The actual boundary between the core and rim of each grain on which one is developed is exceptionally sharp, as is visible in Figure 5. This degree of sharpness is very similar to that observed by one of the authors (JRC) and his co-workers on gold grains from numerous localities within the United States.

Boyle (1979, p. 384) favors gold-rim formation by precipitation from gold-bearing solutions, and Giusti (1983, 1986) describes the occurrence of porous, "new gold" that he believed to be forming on the exteriors of grains. Mann (1984) and Webster and Mann (1984) describe the formation of dendrites of gold and gold-rich rims developing on nuggets during lateritic weathering; these are attributed to the reprecipitation of secondary gold by reduction from gold chloride-bearing solutions. Warren (1982) has described gold crystals forming in soil zones above placer deposits; he attributed their formation to precipitation from gold lode soluble by cyanide produced by cyanogenic plants.

The irregular distribution of the gold-enriched rims, the sharpness of the boundaries between the rims and the cores of grains, and the occurrence of euhedral and unabraded gold crystals are all consistent with a mechanism by which gold is precipitated on pre-existing gold grains either during transport or after deposition in the placer. The higher fineness rims on the Lilesville paleoplacer nuggets exhibit a considerable degree of porosity not observed within the cores of the grains nor along the margins of grains without rims. Such porosity is consistent with a silver leaching model of formation but could also result from the precipitation of "new gold" such as suggested by Giusti (1983).

#### ACKNOWLEDGMENTS

We are grateful to Hedrick Industries and W.R. Bonsal for permission to sample, work and report upon the gold recovered from their operators. We are indebted to Todd Solberg for the electron microprobe analyses, to John Groen for the SEM photograph, to Marjorie McKinney for sample preparation, to Margie Sentelle for typing the manuscript, and to Llyn Sharp for her help in figure preparation. This research has been supported by the Department of the Interior's Mineral Institutes program administered by the U.S. Bureau of Mines under allotment grant no. G1174151 given to Virginia Polytechnic Institute and State University.

## REFERENCES

- Berry, W.E. (1916) The flora of the Citronelle Formation. U.S. Geol. Surv. Prof Paper 98-L, p. 193-108.
- Boyle, R.W. (1979) The geochemistry of gold and its deposits. Geol. Survey Canada Bull. 280, 584 p.
- Brown, P. et al. (1985) Geologic Map of North Carolina. North Carolina Dept. Natural Resources and Community Development.
- Butler, J.R. and Fullagar, P.D. (1975) Lilesville and Pageland plutons and the associated meta-rhyolites, eastern North Carolina slate belt. Geol. Soc. Am., Abstracts with Program, v. 7, p. 475.
- Callahan, J.E. and Craig, J.R. (1989) The potential for heavy minerals in the Lilesville, North Carolina, sand and gravel deposits. In A.J.W. Zupan, ed., 24th Forum on the Geology of Industrial Minerals, Proc. Vol., in press.
- Cook, R.B. and Nelen, J.A. (in press) The occurrence and exploration significance of gold in Cretaceous sediments of the Alabama coastal plain. In C.M. Leshner, R.B. Cook, and L.S. Dean, eds., Gold Deposits of Alabama, Geol. Surv. Alabama Bull.
- Cooley, T.W. (1970) Post-Cretaceous stratigraphy of the central sandhills region, North and South Carolina. Unpub. Ph.D. dissertation, Univ. North Carolina, 137 p.
- Craig, J.R. and Vaughan, D.J. (1981) Ore Microscopy and Ore Petrography. Wiley Interscience, New York, 406 p.
- D'Agostino, J.P. and Rowe, W.D. (1986) Mineral Occurrences of the Charlotte 1° x 2° Quadrangle, North Carolina and South Carolina. U.S. Geol. Surv., Misc. Field Studies Map MF-1793.
- D'Agostino, J.P. and Whitlow, S.I. (1989) Gold in fossil placers in Triassic sedimentary rock of the Wadesboro basin. In J.E. Gair, eds., Mineral Resources of the Charlotte 1° x 2° Quadrangle, North Carolina and South Carolina. Geol. Surv. Prof. Paper 1462, p. 163-166.
- D'Agostino, J.P., Whitlow, J.W., and Perkins, T. (1987) Locations of native gold seen in panned concentrates from Charlotte 1° x 2° quadrangle, North Carolina and South Carolina. U.S. Geol. Surv. Open-file Report 87-367, 27 p.
- D'Agostino, J.P., Whitlow, S.I., and Gair, J.E. (1989) Colluvial deposits of gold and other minerals. In J.E. Gair, eds., Mineral Resources of the Charlotte 1° x 2° Quadrangle, North Carolina and South Carolina. Geol. Surv. Prof. Paper 1462, p. 160-162.
- Desborough, G. (1970) Silver depletion indicated by microanalysis of gold from placer occurrences, western United States. Econ. Geol., v. 65, p. 304-311.
- Desborough, G., Raymond, W.H., and Iagmin, P.J. (1970) Distribution of silver and copper in placer gold derived from the northeastern part of the Colorado Mineral Belt. Econ. Geol., v. 65, p. 937-944.
- Ferguson, H.G. (1924) Geology and ore deposits of the Manhattan District, Nevada. U.S. Geol. Surv. Bull. 723, 163 p.
- Fisher, M.S. (1935) The origin and composition of alluvial gold, with special reference to the Morobe Goldfield, New Guinea. Bull. Inst. Mining and Metall. (London), No. 365, 46 p.
- Fisher, N.H. (1945) The fineness of gold, with special reference to the Morobe Goldfield, New Guinea. Econ. Geol., v. 40, p. 449-495, 537-563.
- Giusti, L. (1983) The distribution, grades, and mineralogical composition of gold-bearing placers in Alberta. Unpublished M.S. thesis, Univ. Alberta, Edmonton, Alberta, 396 p.
- Giusti, L. (1986) The morphology, mineralogy, and behavior of "fine-grained" gold from placer deposits of Alberta: sampling and implications for mineral exploration. Can. J. Earth Sci., v. 23, p. 449-495.

- Groen, J.C. (1987) Gold-enriched rims on placer gold grains: An evaluation of formational processes. M.S. thesis, Virginia Polytechnic Institute and State University, Blacksburg, 72 p.
- Johnson, W.A. and Uglow, W.L. (1924) Placer and vein gold deposits of Barkerville and Cariboo District, British Columbia. Geol. Surv. Canada Mem. 149, 246 p.
- Knight, J. and McTaggart, K.C. (1986) The composition of placer and lode gold from the Fraser River drainage area, southwestern British Columbia. Can. Geol. J. CIM, v. 1, p. 21-30.
- Mann, A.W. (1984) Mobility of gold and silver in lateritic weathering profiles; some observations from Western Australia. Econ. Geol., v. 79, p. 38-49.
- Matson, C.G. (1916) The Pliocene Citronelle Formation. U.S. Geol. Surv. Prof. Paper 98-L, p. 167-192.
- McCrone, W.C., Draftz, R.G., and Delly, J.G. (1969) The Particle Atlas. Ann Arbor Science Pubs Inc., 406 p.
- Porcher, S. (1882) On an interesting specimen of native gold, from Montgomery Co., Virginia. The Virginias, v. 3, p. 3.
- Pretorius, D.A. (1981) Gold and uranium in quartz-pebble conglomerates. Econ. Geol., 75th Anniv. Vol., p. 117-138.
- Ramdohr, P. (1965) Rheingold als Seifenmineral. Baden-Württemberg Geol. Landesamtes Jahreshafte, v. 7, p. 87-95.
- Ramdohr, P. (1969) The Ore Minerals and Their Intergrowths. Pergamon Press, Oxford, England, 1174 p.
- Sharp, W.E. (1988) Auriferous terrace gravels on Little Fork Creek, Chesterfield County, South Carolina. In D.T. Secor, ed., Southeastern Geological Excursions, Guidebook for Geological Excursions held in connection with meeting of the Southeastern Section of Geological Society of America, p. 19-23.
- Smith, P.S. (1913) The fineness of gold in the Fairbanks District, Alaska. Econ. Geol., v. 8, p. 449-454.
- Stumpfl, E.F. and Clark, A.M. (1965) Electron-probe microanalysis of gold-platinoid concentrates from southeast Borneo. Trans. Inst. Mining and Metall., v. 74, p. 933-946.
- Warren, H.V. (1982) The significance of a discovery of gold crystals in overburden. In A.A. Levonson, ed., Precious Metals in the Northern Cordillera. Assoc. Explor. Geochem., p. 45-51.
- Webster, J.G. and Mann, A.W. (1984) The influence of climate, geomorphology and primary geology on the supergene migration of gold and silver. J. Geochem. Explor., v. 22, p. 21-42.

# THE USE OF RELICT PHASES WITH PLACER GOLD IN CHARACTERIZING LODES

Alan J. Driscoll, Jr.,\* Donald L. Hall,\*\* and James R. Craig\*\*

\*5247 Dunleigh Drive, Burke, Virginia 22015

\*\*Department of Geological Sciences, Virginia Polytechnic Institute and State University  
Blacksburg, Virginia 24061

## ABSTRACT

Placer gold deposits represent the earliest exploration guides to lode deposits. It has long been recognized that placer deposits of gold, platinum group metals or other ore minerals indicate the presence of lode deposits upstream, and that the individual placer minerals may provide information on the distance of transport, residence time, and lode composition.

Single-phase placer grains or associated detrital minerals generally dominate the fine fraction of sediments, but careful examination commonly reveals the presence of significant numbers of multiphase grains. Quartz is the most frequently observed phase attached to placer gold, but a variety of other phases have also been encountered. The presence of these "relict" phases provides an opportunity to extract valuable information on the nature of the lode deposit.

Exploration programs commonly involve soil and stream sediment sampling, followed by drilling. While drilling yields essential information on the geology, grade and tonnage of a deposit, it also requires significant financial commitment. An intermediate exploration phase involving careful analysis of placer samples can provide useful data about the deposit without major commitments such as land acquisition and drilling.

Examination of placer gold from the Brush Creek deposit in southwestern Virginia serves as an example. Fluid inclusion and petrographic studies of relict phases attached to placer gold grains have constrained not only the timing, but also the P-T conditions of the lode formation. Relict quartz textures indicate that gold mineralization post-dated mylonitization associated with the Fries fault. Furthermore, fluid inclusion compositions suggest affinities for both detachment fault and epithermal type gold deposits.

## INTRODUCTION

The discovery of many major gold mines and districts has resulted from the initial discovery of placer gold in streams or rivers draining the area where primary gold-bearing deposits occur. For example, the first gold mine in the United States (the Reed Mine in North Carolina), and mines in the Mother Lode District, California, resulted from the prior discovery of placer gold. Undoubtedly, the search for placer gold served as one of the earliest and most effective means of exploration. The presence of gold in the alluvium has long been recognized as indicating the existence of a lode deposit upstream. Other minerals in the alluvium, spatially related to the ore minerals *may* provide information about the lode deposit, but the problem, of course, is that their relationship to the ore minerals is often poorly understood. This situation has been recognized in many provenance studies, including those on the world's largest gold deposits in the Witwatersrand basin of South Africa (Hallbauer and Kable, 1982).

In addition to indicating *where* a lode may occur, placer grains of gold, platinum-group metals (PGM), and other placer ore minerals can help to characterize the lode. In order for this to have merit, the placer grains must retain chemical or physical characteristics, or signatures, of the lode. Cabri and Harris (1975) have applied the concept of chemical signatures to alluvial PGM alloys with considerable success. They have shown convincingly that there is a strong relationship between the composition of placer PGM and the inferred source rock. Those alluvial grains derived from concentrically zoned or "Alaska Type" intrusions have Pt\*100/ (Pt+Ir+Os) ratios greater than 86, while those derived from ophiolites, or "Alpine Type" deposits have Pt\*100/ (Pt+Ir+Os) ratios of 36 or less. Clearly, though they may have been partially altered, these alluvial samples have retained at least some chemical characteristics of the source lodes.

The composition of alluvial gold is not as useful as that of alluvial PGM in evaluating associated lodes, primarily because the ranges and causes of variability of natural gold finenesses are not well understood, and because gold occurs in a wide variety of geological environments. Nevertheless, studies of the variations of natural gold compositions and differences between districts have begun to reveal some potential utility for exploration (Antweiler and Campbell, 1977; Craig and Rimstidt, 1985; Craig and Solberg, 1986). Commonly however, alluvial gold is found with other *attached* phases that retain both chemical and physical characteristics of the lode from which they were derived. These "relict" phases may provide important information about that lode.

This paper will discuss the variety of relict phases that are found with placer gold, the information these phases can offer, and as an example, will discuss what has been learned by this type of work done on alluvial gold grains from the Brush Creek deposit in southwestern Virginia. The term "relict" will be used throughout the paper to describe phases that have remained attached to, or intergrown with alluvial gold since they were weathered from the lode deposit.

## THE UTILITY OF RELICT PHASES

### Mineralogy and Textures

Although the vast majority of placer gold grains consist solely of electrum, a significant percentage of these grains in most placers have small fragments of other minerals included or attached. Quartz is the most commonly reported relict phase found with alluvial gold, but feldspars (Foster et al., 1978; this study), micas (this study), ilmenite (Cox and Singer, 1986; this study), magnetite (Cox and Singer, 1986) pyrite (this study), garnet (Barker, 1986), and rock fragments (Barker, 1986) have also been found.

The association of relict phases with alluvial gold may be used to suggest and eliminate possible types of lode deposits from which the gold could have been derived. Relict phases may have certain characteristics that can be identified in the placer grain, and then sought in either stream sediments or outcrops. These characteristics may include mineralogy, deformational textures, fluid inclusion character, color, trace element content, and cathodoluminescence.

The presence of relict quartz has limited utility in constraining the conditions of ore formation, because quartz is common in such a wide range of geological environments. Nevertheless, quartz can still provide useful information in terms of its texture. Although the quartz may suffer significant abrasion during weathering, this process does not alter its internal structure. Hence, any initial metamorphic or deformational textures are preserved,

even in very small quartz relicts. Furthermore, quartz commonly contains fluid inclusions that may preserve information on the conditions and mechanisms of formation.

Relict feldspar can not only help constrain the source of the alluvial gold, but can also serve as a geothermometer (Smith, 1974). Furthermore, the structural state of feldspars can be a useful indicator of the environment of ore deposition (Cerny and Chapman, 1986). For instance, crystallization at high temperatures followed by rapid cooling will result in a highly disordered feldspar, while crystallization at lower temperatures or very slow cooling will probably yield more highly ordered feldspar.

Relict oxide minerals can permit the estimation of limits on oxygen and/or sulfur activity, depending on the particular phases present.

Sulfide minerals, though commonly coexisting with gold in lodes, do not readily survive the rigors of fluvial transportation. Their presence as relicts generally indicates close proximity to the lode source; furthermore, they also permit estimations of limits on sulfur and/or oxygen fugacity.

The presence of a relict phase with gold does not necessarily mean that the two phases are cogenetic, it only means they coexisted in the lode. As with any interpretation then, care and discretion must be exercised.

#### Fluid Inclusions and Isotopes

The nature of fluid inclusions associated with many different types of ore deposits and their utility as petrologic tools has been documented in hundreds of papers and is well summarized by Roedder (1984). Accordingly, the study of fluid inclusions in relict quartz grains may help to not only characterize the trapped fluid, but also to constrain the possible types of deposits represented by the lode. Of particular interest are the compositions of the fluid inclusions. Figure 1a, prepared from many sources in Roedder (1987), illustrates CO<sub>2</sub>-NaCl relationships in major ore deposit types. The presence of CO<sub>2</sub> or other non-condensable gases may be quickly determined by crushing experiments, and in some instances may be quantified microthermometrically, or through micro-Raman techniques. Salinities of appropriate inclusions can be measured on a standard heating/freezing stage. Homogenization temperatures, while not as useful as compositional data, can still be important in distinguishing between deposit types. Wilkins et al. (1986) have grouped some major ore deposit types as a function of the salinity and homogenization temperatures of their fluid inclusions (Fig. 1b).

The relict minerals attached to gold grains may be sufficient to provide isotopic data on the host lode (for instance, oxygen isotopic measurements can be made with as little as 5 mg of quartz). These measurements, coupled with temperature estimates and information on isotopic fractionation can provide an estimate of the isotopic composition of the fluid responsible for mineralization. This in turn may elucidate the source of the fluids and hence the environment of ore deposition. Alternatively, if two coexisting minerals (e.g., two sulfides) can be separated and the fractionation between this pair is known, an estimate of temperature, as well as the isotopic composition of the fluid, can be made. This temperature estimate can then be combined with fluid inclusion compositions and densities to provide an estimate of pressure.

In summary, techniques commonly employed in advanced petrologic studies, but considered to be inapplicable to placer deposits, take on a new importance with the application to exploration, as these techniques can yield crucial information for minimal costs.

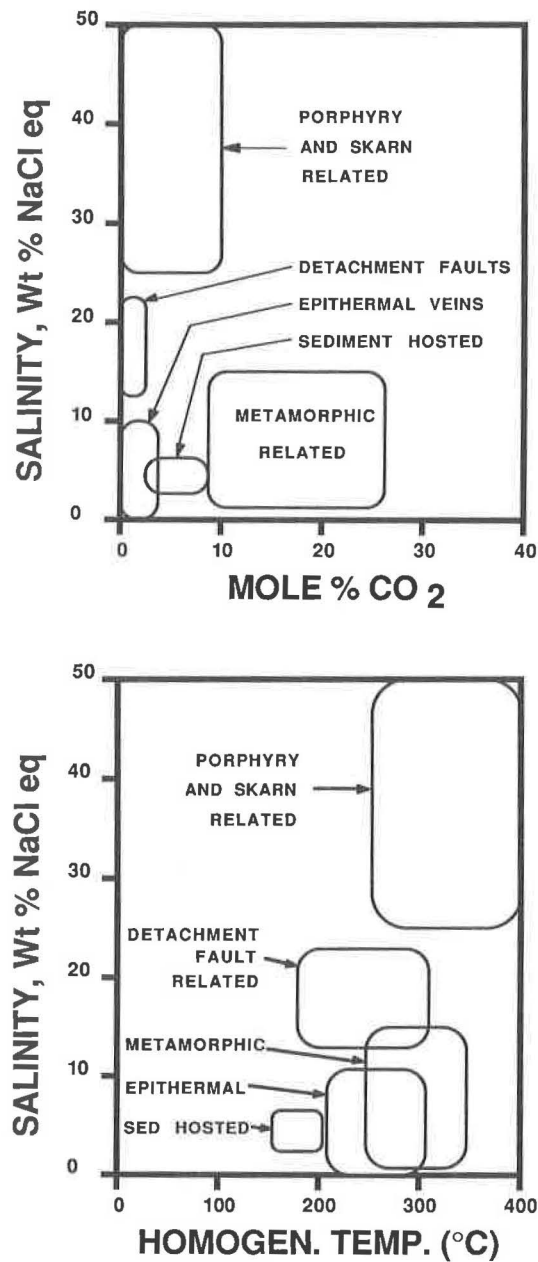


Figure 1. (A) CO<sub>2</sub> vs. salinity relationships for fluid inclusions associated with the indicated deposit types (prepared from many sources in Roedder, 1987). (B) Homogenization temperature (Th) vs. salinity relationships for several types of deposits (modified from Wilkins et al., 1986).

To illustrate the utility of these techniques in examining alluvial gold, we will now turn to the Brush Creek prospect.

## AN EXAMPLE FROM THE BRUSH CREEK GOLD OCCURRENCE, SW VIRGINIA

### Geology

The Brush Creek gold occurrence is located at the border of Floyd and Montgomery counties, in the Blue Ridge province of southwestern Virginia (Fig. 2). Placer gold was discovered in 1879, and after a minor gold rush that produced an estimated 1500 troy ounces, was mined intermittently until 1920 (Fontaine, 1882; Luttrell, 1966; Sweet, 1980, 1983). The deposit lies within the Fries fault, a major ductile deformation zone (DDZ) that extends for many miles to the northeast and southwest along the Blue Ridge. The DDZ in the vicinity of Brush Creek is bounded on the northwest by the Pilot gneiss, and on the southeast by the Little River gneiss (Fig. 2). The DDZ itself was originally described as a gneiss (Fontaine, 1882), but is now recognized as a mylonite (Kaygi, 1979) as illustrated in Figure 3.

### Sample Preparation

Placer gold grains recovered from stream sediments by hand picking from panned concentrates, or under a binocular microscope. Representative material from the coarse fractions was carefully inspected, and thin sections were prepared from cobbles wherever gold was found. Gold grains with relict phases were prepared for either microthermometry or electron microprobe analysis. Samples intended for microthermometric measurements were mounted to a glass slide with a drop of high temperature epoxy (Epo-tek) and cured at 100°C for approximately one hour. The sample was polished on one side then mounted to a second slide with "super-glue." The glass was ground off the unpolished side, and that side was polished as well. The "super-glue" was then dissolved in acetone, releasing a doubly polished epoxy chip ideal for fluid inclusion work. Samples intended for electron microprobe analysis were mounted in standard epoxy and polished on one side.

### Mineralogy and Textures

Placer gold grains recovered from streams with smaller drainage basins were generally found to lack gold-enriched rims (Driscoll, 1989), and to contain the largest proportions of relict phases. Quartz is the most commonly found relict phase, and is of two varieties. The first variety is moderately deformed, displaying undulose extinction and minor recrystallization, whereas the second variety is completely undeformed, exhibiting sharp extinction. Figure 4 is an example of gold with moderately deformed quartz. The grain boundaries of the recrystallized quartz in this sample are decorated with small particles of gold (Fig. 5). The sample in Figure 6 consists of gold within moderately deformed quartz, that in turn cross-cuts the mylonitic foliation in an earlier generation of highly deformed quartz.

One sample consists of gold, quartz, and limonite. Polishing of the surface of this grain revealed a euhedral cubic pseudomorph of limonite after pyrite. The euhedral form of the pyrite suggests that it crystallized under static conditions, and in open space.

Further evidence for open-space mineralization is given by a sample of breccia, consisting of deformed quartz clasts with interstitial sulfide mineralization (Fig. 7).

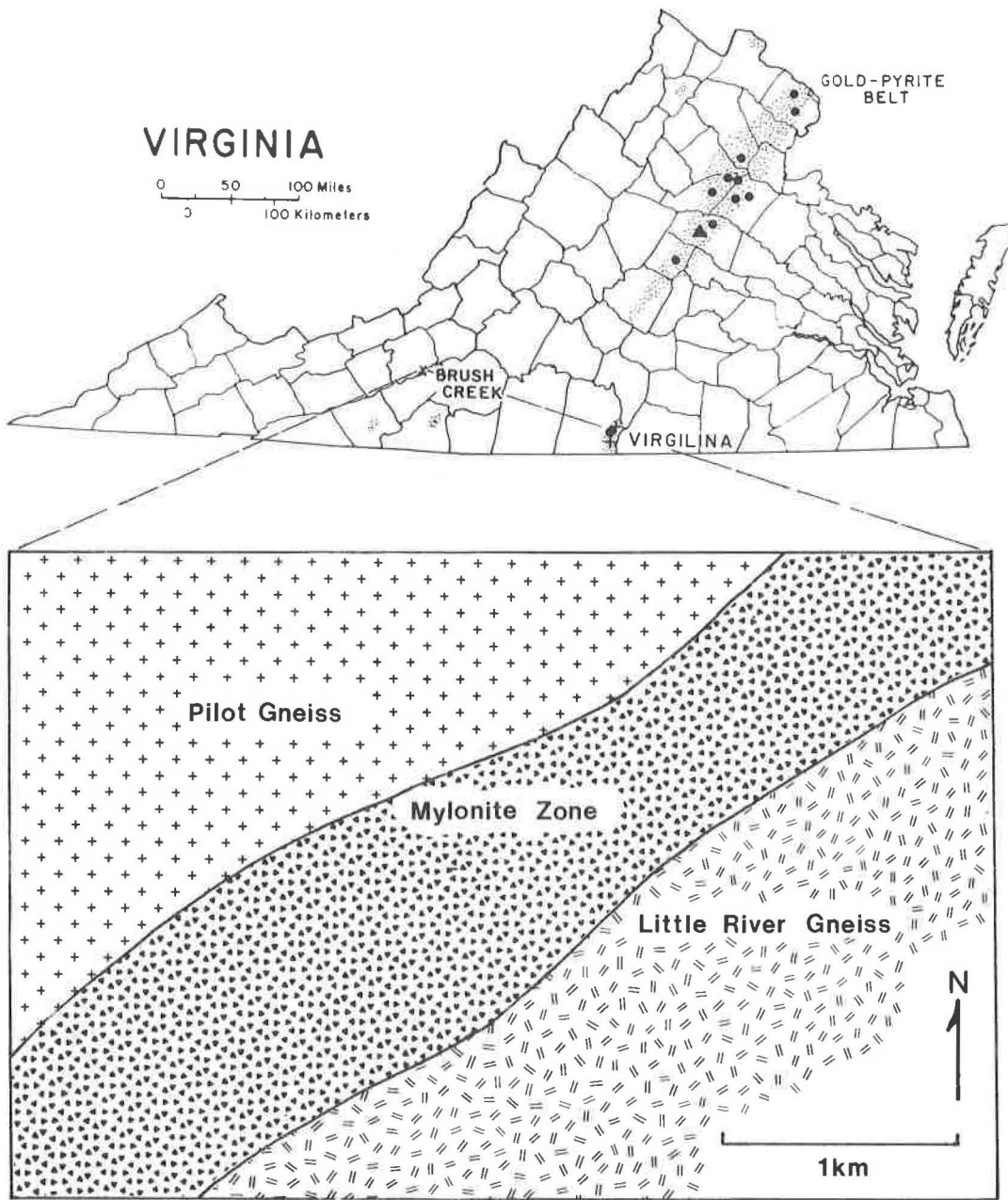


Figure 2. Location of Brush Creek and other significant gold occurrences in Virginia, and a highly generalized geologic map of field area. The gold at Brush Creek is derived from the mylonite zone.

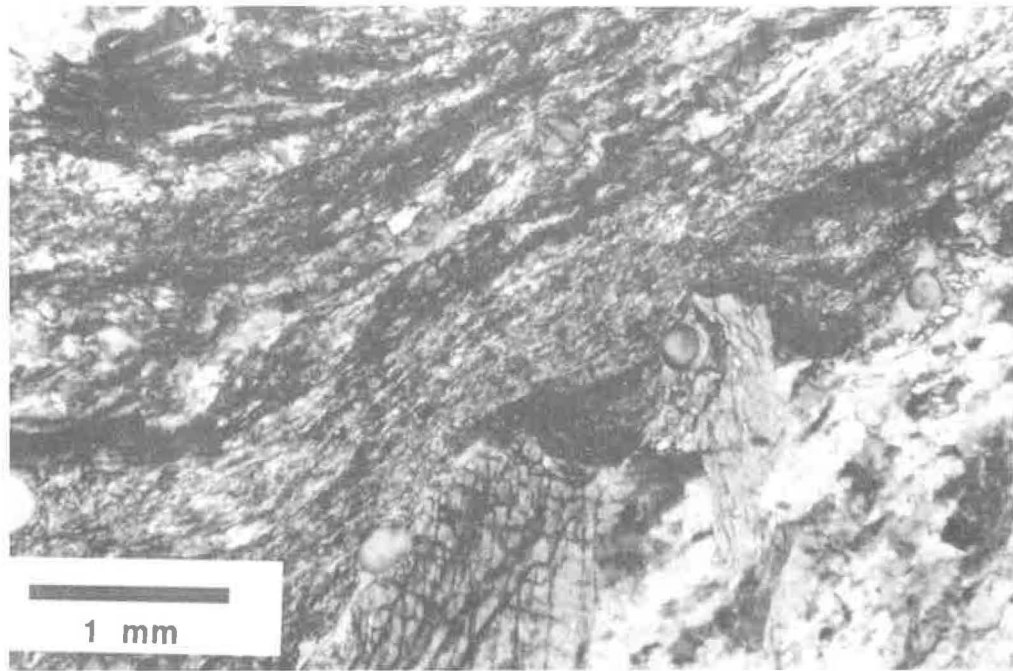
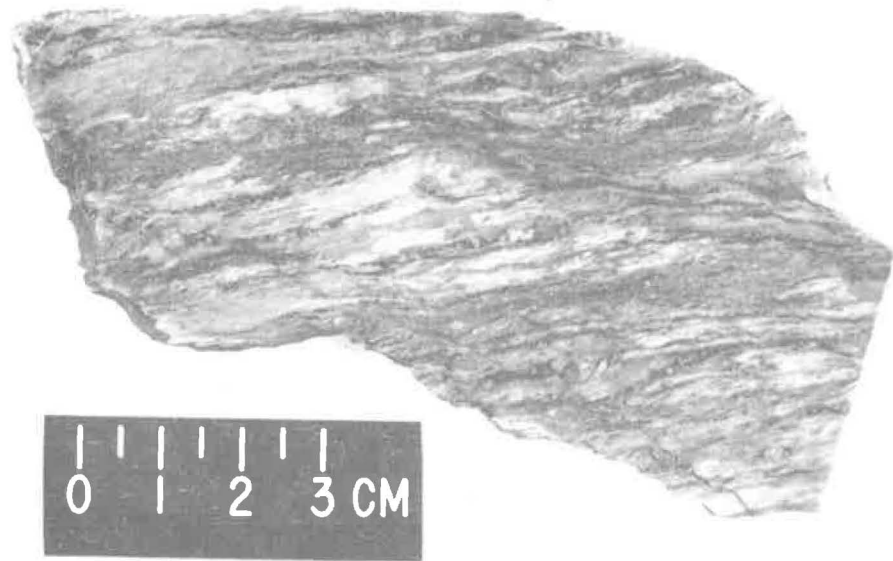


Figure 3. (A) Hand sample and (B) thin section of mylonitic gneiss from Brush Creek, Virginia, showing foliation defined by chlorite.

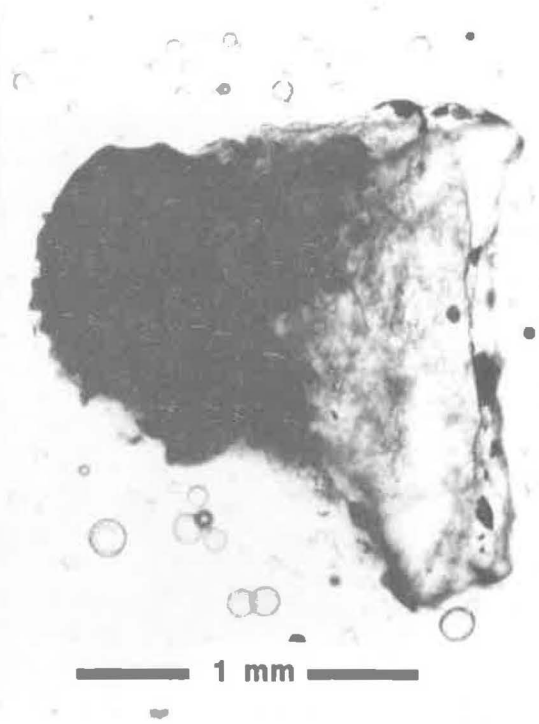


Figure 4. (A) Reflected light, and (B) transmitted light photomicrograph of placer gold grain with relict quartz from Brush Creek, Virginia.

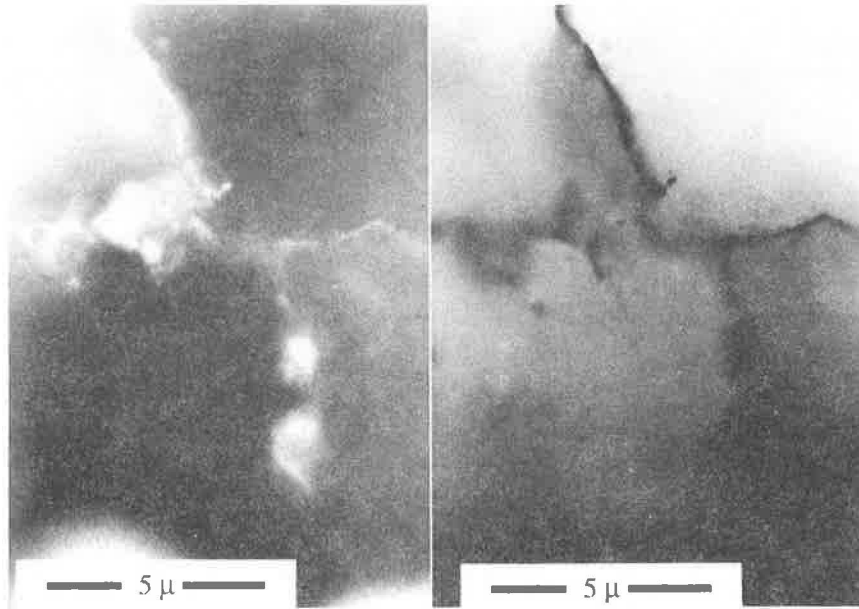


Figure 5. (A) Reflected light, and (B) transmitted light photomicrograph of gold particles decorating quartz grain boundaries in sample shown in Figure 4.

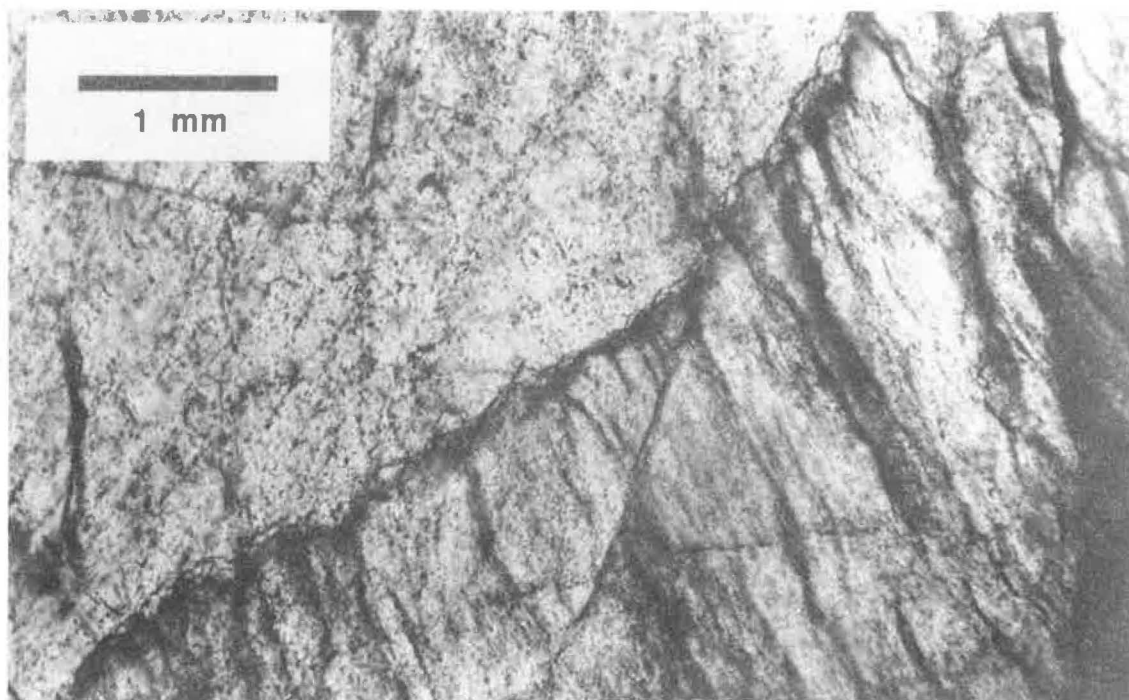


Figure 6. Photomicrograph of a thin section showing younger auriferous quartz (gold grain is just outside the field of view to the upper left) cross-cutting mylonitic foliation in earlier barren quartz (lower right) in sample from Brush Creek, Virginia.

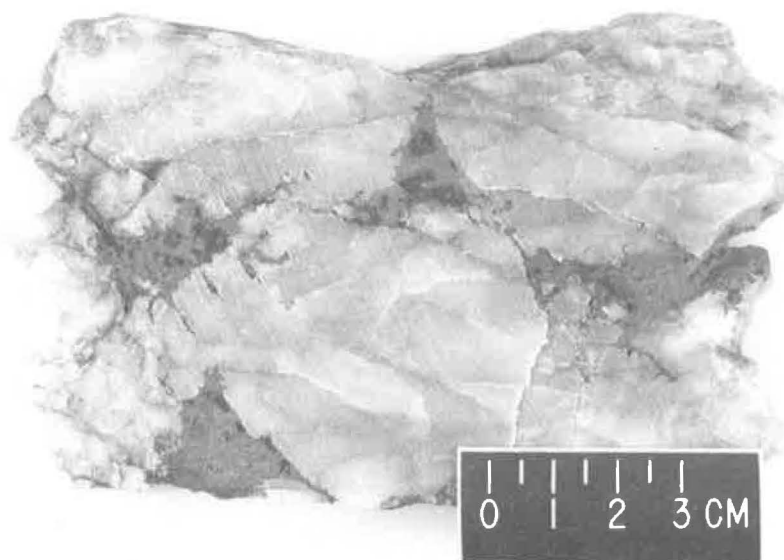


Figure 7. Hand sample from Brush Creek, Virginia, of quartz breccia with interstitial sulfide mineralization.

Three gold samples were found to have a total of 6 relict feldspar grains (Fig. 8). These were analyzed by electron microprobe and found to be virtually pure orthoclase. Some of these feldspar grains display moderate undulose extinction, while others are undeformed. One of these samples also contains a relict mica grain that optically appeared to be chlorite (Fig. 8), but microprobe analysis was inconclusive.

Two gold samples contain relict ilmenite that is enriched in manganese. One of these samples consists of a series of interleaved wedges of gold, ilmenite, and quartz (Fig. 9). In the other sample, the ilmenite grain is separated from its gold host by a rim or zone that is depleted in Fe and Mn, and enriched in Al, Si, and Na (Fig. 10). From their textural relationship with the gold, both of these relict ilmenite grains appear to have been present in the host rock prior to gold mineralization.

### Fluid Inclusions

Fluid inclusions suitable for study are present in relict quartz attached to placer gold, and in gold-bearing quartz cobbles collected along with the placer grains. Fluid inclusions were studied using standard microthermometric techniques, employing a U.S.G.S-type gas-flow, heating-freezing stage (Werre et al., 1979) for data collection. This stage was calibrated at the triple point of CO<sub>2</sub> (-56.6°C), the freezing point of water (0.0°C) and the critical point of water (374.1°C) using synthetic fluid inclusions (Sterner and Bodnar, 1984). In addition to microthermometry, a crushing stage and Raman microprobe were used to assess the gas contents of inclusions.

Three distinct fluid inclusion populations were noted based on phase ratios, compositions, morphologies and/or textural relationships among quartz, gold and fluid inclusions. Type 1 inclusions, the earliest-formed type consists of two fluid phases, liquid and vapor, at room temperature. They range from 3-10 µm in size and decorate grain boundaries of recrystallized quartz, lie along healed, intergranular and intragranular microfractures, or occur as randomly-oriented groups in the centers of grains. They occur only in deformed quartz and are not spatially related to gold grains. Type 1 inclusions are characterized by apparent eutectic temperatures (Te) of -50° to -60°C, final melting temperatures of ice (Tm ice) of -17° to -33°C (Fig. 12, top) and homogenization temperatures (Th) of 150° ± 50°C. These data suggest that the inclusions contain significant amounts of CaCl<sub>2</sub> ± MgCl<sub>2</sub> in addition to NaCl. Modelling the low temperature behavior of Type 1 inclusions in the system CaCl<sub>2</sub>-NaCl-H<sub>2</sub>O suggests that they contain 20-27 wt % total salt (Oakes and Bodnar, 1988). In addition, a final melting point of -33°C implies a maximum NaCl/(NaCl+CaCl<sub>2</sub>) weight ratio of 0.2, or a Na/Ca atomic ratio of 0.5, for these inclusions. Evidence for necking and partial decrepitation is common in Type 1 inclusions and probably accounts for the scatter in homogenization temperatures. The combination of these effects can produce both lower and higher densities, thus making Th of limited utility in these inclusions. Type 1 inclusions are identical to those found by Kirby et al. (1988) in mylonitic gneiss and mylonitic quartz segregations within the Fries fault (Fig. 11). These authors have shown that CaCl<sub>2</sub>-NaCl-H<sub>2</sub>O fluid inclusions record the fluid present in the late stages of mylonitization.

Type 2 inclusions average 2-3 µm in size and occur along healed intergranular and intragranular microfractures in deformed quartz, but were not found along grain boundaries. They are associated with gold in moderately deformed quartz. These inclusions are dominantly one-phase liquids at room temperature although two-phase liquid + vapor inclusions (slightly larger in size) with variable liquid/vapor ratios coexist with one phase types. Close inspection of two-phase inclusions often reveals microfractures that emanate from the inclusion walls and propagate into the surrounding quartz host. It is interpreted

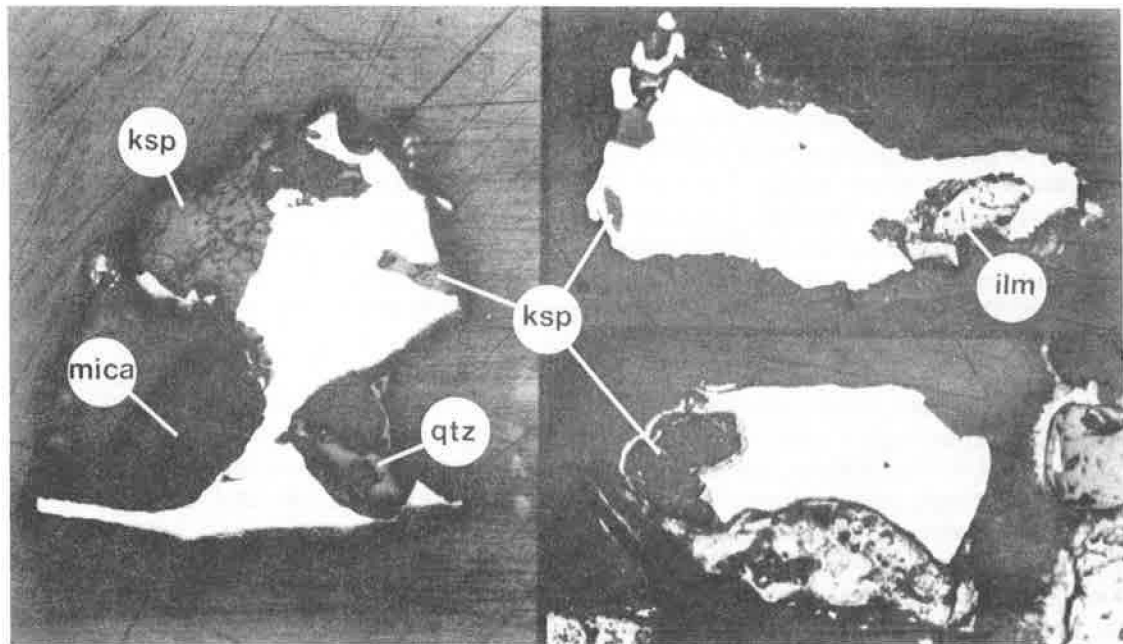


Figure 8. Photomicrographs of placer gold grains from Brush Creek, Virginia, indicating relict phases of feldspar, quartz, ilmenite, and mica.

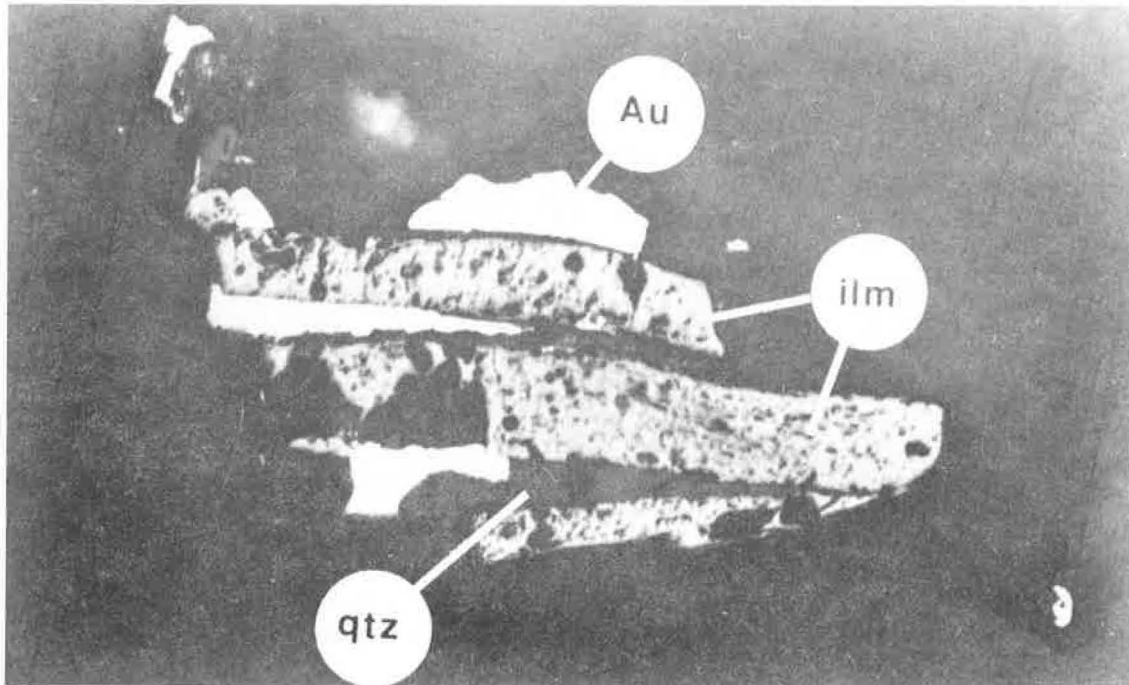


Figure 9. Photomicrograph of placer gold (AU) grain with relict ilmenite (ILM) and quartz (QTZ) from Brush Creek, Virginia.

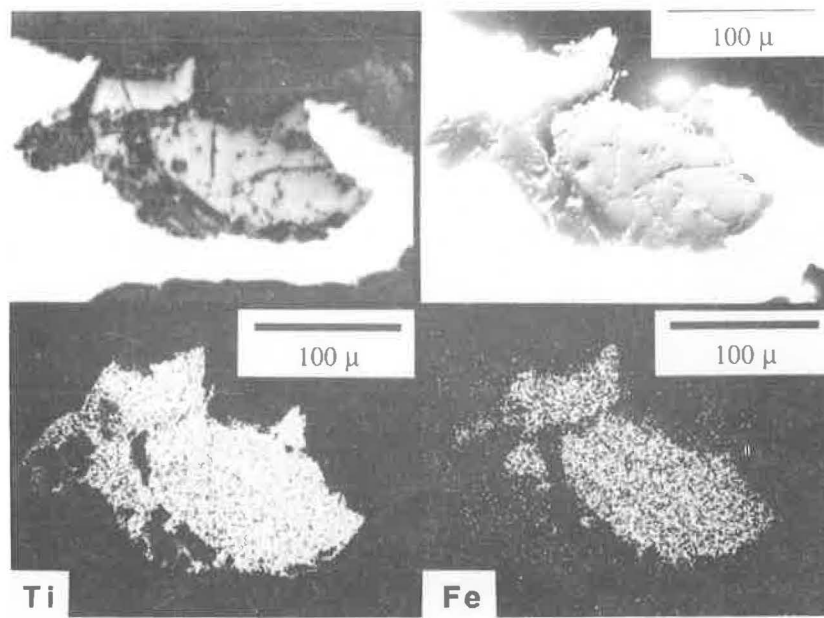


Figure 10. Photomicrograph (enlarged view) of placer gold (AU) grain with relict ilmenite (ILM) shown in Figure 8. (A) Reflected light, (B) backscattered electron image, (C) X-ray map for titanium, and (D) X-ray map for iron.

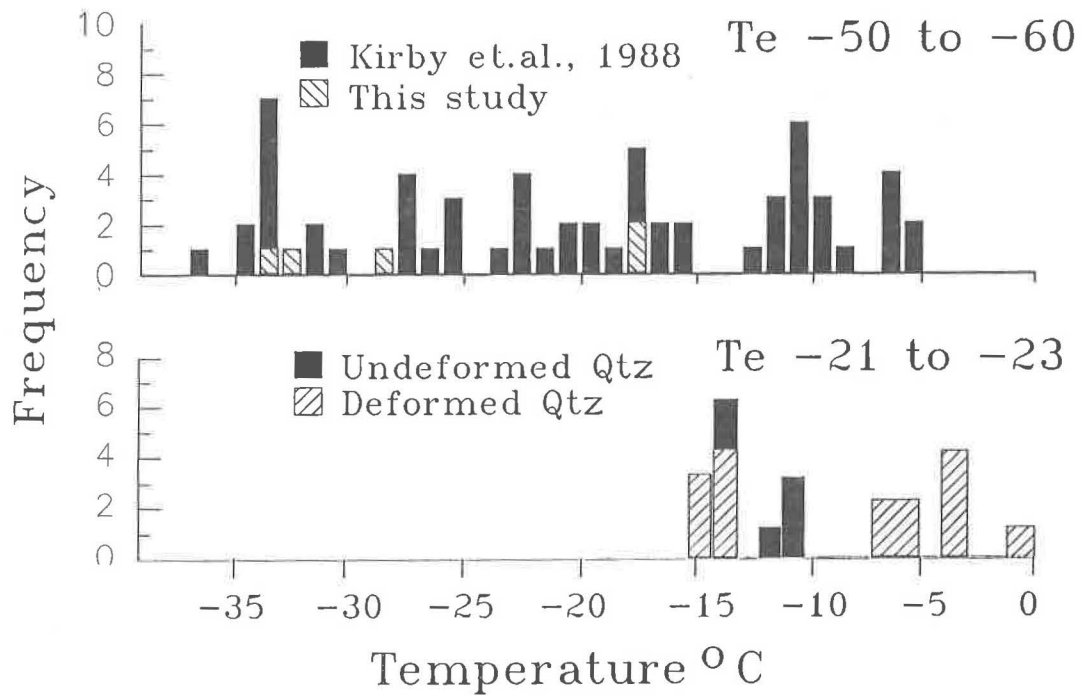


Figure 11. Ice melting temperatures of fluid inclusions in barren, mylonitic quartz (top), and auriferous quartz (bottom) from Brush Creek, Virginia.

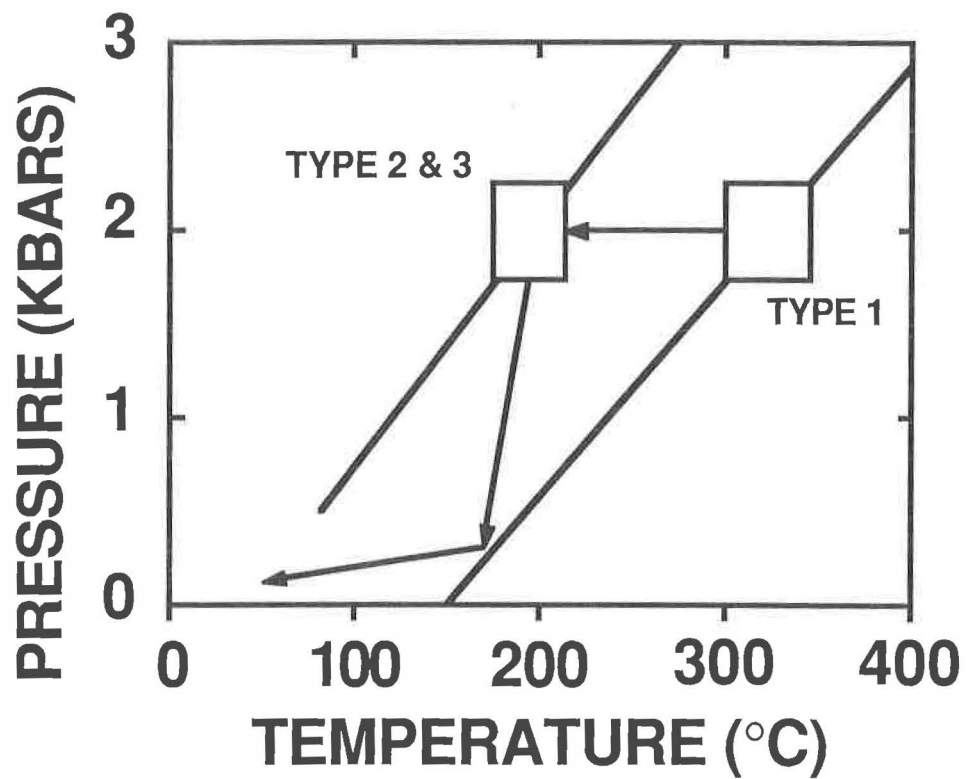


Figure 12. Isochores for fluid inclusions in barren (Type 1) quartz, and auriferous (Type 2 and 3) quartz. Schematic uplift path for Brush Creek rocks is initially isobaric, and then strongly isothermal.

that the two-phase inclusions partially decrepitated during uplift in response to internal over-pressures. The brittle nature of decrepitation suggests that it occurred at relatively low temperatures and probably fairly late in the uplift history. The relationship between inclusion size and the internal pressure required for decrepitation (Bodnar et al., 1989) indicates that about 2 kb of internal over-pressure is necessary to initiate decrepitation in these inclusions. This observation has significant implications for P-T conditions of trapping and uplift paths, as described below.

Type 2 inclusions display final melting temperatures of  $-0.4^{\circ}$  to  $-6.6^{\circ}\text{C}$  (Fig. 11), corresponding to salinities of 1 to 10 wt % NaCl equivalent (Hall et al., 1988). Reliable eutectic temperatures could not be measured on these inclusions due to their small size. As most inclusions were one-phase liquids, and vapor-absent phase transitions are generally metastable (Roedder, 1984), melting temperatures were measured on inclusions that were already two-phase, or that were made two-phase by partial decrepitation during heating. The compositions of initially two-phase inclusions and those that were rendered two-phase in the laboratory, are similar, further supporting that the two-phase Type 2 inclusions have partially decrepitated.

Crushing studies of Type 2 inclusions revealed that very minor quantities of gases are dissolved in the aqueous phase. When one-phase, Type 2 inclusions are opened during crushing, this gas exsolves, is expelled into the surrounding immersion oil, and dissolves into the oil in a few seconds. The vapor phase expelled from each inclusion has a diameter 1-2 times that of the original inclusion. If the aqueous portion of the inclusion is taken to be pure  $\text{H}_2\text{O}$ , the density of  $\text{CO}_2$  at 1 atmosphere and  $25^{\circ}\text{C}$  indicates that less than 0.5 mole % gas is dissolved in these inclusions. Raman spectroscopy on both one- and two-phase Type 2 inclusions failed to detect any  $\text{CO}_2$ ,  $\text{CH}_4$ ,  $\text{N}_2$  or sulfur species. This is consistent with our crushing tests, because the detection limit for most of the above species with Raman spectroscopy is on the order of 1-2 mole %.

Type 3 inclusions are 2-5  $\mu\text{m}$  in size, occur in both deformed and undeformed (i.e. late-stage) quartz, and are associated with gold in undeformed quartz. They are similar to Type 2 inclusions in that they occur along healed intergranular and intragranular microfractures and are mostly one-phase liquids. Two-phase liquid + vapor inclusions show evidence for partial decrepitation, much like Type 2 inclusions. Apparent eutectic temperatures of  $-21^{\circ}$  to  $-23^{\circ}\text{C}$  were measured for Type 2 inclusions, suggesting NaCl  $\pm$  KCl as the dominant salts. Final melting temperatures of ice range from  $-10^{\circ}$  to  $-15^{\circ}\text{C}$  (Fig. 11, bottom). Modelling these fluids in the system NaCl-KCl- $\text{H}_2\text{O}$  suggests total salinities of 14 to 22 wt % (Hall et al., 1988). The melting temperature of hydrohalite or sylvite along the hydrohalite-ice, or sylvite-ice cotectics, respectively, could not be measured due to the small size of these inclusions. Accordingly, Na/K ratios could not be determined. However,  $T_m$  ice of  $-14.5^{\circ}\text{C}$  implies NaCl/(NaCl+KCl) weight ratios greater than 0.4 (Na/K ratios  $> 0.85$ ). Crushing tests revealed amounts of dissolved gases comparable to those found in Type 2 inclusions.

Isochores were constructed for the three fluid inclusion populations based on their estimated compositions and densities (Fig. 12). Because the isochores of  $\text{CaCl}_2$ -NaCl- $\text{H}_2\text{O}$  solutions are not well-known, these inclusions were treated as NaCl solutions of approximately equivalent salinity and density. The densities of one-phase, Type 2 and 3 inclusions were approximated by assuming the solution was vapor-saturated at room temperature (i.e., that the  $T_h$  of these two inclusion types is  $25^{\circ}\text{C}$ ). Internal pressures greater than 1 bar, as verified by crushing studies, suggest that the true isochores may be displaced slightly to higher pressures at a given temperature. This will result in under estimation of trapping pressures if a given trapping temperature is assumed.

## Interpretation

The contrast in deformation states between the auriferous and barren quartz clearly indicates that the gold mineralization post-dated the mylonitization. Furthermore, the two varieties of auriferous quartz (undeformed and moderately deformed) suggest either multiple episodes of mineralization, or that mineralization extended over an interval that was only partly synchronous with deformation. This is born out in part by our fluid inclusion studies.

The euhedral relict limonite pseudomorph in one of the alluvial gold samples, the interstitial sulfide mineralization of the breccia (Fig. 7), and the presence of euhedral quartz fragments found in stream sediments with high gold values, all suggest that some of the gold mineralization occurred as open-space filling.

Integration of fluid inclusion data with mineralogical and textural criteria places reasonable constraints on the P-T conditions of the gold mineralization, and on the P-T path experienced by rocks at Brush Creek (Fig. 12). The common assemblage in the mylonite zone, of albite + chlorite  $\pm$  epidote, the rarity of biotite, and the lack of garnet suggests that the prevailing metamorphic grade recorded is lower greenschist facies. Furthermore, the fact that chlorite usually defines the mylonitic foliation in these rocks suggests that this grade was attained during mylonitization. The highest temperature recorded by the mylonitization then, was that of lower greenschist facies or, conservatively, 350°C. With this temperature, and the isochore estimated for Type 1 fluid inclusions, the pressure during late mylonitization must have been on the order of 2-2.5 kb. The estimated isochores for Type 2 and 3 inclusions, the types associated with gold mineralization, coupled with the observation that a differential pressure of about 2 kb was attained between Type 2 and 3 inclusions and the matrix during uplift, requires that the uplift path be initially isobaric and then strongly isothermal (Fig. 12). These relationships also imply minimum and maximum temperatures of gold mineralization of 150°C and 200°C, respectively, and suggest that accompanying pressures were near 2 kb.

The data presented in the foregoing discussion indicate that gold mineralization at Brush Creek was probably epithermal, and associated with brittle fracture of rocks within the Fries fault zone, but clearly post-dated the latest mylonitization associated with the fault. This precludes the possibility of a "shear zone-type" deposit, and accordingly, has significant implications regarding any proposed exploration strategy. For example, a shear zone-type ore body would likely be tabular, and conformable to the shear zone, whereas a vein-type epithermal deposit could have any number of orientations and/or morphologies.

## CONCLUSIONS

Although the technique of studying placer samples to characterize lode deposits may be applicable in only a limited number of cases, it can serve as an excellent exploration method where it *is* applicable. Recognition of the *presence* of certain relict phases may lead to more effective soil or stream sediment sampling programs. Recognition of certain *textures* in relict phases may suggest tectonic or structural relationships that could have influenced mineralization. Finally, knowledge of the *P-T conditions* during mineralization, as determined from fluid inclusion studies, isotopic studies, other geothermometers, geobarometers, or even geochronometers may help reveal the temporal and spatial relationship of the mineralization to the regional geology. Any of this information could have a significant influence on an exploration strategy.

For relatively little cost, and no commitment, a great deal of information can be obtained, in appropriate situations, by careful analysis of placer samples. The techniques are well established in various geological disciplines, but the application of these techniques to placer samples for exploration has been unrealized.

#### ACKNOWLEDGMENTS

We are grateful to Todd Solberg for his assistance in the microprobe analyses, to Llyn Sharp for her help with the photography and graphics, to Jean Cline and Ron Sheets for early reviews of the manuscript, and to Cheryl Knight for the Raman analyses. Steve Mittwede's critical review, and suggestions from Don Rimstidt, Larry Turner and Robert Cook are greatly appreciated. Kim Joseph deserves special thanks for her patience. This research has been supported by the Department of the Interior's Minerals Institute Program administered by the U.S. Bureau of Mines under allotment grant number G1174151 given to Virginia Polytechnic Institute and State University. Funding was also provided by the Virginia Division of Mineral Resources.

#### REFERENCES

- Antweiler, J.C. and Campbell, W.L., 1977, Application of gold compositional analyses to mineral exploration in the United States. *J. Geochem. Expl.*, 8, 17-29.
- Barker, J.C., 1986, Placer gold deposits of the Eagle Trough, Upper Yukon River Region, Alaska. U.S. Bur. of Mines, Inf. Circ. 9123, 23 p.
- Bodnar, R.J., Binns, P.R., and Hall, D.L., 1989, Synthetic fluid inclusions. VI. Quantitative evaluation of the decrepitation behavior of fluid inclusions in quartz at one atmosphere confining pressure. *J. Met. Geol.*, 7, pp. 229-242.
- Cabri, L.J. and Harris, D.C., 1975, Zoning in Os-Ir alloys and the relation of the geological and tectonic environment of the source rocks to the bulk Pt: Pt+Ir+Os ratio for placers. *Can. Mineral.*, 13, 266-274.
- Cerny, P., and Chapman, R., 1986, Adularia from hydrothermal vein deposits: Extremes in structural state. *Can. Mineral.*, 24, 717-728.
- Craig, J.R., and Rimstidt, J.D., 1985, Gold: Compositional variations in naturally occurring alloys. *Geol. Soc. Am., Abstracts with Programs*, 17, 55.
- Craig, J.R. and Solberg, T.N., 1986, Compositional signatures in some Appalachian gold occurrences. *Proc. Int. Min. Assoc.*, 13th meeting, Varna, Bulgaria, Pub. House of Bulgarian Academy of Sci., p. 213-222.
- Cox, D.P., and Singer, D.A., eds., 1986, Mineral deposit models. U.S. Geol. Surv. Bull. 1693, 379 p.
- Driscoll, Alan J., Jr., 1989, Lode gold deposit characterization using evidence from stream sediments: An example from Brush Creek, Montgomery County, Virginia. Unpublished M.S. thesis, VPI & SU, Blacksburg, VA, 71 p.
- Fontaine, W.M., 1882, Notes on Virginia geology: The Brush Creek, Va., gold district. In *The Virginias*, 3, 108.
- Foster, R.L., Foord, E.E., and Long, P.E., 1978, Mineralogy and composition of Jamison Creek particulate gold, Johnsville Mining District, Plumas Co., Calif. *Econ. Geol.*, 73, 1175-1183.
- Hall, D.L., Sterner, S.M., and Bodnar, R.J., 1988, Freezing point depression of NaCl-KCl-H<sub>2</sub>O solutions. *Econ. Geol.*, 83, 197-202.
- Hallbauer, D.K., and Kable, E.J.D., 1982, Fluid inclusions and trace element content of quartz and pyrite pebbles from Witwatersrand Conglomerates: Their significance with respect to the genesis of primary deposits. In Amstutz, G.C., et. al., eds., *Ore Genesis: The State of the Art*, Springer-Verlag, Berlin, p. 742-752.

- Kaygi, P.B., 1979, The Fries Fault near Riner, Virginia: An example of a polydeformed, ductile deformation zone. Unpublished M.S. thesis, VPI & SU, Blacksburg, VA, 165 p.
- Kirby, C.S., Driscoll, A.J. Jr., Bodnar, R.J., Law, R.D., 1988, Importance of fluid composition in the mylonitization process: A shear zone as a conduit for  $\text{CaCl}_2$ - $\text{NaCl}$  brines. *Geol. Soc. Am., Abstracts with Programs*, 20, A332.
- Luttrell, G.W., 1966, Base and precious-metal and related ore deposits of Virginia. Va. Div. of Min. Resources, *Min. Resources Report* 7, 167 pp.
- Oakes, C.S., and Bodnar, R.J., 1988, Phase equilibria in the system  $\text{NaCl-CaCl}_2\text{-H}_2\text{O}$ : The ice liquidus. *Geol. Soc. Am., Abstracts with Programs*, 20, A390.
- Roedder, E., 1984, Fluid inclusions. In Ribbe, P.H., ed., *Mineral. Soc. Am., Reviews in Mineralogy*, 644 p.
- Roedder, E., ed., 1987, *Fluid Inclusion Research*, Vol. 20. The University of Michigan Press, Ann Arbor, 559 p.
- Smith, J.V., 1974, *Feldspar Minerals*, Vol. 1. Springer-Verlag, New York.
- Sternner, S.M., and Bodnar, R.J., 1984, Synthetic fluid inclusions in natural quartz I. Compositional types synthesized and applications to experimental geochemistry. *Geochim. Cosmochim. Acta*, 48, 2659-2668.
- Sweet, P.C., 1980, Gold in Virginia. Va. Div. Min. Resources, *Pub.* 19, 77 p.
- Sweet, P.C., 1983, Virginia gold—Resource data. Va. Div. Min. Resources, *Pub.* 45, 196 p.
- Werre, R.W. Jr., Bodnar, R.J., Bethke, P.M., and Barton, P.B. Jr., 1979, A novel gas-flow fluid inclusion heating/freezing stage. *Geol. Soc. Am., Abstracts with Programs*, 11, 539.
- Wilkins, J., Jr., Beane, R.E., and Heidrick, T.L., 1986, Mineralization related to detachment faults: A model. In Beatty, B. and Wilkinson, P.A.K., eds., *Arizona Geol. Soc. Digest*, 16, 108-117.

A GEOCHEMICAL INVESTIGATION OF THE MASON MOUNTAIN SPERRYLITE  
OCCURRENCE, MACON COUNTY, NORTH CAROLINA

Robert B. Cook\* and James R. Burnell\*\*

\*Department of Geology, Auburn University, AL 36849

\*\*E.C. Jordan, Inc., P. O. Box 7050, Portland, ME 04112

ABSTRACT

Sperrylite ( $PtAs_2$ ) was initially discovered in the United States as a rare accessory mineral recovered during the placer mining of gem corundum and rhodolite garnet in streams draining Mason Mountain, Macon County, North Carolina. In-place sperrylite was subsequently found associated with sulfide-rich garnet-biotite gneiss near the summit of the mountain. The potential economic significance of the occurrence was ignored until 1982 when it was evaluated by stream-sediment and rock geochemistry.

Of 38 panned concentrate, stream-sediment samples representing a  $50 \text{ km}^2$  area, ten contained Pt in amounts up to 200 ppb. Arsenic contents varied between 2 and 8 ppm. Pd did not exceed 5 ppb in any sample. The highest Pt values were for samples collected from streams draining the western one-half of Mason Mountain. Coincidentally collected silt stream-sediment samples did not contain Pb, Zn, or Cu in anomalous amounts.

Rock analytical data were uniformly negative with respect to Pt-group elements, with the exception of weakly foliated biotite-garnet-pyrrhotite rock exposed in bald, iron-stained outcrops along the southwest slope of the mountain, a sample of which contained 15 ppb Pt. Sulfide-rich rock from a prospect midway up the south slope of the mountain's west end contained up to 0.81% Cu, 3.62% Pb, 0.55% Zn, 36 ppm Ag, and no detectable Pt-group metals or Au. The Co, Ni, and Cr contents of sulfide-rich rock samples are relatively low, reaching maximum values of 80, 95, and 300 ppm, respectively. Siliceous units associated with sulfide occurrences are anomalously aluminous and magnesian with values ranging up to 27.1%  $Al_2O_3$  and 13.4% MgO for garnet-sillimanite-biotite schist and galena-bearing garnet-biotite gneiss, respectively. The sperrylite occurrence does not appear to represent ore-related mineralization and is of mineralogical interest only.

INTRODUCTION

Platinum group metals were reported as rare constituents of heavy mineral concentrates produced during the early years

of gold mining in both Georgia (Stephenson, 1871) and North Carolina (Genth, 1891). The occurrences included rather diverse terranes of both the Blue Ridge and Piedmont Provinces. Although no significant attempt was made to identify the source of the platinum, its occurrence in Georgia was verified almost a century later in streams draining poorly known crystalline rocks generally north of the Brevard Zone in White County by Hurst and Otwell (1964) and in Habersham County by Hurst and Crawford (1964).

In an event unrelated to gold mining, sperrylite ( $\text{PtAs}_2$ ) was discovered in 1894 at the mouth of Ned Wilson Branch along the Caler Fork of Cowee Creek, about 5 miles north of Franklin, Macon County, North Carolina (Hidden, 1898; Hidden and Pratt, 1898; Kemp, 1902). The discovery was accidental, resulting from a heavy mineral study of material found during the alluvial mining of corundum and the gem garnet rhodolite. Fifty-five sperrylite crystals, the largest being 0.2 mm in diameter, were initially submitted to S. L. Penfield for identification (Hidden, 1898). The sperrylite occurred in both nugget-like masses and cubo-octahedral crystals. According to Hidden, sperrylite was also identified in heavy mineral suites from four other gem placer operations both east and west along the Caler Fork of Cowee Creek.

A subsequent paper by Hidden and Pratt (1898) described the separation of 300 sperrylite crystals from heavy mineral concentrate collected from a new location on Mason Branch, about two miles southwest of the initial discovery site. The total weight of these crystals was one milligram with the largest crystal being 0.4 mm in diameter. The heavy mineral suite containing the placer sperrylite was unusual, containing minor gold, relatively abundant corundum, bronzite, cordierite, aluminosilicates, and various spinel group minerals. Ultimately, the apparent source of the placer sperrylite was discovered by Hidden and Pratt 0.8 km north of the Mason Branch gem placer near the summit of Mason Mountain. Here, crystals of sperrylite were panned from weathered residuum derived from an outcrop of garnet-biotite-sulfide gneiss.

Subsequent published data relating specifically to the Mason Mountain sperrylite occurrence are lacking. Henderson (1931) described the mineralogy of material collected at the "rhodolite quarry" on the west end of the mountain, an occurrence apparently unrelated to that containing the sperrylite. Heinrich (1950) made corrections in the mineralogical work of Henderson (1931) and proposed a paragenetic scheme for the quarry rhodolite occurrence. Neither paper describes significant sulfide minerals and Henderson points out that the locality of his study is areally and perhaps geologically distinct from that described by Hidden and Pratt (1898).

It appears that the very presence and possible economic significance of the Mason Mountain platinum occurrence has been overlooked by modern exploration geologists, primarily due to the age of the original reports. Consequently, the present study was undertaken to identify the initial in-place sperrylite discovery site and to generate preliminary geochemical data upon which future work could be based.

### General Geology

Mason Mountain is within a poorly-characterized portion of the western North Carolina Blue Ridge Province lying between the Hayesville and Shope Fork faults (fig. 1). The general tectonic setting of the area has been described by Hatcher and others (1980). Immediately adjacent areas have been described in somewhat greater detail by McSween and Hatcher (1985) and Kittelson and McSween (1987). Projection of units shown on maps included in these works indicates that the Mason Mountain area is underlain by undifferentiated rocks of the Coweeta Group and Tallulah Falls Formation. The study area is shown as biotite schist and gneiss, and layered gneiss and migmatite on the geologic map of the Knoxville 1:250,000 quadrangle (Hadley and Nelson, 1971). On the most recent North Carolina state geologic map (North Carolina Department of Natural Resources and Community Development, 1985) the area is included within a general zone of Precambrian hypersthene granulite dominated by locally migmatitic biotite gneiss interlayered with biotite gneiss and amphibolite.

### METHODS

An approximately 50 km<sup>2</sup> area centering around Mason Mountain was evaluated by panned stream-sediment concentrate and silt geochemistry, reconnaissance geologic mapping, and rock geochemistry. The examined area includes the southeast part of the Alarka 7-1/2" Quadrangle, the southwest part of the Greens Creek 7-1/2" Quadrangle, the northwest part of the Corbin Knob 7-1/2" Quadrangle and the northeast part of the Franklin 7-1/2" Quadrangle (fig. 1).

Heavy mineral concentrate stream-sediment samples were collected at 38 sites by carefully panning approximately equal initial volumes of gravel dug from active channel deposits. Concentrates were analyzed commercially for Pt, Pd, Au, and As. Pt and Pd were determined by neutron activation analysis with 5 ppb detection limits. Au was analyzed by standard fire assay preparation and atomic absorption spectrophotometric (AAS) finish with a detection limit of 5 ppb. Arsenic was determined by standard AAS techniques with an analytical detection limit of 1 ppm.

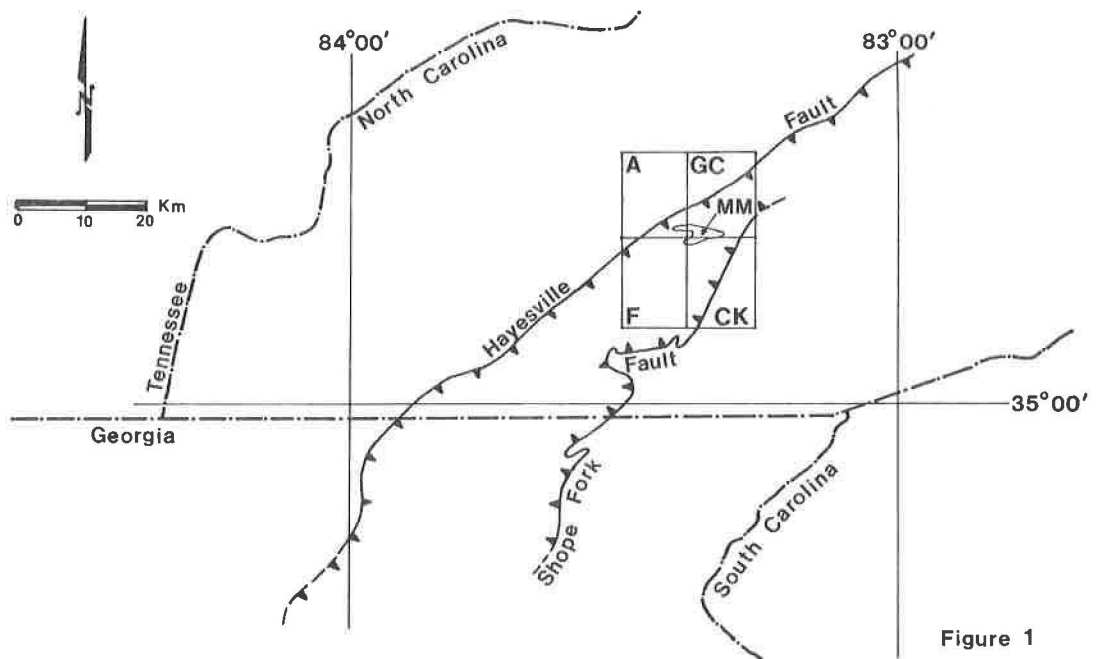


Figure 1

Figure 1. General location of Mason Mountain (MM), Macon County, North Carolina. The 7.5-minute quadrangles shown are the Alarka (A), Greens Creek (GC), Corbin Knob (CB) and Franklin (F).

Coincidentally collected silt samples were analyzed for Cu, Pb, and Zn by standard AAS techniques with a detection limit of 1 ppm for each element.

Rock samples were analyzed commercially for a variety of geochemical parameters. In addition to Pt, Pd, Au, and As determinations by the above described techniques, a number of rock samples were analyzed for Cu, Pb, Zn, Ag, Ni, and Co by standard AAS methods with 1 ppm detection limits. Obviously mineralized samples were analyzed by neutron activation for Ru, Rh, Pt, Re, Os, Ir, and Pd with detection limits of 5, 1, 5, 1, 3, 0.1, and 5 ppb, respectively. Neutron activation whole rock analyses were obtained commercially for rocks associated with sulfide mineralization.

## RESULTS

The presence of trace Pt in streams draining Mason Mountain is confirmed by stream sediment geochemistry. Drainages containing anomalous Pt are not characterized by coincident Pd, As, Cu, Pb, or Zn in elevated amounts.

Reconnaissance mapping on Mason Mountain has identified previously unreported prospects on its south slope and west end. Rock samples from the south slope prospects contain very anomalous Cu, Pb, Zn, Ag, and Au. A pyrrhotite-rich sample collected from a prospect area associated with bald sulfidic outcrops contains trace (15 ppb) Pt.

### Stream-Sediment Geochemistry

Heavy mineral concentrate stream-sediment geochemistry (Table 1) has confirmed the presence of sporadic trace Pt in streams draining both the north and south flanks of Mason Mountain (fig. 2). Ten of 38 panned concentrate samples contain Pt in amounts up to 200 ppb. Nine of these ten anomalous samples represent streams originating on the flanks of Mason Mountain. No sample contained Pd in amounts greater than the analytical detection limit. The As content of all samples is low, ranging between 2 and 8 ppm. Trace amounts of Au are widely distributed throughout the area, all samples containing detectable Au in amounts up to 10,300 ppb. Gold was visible in all samples containing greater than 1000 ppb Au.

Silt samples collected coincidentally with panned concentrate samples contained Cu, Pb, and Zn in low amounts ranging up to 94, 31, and 129 ppm, respectively (Table 2). There is no apparent statistical correlation between Pt, Au, As, Cu, Zn and Pb in stream sediment samples, nor is there a

Table 1. Panned stream-sediment concentrate analytical data, Mason Mountain area, Macon County, North Carolina

Sample #	Pt ppb	Pd ppb	Au ppb	As ppm
1	150	N.D. <sup>1</sup>	10300	4
2	N.D.	N.D.	15	6
3	N.D.	N.D.	6200	6
4	200	N.D.	15	6
5	N.D.	N.D.	140	4
6	N.D.	N.D.	15	6
7	N.D.	N.D.	30	3
8	N.D.	N.D.	5	2
9	100	N.D.	25	3
10	N.D.	N.D.	10	2
11	100	N.D.	30	3
12	100	N.D.	10	3
13	N.D.	N.D.	10	3
14	N.D.	N.D.	5	2
15	100	N.D.	5	3
16	100	N.D.	10	4
17	100	N.D.	10	3
18	N.D.	N.D.	5	3
19	N.D.	N.D.	60	3
20	N.D.	N.D.	15	6
21	100	N.D.	5	3
22	N.D.	N.D.	5	3
23	N.D.	N.D.	345	2
24	N.D.	N.D.	150	2
25	N.D.	N.D.	35	3
26	N.D.	N.D.	35	8
27	N.D.	N.D.	100	6
28	N.D.	N.D.	40	3
29	N.D.	N.D.	15	2
30	N.D.	N.D.	10	4
31	N.D.	N.D.	15	3
32	N.D.	N.D.	5	2
33	N.D.	N.D.	15	4
34	100	N.D.	5	3
M1	N.D.	N.D.	65	3
M2	N.D.	N.D.	40	3
M3	N.D.	N.D.	15	3
M4	N.D.	N.D.	50	2

<sup>1</sup>Below analytical detection limit.

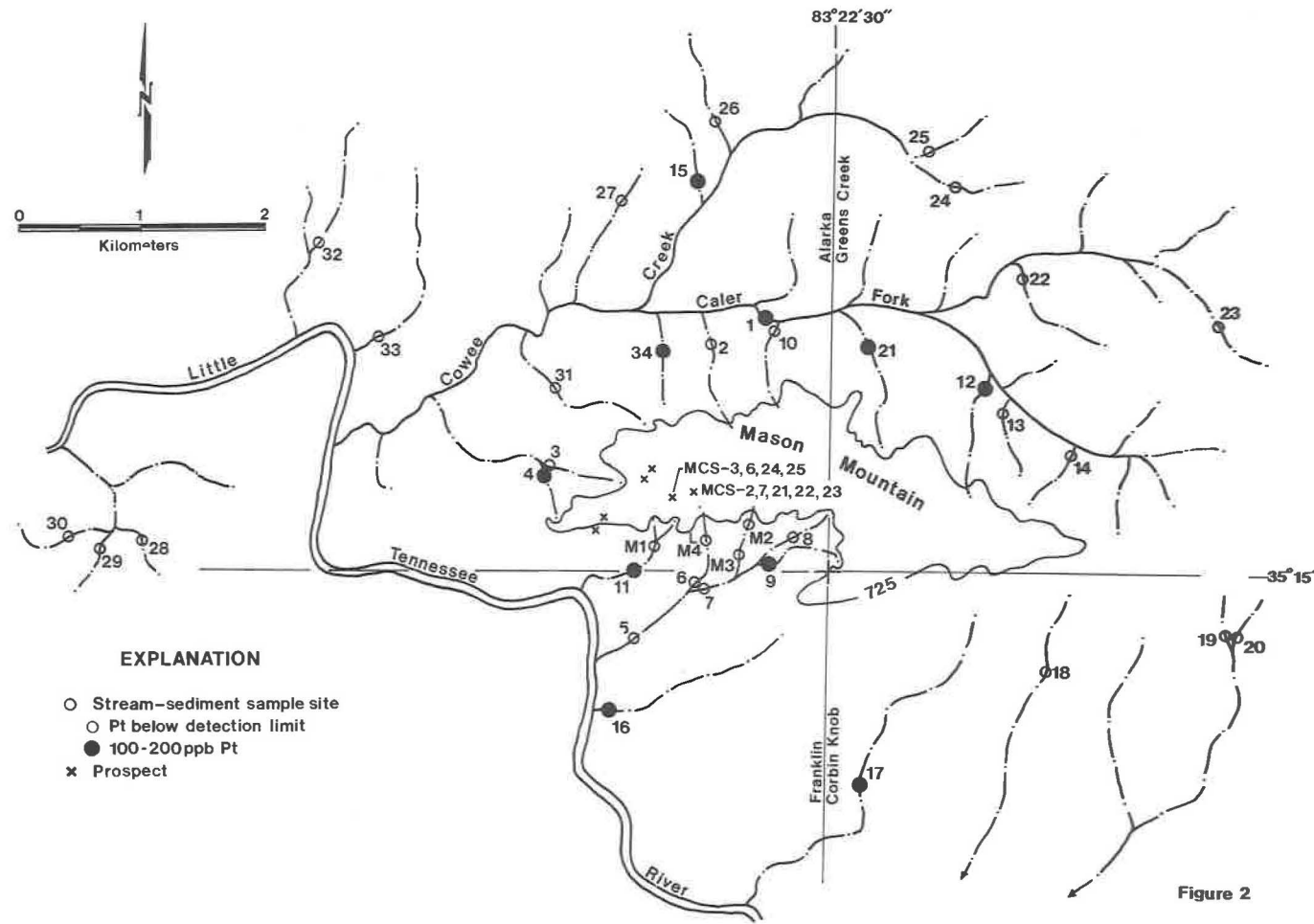


Figure 2

Figure 2. Stream-sediment and rock sample locations on parts of the Alarka, Greens Creek, Corbin Knob, and Franklin 7.5-minute quadrangles, Macon County, North Carolina. Mason Mountain is indicated by the 725-meter contour line.

Table 2. Stream-sediment analytical data, Mason Mountain area, Macon County, North Carolina

Sample #	Cu ppm	Pb ppm	Zn ppm
1	39	10	85
2	31	13	67
3	42	8	105
4	82	6	79
5	27	13	53
6	86	7	87
7	25	5	47
8	24	13	52
9	29	7	59
10	20	6	53
11	94	11	78
12	51	6	62
13	31	5	57
14	46	5	121
15	33	9	69
16	22	9	56
17	37	19	80
18	27	9	60
19	10	6	41
20	14	6	44
21	37	18	78
22	37	5	54
23	72	10	129
24	24	6	45
25	31	25	88
26	43	31	92
27	39	26	80
28	28	12	61
29	13	15	46
30	37	31	87
31	21	11	63
32	25	12	77
33	19	17	48
34	20	14	52
M1	92	11	64
M2	78	9	56
M3	88	12	61
M4	85	10	72

pronounced geographic association between samples containing relatively large amounts of two or more of these elements.

### Prospect Examinations

Traverses walked across the central and western portions of Mason Mountain resulted in the identification of several previously unreported prospects (fig. 2). Prospects associated with bald outcrops along the south slope of the mountain are characterized by relatively abundant pyrrhotite in float, outcrop and dump material. Prospects contiguous to and on strike with the rhodolite mine at the west end of the mountain contain only sparse sulfides and apparently were dug in search of gem garnet. These prospects are not considered further in this paper.

The most extensive prospect found on Mason Mountain lies approximately 0.5 km north of stream sediment sample site M4 (fig. 2). The prospect is marked by an open cut that ends in what appears to be a caved adit, and dumps suggestive of several hundred feet of underground workings. Dominant rock types observed in outcrop and as dump material are biotite-quartz gneiss and schist that contain locally very abundant, coarse-grained garnet porphyroblasts of the rhodolite variety. Sillimanite is locally very abundant.

Mineralized dump material contains fine- to medium-grained galena, pyrite, sphalerite and chalcopyrite in a generally fine-grained, gray siliceous biotite-garnet-quartz gneiss. Analyses of grab and chip samples (NCS-21, NCS-22, and NCS-23; Table 3) indicate the presence of Pb, Cu and Zn in amounts up to 23,200 ppm, 8120 ppm and 5500 ppm, respectively. Silver occurs in amounts up to 36 ppm while Au, Pt and Pd are not present in amounts above the analytical detection limit. Polished section examination did not result in the identification of platinum group minerals.

Approximately 400 m west of the above described prospect is an area of bald, iron-stained, sulfide-bearing siliceous gneiss that is marked by several shallow prospect openings (fig. 2). Composite chip samples collected at this site (Samples NCS-24 and NCS-25; Table 3) contain low though anomalous Cu, Pb, Zn and Ag. Both samples contain anomalous gold but do not contain Pt or Pd in detectable amounts. Polished section examination indicates that pyrrhotite is the dominant iron sulfide mineral with paragenetically later, subordinate chalcopyrite, galena and sphalerite. Sperrylite or other platinum group minerals were not identified in polished sections of samples collected at this site.

Examination of float boulders downslope from the general bald outcrop area resulted in the discovery of several

Table 3. Rock sample trace metal analyses, Mason Mountain prospect areas, Macon County, North Carolina

Sample #	Pt ppb	Pd ppb	Au ppb	Ag ppm	Cu ppm	Pb ppm	Zn ppm	Co ppm	Ni ppm	As ppm
NCS-3	15	N.D.	N.D.	1	1460	14	460	41	45	3
NCS-21	N.D. <sup>1</sup>	N.D.	N.D.	25	5375	10,900	370	15	10	2
NCS-22	N.D.	N.D.	N.D.	27	5700	23,200	5500	6	8	3
NCS-23	N.D.	N.D.	N.D.	36	8120	18,900	480	7	9	2
NCS-24	N.D.	N.D.	100	56	1050	510	410	20	23	3
NCS-25	N.D.	N.D.	245	32	230	76	110	19	26	3

<sup>1</sup>Below analytical detection limit.

- NCS-3 massive garnet-biotite-pyrrhotite rock.  
 NCS-21 garnet-biotite-quartz gneiss with fine-grained pyrite, chalcopyrite and galena.  
 NCS-22 very siliceous garnet-biotite-sulfide gneiss.  
 NCS-23 siliceous biotite-sulfide gneiss with very coarse-grained garnet porphyroblasts.  
 NCS-24 massive pyrrhotite-garnet rock.  
 NCS-25 massive pyrrhotite-garnet rock.

samples of massive pyrrhotite-garnet-biotite-quartz rock. Analysis of this rock (NCS-3; Table 3) indicates the presence of 15 ppb Pt. The rock is unusual with respect to other analyzed samples in that it contains relatively small amounts of Pb and Ag and relatively large amounts of Co and Ni. Analyses for the other Pt group metals identified trace Ir in amounts up to 0.8 ppb. Polished section examination did not result in the identification of Pt group minerals in these samples.

Rocks cropping out in the general area of the south slope prospects are predominantly gneisses that contain variable amounts of garnet, quartz, sillimanite and biotite with locally significant pyrrhotite and orthopyroxenes. Whole-rock analyses of major prospect area rock types are given in Table 4. Sample locations are shown on figure 2.

Sillimanite-biotite-garnet gneiss and massive garnet-biotite-pyrrhotite rock (NCS-2 and NCS-3) are characterized by low  $\text{SiO}_2$  coupled with relatively large amounts of  $\text{Al}_2\text{O}_3$ , MgO,  $\text{K}_2\text{O}$ ,  $\text{Fe}_2\text{O}_3$  and  $\text{TiO}_2$ . Very coarse-grained garnets in pyrrhotite-rich sample NCS-3 are intensely deformed. Fractures are healed with pyrrhotite and locally garnets and biotite are altered along fractures and grain boundaries to a very fine-grained talc-like mineral.

In contrast, garnet-quartz-sillimanite gneiss and garnet-biotite-quartz gneiss (NCS-6 and NCS-7) contain relatively abundant  $\text{SiO}_2$ , large to moderate quantities of  $\text{Al}_2\text{O}_3$  and  $\text{Fe}_2\text{O}_3$ ; and sparse CaO,  $\text{Na}_2\text{O}$ ,  $\text{K}_2\text{O}$ , MnO, and  $\text{TiO}_2$ . Garnets in NCS-6 are poikiloblastic with concentric and snowball inclusions. Sillimanite occurs in distinct bands that wrap around and enclose garnets.

Apparently altered, relatively fine-grained rock (NCS-21) containing pyrite, chalcopyrite and galena is characterized by an intermediate  $\text{SiO}_2$ , relatively low  $\text{Al}_2\text{O}_3$ , and a high MgO content. Quartz is strained and locally recrystallized. The garnet is poikiloblastic and of the distinct rose-violet rhodolite color.

#### CONCLUSIONS

Platinum has been identified in amounts up to 200 ppb in heavy mineral concentrates obtained from streams draining Mason Mountain. Although sperrylite was not found in either heavy mineral concentrates or rock samples, the original Hidden (1898) and Hidden and Pratt (1898) reports are considered to be confirmed. The apparent stream sediment platinum anomalies are not accompanied by anomalous Cu, Pb, and Zn in coincidentally collected silt samples nor by anomalous Pd or As in heavy mineral concentrates.

Table 4. Whole-rock analytical data, Mason Mountain prospect areas, Macon County, North Carolina

	NCS-2	NCS-3	NCS-6	NCS-7	NCS-21
SiO <sub>2</sub>	42.3	35.7	62.3	63.4	53.0
Al <sub>2</sub> O <sub>3</sub>	27.1	19.5	22.0	11.5	15.3
CaO	1.1	0.8	0.3	0.5	0.7
MgO	8.4	11.3	3.8	11.6	13.4
Na <sub>2</sub> O	1.3	0.2	0.1	0.3	0.3
K <sub>2</sub> O	3.8	2.4	0.1	1.9	0.8
Fe <sub>2</sub> O <sub>3</sub>	12.0	24.2	9.7	8.7	11.7
MnO	0.4	0.6	0.3	0.3	0.3
TiO <sub>2</sub>	1.3	1.3	0.1	0.9	0.8
P <sub>2</sub> O <sub>5</sub>	0.3	0.2	0.1	0.1	0.4
Cr <sub>2</sub> O <sub>3</sub>	0.03	0.02	0.02	0.03	0.03
S	0.04	4.40	0.06	0.06	1.28
Total	98.07	100.62	98.88	99.29	98.01

NCS-2 sillimanite-biotite-garnet gneiss.  
 NCS-3 massive garnet-biotite-pyrrhotite rock.  
 NCS-6 garnet-quartz-sillimanite gneiss.  
 NCS-7 garnet-biotite-quartz gneiss.  
 NCS-21 garnet-biotite-quartz gneiss with fine-grained pyrite, chalcopyrite and galena.

Prospects characterized by sulfide-rich garnet-biotite-quartz rocks occur on the south flank of the western segment of the mountain. Other workings at the west end of the mountain appear to be only rhodolite garnet prospects. The most intensely prospected site on the mountain's south slope is characterized by rocks containing very anomalous amounts of Cu, Pb, Zn and Ag while a bald, iron-oxide stained prospect area is characterized by anomalous Au, Cu, and, in one float sample, Pt. This site is ideally situated to have supplied sperrylite to the Mason Branch rhodolite mine and is consistent with the in-place sperrylite discovery site description provided by Hidden and Pratt (1898).

The host rocks for both sulfide prospect areas have undergone very high-grade regional metamorphism and intense deformation. Locally, these rocks are relatively deficient in SiO<sub>2</sub> and enriched in MgO; however, mineralogically they do not appear to have been derived from a typical mafic igneous rock suite as might be expected in a platiniferous environment. As such, the Mason Mountain sperrylite occurrence is genetically enigmatic. It does not appear to conform to any of the typical economic Pt metal depositional environments as described by Mertie (1969). The lack of identifiable sperrylite in any polished section, relatively low Pt content of mineralized rock, and original discovery in weathered residuum derived from sulfide-rich rock suggest that at least some of the sperrylite may be of supergene origin, a circumstance implied for some sperrylite of the New Rambler, Wyoming, deposit by McCallum and others (1976). Consequently, the Mason Mountain sperrylite occurrence is considered to be a mineralogical curiosity without economic importance.

#### ACKNOWLEDGMENTS

Grateful appreciation is extended to Dr. Bruce A. Bouley, Chief Geologist of Callahan Mining Corporation, for permission to publish the data contained herein. The study benefited markedly from the helpful guidance and suggestions of King Troensegaard. Critical review by James Saunders greatly improved the manuscript.

#### REFERENCES CITED

- Genth, F. A., 1891, The minerals of North Carolina: U.S. Geological Survey Bulletin 74, 14 p.
- Hadley, J. B., and Nelson, A. E., 1971, Geologic map of the Knoxville Quadrangle, North Carolina, Tennessee, and South Carolina: U.S. Geological Survey, Miscellaneous Geologic Investigations, Map I-654.

- Hatcher, R. D., Jr., Butler, J. R., Fullagar, P. D., Secor, D. T., and Snoke, A. W., 1980, Geologic synthesis of the Tennessee-Carolinas-northeast Georgia southern Appalachians, *in* Wones, D. R. (ed.), *The Caledonides in the U.S.A.: International Geological Correlation Program, Memoir 2*, p. 83-90.
- Henderson, E. P., 1931, Notes on some minerals from the rhodolite quarry near Franklin, North Carolina: *American Mineralogist*, v. 16, pp. 563-638.
- Heinrich, E. W., 1950, Paragenesis of the rhodolite deposit, Mason's Mountain, North Carolina: *American Mineralogist*, v. 35, pp. 764-771.
- Hidden, W. E., 1898, Occurrence of sperrylite in North Carolina: *American Journal of Science*, v. 6, 381 p.
- Hidden, W. E. and Pratt, J. H., 1898, On the associated minerals of rhodolite: *American Journal of Science*, v. 6, pp. 463-468.
- Hurst, V. J. and Crawford, T. J., 1964, Exploration of mineral deposits in Habersham County, Georgia: U.S. Department of Commerce Area Redevelopment Administration, 180 p.
- Hurst, V. J. and Otwell, W. L., 1964, Exploration of mineral deposits in White County, Georgia: U.S. Department of Commerce Area Redevelopment Administration, 166 p.
- Kemp, J. F., 1902, The geological relations and distribution of platinum and associated metals: U.S. Geological Survey Bulletin 193, pp. 58-59.
- Kittleson, R. C., and McSween, H. Y., 1987, The amphibolite to granulite transition in the Blue Ridge, Macon County, North Carolina: Geological Society of America, Abstracts with Programs, v. 19, no. 2, p. 93.
- McCallum, M. E., Loucks, R. R., Carlson, R. R., Cooley, E. F., and Doerge, T. A., 1976, Platinum metals associated with hydrothermal copper ores of the New Rambler mine, Medicine Bow Mountain, Wyoming: *Economic Geology*, v. 71, pp. 1429-1450.
- McSween, H. Y., and Hatcher, R. D., 1985, Ophiolites(?) of the southern Appalachians Blue Ridge, *in* Field Trips in the southern Appalachians, University of Tennessee Studies in Geology, v. 9, pp. 144-170.
- Mertie, J. B., Jr., 1969, Economic geology of platinum metals: U.S. Geological Survey Professional Paper 630, 120 p.
- North Carolina Department of Natural Resources and Community Development, 1985, Geologic map of North Carolina: North Carolina Geological Survey, map.
- Stephenson, M. F., 1871, Geology and mineralogy of Georgia: Globe Publishing Company, Atlanta, 30 p.

# THE CENTRAL PIEDMONT METALLOGENIC PROVINCE, SOUTH CAROLINA<sup>1</sup>

Steven K. Mittwede<sup>2</sup>  
South Carolina Geological Survey  
5 Geology Road, Columbia, South Carolina 29210-9998

## Abstract

Diverse types of metallic and non-metallic mineral deposits occur proximal to the Piedmont terrane-Carolina terrane boundary in the central Piedmont of South Carolina. Stratiform Sn (+ Au, W), disseminated and vein Au, massive and vein sulfide (Cu + Pb), "vermiculite", talc and manganese schist deposits are known in the central Piedmont although mining activity, at present, is confined to some of the non-metallic resources. Even though the mineral deposits described here occur in two terranes, the similarities in their tectonostratigraphic settings, the petrotectonic processes by which they formed, and their spatial relationships commend them to be classified as a single metallogenic province, here termed the "central Piedmont metallogenic province".

Much of the mineralization known in the central Piedmont is related to calc-alkaline arc development and, hence, is considered volcanogenic or due to hydrothermal alteration/concentration processes. Some of the vein mineralization probably is metamorphogenic but, even in these cases, the original concentration of gold or base metals was likely volcanogenic and syngenetic with volcanic activity.

The volcanic-arc building processes that produced many of the mineral deposits in the Kings Mountain belt (Carolina terrane) were related to accretionary tectonics, specifically, the impingement of Laurentia (Piedmont terrane) by the exotic Carolina arc edifice. Some of the Inner Piedmont belt (Piedmont terrane) mineralization is probably older and likely formed in intra-arc or back-arc rift zones.

## Introduction

Metallogeny, the study of the genesis of metallic and nonmetallic mineral deposits with emphasis on their time-space distribution relative to regional tectonic features, has greatly facilitated mineral exploration in the wake of the widespread acceptance of plate tectonic theory. The recognition of metallogenic provinces (especially those containing types of mineralization targeted in a particular exploration program) is invaluable in the context of exploration planning. Several important volumes (for example, Strong, 1976; Hutchison, 1983; Sawkins, 1984) have applied the concepts of metallogeny and contain global mineral deposit data which have been effectively synthesized and interpreted in light of regional tectonic frameworks. Also, individual papers dealing with specific metallogenic provinces/regional models have been published (for example, the Tethyan-Alpine-Himalayan belt: Dixon and Pereira, 1974; Evans, 1975; Jankovic,

---

<sup>1</sup> This paper is a modified version of the text of a talk entitled "Metallogeny of an accretionary plate margin in the central Piedmont of the southern Appalachians" that was presented at the 1989 Southeastern Section of the Geological Society of America.

<sup>2</sup> Present address: Terrane Exploration Services, 2523 Huguenot Springs Road, Midlothian, Virginia 23113.

1980; Jankovic and Petrascheck, 1987), including some pertaining to the southern Appalachian Piedmont (Feiss and Hauck, 1980; Cook and Bittner, 1987). Unfortunately, there are large gaps in the metallogenic-model coverage. One such area for which no model has been developed is the central Piedmont of South Carolina. There are a number of reasons for this omission: 1) there has been, until recently, little detailed geological work in the central Piedmont, possibly because of the structural complexity and lament over scarce exposure and deep weathering; 2) most of the known mineral deposits of the central Piedmont appear to be much smaller than many exploration companies are willing to consider; 3) although there has been some gold exploration in the Kings Mountain belt, most serious exploration efforts have focused on the Carolina slate belt.

The purpose of this paper is to compile and synthesize mineral resource information for the central Piedmont of South Carolina and to evaluate the various mineral deposits or types of mineralization in light of the tectonostratigraphic framework. Admittedly, some of the discussions herein are long and fairly detailed while others are almost cursory. Hopefully though, this review of previous work combined with the presentation of some new geological and geochemical data will encourage future exploration efforts.

For present usage, the "central Piedmont" is defined, somewhat arbitrarily, as that part of the Piedmont physiographic province proximal to (within 25 km of) the Piedmont terrane-Carolina terrane boundary. This area comprises the eastern edge of the Inner Piedmont geologic belt, and the western edge of the Carolina terrane (including all or parts of the Kings Mountain/Lowndesville and Charlotte geologic belts).

### Paleoenvironmental Interpretations

Glover and others (1983) suggested that the Inner Piedmont belt (IPB) was the least known belt of the central and southern Appalachians. Because of the paucity of detailed geological work in most parts of the IPB, interpretations of paleoenvironmental conditions can be made only tentatively. Glover and others (1983) reported that the IPB contains mica schist, paragneiss and quartzite of probable epiclastic origin, layered metavolcanic rocks and amphibolite and, rarely, marble. Secor and others (1986, p. 1347) contended that the schist and paragneiss of the IPB were "derived from upper Proterozoic and/or lower Paleozoic continental slope and rise sediments deposited off the southeastern edge of the Laurentian plate." Although the IPB heretofore has been considered predominantly metasedimentary (that is, mostly paragneiss), the presence of locally significant amounts of amphibolite with basaltic (MORB-like) composition, banded iron-formation and manganiferous horizons does not support this earlier opinion. Acceptable tectonic models must incorporate and explain the presence of extensive amphibolite units as well as scattered metamorphosed ultramafites which are fairly common in the northwestern flank of the IPB. Significantly, for the early Paleozoic phase of its development, the Piedmont terrane has been labelled the "Piedmont arc" (Hatcher, 1987, Fig. 4). The section of this paper (below) on the Thicketty Mountain area presents some evidence for a significant felsic metavolcanic component in the IPB.

The Carolina terrane (the Kings Mountain belt and belts to the east) has been identified as a volcanic island-arc association (Hatcher, 1987; Mittwede, 1988c; Horton and others, 1989). The central part of the terrane (Charlotte belt) comprises mainly high-grade plutonic and related metavolcanic rocks, while the

flanks (Kings Mountain and Carolina slate belts) are composed mostly of felsic metatuffs and associated fine-grained marine metasedimentary rocks. Rocks of the Carolina terrane are of dominantly calc-alkaline volcanic origin with rhyodacite, which is more abundant than basalt and andesite, probably comprising more than half of the sequence (Glover and others, 1983). At the northwestern edge of the Kings Mountain belt in the Carolinas, the Blacksburg Formation (Gaffney terrane of Horton and others, 1989) consists of abundant mica schist and phyllite, some quartzite, marble, calc-silicate rock and amphibolite. Although some would suggest that the Blacksburg Formation has North American affinities (Hatcher, 1987), recent mapping (Mittwede, 1989b, c) in Pacolet Mills and Gaffney quadrangles found that the metavolcanic and associated metasedimentary rocks of the Blacksburg Formation are not sufficiently distinct from similar rocks of the Battleground Formation to warrant recognizing it as a distinct tectonostratigraphic entity.

### Mineralization of the Piedmont terrane

#### Thicketty Mountain area

The Thicketty Mountain area, as used here, includes parts of the Chesnee, Boiling Springs South, Blacksburg North, Cowpens and Gaffney (U.S.G.S.) 7.5-minute topographic quadrangles in northwestern Cherokee County. This boron-metals subprovince (Fig. 1) is defined on the basis of anomalous tourmaline concentrations (particularly tourmalinite and tourmaline-bearing leucosomes) and occurrences of gossanous ("brown ore") iron formation and aluminosilicate (kyanite and sillimanite) mineralization. This subprovince (Fig. 1) may extend as far east as the Kings Mountain shear zone in Gaffney and as far south as Pacolet Mills. The Thicketty Mountain subprovince extends north into Rutherford and Cleveland counties, North Carolina, but its northern limit has not been determined.

Mittwede (1984a, b; 1985a, b; 1986) previously described the geological setting of the area and reported the mineralogical and stream-sediment geochemical anomalies. Au, Sn, W and, locally, Zn are above background levels in some heavy-mineral concentrates (Mittwede, 1985a). Although these metal anomalies have not been traced to bedrock sources, tin (as cassiterite) is known to occur in some stratiform, tourmaline-bearing leucosomes (Carr and others, 1984; Moore and others, 1985; Rowe and Moore, 1988).

New grab-sample, whole-rock analyses (Table 1) of material from the Thicketty Mountain area did not show anomalies for these metals, but unusually high concentrations of Ag are associated with tourmaline-rich and calc-silicate rocks. Two samples of tourmalinite (boron-rich exhalites/chemical sediments; Slack and others, 1984; Plimer, 1987) one thin-banded and one thick-banded (illustrated by Mittwede, 1984b), also were analyzed and were found to contain 4.9 and 2.2 ppm Ag, respectively. A single sample of "brown ore" showed 18 ppm Te and, generally, rocks of the area tend to have somewhat elevated Pb, Zn and Sb contents (Table 1). The "brown ore" gossans were produced by weathering of pyrite-rich exhalites, and this low-grade iron ore apparently was mined as early as the colonial period (Moss, 1972).

Chemical sediments (tourmalinites and thin beds of tourmaline schist) and tourmaline-bearing leucosomes occur as stratiform units within the upper-amphibolite-facies metamorphic rocks of the area. The main map units (Fig. 2) are 1) a gneiss unit (mainly biotite-quartz-feldspar gneiss) which is overlain by 2) a

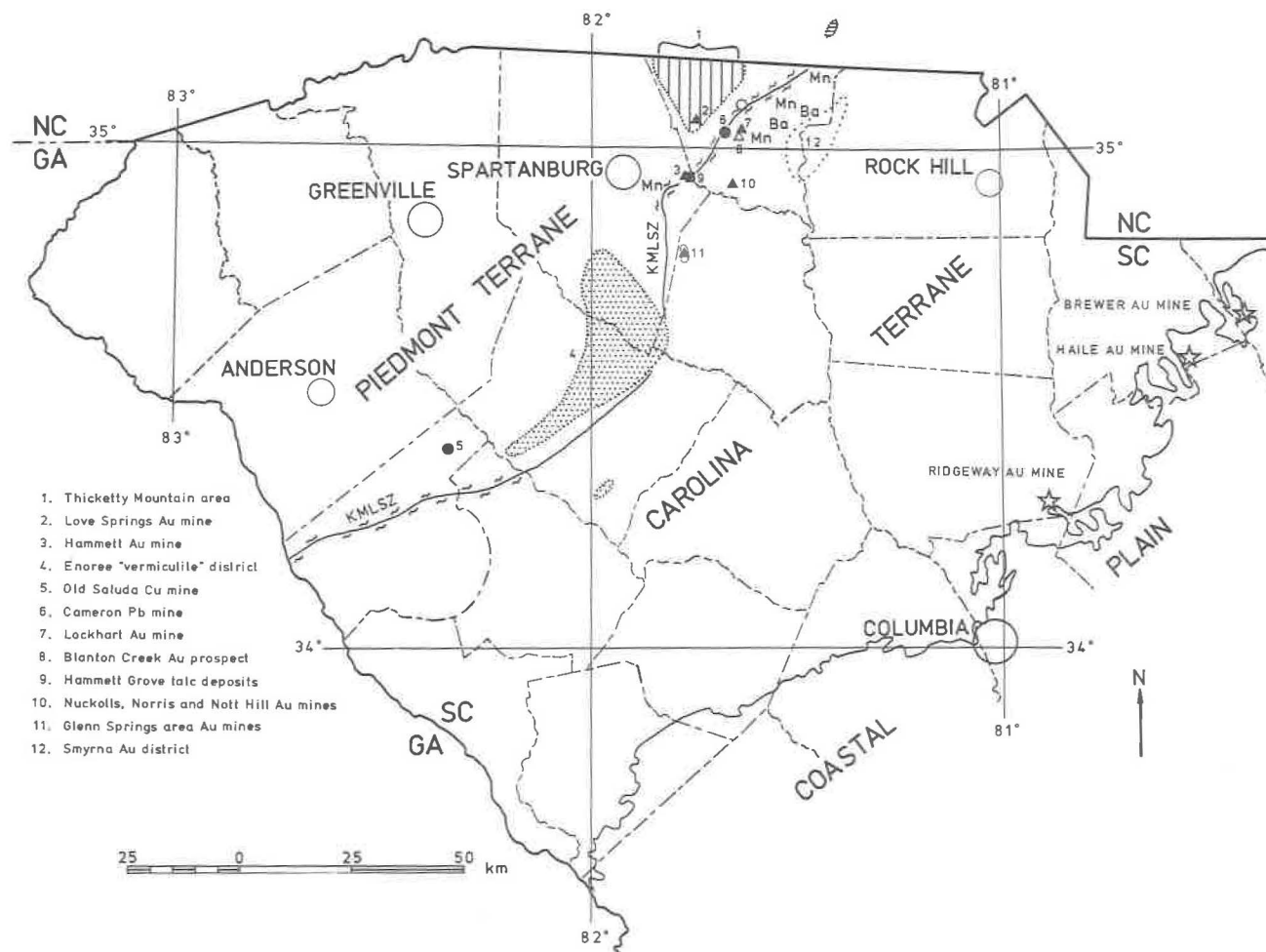


Fig. 1. Metallogenic map of the central Piedmont of South Carolina. Explanation of symbols and patterns: vertical-lined pattern = Thicketty Mountain boron-metals subprovince; stippled pattern = Enoree "vermiculite" district and "Cross Hill outlier"; solid triangles = old gold mines; open triangles = old gold prospects; solid circles = base-metal deposits; open circle = Ross tin mine; solid square = talc deposits; coarse-dotted line = Smyrna gold district; Mn = manganiferous schist of the Battleground Formation (generalized); Ba = barite mineralization (generalized); horizontal-lined pattern in North Carolina = spodumene-pegmatite district between Kings Mountain and Bessemer City (shown for reference, not discussed in text). KMLSZ = Kings Mountain-Lowndesville shear zone (marks the approximate boundary between the Piedmont terrane and Carolina terrane). Large stars along the eastern edge of the Carolina terrane denote active gold mines.

Table 1. Chemical analyses of selected rock samples from the Thicketty Mountain area.

	BN-21	BSS-13	BSS-39	BSS-402	Ch-15	Ch-Fe	Co-44	Co-49
SiO <sub>2</sub>	73.89	36.47	63.26	75.21	75.29	33.49	77.08	60.18
TiO <sub>2</sub>	.03	.09	1.25	.05	.02	.74	.03	1.31
Al <sub>2</sub> O <sub>3</sub>	14.68	59.02	20.29	13.28	14.04	13.37	13.11	21.31
Fe <sub>2</sub> O <sub>3</sub>	1.07	1.53	3.65	1.31	1.11	40.56	.52	5.31
MgO	.01	.01	1.48	.07	.01	.53	.01	1.20
MnO	.05	.01	.02	.18	.04	.03	.02	.01
CaO	.37	.15	.09	1.13	.23	.08	1.26	.16
Na <sub>2</sub> O	4.28	.41	.98	3.26	1.63	.17	2.97	.69
K <sub>2</sub> O	4.80	.72	4.54	4.31	5.33	.04	3.66	4.98
P <sub>2</sub> O <sub>5</sub>	.20	.01	.04	.08	.14	.15	.04	.02
S	.01	.02	.17	.03	.02	.08	<.01	.02
LOI	.44	1.43	4.32	.28	1.20	10.83	1.17	3.50
Total	99.83	99.87	100.09	99.19	99.06	100.07	99.87	98.69
Au (ppb)	<5	<5	<5	<5	<5	<5	<5	<5
Ag	<.2	<.2	.6	2.2	<.2	1.2	<.2	1.1
As	<5	<5	<5	<5	<5	<5	<5	<5
B	9	4	8	6	2	43	6	11
Ba	31	55	508	45	17	16	146	510
Be	1.2	2.1	2.3	1.2	1.2	4.2	.7	6.6
Bi	<2	<2	10	<2	<2	95	<2	4
Cd	<1	<1	1	<1	<1	5	<1	<1
Ce	<5	13	39	9	<5	59	14	<5
Co	2	1	6	1	1	3	2	5
Cr	157	51	168	251	167	84	150	191
Cu	22	33	32	7	5	66	7	47
Ga	16	21	32	13	11	19	13	16
La	1	3	5	5	1	14	3	1
Li	10	73	4	1	3	9	<1	7
Mo	5	3	8	4	4	6	3	8
Nb	<1	<1	2	<1	<1	6	<1	2
Ni	13	5	7	6	3	2	2	3
Pb	100	56	78	81	88	87	95	69
Rb	<20	<20	<20	<20	<20	<20	<20	<20
Sb	25	21	45	27	32	75	19	40
Sc	<1	1	16	<1	<1	4	<1	11
Sn	<20	<20	<20	<20	<20	<20	<20	<20
Sr	18	20	75	30	25	17	90	57
Ta	<10	<10	<10	<10	<10	28	<10	<10
Te	<10	<10	<10	<10	<10	17	<10	<10
Tl	<10	<10	<10	<10	<10	<10	<10	<10
V	4	23	157	4	1	96	1	106
W	<10	<10	<10	<10	<10	<10	<10	<10
Y	2	<1	2	6	<1	2	3	<1
Zn	59	50	74	39	49	81	21	20
Zr	2	26	12	40	11	31	28	25

Sample explanations: BN-21 (tourmaline-bearing leucosome, Blacksburg North quadrangle); BSS-13 (massive kyanite, Boiling Springs South quadrangle); BSS-39 (pyrite-rich exhalite or altered volcanic rock); BSS-402 (tourmaline- and garnet-bearing leucosome); Ch-15 (tourmaline- and garnet-bearing leucosome, Chesnee quadrangle); Ch-Fe (gossanous "brown ore" iron formation); Co-44 (opalescent blue-quartz, felsic-volcanic rock, north slope of Thicketty Mountain, Cowpens quadrangle); Co-49 (tourmaline-bearing quartz-muscovite schist).

Analyst: Bondar-Clegg and Company, Ltd., North Vancouver, British Columbia. Method: plasma emission (DCP and ICP) spectroscopy.

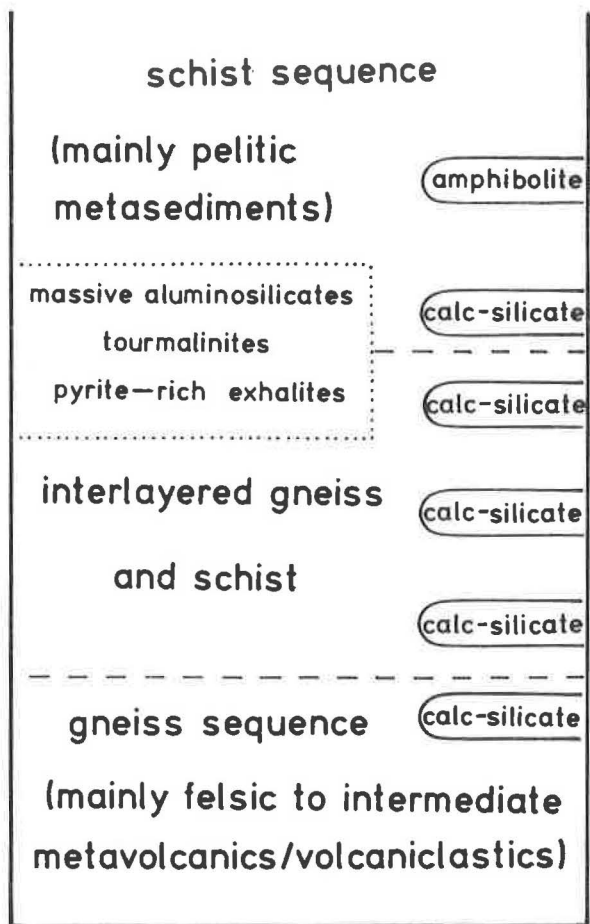


Fig. 2. Interpretive-composite stratigraphic sequence for the Thicketty Mountain area.

moderately aluminous schist unit that locally contains sillimanite or kyanite. Mapping by Mittwede (1985b) found that the gneiss-schist contact is gradational, so that an interval of interlayered gneiss and schist separates the main units. Pyritic exhalites, tourmaline-rich rocks and thin, blocky to tabular layers of calc-silicate rock tend to be concentrated near the gneiss-schist contact (Fig. 2). As noted by Lieber (1858), Thicketty Mountain is blanketed by aluminous schist, and little gneiss crops out in the immediate vicinity of the mountain.

A small but mappable felsic-rock unit that crops out on the north slope of Thicketty Mountain is of particular interest (Mittwede, 1984b). This resistant rock is composed of quartz, plagioclase and microcline with accessory garnet and chlorite. Quartz in this rock has an opalescent blue aspect, reflecting the presence of minute rutile inclusions. A chemical analysis of this rock (Table 1) gives a composition compatible with a rhyolitic precursor. Mittwede (1984b) interpreted this distinctive unit to be a felsic-volcanic center, and this analysis supports an interpretation of this unit as a rhyolitic flow-dome. This felsic unit may be analogous to the "white rhyolite" domes that characterize many Kuroko-type deposits (Franklin and others, 1981). Kuroko-type deposits are considered arc-related rift deposits (Sawkins, 1984).

Tourmalinites are stratabound (often stratiform) lithologic units that are broadly concordant with their enclosing host rocks and contain at least 15 to 20 percent tourmaline by volume (Slack and others, 1984). Stratiform tourmalinites are significant minor rock types in many of the regional metamorphic terranes of the world, and are closely associated with a variety of mineral deposits, including massive sulfides (Ethier and Campbell, 1977; Slack, 1982), tin and tungsten (Plimer, 1980; 1987), and gold (Fleischer and Routhier, 1973; McArdle and others, 1989).

Mittwede (1986) reviewed the stratiform tourmaline rocks of the Thicketty Mountain area but, since then, a significant amount of new information is available concerning the tourmaline-bearing and, locally, cassiterite-bearing leucosomes mentioned above. Rowe and Moore (1988) noted the concordant, stratiform nature of the leucosomes, but suggested that these lenticular units formed by anatexis during regional metamorphism. They interpreted the leucosomes as segregates from the host gneisses which formed by partial melting. They believed that this process remobilized and concentrated detrital tin which was presumably present in the sedimentary protolith. Interestingly, most of the leucosomes have compositions compatible with a felsic-intermediate volcanic precursor (Table 1; Rowe and Moore, 1988), allowing their interpretation as rhyolitic to dacitic flows. These boron-rich units may be vaguely analogous to tin-bearing "topaz rhyolites" that have been recognized and described elsewhere (for example, Christiansen and others, 1986).

Concerning tin mineralization, the only historical tin producer in South Carolina, the Ross mine, was located in Gaffney, north-central Cherokee County (Fig. 1). Graton (1906) and Sloan (1908) described the deposit as a concordant (or "interfoliated"), cassiterite-bearing pegmatite dike; Graton reported that amphibolite was the country rock, and Sloan described the dike as occurring at the contact between "pyroxenite" (amphibolite?) and "aplite gneiss". It seems likely that the mineralization at the Ross mine was hosted by a stratiform leucosome such as those discussed above.

The dense, gray calc-silicate rocks that occur near the gneiss-schist contact in the Thicketty Mountain area were interpreted as metamorphosed calcareous, quartz-rich sediments by Mittwede (1984a). Interestingly, Plimer (1987) reported that calc-silicate rocks, in places, are associated with stratiform scheelite deposits and tourmalinite. He suggested that "the calc-silicate progenitor

was probably an impure dolomitic carbonate sediment" (Plimer, 1987, p. 282). New chemical analyses (Table 2) of calc-silicate rocks from the Thicketty Mountain area indicate that these rocks may have been impure limey sediments or volcanic rocks that were subjected to hydrothermal alteration. The relatively high  $\text{SiO}_2$  contents and elevated - but not extremely high - CaO contents suggest that the calc-silicate rocks may represent zones of carbonate alteration or, as a third alternative, be interpreted as Ca-rich exhalites/brines, such as those that produce some evaporite-horizons. The analyzed samples of calc-silicate rock contain 1.5-2.2 ppm Ag as well as relatively high Bi, Co, La, Ni, Sr, Y and Zr (Table 2).

Massive kyanite (Table 1) and sillimanite occur at Thicketty Mountain and, locally, along the ridge that extends northeast from Thicketty Mountain. In places, kyanite-rich rocks are associated with paragonite-bearing rocks; ilmenite-tourmaline-quartz-kyanite granofels also has been identified.

Massive kyanite is much more prevalent than massive sillimanite, although acicular to fibrolitic sillimanite is abundant in the areally extensive schist unit. The schist, where fairly aluminous, probably reflects an early phase of sericitic alteration. Where massive, the aluminosilicates are interpreted as metamorphosed argillic alteration zones.

The aluminosilicate mineralization in the Thicketty Mountain area is similar to some aluminous alteration associated with gold deposits of the Carolina slate belt. Although obviously at higher metamorphic grade, massive kyanite and sillimanite in the vicinity of Thicketty Mountain compare favorably with pyrophyllite-andalusite and/or kyanite-bearing assemblages at Graves Mountain, Georgia, Robbins, North Carolina and at Faulkner, Boles, Parsons and Little Mountains, South Carolina.

Carpenter and Allard (1982) suggested that aluminosilicate assemblages, particularly Al-rich assemblages that originate near felsic-volcanic centers, are a valuable exploration tool in metavolcanic terrains. Altered volcanic rocks of this type host gold and base-metal deposits throughout the world. Certainly the presence of mineralogical anomalies (in the sense of Allard and Carpenter, 1988), such as aluminosilicate mineralization and tourmaline concentrations, chemical sediments (tourmalinite and pyritic exhalite), a likely felsic-volcanic system and stream-sediment geochemical anomalies make the Thicketty Mountain area one of the more favorable exploration targets in the Inner Piedmont belt of South Carolina.

#### Love Springs and Hammett Au Mines

The Love Springs (old Palmer) gold mine, reported by Sloan (1908), is located on the southwestern side of Rocky Ford Creek in southwestern Cherokee County, 4.7 km N47°E of the intersection of South Carolina Highway 110 and U.S. Highway 29 in Cowpens (Fig. 1). The mine was a placer operation that reportedly yielded valuable quantities of gold (Sloan, 1908). Sloan (1908) also noted that some prospect pits were sunk on quartz veinlets that cut the mica schist-country rock. He reported that tourmaline, hornblende (?), monazite and corundum were accessory minerals in the schist. Effects of this early mining activity are still apparent on the land surface. Small pits and low mounds of rounded fragments of vein quartz, some with black tourmaline, were observed during a recent investigation of the property (Mittwede, 1986).

The Hammett (Hamet or Crocker) mine was mentioned in the early geological reports of Tuomey (1844), Lieber (1858) and Sloan (1908). The mine

Table 2. Chemical analyses of calc-silicate rocks from the Thicketty Mountain area (southern one-half of the Boiling Springs South 7.5-minute quadrangle).

	BSS-46	BSS-55	BSS-140
SiO <sub>2</sub>	72.55	71.05	75.31
TiO <sub>2</sub>	.58	.58	.60
Al <sub>2</sub> O <sub>3</sub>	11.77	10.54	10.37
Fe <sub>2</sub> O <sub>3</sub>	3.78	3.97	4.12
MgO	2.23	2.38	1.97
MnO	.10	.15	.14
CaO	7.26	8.17	5.42
Na <sub>2</sub> O	.38	.81	.12
K <sub>2</sub> O	.06	.39	.08
P <sub>2</sub> O <sub>5</sub>	.12	.10	.14
S	.17	.07	.04
LOI	.45	1.03	1.04
Total	99.45	99.24	99.35

Au (ppb)	<5	<5	<5
Ag	1.5	1.5	2.2
As	<5	<5	104
B	9	8	8
Ba	65	107	161
Be	3.2	1.4	1.8
Bi	14	17	11
Cd	1	1	<1
Ce	66	76	40
Co	16	15	16
Cr	195	223	456
Cu	39	30	29
Ga	16	15	13
La	21	36	17
Li	5	18	3
Mo	4	4	5
Nb	11	9	8
Ni	67	49	39
Pb	59	60	55
Rb	<20	<20	<20
Sb	27	28	26
Sc	15	17	11
Sn	<20	<20	<20
Sr	134	212	144
Ta	<10	<10	<10
Te	<10	<10	<10
Tl	<10	<10	<10
V	62	60	63
W	<10	<10	<10
Y	16	37	27
Zn	75	60	90
Zr	110	69	100

Analyst: Bondar-Clegg and Company, Ltd., North Vancouver, British Columbia. Method: plasma emission (DCP and ICP) spectroscopy.

is located 4.76 km N16°W of the junction of South Carolina Highway 150 and U.S. Highway 176 in Pacolet (Fig. 1). Quartz veins at the mine reportedly yielded free gold, but adjacent placer deposits constituted the main source of the metal. McCauley and Butler (1966) noted that this mine is one of the oldest in the state, with work (according to Lieber, 1858) having begun thirty or forty years before Lieber's survey. Sloan (1908) reported that mica schist ("mica slate") is the country rock for a northwest-trending quartz vein. Float blocks containing abundant black tourmaline are scattered about near the mine workings and may represent the material targeted by the early miners. Similar vein-like quartz-tourmaline rocks, locally with an accessory green mica, are found in the same structural-stratigraphic position (along the western edge of the Hammett Grove Meta-igneous Suite) along strike to the southwest; collectively, these rocks may mark a fault related to the emplacement of the Hammett Grove Suite (Mittwede, 1986). The veins that purportedly yielded the gold were probably metamorphogenic, although concentration of silica, boron and gold may reflect volcanogenic enrichment or exhalative activity. The boron and gold may be genetically related to anomalous concentrations of the same elements in the Thicketty Mountain area.

Grab samples of tourmaline-bearing, quartz-vein material were taken at each of these old mines, but assays showed no gold or any other metals of interest (Table 3).

#### Enoree "Vermiculite" District

Potassic ultramafic rocks, termed biotitites by Libby (1975), occur in an arcuate zone (Fig. 1) that extends from Ware Shoals north to the community of Moore. Butler (1989) commented that these Enoree-district ultramafites are unique in the southern Appalachians. This district hosts possibly the most collectively important vermiculite deposits of North America (Maybin and Carpenter, 1989). The "vermiculite" forms in response to weathering in the upper parts of the biotitite bodies in the district.

Two petrographic types of biotitite are distinguished on the basis of the biotite-weathering-product (Libby, 1975). Biotite from the talc-bearing, "V-biotitite" weathers to vermiculite, while biotite from the feldspar-bearing, "HB-biotitite" weathers to hydrobiotite. A weathering origin for the vermiculite/hydrobiotite is demonstrable in the field; Libby (1975) observed that alteration of biotite by meteoric water/groundwater in an abandoned mine produced partial expansion of the biotite structure in less than two years. Weathering of biotite results in  $K_2O$  loss, oxidation and partial hydration.

The physical characteristics of "vermiculite" commend it to a variety of uses, from applications in horticulture to use in lightweight construction materials. Until recently, exploration for "vermiculite" in the area was limited to simple visual identification in road cuts or soils. Maybin and Carpenter (1989) pioneered stream-sediment/soil geochemical exploration that utilizes the high Cr and Ni contents (and to some extent, Co and Cu) of the biotite-rich ultramafites as well as the unusually high P content of the biotitites to locate and define potential ore bodies.

Biotitites of the Enoree district are most similar compositionally to orenditic lamproites of western Australia, and were interpreted by Libby (1975) as the metamorphosed equivalents of mantle-derived rocks. Libby (1975) suggested that the magmas that produced the biotitite plutons were probably initially generated by partial melting of upper mantle material containing low

Table 3. Trace-element analyses of selected rock samples from gold mines of the central Piedmont (in ppm).

	Co-LS	G-BCP	G-LM	GS-WMm	GS-WMq	P-172
Au (ppb)	<5	<5	<5	<5	144	<5
Ag	<.2	<.2	<.2	.8	.2	<.2
As	<5	<5	<5	<5	<5	<5
B	51	48	71	4	<2	116
Ba	3	4	2	118	218	16
Be	1.9	1.3	1.3	2.5	2.1	1.4
Bi	<2	<2	<2	<2	<2	<2
Cd	<1	<1	<1	<1	<1	<1
Ce	<5	<5	<5	<5	10	<5
Co	1	1	2	3	2	2
Cr	230	224	249	65	103	299
Cu	6	6	6	16	11	6
Ga	8	8	8	26	16	9
La	<1	<1	<1	<1	4	<1
Li	5	5	5	33	22	5
Mo	2	2	2	11	11	3
Nb	<1	<1	<1	<1	<1	<1
Ni	5	6	6	3	2	10
Pb	14	10	13	59	50	15
Rb	<20	<20	<20	25	<20	<20
Sb	<5	<5	<5	38	21	<5
Sc	<1	<1	<1	7	3	<1
Sn	<20	<20	<20	<20	<20	<20
Sr	5	9	28	6	16	15
Ta	<10	<10	<10	<10	<10	<10
Te	<10	<10	<10	<10	<10	<10
Tl	<10	<10	<10	<10	<10	<10
V	4	5	10	57	18	7
W	<10	<10	<10	<10	<10	<10
Y	<1	<1	<1	<1	<1	<1
Zn	10	9	12	26	18	14
Zr	2	1	1	138	61	2

Sample explanations: Co-LS (tourmaline-bearing vein quartz from the Love Springs gold mine, Cowpens quadrangle); G-BCP (tourmaline-bearing vein quartz from the Blanton Creek gold prospect, Gaffney quadrangle); G-LM (tourmaline-bearing vein quartz from the Lockhart gold mine); GS-WMm (sericite-rich altered volcanic rock from the West gold mine, Glenn Springs quadrangle); GS-WMq (silica-rich altered volcanic rock from the West gold mine); P-172 (tourmaline-bearing quartz vein from the Hammett gold mine, Pacolet quadrangle).

Analyst: Bondar-Clegg and Company, Ltd., North Vancouver, British Columbia. Method: plasma emission (DCP and ICP) spectroscopy.

concentrations of phlogopite in the presence of a  $\text{CO}_2\text{-H}_2\text{O}$  fluid and/or unusually high concentrations of  $\text{P}_2\text{O}_5$  and  $\text{TiO}_2$ . Mittweede (1988c) suggested that these unusual rocks may have formed as suprasubduction zone melts which were contaminated by sediments derived from the proto-Inner Piedmont belt or, alternatively, as products of incipient-rift-related melting beneath the Laurentian plate margin.

It is notable that the arcuate zone of biotite occurrences coincides with the gap between the southern terminus of the Kings Mountain belt and the northern end of its probable equivalent, the Lowndesville belt (Mittweede, 1988c). This spatial situation may reflect some fundamental tectogenetic process that operated during accretion of the exotic Carolina arc terrane.

### Old Saluda Cu Mine

The old Saluda copper mine (Fig. 1), located near Donalds in northern Abbeville County (Fig. 3), is the only massive sulfide deposit known in the Piedmont terrane in South Carolina. According to Bynum (1982), the mine was operated during the early 1900's by four or five men. Sloan (1908) made no mention of the property so, presumably, the mine had not yet been opened. In 1967, Tennessee Copper Company drilled 28 core holes (Fig. 3) along the strike of the sulfide deposit (cores and logs are stored at the South Carolina Geological Survey).

Drilling revealed sulfide veinlets, disseminated sulfides and zones of massive sulfides. Most of the sulfides and associated iron-formation (quartz-magnetite-minor pyrrhotite and pyrite) occur near the top of a mafic-rock sequence; that is, near a volcanic-sedimentary interface. The sulfide mineralization consists of approximately 70 percent pyrrhotite, 5 percent pyrite and up to 15 percent chalcopyrite (Bynum, 1982), but recent examination of the core and assay values of up to 7.28 percent Cu (core hole #6) suggest that even greater amounts of chalcopyrite are present locally. According to analyses of core samples, Zn reaches 1.03 percent (core hole #12), Ag 0.70 ounces/ton and Au 0.02 ounces/ton (core hole #8). Little or no Pb is associated with the deposit. The thickest sulfide zone is about 75 cm (core hole #6).

An idealized, somewhat interpretive stratigraphic sequence, compiled from the core logs, is given in Figure 4. Bynum (1982) interpreted the felsic igneous assemblage (Figs. 3 and 4) as felsic metavolcanic rocks, the amphibolite-amphibole gneiss unit as metabasaltic flows and tuffs, and the biotite gneiss unit as metamorphosed graywacke and arkosic metasandstones. Furthermore, Bynum (1982) invoked a Besshi-type volcanogenic model to explain this sulfide deposit.

The descriptions of geological environments of Besshi-type deposits, including associated rock types and tectonic settings (Franklin and others, 1981; Fox, 1984; Cox, 1986), are consistent with Bynum's (1982) characterization and interpretation of the old Saluda deposit. As noted by Franklin and others (1981), Besshi-type deposits occur in strata consisting of subequal amounts of clastic sedimentary rocks and basalt, usually near a tectonic boundary (such as between ocean crust and one of the following: an island arc; a craton; continental crust). Cox (1986) reported that, although the tectonic setting may be uncertain, Besshi deposits possibly form at spreading ridges underlying terrigenous sediment at a continental slope, or in a rifted basin in an island arc/backarc. Besshi-type deposits usually are related to rifting and form subaqueously, and their universal association with mafic volcanic rocks suggests that they are volcanogenic (Fox,

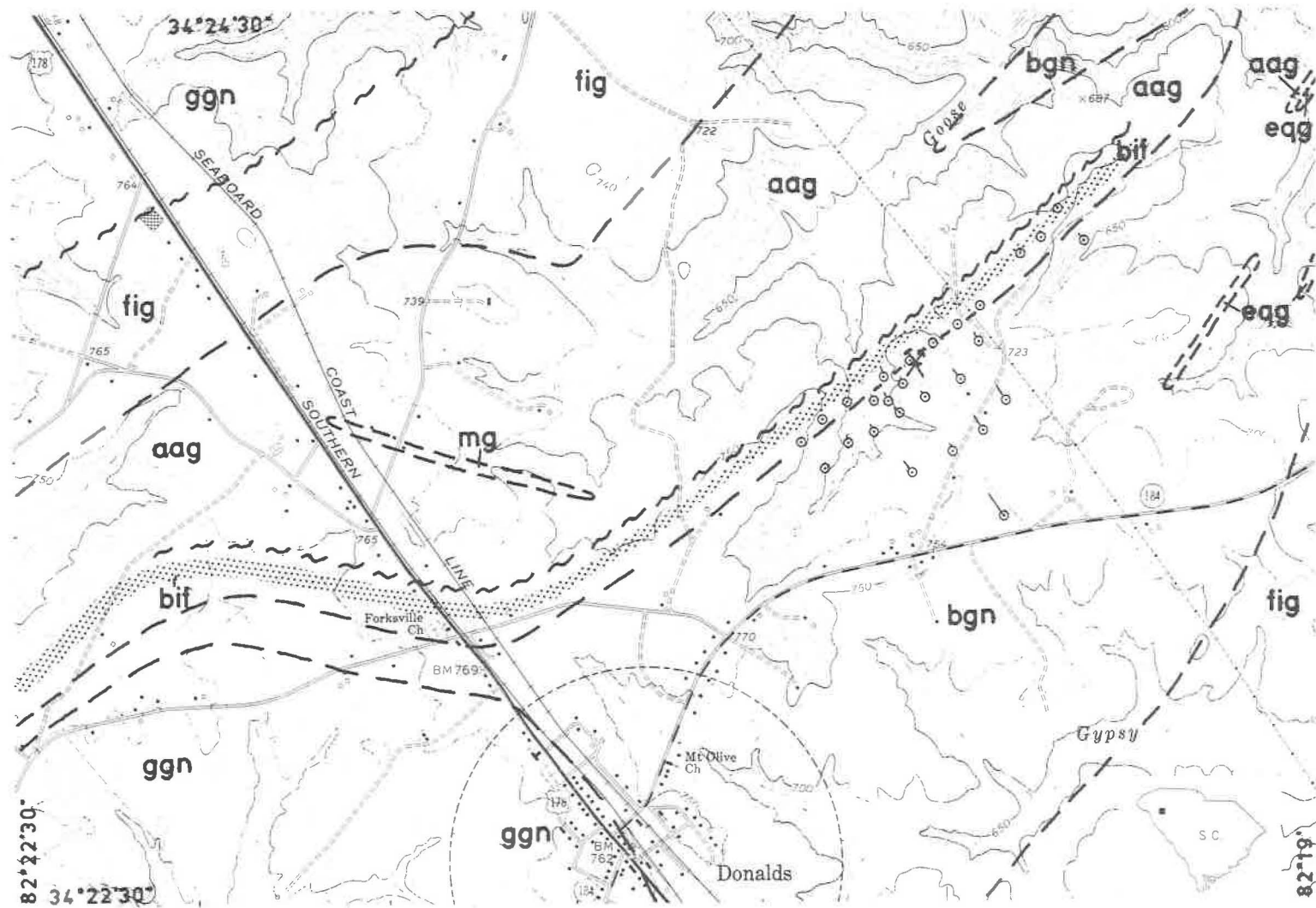


Fig. 3. Geologic map of part of the Ware Shoals West quadrangle (after Bynum, 1982), showing location of drill holes (dots within small circles) in the vicinity of the old Saluda copper mine. Explanation: fig = felsic igneous gneiss assemblage; aag = amphibolite and amphibole gneiss assemblage; bgn = biotite gneiss and schist assemblage; ggn = granitic gneiss assemblage; eag = epidote-quartz granofels; mg = magnetite-epidote-quartz granofels; bif = banded iron-formation. Stippled area highlights iron-formation.

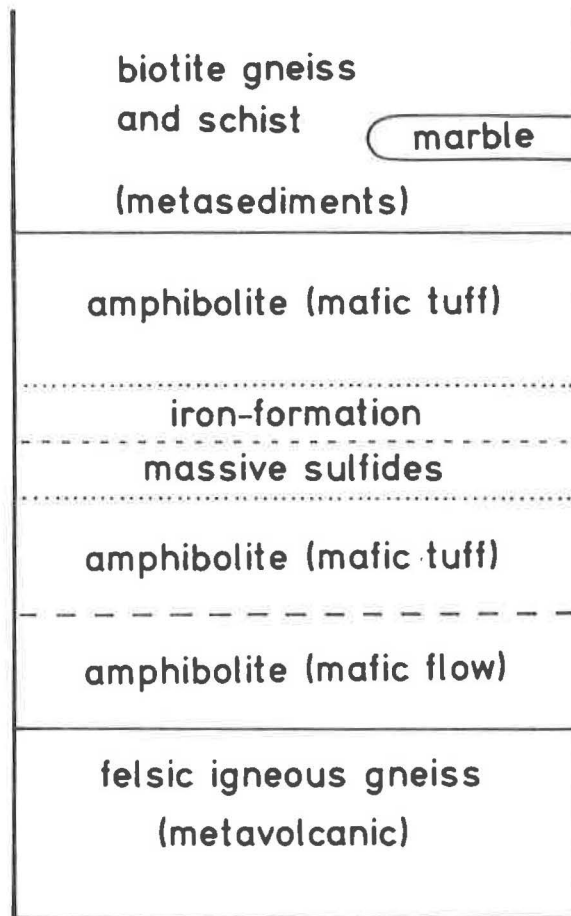


Fig. 4. Interpretive-composite stratigraphic sequence for the old Saluda Cu mine area.

1984). Cox (1986) indicated that Besshi-type mineralization may be the result of deposition by submarine hot springs.

Based upon these definitions and explanations, it seems reasonable to adopt a Besshi-type model to explain this deposit near Donalds. In some ways, the Glenn Springs-area gold deposits (discussed below), associated with mafic metavolcanic rocks and with some copper mineralization, are similar to the old Saluda deposit and could be related metallogenically. In any case, the spatial relationship of the old Saluda mineralization to mafic metavolcanic rocks and iron-formation support its classification as a volcanogenic-exhalative deposit.

## Mineralization of the Carolina terrane

### Cameron Pb Mine

The Cameron mine (Fig. 1), located in the Kings Mountain shear zone approximately five kilometers south of Gaffney (Mittwede, 1989c) and 2.55 km N50°W of the intersection of S.C. Highway 18 and Cherokee County Road 70, was a supplier of lead ore for the Confederate smelter at Norfolk, Virginia during the War Between the States (Sloan, 1908). The Cameron mine opened originally as a copper prospect/mine, but was worked subsequently for lead (Graton, 1906; Keith and Sterrett, 1931). Sloan (1908) reported that the mine produced only a few hundred tons of lead ore.

Lieber (1858) and Graton (1906) reported that the sulfide-bearing vein upon which the mine was developed was 60-75 cm wide and parallel to the foliation of the country rock. Graton (1906) noted that the vein consisted principally of quartz, coarsely crystalline siderite, and chlorite. Recent work in the area (Mittwede and Dockal, 1986; Mittwede, 1989c) has confirmed many of the observations of earlier investigators, but certain mineralogical and textural evidence suggests that the Cameron vein mineralization was superimposed on a pre-existing mineralized zone.

Mineralogically, the Cameron deposit (magnesian siderite (Table 4), quartz, chlorite, galena, chalcopyrite and pyrite) is remarkably similar to sedimentary, carbonate-silicate facies iron-formation, perhaps not unlike Algoma-type iron-formation which is characteristic of many Archean greenstone belts (Evans, 1980). The close proximity of the Cameron deposit to quartzite and mafic metavolcanic rocks, as well as the other interlayered metasedimentary and metavolcanic rocks of the Kings Mountain belt (Figs. 5 and 6), is similar to the graywacke-volcanic association typical of Algoma-type iron-formation (Evans, 1980).

If the Cameron deposit, in part, represents metamorphosed iron-formation, the original sediment from which it formed probably included bedded siderite, chert, and one or more iron silicates/septechlorites (such as greenalite or chamosite). Following this depositional event, possibly as chemical sediments/exhalites, an episode of brecciation produced septechlorite and siderite lithoclasts. Subsequently, chlorite (aphrosiderite) veinlets and quartz euhedra formed, probably during metamorphism. During Alleghanian(?) cataclasis in the Kings Mountain shear zone, the mineralized sequence was fractured/brecciated. This deformation allowed the formation of chlorite (ripidolite) fracture fills and replacements of siderite and aphrosiderite. Finally, ferroan dolomite and quartz fracture fills and replacements formed. It was during this last event that sulfide minerals were mobilized and deposited (Mittwede and

Table 4. Major-oxide analyses (weight percent) of siderite from the Cameron lead mine dump.

	CM-1	CM-2
SiO <sub>2</sub>	1.97	1.56
TiO <sub>2</sub>	<.01	.02
Al <sub>2</sub> O <sub>3</sub>	.28	.23
Fe <sub>2</sub> O <sub>3</sub>	6.91	-
FeO	38.48	45.15
MgO	9.79	9.44
MnO	.71	.77
CaO	1.37	2.67
Na <sub>2</sub> O	.09	.10
H <sub>2</sub> O+	.18	.20
CO <sub>2</sub>	39.34	40.07
Total	99.12	100.21

Other oxides below detection and their lower limits of detection (in parentheses): K<sub>2</sub>O (.10), P<sub>2</sub>O<sub>5</sub> (.01), BaO (.01), SrO (.01), ZrO<sub>2</sub> (.01).

Analyst: Paul Burgener, Technical Services Laboratories, Mississauga, Ontario. Method: ICP.

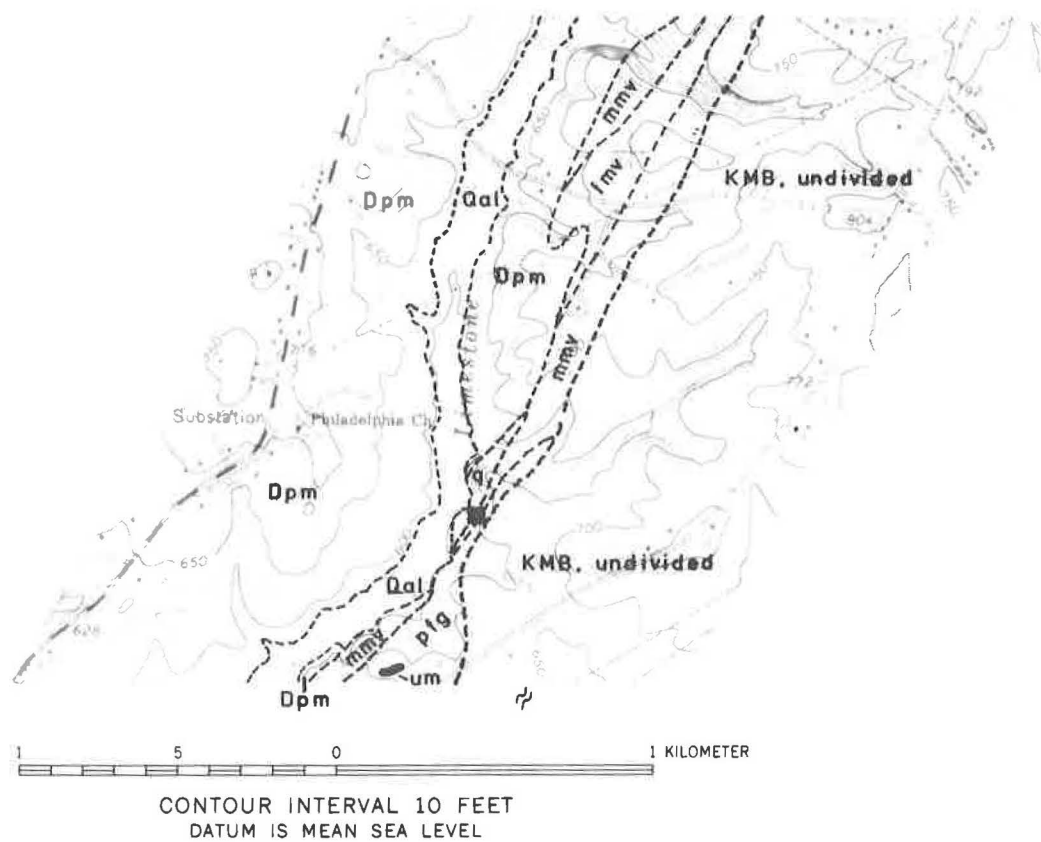


Fig. 5. Geologic map of the old Cameron Pb mine area (after Mittwede, 1989c).  
 Explanation: Dpm = Devonian Pacolet Mills granitic pluton; Qal = Quaternary alluvium; mmv = mafic metavolcanic rocks; fmv = felsic metavolcanic rocks; q = quartzite; pfg = pegmatitic felsic gneiss; um = ultramafic rock (metapyroxenite); KMB, undivided = Kings Mountain belt rocks (interlayered metasedimentary and metavolcanic rocks); solid square = Cameron mine.

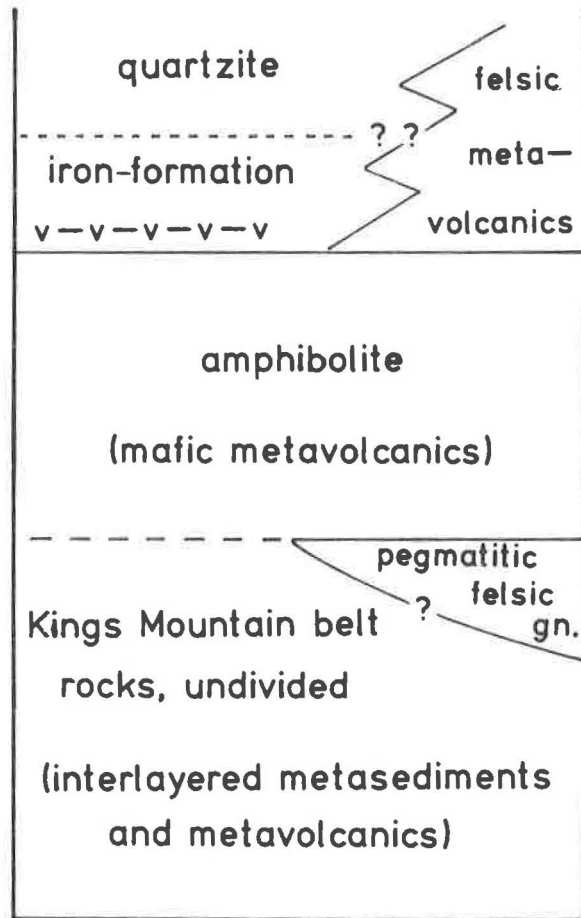


Fig. 6. Interpretive-composite stratigraphic sequence for the old Cameron Pb mine area. Explanation: v-v-v = vein.

Dockal, 1986). The Cameron "vein" is similar to concordant lenses of beds of silica described from some iron-formation-related gold deposits (Gilmour, 1985).

None of the samples collected at the Cameron mine contain detectable gold, but the Austin (or Nott) placer (Lieber, 1858; Graton, 1906; Sloan, 1908) was located somewhere near the Cameron mine and was worked in the 1850's (Sloan, 1908). Lieber (1858) even suggested that the Austin deposit may have been derived from the Cameron vein. Spectrographic trace-element analyses (Tables 5 and 6) show that some samples from the Cameron mine contain >10,000 ppm Pb, up to 5,000 ppm Cu, and up to 100 ppm Ag. Sloan (1908) reported that the galena at the Cameron mine was argentiferous.

#### Lockhart Au Mine and Blanton Creek Au Prospect

The Lockhart mine (mentioned briefly by Tuomey, 1848) and the Blanton Creek prospect (located 2.82 km N45°E and 0.85 km N60°E of the intersection of S.C. Highway 18 and Cherokee County Road 70, respectively) were developed on a tourmaline-bearing quartz vein southeast of Gaffney (Fig. 1). Locations for both "deposits" were given by Keith and Sterrett (1931). The two deposits are located 2.06 km apart and the vein trends about N40°E. At both, white vein quartz, much of which contains acicular to stubby-prismatic black tourmaline crystals, occurs in abundance around the old workings. Supposedly, free gold was present locally in the vein, but grab samples from each location showed no gold when assayed (Table 3). The mineralogy and texture of the Lockhart-Blanton Creek vein suggest that it is probably metamorphogenic.

#### Manganiferous Schist of the Battleground Formation

Manganiferous quartz-mica schist, assigned to the Jumping Branch Manganiferous Member of the Battleground Formation (Horton, 1984), is associated with felsic metavolcanic rocks in the Kings Mountain belt. Often, the manganiferous schist is accompanied by conformable beds of very dense, fine-grained gondite (coticule). The manganiferous unit extends from the Corinth community (south of Gaffney) northeast into the Kings Creek area and on into North Carolina (Fig. 1). Mittwede (1988a) also reported that steeply dipping manganiferous schist holds up the prominent ridge south of White Stone, about 5 km west of Pacolet in east-central Spartanburg County.

Horton and others (1981) suggested that the manganese and associated iron of the Kings Mountain belt manganiferous schists may have been derived by chemical weathering and leaching of volcanic glass, or formed as distal volcanic exhalative deposits of submarine hydrothermal vents. Bennett (1987) described apparently similar rocks from the Cambrian Harlech Grits Group of North Wales and likewise suggested that the syngenetic/syndiagenetic manganese mineralization there was a result of the submarine exhalation of manganese-rich hydrothermal fluids. Considering the close association of the Jumping Branch Manganiferous Member to metavolcanic rocks (and alteration; for example, sericite schist) in the Battleground Formation, it is reasonable to conclude that the manganese mineralization is indeed volcanogenic. Stanton (1972) presented an excellent summary of manganese deposits of volcanic affiliation. Stanton suggested that hot springs are almost certainly the major source of manganese in volcanic environments and, hence, most of these manganese deposits can be termed "exhalative-sedimentary".

Table 5. Spectrographic trace-element analyses (in ppm) of vein material from the Cameron lead mine dump. Lower limits of detection in parentheses.

		1	2	3	4	5	6
Ag	(1)	50	3	5	10	100	1
B	(10)	-	10	-	-	-	70
Ba	(10)	70	50	-	-	-	100
Be	(2)	3	2	-	-	-	3
Bi	(10)	100	-	-	-	150	-
Cr	(10)	-	-	20	-	10	-
Cu	(2)	70	15	5000	5000	1000	1500
Ga	(10)	-	-	-	-	-	10
La	(20)	-	20	20	20	20	20
Mn	(10)	5000	70	200	1000	150	150
Mo	(2)	15	-	-	2	-	50
Ni	(5)	10	5	20	10	15	10
Pb	(10)	> 10000	300	100	30	5000	1000
Sc	(10)	10	-	-	-	-	-
Sr	(100)	200	-	-	-	-	-
Ti	(20)	200	300	1500	50	700	500
V	(10)	20	15	30	10	30	10
Zr	(20)	-	50	30	-	30	100

Other elements below detection and their lower limits of detection: As (200), Cd (50), Co (5), Ge (20), Nb (20), Sb (100), Sn (10), W (50), Y (10), Zn (200).

Analyst: Gordon H. VanSickle, Skyline Labs, Wheat Ridge, Colorado. Method: semi-quantitative D.C. arc emission spectrography.

Table 6. Spectrographic trace-element analyses (in ppm) of siderite samples from the Cameron lead mine dump. Lower limits of detection in parentheses.

		1	2	3	4	5	6	7	8
Ba	(10)	10	10	10	10	10	10	-	10
Cr	(10)	-	-	-	-	-	10	-	-
Cu	(2)	20	-	-	7	-	5	-	-
Ga	(10)	15	15	10	10	10	10	-	10
Mn	(10)	7000	5000	5000	7000	5000	7000	3000	5000
Mo	(2)	20	10	10	15	15	20	10	15
Ni	(5)	10	10	5	15	5	5	-	-
Pb	(10)	100	-	-	-	-	-	-	-
Sc	(10)	-	-	-	10	-	-	-	10
Ti	(20)	20	-	20	-	20	100	20	30
V	(10)	10	10	20	10	15	10	10	20
Y	(Y)	-	-	-	-	-	10	-	-

Other elements below detection and their lower limits of detection (in parentheses): Ag (1), As (200), B (10), Be (2), Bi (10), Cd (10), Co (5), Ge (20), La (20), Nb (20), Sb (100), Sn (10), Sr (100), W (50), Zn (200) and Zr (20).

Analyst: Gordon H. VanSickle, Skyline Labs, Wheat Ridge, Colorado. Method: semi-quantitative D.C. arc emission spectrography.

Manganiferous schist is used as a filler in common brick or as a coloring agent in special face brick. It currently is mined near Kings Creek for these applications. Furthermore, these manganese concentrations should be explored not only for their manganese content, but also for associated metals as manganiferous units are good geochemical marker horizons for base metals and/or gold (for example, Wonder and others, 1988 and references therein).

### Talc Deposits of the Hammett Grove Suite

Two deposits of paint- to filler-grade talc occur within the altered (steatitized and serpentinitized) rocks of the Hammett Grove Meta-igneous Suite (Mittwede, 1989d) near Pacolet Mills (Fig. 1). The talc-rich rocks, mostly soapstone with lesser talc schist (and some antigorite-serpentinite enclaves), are composed of talc (50-80 percent), clinoamphibole (5-15 percent), chlorite (2-10 percent) and variable, minor or trace amounts of opaque minerals, calcite, antigorite and anthophyllite. A calculation of reserves indicates that there may be 1 to 1.5 million tons of talc ore in each of the deposits. One of the prospects, located near Hammett Grove Church and bounded on the south by the Pacolet River, was leased recently by Southern Talc Company of Chatsworth, Georgia.

The talc in these deposits formed as part of a cooling assemblage by retrogression following the metamorphic thermal peak (Mittwede, 1989a). The preponderance of talc-rich rocks indicates that the Hammett Grove ultramafites (originally Iherzolites or harzburgites) reached a compositional plateau within the stability range of talc during cooling after attainment of middle- to upper-amphibolite facies conditions.

The Hammett Grove Suite was interpreted as a dismembered, metamorphosed and variably deformed ophiolite fragment by Mittwede (1989a) and was considered a marker of the suture between the Piedmont terrane and the exotic Carolina terrane (Mittwede, 1988c). Although the Suite is located in the Inner Piedmont belt (that is, west of the Kings Mountain shear zone), it is included in the discussion of Carolina terrane mineralization because it is believed to have been derived from the Carolina terrane by thrusting (Mittwede, 1989a).

### Nuckolls, Norris and Nott Hill Au Mines

The Nuckolls, Norris and Nott Hill mines, developed on gold-bearing quartz veins and described by Tuomey (1848), Lieber (1858), and Mittwede (1988b), are situated close together on a conical hill, 3.18 km S80°W of the junction of South Carolina Highways 18 and 211 in southern Cherokee County (Fig. 1). The extensive workings include caved shafts, at least one adit, and numerous pits and short trenches. White vein quartz crops out in several of the workings and is strewn about widely on the land surface.

The deposits were described by earlier workers as funnel-shaped, "saccharoid" (coarsely crystalline) quartz veins, all of which were reported to have northeasterly strikes, parallel to the foliation in the country rocks. The concordant nature of the veins indicates that they were either folded with the country rocks or entered along pre-existing structures. The granular, coarsely crystalline texture of the veins suggests that they recrystallized during metamorphism and, therefore, belong to an early, possibly volcanogenic, vein system. Tuomey (1848) and Lieber (1858) reported that the veins were steeply dipping and passed upward through granite and into mica schist that capped the hilltops. No schist was

found during recent mapping of the area, but the veins are probably related to granodioritic, subvolcanic intrusive rocks of the Polecat Creek suite (Mittweide, 1989b). Rhyolitic to dacitic plagioclase-crystal tuffs and rhyolitic-rhyodacitic quartz-crystal tuffs ("porphyrys") also are common in the vicinity.

The veins carried free gold which was most abundant where the veins were rich in "brown ore". The only gangue or accessory minerals that have been found are quartz, pyrite, limonite and, locally, muscovite. Six grab samples of vein quartz (some of which contained visible limonite and/or pyrite) all had amounts of gold above background levels, and three were highly anomalous (550, 615 and 7480 ppb) with respect to gold.

### Glenn Springs Area Au Mines

Historically, the greatest production of gold in the South Carolina central Piedmont came from five mines in the vicinity of Glenn Springs. Located in western Union County (Fig. 1), these mines were called the Fair Forest mines by early workers (Tuomey, 1848; Lieber, 1858). Sloan (1908) separately described each property, including the Mud (or Harman) mine, the Nott mine, the Ophir (or Thompson) mine, the West mine, and the Bogan mine.

Country rocks to the gold-bearing quartz veins at the Mud and Nott mines are mafic metavolcanic rocks (amphibolite and amphibole gneiss), described by Sloan (1908) as biotite and hornblende slates. The veins and the country rocks have steep dips to the SE and strike N10-23°E. In addition to gold, Sloan (1908) reported copper mineralization in the form of chalcopyrite and native copper.

A different style of mineralization is found at the Ophir and West mines where gold is disseminated in siliceous and aluminous (sericitic) alteration (Table 3) or concentrated in later veins. Grab samples of sericitic and siliceous rocks from the West mine (Table 7) have compositions compatible with felsic volcanic precursors that have undergone potassium metasomatism, based upon the supposed inertness of  $Al_2O_3$  and  $TiO_2$  during metamorphism and alteration.

The Bogan mine was developed on a quartz vein that was described by Sloan (1908, p. 38) as "more saccharoidal than the West Springs group". Placer deposits were worked to a modest extent at the West and Bogan mines.

Exploration activity has continued to present in the Glenn Springs area. BP Minerals America held a recent lease on the West mine and conducted a limited drilling program. U.S. Borax and FMC have had drilling programs at the Ophir mine within the last decade (core and data stored at the South Carolina Geological Survey). Logs of core taken by U.S. Borax at the Ophir mine indicate that mineralized zones range in thickness from one to six meters and carry grades of .06 to .09 ounces Au/ton, but these zones apparently are not laterally extensive. Pyritic quartz-sericite schist and silicified tuff (usually within a section of mafic metavolcanic rock) host the gold mineralization or, locally, gold may be concentrated in quartz veins. In addition to quartz veins, epidosite veins, carbonate-filled fractures and meta-ultramafic/metamafic (metapyroxenite to metadiorite) dikes were intersected in some core holes. The latter are significant in that they are probably part of the Mean Crossroads suite of Dennis (1988). This suite of related meta-igneous rocks was interpreted by Dennis (1988) and Dennis and Shervais (1988) as a product of intra-arc rifting. Since the mafic/ultramafic dikes obviously cut across the mineralized alteration zones, the Mean Crossroads suite is clearly younger than the syn- or epigenetic alteration and mineralization and probably the main episode of arc building.

Table 7. Major-oxide analyses (weight percent) of altered volcanic rocks from the West gold mine.

	GS-WMm	GS-WMq
SiO <sub>2</sub>	71.96	79.96
TiO <sub>2</sub>	.36	.21
Al <sub>2</sub> O <sub>3</sub>	14.71	10.71
Fe <sub>2</sub> O <sub>3</sub>	4.30	1.72
MgO	.77	.28
MnO	.03	.02
CaO	.08	.08
Na <sub>2</sub> O	.26	.06
K <sub>2</sub> O	4.75	4.71
P <sub>2</sub> O <sub>5</sub>	.06	.06
LOI	2.49	1.62
S	.04	.01
Ba	.02	.04
Cr	.01	.02
Total	99.80	99.49

Sample explanations: GS-WMm = sericite-rich; GS-WMq = silica-rich.

Analyst: Bondar-Clegg and Company, Ltd., North Vancouver, British Columbia. Method: plasma emission (DCP and ICP) spectroscopy.

The disseminated gold mineralization and related alteration zones in the Glenn Springs area are volcanogenic and were likely syngenetic with mafic and/or felsic volcanism. Where gold occurs in veins, it is assumed that the veins and mineralization were volcanogenic, metamorphogenic or both.

### Smyrna Au District

Butler (1981) discussed the geology and mineralization of the Smyrna district (Fig. 1). The district is characterized by gold-bearing quartz-pyrite veins and more than 50 old mines and prospects. Butler suggested that this swarm of gold-quartz veins formed in the upper parts of shallow (subvolcanic) intrusions and in altered zones in the superjacent volcanic rocks. Overlying barite (such as the Kings Creek barite deposit; see Sharp and Hornig, 1981, and references therein) and manganese deposits (Fig. 1) were interpreted to have a volcanic-exhalative origin, formed during the waning stages of igneous activity. Butler pointed out that some of the Smyrna district veins are not hydrothermal-volcanogenic but, rather, metamorphogenic.

An added note concerning barite: barite can be an important guide to base- and precious-metal deposits. For example, bedded and vein barite is associated with the ores in the Buchans polymetallic sulfide deposits, Newfoundland and the classic Kuroko massive sulfide deposits, Japan (Sawkins, 1984), and with gold deposits in the important Hemlo camp, Ontario (Patterson, 1984). The barite deposits in the central Piedmont of South Carolina may be indicators of undiscovered metallic mineralization. Interestingly, minor amounts of galena are associated with the barite at Kings Creek (LeHuray, 1982).

### Exploration Potential

For all intents and purposes, the Inner Piedmont belt is terra incognita with respect both to the understanding of its geologic framework and its mineral deposits. The presence of what are considered chemical sedimentary/exhalative units (for example, tourmalinites, iron-formations and manganese formations or gondites) as well as many isolated mines or prospects outside of the more well-known mining districts make the Inner Piedmont belt a tantalizing metals exploration target. However, companies that have ventured into the Inner Piedmont belt, to this point, have received little encouragement for their efforts. Unfortunately, the majority of such efforts have been either hopelessly broadbrush or wastefully cursory. Because of the complex structure and typically very scarce exposure, work in this belt has been nearly taboo. The discovery of an economic mineral deposit in the Inner Piedmont belt will require agonizing scrutiny, excellent mapping (with a prerequisite of identifying and utilizing distinctive marker units), and an unreserved, unbridled commitment to core drilling. A regional lithogeochemical sampling program would be a tremendous boon to exploration efforts; such a program would facilitate the identification of Inner Piedmont belt protoliths (particularly the recognition of volcanic components) and allow determination of (or better constrain) paleoenvironments.

Given the recent recognition of an important stream-sediment/soil geochemical exploration technique for vermiculite, and the sheer number of biotite bodies that seem to be present, it is likely that more vermiculite deposits will be discovered. Hence, the Enoree district will remain a dominant producer for years to come. Other industrial minerals, such as talc, graphite and

aluminosilicates, are known in the Inner Piedmont belt, but discovery of an economically important deposit will require concerted effort and commitment.

The situation in the Carolina terrane, specifically the Kings Mountain belt, is not so bleak. There has been significant historical gold production from two districts in the Kings Mountain belt, namely the Smyrna and Glenn Springs districts. Most of the vein deposits in these areas are likely too small to receive the attention of large exploration companies, but disseminated deposits like those at the Ophir and West mines near Glenn Springs will continue to lure the gold hunters. It is quite possible that other deposits of the Glenn-Springs type are present in other parts of the Kings Mountain belt volcanic sequence. Some companies in recent years have explored the gold potential of some of the Kings Mountain belt iron-formations and have been moderately encouraged but, for the most part, the whole area has remained a teaser for those seeking precious metals.

The numerous, relatively late shear zones in the Kings Mountain belt, especially those that transect favorable volcanic sequences, must be considered prime exploration targets. A recently discovered example is the Jones Creek shear zone (Mittweide, 1989b); metatuffaceous rocks (including blue-quartz eye tuffs or "porphyrys") in the vicinity of Jones Creek host aluminous and chloritic hydrothermal alteration as well as local sulfide enrichments. Coarse crystals of staurolite are plentiful in Jones Creek stream sediments. Sericite schist in the area runs 10-30 ppb gold - not much, but well above background levels. Additionally, the Jones Creek shear zone is located near the known mineralization of the old Nuckolls, Norris and Nott Hill mines discussed above.

Manganiferous and sericite schist will continue to be in demand by the brick industry. The reserves of both in the Kings Creek area and along strike to the southwest will easily meet the demand of the brick manufacturers in the region, although some effort will be necessary to find 1) deposits of the size required by the industry and 2) favorable land situations.

## Conclusions

The diverse mineral deposits in the central Piedmont metallogenic province cannot be simply or definitively classified, but it is clear that many are volcanogenic. Most of the mineralization in the Kings Mountain belt portion of the Carolina terrane is associated with calc-alkaline metavolcanic rocks that formed in response to or are products of continent-arc convergence, that is, accretion of the exotic Carolina volcanic-arc terrane to the enigmatic Piedmont terrane (Fig. 7). Some of the mineralization in the Inner Piedmont portion of the Piedmont terrane probably is related to earlier, intra-arc or back-arc rifting of the "Piedmont arc" of Hatcher (1987).

## Acknowledgements

This work was completed as a South Carolina Geological Survey (SCGS) mineral resources project. I appreciate the encouragement and practical help provided me by Butch Maybin, Alan-Jon Zupan, Ole Olson and Lou Price, all of SCGS. An earlier version of this paper was reviewed by Gilles Allard (University of Georgia), Bob Cook (Auburn University), and Butch Maybin (SCGS); profuse thanks for their comments and suggestions which improved the paper.

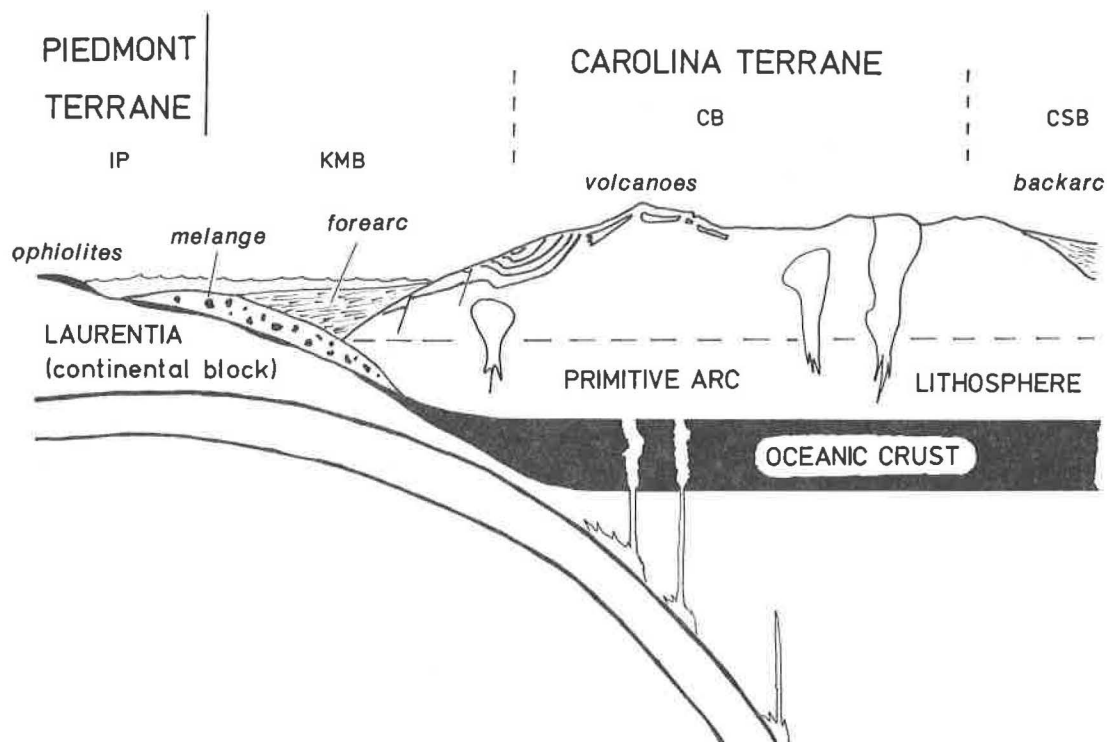


Fig. 7. Tectonic cartoon of the central Piedmont showing early- to middle-Paleozoic accretionary zone between the Piedmont terrane and Carolina terrane. Explanation: IP = Inner Piedmont belt; KMB = Kings Mountain belt; CB = Charlotte belt; CSB = Carolina slate belt. Ophiolites and melanges portrayed here are envisioned per the descriptions and interpretations of Mittwede (1988c) and Mittwede and Maybin (1989). Although the Piedmont terrane is here shown as a continental block, its partial volcanic character cannot be denied. The Piedmont terrane likely originated as a continental-margin arc.

## References

- Allard, G. O., and Carpenter, R. H., 1988, Mineralogical anomalies in metamorphosed terrains; a neglected but promising exploration tool: International Conference -Geochemical Evolution of the Continental Crust, Pocos de Caldas, Brazil 1988, Abstracts Volume, p. 229-236.
- Bennett, M. A., 1987, Genesis and diagenesis of the Cambrian manganese deposits, Harlech, North Wales: *Geological Journal*, v. 22, p. 7-18.
- Butler, J. R., 1981, Gold and related deposits of the Smyrna district, York and Cherokee Counties, South Carolina *South Carolina Geology*, v. 25, p. 9-20.
- Butler, J. R., 1989, Review and classification of ultramafic bodies in the Piedmont of the Carolinas, in Mittwede, S. K. and Stoddard, E. F., eds., *Ultramafic rocks of the Appalachian Piedmont: Geological Society of America Special Paper 231*, p. 19-31.
- Bynum, F. J., Jr., 1982, The geology of the south one-half of the Ware Shoals West quadrangle, S.C.: unpublished M. S. thesis, University of Georgia, Athens, 97 p.
- Carpenter, R. H., and Allard, G. O., 1982, Aluminosilicate assemblages: An exploration tool for metavolcanic terrains of the Southeast, in Allard, G. O., and Carpenter, R. H., eds., *Exploration for Metallic Resources in the Southeast: University of Georgia Department of Geology and Center for Continuing Education*, p. 1-4.
- Carr, R. S., III, Dean, L. S., Unger, H. E., and Reely, B. T., 1984, Stratiform tin mineralization in the Inner Piedmont belt of North and South Carolina: *Geological Society of America Abstracts with Programs*, v. 16, p. 464.
- Christiansen, E. H., Sheridan, M. F., and Burt, D. M., 1986, The geology and geochemistry of Cenozoic topaz rhyolites from the western United States: *Geological Society of America Special Paper 205*, 88 p.
- Cook, R. B., and Bittner, E., 1988, Tectonic modeling as a guide to base and precious metal exploration in the southernmost Appalachian orogen, in Kisvarsanyi, G., and Grant, S. K., eds., *North American Conference on Tectonic Control of Ore Deposits and the Vertical and Horizontal Extent of Ore Systems: Rolla, Missouri, University of Missouri-Rolla*, p. 471-481.
- Cox, D. P., 1986, Descriptive model of Besshi massive sulfide, in Cox, D. P. and Singer, D. A., eds., *Mineral Deposit Models: U. S. Geological Survey Bulletin 1693*, p. 136-138.
- Dennis, A., 1988, Preliminary report on the geology of the Glenn Springs-Jonesville area and tectonic model, in Secor, D. T., Jr., ed., *Southeastern Geological Excursions: Columbia, South Carolina Geological Survey*, p. 226-249.
- Dennis, A. J. and Shervais, J. W., 1988, Field relationships and geochemistry of arc-related mafic-ultramafic intrusives in the southern Kings Mountain belt: *Geological Society of America Abstracts with Programs*, v. 20, p. 260.
- Dixon, C. J., 1974, Plate tectonics and mineralization in the Tethyan region: *Mineralium Deposita*, v. 9, p. 185-198.
- Ethier, V. G., and Campbell, F. A., 1977, Tourmaline concentrations in Proterozoic sediments of the southern Cordillera of Canada and their economic significance: *Canadian Journal of Earth Sciences*, v. 14, p. 2348- 2363.
- Evans, R. M., 1975, Mineralization in geosynclines - the Alpine enigma: *Mineralium Deposita*, v. 10, p. 254-260.
- Evans, A. M., 1980, *An introduction to ore geology*: New York, Elsevier, 231 p.
- Feiss, P. G., and Hauck, S. A., 1980, Tectonic setting of massive-sulfide deposits in the southern Appalachians, U.S.A., in Ridge, J. D., ed.,

- Proceedings of the Fifth Quadrennial IAGOD Symposium, v. I: Stuttgart, E. Schweizerbart'sche Verlagsbuchhandlung, p. 567-580.
- Fleischer, R., and Routhier, P., 1973, The "consanguineous" origin of a tourmaline-bearing gold deposit; Passagem de Mariana (Brazil): *Economic Geology*, v. 68, p. 11-22.
- Fox, J. S., 1984, Besshi-type volcanogenic sulphide deposits-a review: *CIM Bulletin*, v. 77, p. 57-68.
- Franklin, J. M., Lydon, J. W., and Sangster, D. F., 1981, Volcanic-associated massive sulfide deposits, *in* Skinner, B. J., ed., *Economic Geology 75th Anniversary Volume*: p. 485-627.
- Gilmour, P., 1985, Gold associated with iron formation and related sediments: *Society of Mining Engineers Preprint Number 85-83*, 9 p.
- Glover, L., III, Speer, J. A., Russell, G. S., and Farrar, S. S., 1983, Ages of regional metamorphism and ductile deformation in the central and southern Appalachians: *Lithos*, v. 16, p. 223-245.
- Graton, L. C., 1906, Reconnaissance of some gold and tin deposits of the southern Appalachians: *U. S. Geological Survey Bulletin* 293, p. 9-118.
- Hatcher, R. D., Jr., 1987, Tectonics of the southern and central Appalachian internides: *Annual Reviews of Earth and Planetary Science*, v. 15, p. 337-362.
- Horton, J. W., Jr., 1984, Stratigraphic nomenclature in the Kings Mountain belt, North Carolina and South Carolina, *in* *Stratigraphic Notes, 1983*: U. S. Geological Survey Bulletin 1537-A, p. A59-A67.
- Horton, J. W., Jr., Butler, J. R., Schaeffer, M. F., Murphy, C. F., Connor, J. M., Milton, D. J., and Sharp, W. E., 1981, Field guide to the geology of the Kings Mountain belt between Gaffney, South Carolina and Lincolnton, North Carolina, *in* Horton, J. W., Jr., Butler, J. R., and Milton, D. J., eds., *Geological investigations of the Kings Mountain belt and adjacent areas in the Carolinas: Carolina Geological Society Field Trip Guidebook 1981*, p. 213-247.
- Horton, J. W., Jr., Drake, A. A., Jr., and Rankin, D. W., 1989, Tectonostratigraphic terranes and their Paleozoic boundaries in the central and southern Appalachians, *in* Dallmeyer, R. D., ed., *Terranes in the Circum-Atlantic Paleozoic orogens*, Geological Society of America Special Paper 230, p. 213-245.
- Hutchison, C. S., 1983, *Economic deposits and their tectonic setting*: New York, Wiley, 365 p.
- Jankovic, S., 1980, Porphyry-copper and massive-sulfide ore deposits in the northeastern Mediterranean, *in* Ridge, J. D., ed., *Proceedings of the Fifth Quadrennial IAGOD Symposium, v. I: Stuttgart, E. Schweizerbart'sche Verlagsbuchhandlung*, p. 431-444.
- Jankovic, S., and Petrascheck, W. E., 1987, Tectonics and metallogeny of the Alpine-Himalayan belt in the Mediterranean area and western Asia: *Episodes*, v. 10, p. 169-175.
- Keith, A., and Sterrett, D. B., 1931, Description of the Gaffney and Kings Mountain quadrangles: *U. S. Geological Survey Geological Atlas Folio Series*, no. 222, 13 p.
- LeHuray, A. P., 1982, Lead isotopic patterns of galena in the Piedmont and Blue Ridge ore deposits, southern Appalachians: *Economic Geology*, v. 77, p. 335-351.
- Libby, S. C., 1975, The origin of potassic ultramafic rocks in the Enoree "vermiculite" district, South Carolina: unpublished Ph. D. dissertation, Pennsylvania State University, 116 p.

- Lieber, O. M., 1858, Report on the survey of South Carolina; being the second annual report: Columbia, South Carolina, 145 p.
- Maybin, A. H., III, and Carpenter, R. H., 1989, Geochemistry, a new approach for vermiculite exploration in South Carolina: Proceedings, 24th Forum on the Geology of Industrial Minerals, in press.
- McArdle, P., Fitzell, M., Oosterom, M. G., O'Connor, P. J., and Kennan, P. S., 1989, Tourmalinite as a potential host rock for gold in the Caledonides of southeast Ireland: *Mineralium Deposita*, v. 24, p. 154-159.
- McCauley, C. K., and Butler, J. R., 1966, Gold resources of South Carolina: South Carolina Division of Geology, Bulletin 32, 78 p.
- Mittwede, S. K., 1984a, The geology and mineral resource potential of the Thicketty Mountain area, S.C.: unpublished M.S. thesis, University of South Carolina, 59 p.
- Mittwede, S. K., 1984b, Tourmalinite, anomalous tourmaline concentrations, and iron formation as exploration guides in northwestern Cherokee County, South Carolina: *South Carolina Geology*, v. 27, p. 6-12.
- Mittwede, S. K., 1985a, Geochemical and mineralogical anomalies in the Thicketty Mountain area, Cherokee and Spartanburg counties, South Carolina: *South Carolina Geology*, v. 28, p. 7-10.
- Mittwede, S. K., 1985b, Geologic map of the southern half of the Boiling Springs South 7.5-minute quadrangle, South Carolina and North Carolina: South Carolina Geological Survey Open-File Report 51.
- Mittwede, S.K., 1986, Tourmaline in South Carolina: A review: *South Carolina Geology*, v. 30, p. 47-69.
- Mittwede, S. K., 1988a, Road log for stops in the Ora, Pacolet and Pacolet Mills quadrangles - Field trip 7: A geological transect through the suspect terranes of the Appalachian Piedmont from the Fall Line through the Inner Piedmont, in Secor, D. T., Jr., ed., *Southeastern Geological Excursions: Columbia, South Carolina Geological Survey*, p. 250-265.
- Mittwede, S. K., 1988b, Gold mineralization and its relationship to volcanic stratigraphy in the Kings Mountain belt, Pacolet Mills quadrangle, South Carolina: *Geological Society of America Abstracts with Programs*, v. 20, p. 281.
- Mittwede, S. K., 1988c, Ultramafites, melanges, and stitching granites as suture markers in the central Piedmont of the southern Appalachians: *Journal of Geology*, v. 96, p. 693-707.
- Mittwede, S. K., 1989a, The Hammett Grove Meta-igneous Suite; a possible ophiolite in the northwestern South Carolina Piedmont, in Mittwede, S. K. and Stoddard, E. F., eds., *Ultramafic Rocks of the Appalachian Piedmont: Geological Society of America Special Paper 231*, p. 45-62.
- Mittwede, S. K., 1989b, Geologic maps of the Pacolet and Pacolet Mills 7.5-minute quadrangles, South Carolina: South Carolina Geological Survey Open-File Report 64.
- Mittwede, S. K., 1989c, Geologic map of the Cameron lead mine area, Gaffney 7.5-minute quadrangle, Cherokee County, South Carolina: South Carolina Geological Survey Open-File Report 65.
- Mittwede, S. K., 1989d, Mineralogy, origin and evaluation of talc deposits near Pacolet Mills, South Carolina: Proceedings, 24th Forum on the Geology of Industrial Minerals, in press.
- Mittwede, S.K., and Dockal, J. A., 1986, The Cameron mine: Sedimentary iron-formation in the Kings Mountain shear zone: *Geological Society of America Abstracts with Programs*, v. 18, p. 256.

- Mittwede, S. K., and Maybin, A. H., III, 1989, Metamorphosed melange in the central Piedmont of South Carolina: *Journal of Geology*, v. 97, p. 632-639.
- Moore, W. J., Rowe, W. D., Jr., and Eckert, J. R., 1985, Chemistry of Inner Piedmont metamorphic rocks hosting a stratiform tin occurrence near Forest City, NC: *Geological Society of America Abstracts with Programs*, v. 17, p. 668-669.
- Moss, B. G., 1972, *The Old Iron District: a study of the development of Cherokee County - 1750-1897*: Clinton, South Carolina, Jacobs Press, 390 p.
- Patterson, G. C., 1984, Field trip guidebook to the Hemlo area: Ontario Geological Survey Miscellaneous Paper 118, 33 p.
- Plimer, I. R., 1980, Exhalative Sn and W deposits associated with mafic volcanism as precursors to Sn and W deposits associated with granites: *Mineralium Deposita*, v. 15, p. 275-289.
- Plimer, I. R., 1987, The association of tourmalinite with stratiform scheelite deposits: *Mineralium Deposita*, v. 22, p. 282-291.
- Rowe, W. D., Jr., and Moore, W. J., 1988, Chemistry of stratiform Late Proterozoic tin-bearing leucosomes in the Inner Piedmont belt, southeastern United States, in *Proceedings of the Seventh Quadrennial IAGOD Symposium*: Stuttgart, E. Schweizerbart'sche Verlagsbuchhandlung, p. 427-436.
- Sawkins, F. J., 1984, *Metal deposits in relation to plate tectonics*: Berlin, Springer-Verlag, 325 p.
- Secor, D. T., Jr., Snoke, A. W., and Dallmeyer, R. D., 1986, Character of the Alleghanian orogeny in the southern Appalachians; Part III - Regional tectonic relations: *Geological Society of America Bulletin*, v. 97, p. 1345-1353.
- Sharp, W. E., and Hornig, C. A., 1981, The barite deposit at Kings Creek, South Carolina, in Horton, J. W., Jr., Butler, J. R., and Milton, D. J., eds., *Geological investigations of the Kings Mountain belt and adjacent areas in the Carolinas*: Carolina Geological Society Field Trip Guidebook 1981, p. 120-129.
- Slack, J. F., 1982, Tourmaline in Appalachian-Caledonian massive sulfide deposits and its exploration significance: *Institution of Mining and Metallurgy Transactions*, v. 91, Sec. B, p. B81-B89.
- Slack, J. F., Herriman, N., Barnes, R. G., and Plimer, I. R., 1984, Stratiform tourmalinites in metamorphic terranes and their geologic significance: *Geology*, v. 12, p. 713-716.
- Sloan, E., 1908, *Catalogue of the mineral localities of South Carolina*: Columbia, South Carolina Geological Survey Bulletin 2, reprinted 1979, 505 p.
- Stanton, R. L., 1972, *Ore petrology*: New York, McGraw-Hill, 713 p.
- Strong, D. F., ed., 1976, *Metallogeny and plate tectonics*: Geological Association of Canada Special Paper Number 14, 660 p.
- Tuomey, M., 1844, *Report on the geological and agricultural survey of the state of South Carolina*: Columbia, South Carolina, 63 p.
- Tuomey, M., 1848, *Report on the geology of South Carolina*: Columbia, South Carolina, A. S. Johnston, 293 p.
- Wonder, J. D., Spry, P. G., and Windom, K. E., 1988, Geochemistry and origin of manganese-rich rocks related to iron-formation and sulfide deposits, western Georgia: *Economic Geology*, v. 83, p. 1070-1081.

The Rockford Tin District, Alabama Piedmont:  
A Result of Na-Metasomatism Associated with  
Trondhjemitic Alteration of the Rockford Granite?

David J. Wesolowski  
Chemistry Division  
Oak Ridge National Laboratory  
P.O. Box 2008  
Oak Ridge, TN 37831-6110

and

Mark S. Drummond  
Department of Geology  
University of Alabama at Birmingham  
Birmingham, AL 35294

### Abstract

The abundant trondhjemites of the Rockford Granite suite of the Alabama Piedmont are shown to be the result of extensive exchange of normal subsolidus potassic granites with circulating metamorphic fluids which originated in metapelites of the Wedowee Group. The unaltered granites are not highly differentiated and are not enriched in Sn, Li, F or Rb. However, a number of Sn-Ta deposits are associated with the Rockford Granite, consisting of albitized Ta-Sn pegmatites and quartz-muscovite-cassiterite veins. A number of the metals concentrated in the ores are shown to have been leached from the granites during Na-metasomatism. Also, the alteration mineralogy of the granitoids is similar to that observed in the ores. It is suggested that the Sn-Ta mineralization in this district is a result of metamorphic fluid flow rather than magmatic-hydrothermal processes.

### Introduction

Significant tin and tantalum mineralization occurs in a narrow belt within the outcrop area of the Wedowee Group of the northern Alabama Piedmont (Fig. 1). The "Alabama Tin Belt" (Hunter, 1944) or Rockford Tin District has been the focus of recent exploration and drilling by the Callahan Mining Corporation, as discussed by Cook et al. (1987) and Foord and Cook (1989). These authors document intense Na-metasomatism associated with mineralization in the McAllister Ta-Sn deposit, the major ore body in the district (No. 2 in Fig. 1). Albitization is also an important feature of Ta-Sn mineralization in the Two-Bit Pegmatite (No. 1 in Fig. 1) as noted by Tompa (1987). In addition to these pegmatitic ores, numerous quartz-muscovite(+/-tourmaline)-cassiterite veins throughout the district contain a sodium-rich (8-9% paragonite

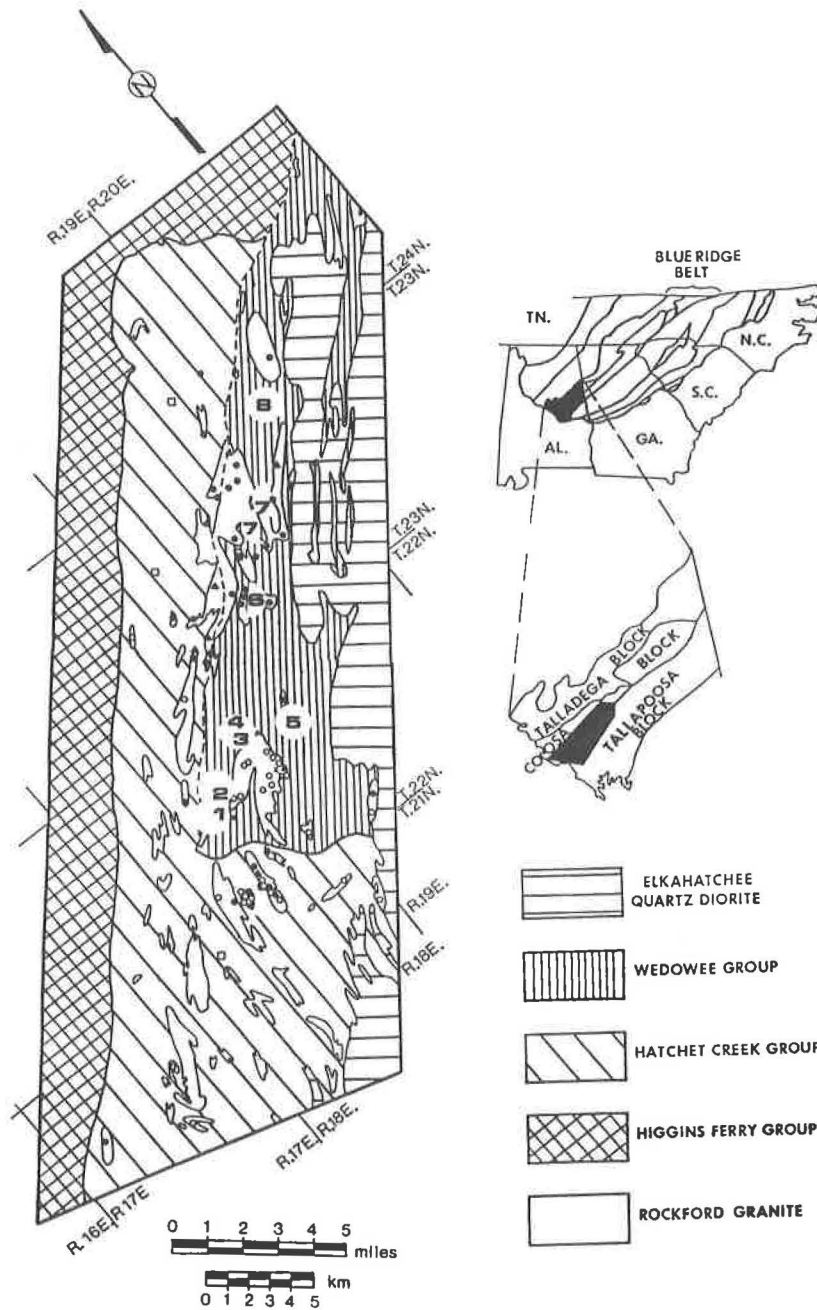


Figure 1. Geologic map of the Rockford District showing the locations of granites (○), granodiorites (x), trondhjemites (●) and transitional granitoids (▲) of the Rockford Granite. Sn and Ta-Sn deposits are numbered and categorized as follows: (1) Two-bit deposit = zoned, complex pegmatite; (2) McAllister deposit = complex pegmatite - albite aplite greisen; (3) Annie Mitchell deposit = quartz-muscovite veins and tourmalinized Wedowee phyllite; (4) County Land deposit = complex pegmatite - aplite; (5) Millsite deposit = pegmatite and quartz-muscovite veins; (6) S-1400 deposit = pegmatite and quartz veins; (7) Manning's Store deposit = quartz-muscovite veins and tourmalinized Wedowee phyllite; and (8) Worthy prospect = pegmatite and quartz-muscovite veins.

component, Foord and Cook, 1989), Li-F-poor muscovite distinctly different from the Li-F-rich mica common in normal Sn greisens.

For several years, the authors have been studying the origins of the Rockford Granite and the post-magmatic processes which have affected it (Drummond, 1986; Drummond et al., 1986, 1988; Wesolowski et al., 1987). These studies have clearly demonstrated that the origin of the trondhjemites of the Rockford District (Fig. 1) was via subsolidus alteration of normal Rockford Granite by Na-rich metasomatic fluids which originated in the host metasediments and infiltrated the intrusives as a result of either directed tectonic stress and/or advective circulation driven by the heat of the cooling intrusives.

Na-metasomatism or "albitization", characterized by replacement of K-feldspar by albite, is a ubiquitous feature of Sn-Ta pegmatite deposits and a very common feature of the granites associated with tin greisens and other types of rare-metal mineralization (Ginzburg, 1956; Serebryakov, 1961; Kinnaird, 1984; Manning and Pichavant, 1988; Taylor, 1979). Traditionally, alteration of this type has been ascribed to reactions between the crystallized upper portions of the source-granite and a magmatic volatile phase separating from a water-saturated melt in the deeper portions of the system (so-called "autometasomatism"). However, the strong evidence for sodic alteration of the Rockford Granite by circulating metamorphic fluids, the trace-element-depletion pattern of the altered intrusives and the position of the major Sn-Ta deposits at the granite-trondhjemite transition in the Rockford District, all suggest a possible metamorphic-fluid origin for the Sn-Ta ores. This paper discusses this hypothesis and offers further supporting arguments.

### Text

Individual plutons of the Rockford Granite suite exhibit a gradational range in Na/K ratios traversing the granite to trondhjemite classifications (Drummond et al., 1986). Even within individual plutons, zones of "granite" and "trondhjemite" (*sensu stricto*) occur and these have been shown to be controlled by the metamorphic fabric, with individual zones concordant with the foliation planes being trondhjemitic or granitic. Detailed petrography reveals that in the more sodic rocks, K-feldspar is extensively replaced by a very sodic oligoclase and biotite is intensely altered to paragonitic muscovite (Drummond et al., 1986). In fact, the paragonite content of this secondary muscovite (8-10 mole %) is similar to muscovite in late-stage "greisen-like pipes" in the McAllister deposit (Foord and Cook, 1989). Other mineralogic changes accompanying Na-metasomatism in the granites include introduction of secondary quartz and zircon

and alteration of primary apatite to Al-epidote.

When the trace element content of average trondhjemite is compared with that of average unaltered Rockford Granite, depletions and enrichments that can be sensibly related to the sodic metasomatism are observed (Figure 2). The breakdown of igneous biotite resulted in the loss of Sn, Li, F, and Fe. Replacement of K-feldspar by sodic-oligoclase ( $An_{14}$ ) resulted in addition of Sr and Na and loss of K, Rb and possibly Pb. Replacement of apatite by epidote is largely responsible for the depletion of P, U and Th in the altered rocks. The depletion in U, Th and K is so dramatic that, as shown by Drummond et al. (1986), zones of trondhjemitic alteration can easily be mapped in the field with the use of a gamma-ray-scintillometer.

The whole rock oxygen isotopic compositions of trondhjemites and granites of the Rockford district are plotted versus the atomic K/Na ratios in Figure 3. The trondhjemites show a linear relationship, with the  $^{18}O$  content increasing with sodium enrichment. The transitional granitoids appear to follow a similar trend, but at somewhat higher K/Na ratios, while the unaltered granitoids exhibit no correlation between these variables. Drummond et al. (1986) interpreted these data as indicating that in the trondhjemites and transitional granitoids, chemical and mineralogical alteration accompanied isotopic exchange with circulating metamorphic fluids, while only isotopic alteration occurred in the granitoids. Since it is obvious that the K/Na ratios in the intrusives are controlled by the degree of Na-metasomatism, it follows that the  $^{18}O$  contents of the intrusives also reflect fluid/rock interaction. If the metasomatic fluids were internally-generated by the crystallizing intrusions, then it would be logical to assume that the resulting "autometasomatism" would, in most cases, reflect declining temperatures from that of the solidus temperature. This would indeed result in a small enrichment in the  $^{18}O$  content of the rock because water in equilibrium with the major rock-forming silicates (quartz, feldspars, micas) becomes increasingly depleted in  $^{18}O$  relative to the minerals with decreasing temperature. However, as shown in Figure 4, path C-D, fluids in equilibrium with K-feldspar and albite (sufficiently close to the  $An_{14}$  metasomatic feldspar for this argument) must cause potassic rather than sodic alteration upon cooling from a higher temperature. Conversely, prograde alteration, while causing sodium enrichment in the rocks, would have resulted in relative depletion in  $^{18}O$ . Thus, the trondhjemite trend in Figure 3 cannot have been generated by "autometasomatism". Wesolowski et al. (1987) concluded from these observations that the metasomatic fluid must have been externally derived.

A detailed examination of the stable carbon and oxygen isotope distributions in the intrusives and host metasediments

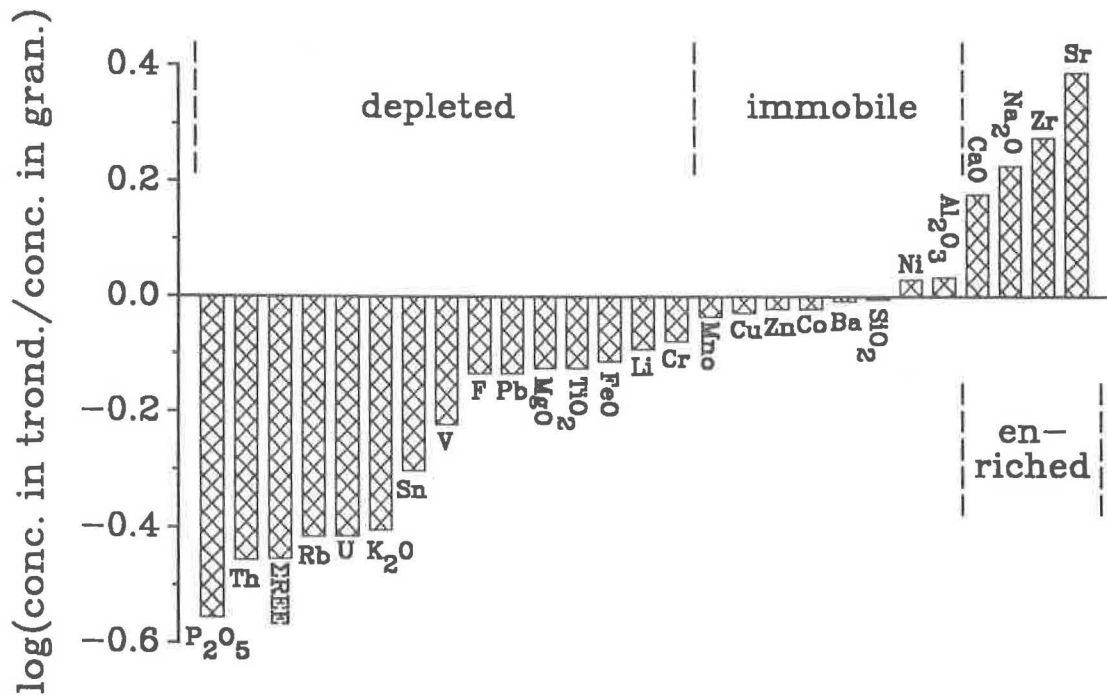


Figure 2. Log<sub>10</sub> of the elemental concentration ratios of average trondhjemite divided by average granite+granodiorite from the Rockford District.

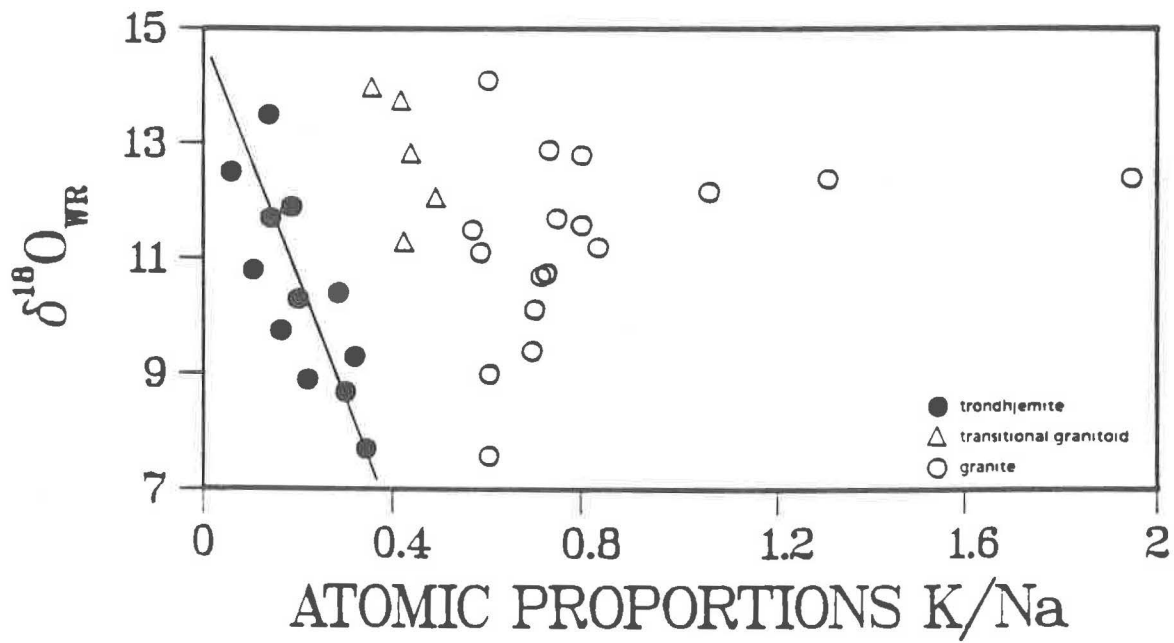


Figure 3. Whole rock oxygen isotope compositions of granitoids of the Rockford district (per mil values relative to SMOW) versus atomic K/Na ratios in the intrusives.

throughout the district demonstrated strong evidence for extensive exchange of the intrusives with a fluid either originating or having completely homogenized with the volumetrically-dominant metapelites of the Wedowee and Hatchet Creek Groups in the region. In fact, the distribution of trondhjemites and granites shown in Figure 1 reflects the chemistry of the host rocks. Trondhjemites are most abundant in the northeastern portion of the study area, where the metapelites of the Wedowee Group contain only one feldspar, sodic oligoclase. Granites are more abundant in the southwest, where the Hatchet Creek Group metapelites and metagraywackes commonly contain K-feldspar as well as plagioclase.

As can be surmised from Figure 4, metamorphic fluids equilibrated with a country rock containing only sodic plagioclase must destroy K-feldspar upon infiltrated granite, until the K/Na ratio in the fluids reaches a sufficient level for K-feldspar to be stable (paths A-D and A'-D defining isothermal and increasing temperature paths, respectively), while fluids entering granite from a two-feldspar country rock will only cause sodic alteration with rising temperatures (path B-D) as might be encountered if the fluid flow is advective.

The oxygen and carbon isotopic studies, in conjunction with petrogenetic modelling (Drummond et al., 1988), indicate that the intrusives had a primary  $\delta^{18}\text{O}$  content of 8-9 per mil. The  $^{18}\text{O}$  enrichment in normal potassic granite shown in Figure 3 is a result of exchange with metamorphic fluids whose K/Na ratio had either started out at equilibrium with the granite mineral assemblage, or reached chemical equilibrium sooner than isotopic equilibrium due to the differing cation and oxygen exchange capacities of the fluid depending on the starting fluid salinity and K/Na ratio. Oxygen and carbon (Wesolowski et al., 1987) isotopic distributions indicate pervasive metamorphic fluid infiltration throughout the district. Both chemically altered and unaltered intrusives experienced this fluid flow to some extent. However, it is clear from Figure 2, that only those fluids which caused chemical alteration (silicate decomposition) of the primary igneous minerals were effective in leaching metals, including Sn, Li, F, U and Th out of the intrusives.

The McAllister Ta-Sn deposit (Foord and Cook, 1989; Cook et al., 1987; Cook, 1986) exhibits a number of the features typical of mineralized zones in the Rockford District. The main body of the deposit is a quartz-alkali-feldspar pegmatite containing a small quartz core bordered by a zone of smoky quartz-alkali feldspar graphic intergrowths. This early, primary pegmatitic stage also contains significant quantities of spodumene, beryl, cassiterite, tapiolite and Fe-rich columbite ( $\text{Nb} > \text{Ta}$ ). This early stage is intensely altered and replaced by saccharoidal albite. Similar albitization is also

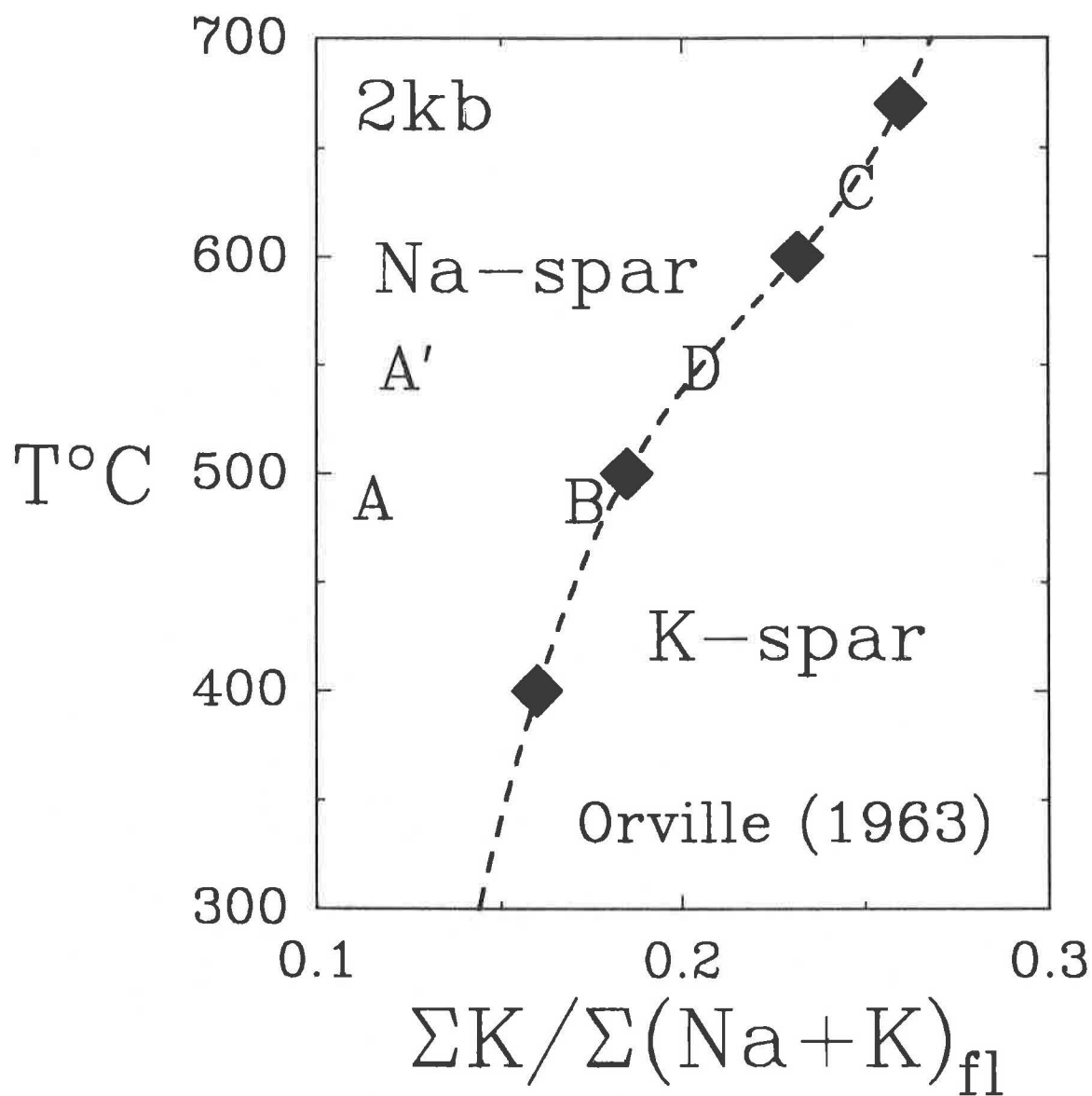


Figure 4. Plot of the molal total K/(Na+K) ratios of chloride brines in equilibrium with albite and K-feldspar at 2 kb (Orville, 1963). The points A-D are discussed in the text.

reported from the Two-Bit pegmatite (Tompa, 1987). Although the relationships are not completely described by Foord and Cook (1989), it appears that columbite-tantalite, Ta-Nb-rich cassiterite and zircon developed during this stage. Finally, "pipes" of quartz+paragonitic muscovite replaced these earlier assemblages. The major economic mineralization, consisting of Mn-Sn-rich wodginite and uranmicrolite, was deposited during this stage. Abundant zircon and rare topaz are intergrown with wodginite and uranmicrolite. No cassiterite was noted from the quartz-muscovite pipes. Other Sn and Sn-Ta deposits of the Rockford District consist of a.) cassiterite-bearing, albitized pegmatites similar to the first two stages of the McAllister deposit; b.) quartz-muscovite veins similar to McAllister stage three, but containing cassiterite; and c.) simple quartz-cassiterite veins. A common feature of other deposits in the district not present in the McAllister deposit is extensive veining and replacement of host rocks by tourmaline. However, Sn mineralization has not been directly linked to boron metasomatism. Throughout the district, mineralization occurs associated with pegmatites in granitoid intrusions and in the Wedowee metasediments and in quartz-muscovite veins in the metasediments.

It is interesting to compare the element trends in the mineralized zones with the Na-metasomatism of the trondhjemites. The ores and their nearby host rocks are enriched in Sn, Li, F, U (Foord and Cook, 1989) and Rb (Dean and Cook, 1987). As shown in Figure 2, these elements were removed from the granites during Na-metasomatism. The ores exhibit strong development of albitization, paragonitic muscovite and secondary zircon, also common features of the trondhjemites. Thus, the chemistry of the metamorphic fluids responsible for Na-metasomatism of the granites was ideal for the formation of ores like those which occur in the district. This is in stark contrast to the chemistry of the unaltered intrusives themselves. Table 1 compares the major and trace element compositions of average unaltered Rockford Granite with specialized granites typically associated with rare-metal mineralization. Note in particular the elevated CaO, MgO and K/Rb and the low contents of SiO<sub>2</sub>, Sn, Li, Rb and F relative to typical rare-metal granites. The low differentiation index of the granites (80-84, Foord and Cook, 1989) and the lack of any trend in Sn vs SiO<sub>2</sub> (Fig. 5) are also atypical of fertile granites associated with rare-metal mineralization.

Taken as whole, the evidence presented above suggests that the Sn-Ta mineralization in the Rockford District may have formed as a result of interaction of the two-feldspar+biotite granites (and the host metasediments) with a regional, Na-rich metamorphic fluid. The unspecialized nature of the Rockford Granite and the lack of abundant Li- and F-rich assemblages in the ores argues against a primary magmatic or autometamorphic origin for the mineralization. The early pegmatitic stage, containing minor spodumene, cassiterite and

Table 1. Comparison of major and trace element compositions of Rockford Granite (unaltered), average Granite and various specialized tin granites.

	I	II	III	IV	V	VI
(wgt %)						
SiO <sub>2</sub>	71.99	71.30	73.38	71.30	74.45	75.49
TiO <sub>2</sub>	0.24	0.31	0.16	0.34	0.07	0.11
Al <sub>2</sub> O <sub>3</sub>	14.73	14.32	13.97	14.80	14.06	13.20
FeO	1.61	2.73	1.82	2.05	1.00	1.59
MnO	0.04	0.05	0.05	0.06	0.03	0.02
MgO	0.48	0.71	0.47	0.48	0.10	0.19
CaO	1.29	1.84	0.75	1.05	0.51	0.85
Na <sub>2</sub> O	3.33	3.68	3.20	3.20	4.11	3.23
K <sub>2</sub> O	3.79	4.07	4.69	5.15	4.32	4.91
P <sub>2</sub> O <sub>5</sub>	0.18	0.12		0.26	0.26	0.04
LOI	1.79	0.82		0.63	0.84	0.73
Total	99.47	100.07	98.49	99.32	99.75	100.36
(ppm)						
Sn	6	3	40	23	44	49
Li	100	30	400	400	324	628
Rb	190	150	580	455	760	699
F	240	800	3700	2400	4000	4100
K/Rb	166	>100	<100	94	47	58

- I. Unaltered Rockford Granite (average of 20 analyses).  
 II. Average granite (major elements - LaMaitre, 1976; Sn, Li, Rb - Taylor, 1965; F - Bailey, 1977; K/Rb - Tischendorf, 1977).  
 III. Average specialized tin granite (Tischendorf, 1977).  
 IV. Cornwall biotite granite (Manning and Pichavant, 1988).  
 V. South Mountain Batholith tin granite (Clarke and Chatterjee, 1988).  
 VI. Average of ten tin granites in Sumatra, Indonesia (Clarke and Stephens, 1987).

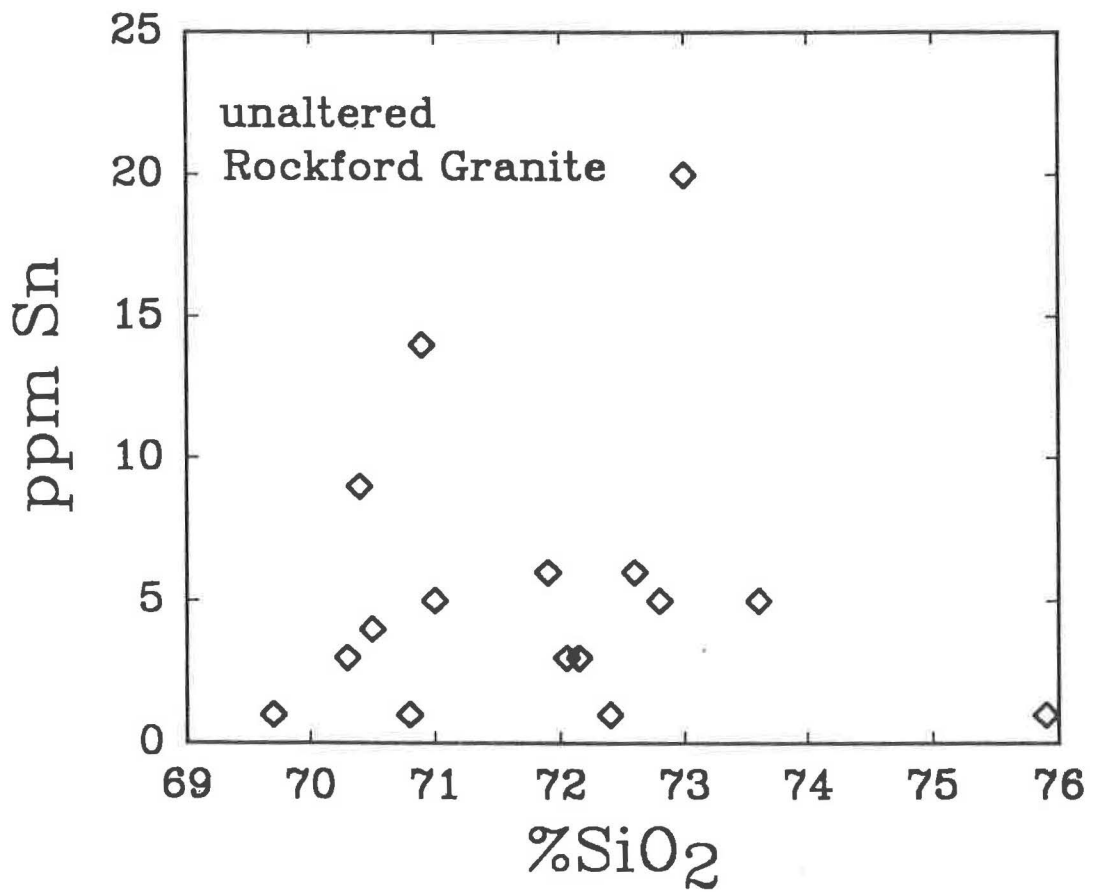


Figure 5. Parts per million tin versus weight percent SiO<sub>2</sub> in unaltered Rockford Granite.

columbite may have formed as a late-stage differentiate of the crystallizing granites, but the lack of zoning and differentiation in the intrusives does not lend convincing support for this scenario. The pegmatites could equally as well have formed via localized partial melting of granite and metasediments as a response to infiltration of a metamorphic fluid enriched in Li, F and B as a result of Na-metasomatism of the granites and two-feldspar metasediments. The presence of high levels of Li, B and F in the metasomatic fluid exiting the altered granites could have facilitated anatexis in the metasediments at temperatures as low as 500-550°C, since these components drastically lower the minimum melting conditions (650°C at P = 5b, water saturated, Luth et al., 1964) of granitic melts (Manning, 1981; Pichavant, 1981; Martin, 1983).

Regardless of the origin of the primary pegmatitic phase, the style of metasomatic alteration of the ores, which was responsible for the bulk of economic Sn-Ta mineralization, is identical to the alteration observed in the trondhjemites. Pichavant (1983) suggests, based on some very preliminary data, that Na-metasomatism can occur in autometasomatic settings as a result of mixing of, presumably magmatically derived, but physically separated, chloride- and boron-rich brines. While tourmaline is common in many of the Rockford ores, no tourmaline is observed in the trondhjemites. A much simpler explanation for sodic alteration is reaction with a fluid which has equilibrated with a sodic host rock, such as the Wedowee metapelites. As shown in Figure 6, a fluid in equilibrium with K-spar and albite at 600°C (point A) must induce potassic alteration upon cooling, resulting in replacement of albite by K-spar. Conversely, a fluid enriched in sodium due to interaction with a sodic host rock will, upon entering a two-feldspar assemblage, replace K-spar with albite. If this fluid (point B in Figure 6) cools sufficiently before reaching the K-spar stability field, muscovite will replace both albite and k-spar. Because of the sodic nature of the fluid, this muscovite will be paragonitic. This second scenario is precisely that observed in both the ores and granitoids in the Rockford District.

A simple mass-balance calculation demonstrates that, at least in the case of tin, the amount of metal removed from granite during formation of trondhjemite is more than sufficient to account for all known Sn deposits of the Rockford District. The outcrop area of trondhjemites is approximately 22 km<sup>2</sup>. Assuming an average thickness of 1 km for each pluton and a density of 2.72 g/cc, this gives 6X10<sup>13</sup> kg of altered material. Average trondhjemite is depleted in Sn by 3 ppm relative to average granite (6 ppm, Table 1), giving 200,000 short tons of Sn removed from the granites during Na-metasomatism. Since all known ore bodies represent a total of less than 300 tons of contained Sn, the amount potentially leached from the granites by metamorphic fluid/rock interactions is nearly 3 orders of magnitude

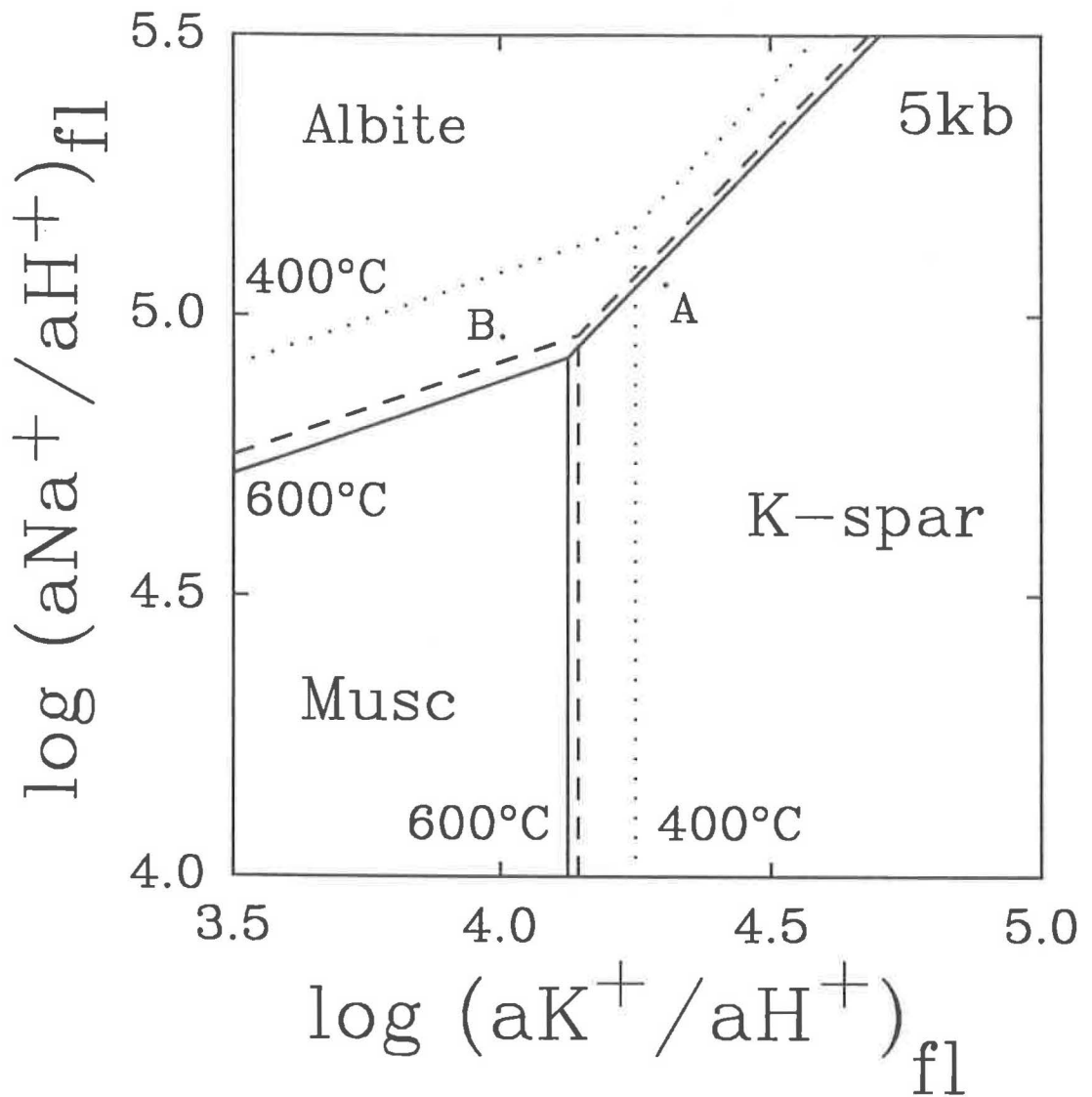


Figure 6. Activity ratios of fluids in equilibrium with K-spar, muscovite, albite and quartz at 600 (solid lines), 500 (dashed lines) and 400°C (dotted lines). The sources of data and the significance of points A and B are discussed in the text.

greater than in all known ores.

Our model for the formation of pegmatites and Sn-Ta mineralization in the Rockford District is depicted in Figure 7. The granites of the Rockford Granite formed by partial melting of metagraywackes of the Hatchet Creek Group and diapirically rose into the Wedowee metapelites during prograde metamorphism (Drummond et al., 1988). Contemporaneous regional metamorphism plus heat from the rising granite-metasediment diapir induced dehydration in the sodic metapelites of the Wedowee Group. The aqueous fluid generated from this process was constrained to flow along planes of foliation parallel to  $\sigma_3$  in a southwesterly direction. Granites and two-feldspar metasediments encountered by this fluid were pervasively altered to sodic assemblages. Destruction of biotite and apatite in the rocks caused enrichment of the fluids in Sn, Li, F, U and probably Nb and Ta. A 1-2 km thick horizon in the Wedowee Group parallel to foliation and  $\sigma_3$  (shaded in Figure 7) was particularly permeable and/or reactive and numerous pegmatites and metasomatic mineralizations occurred along this horizon, the surface outcrop of which constitutes the Alabama Tin Belt as it is known today.

Metamorphic fluid pathways can be traced by synmetamorphic quartz veins in the Rockford District which commonly parallel the  $S_1/S_2$  fabric in the host metasediments. Tourmalinization of Wedowee Group graphitic metapelites occurs adjacent to synmetamorphic quartz-graphite veins (Drummond, 1986), producing tourmaline-rich (20 volume % tourmaline) muscovite schists that are very similar to those described by Galbreath et al. (1988). The source of the B is interpreted to have either resided in protolithic clays (Eugster and Wright, 1960), or in graphite (Douthitt, 1985) and may have been released into solution during metamorphic devolatilization of the metapelites.

Detailed modelling of the chemical evolution of the ore fluids resulting in Sn-Ta mineralization is not the intent of this paper. However, a few broad observations can be made. We know that peak metamorphic conditions of 5 kb and 583-674°C were reached during formation of the granites (Drummond et al., 1988). Temperatures calculated from both chemical and oxygen isotope distributions in the metasomatized trondhjemites cluster around 535°C at 5 kb (Drummond et al., 1988), clearly demonstrating the retrograde nature of the metasomatic event. Abundant saccharoidal albite and quartz-muscovite development in the ore zones suggests temperatures in the 500-400°C range, although no direct geochemical data are available to determine reliable P-T conditions for mineralization. It is unlikely that major, abrupt pressure changes occurred in this deeply-buried sequence during retrograde mineralization. Likewise, significant changes in pH of the fluids were also unlikely, due to the buffering of

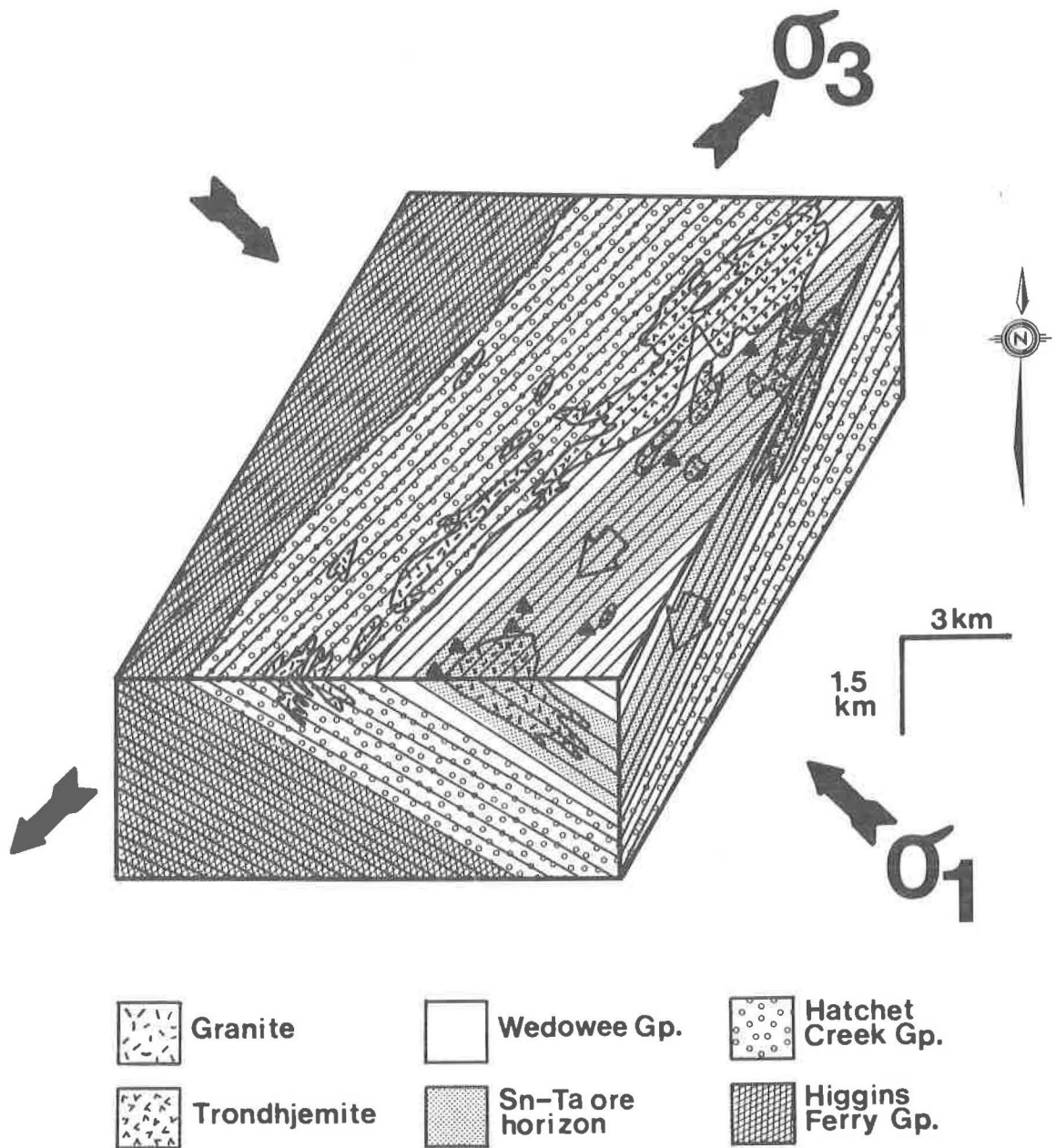


Figure 7. Block diagram showing geologic and ore deposit ( $\Delta$ ) relationships in the Rockford District. On this conceptual model, the arrows in the Sn-Ta ore horizon indicate the metasomatic fluid path relative to the maximum ( $\sigma_1$ ) and minimum ( $\sigma_2$ ) principal stress directions during prograde regional metamorphism.

fluids by rather similar silicate assemblages in all rock types present in the district and the absence of mafics or carbonates. Even abrupt temperature changes were unlikely. However, at least in the case of cassiterite, only minor temperature changes are needed to cause mineralization under these conditions. Figure 8 is a plot of the solubility of cassiterite in an aqueous fluid in equilibrium with graphite, K-feldspar, albite, quartz and muscovite and containing 2 molal total chloride. Data were taken from Wilson (1986) for cassiterite solubility, Bowers et al. (1984) for the silicates, Ohmoto and Kerrick (1977) for the oxygen fugacity of a fluid in equilibrium with graphite at  $f_{CO_2}=f_{CH_4}$ , (Drummond, 1986) and Montoya and Hemley (1975) for the dissociation constants of NaCl, KCl and HCl. Data were available for cassiterite solubility only at 1.5 kb, but the general trends are expected to remain the same at higher pressures. As can be seen, at 535°C, the metasomatic fluid would have been an efficient scavenger of tin released from biotite, while in the 500-400°C range, temperature drops of only a few tens of degrees would have been sufficient to deposit as much as 90% of the Sn contained in the fluid. Unfortunately no data are available at this time for evaluating the solubilities of the complex Nb-Ta-Sn oxides also abundant in the ores.

### Conclusions

The sodic metasomatism of the granites of the Rockford district cannot be easily explained by any process other than exchange of the subsolidus intrusives with a circulating regional metamorphic aqueous fluid. The unaltered granites are in no way typical of the highly specialized granites associated with rare-metal mineralization elsewhere in the world. The major and trace element trends in the metasomatized granites reflect a sympathetic relationship with the mineralized pegmatites and veins. The metasomatic alteration associated with these ores is similar to that observed in the trondhjemites of the district, and the trace metals known to have been mobilized from the granites are precisely those concentrated in the ores. For these reasons, we suggest that the Sn-Ta ores of the Rockford district also formed as a result of regional metamorphic fluid flow. The deposits resulted from scavenging of Sn, Li and F (and probably Nb and Ta) from rocks undergoing extensive alteration of biotite to muscovite. Mineralization probably reflects cooling of the fluids from around 535°C to around 400°C.

Proof of this hypothesis requires much more detailed petrogenetic studies of the ores and pegmatites, coupled with extensive stable and radiogenic isotope and fluid inclusion studies. The dissimilarities between mineralization in the Rockford district and other rare-metal mineralizations worldwide, such as the unspecialized nature of the granites,

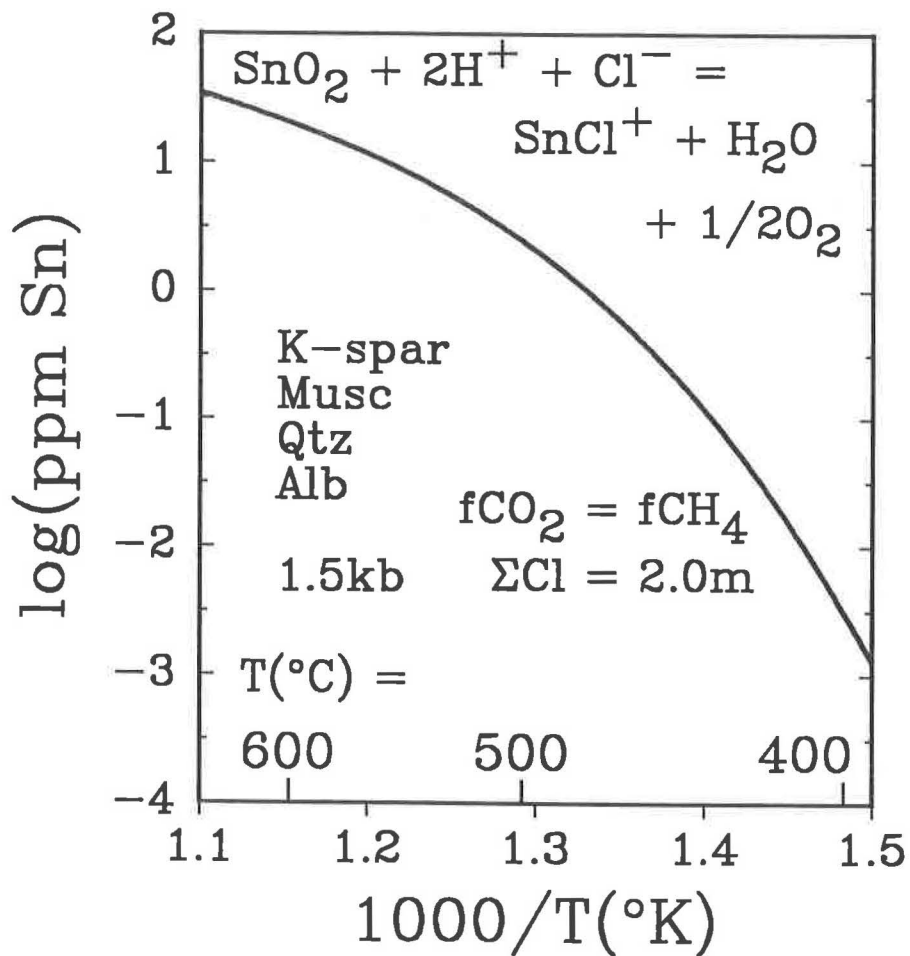


Figure 8. Solubility of cassiterite as a function of temperature in an aqueous fluid in equilibrium with graphite + K-spar + muscovite + albite + quartz at 1.5 kb fluid pressure,  $f\text{CO}_2 = f\text{CH}_4$ , total chloride = 2.0 molal. Sources of data are listed in the text.

the extensive regional sodic metasomatism and the lack of abundant Li-F assemblages in the ores suggest that the Rockford mineralization may be unique. However, if one considers that nearly all rare-metal mineralization associated with batholithic granites is typically confined to the apical portions, and often to small cupolas in the batholiths, it seems rather surprising that more widespread country rock-derived fluid involvement in ore formation and alteration has not been recognized. Certainly, externally-derived fluids play a prominent role in porphyry Cu and Mo and subvolcanic Sn-W-Mo ore systems. Recent work by Carten (1986) on the Yerington District in Nevada documents sodic alteration of the basal portions of an otherwise typical porphyry copper vein system. In addition, the hydrothermal fluids responsible for tin mineralization at Cornwall, England are suggested to be meteoric in origin (Alderton and Moore, 1981; Jackson et al., 1982; and Sams and Thomas-Betts, 1988). Steady state convection of meteoric fluids around the epizonal (1.5-4.0 km) Cornubian plutons (Sams and Thomas-Betts, 1988) may be a shallow level analogue of the deeper level (approx. 15 km) advective metamorphic fluid-granite interaction suggested here for the Rockford Tin District.

Certainly, subsolidus alteration of biotite as a possible source of tin and other metals has often been referred to in the literature of rare-metal systems (Hesp and Rigby, 1971; Jackson et al., 1982; Alderton and Moore, 1981). Perhaps the potential role of metamorphic fluids has simply been neglected due to the great depth and apparent host-rock impermeability in such systems. An interesting possibility is that, if alteration of biotite by high temperature fluids is the only key factor in the formation of rare-metal mineralization, then it seems evident that large portions of the cores of orogenic belts, metasediments and granitoids included, may be potential source rocks. Thus, one might search for deposits of this type (although perhaps not including the pegmatitic assemblages) in metamorphic terranes not directly associated with granitoids.

#### **Acknowledgements**

The authors would like to thank Eugene E. Foord for a very thorough and thoughtful review of this paper. This research was sponsored by a the U. S. Department of Energy, Division of Mathematics and Geosciences, Office of Basic Energy Sciences, grant no. DEAC05-84OR21400 to Martin Marietta Energy Systems and a University of Alabama at Birmingham Faculty Research Grant.

## References

- Alderton, D. H. M. and Moore, F. (1981), New determination of tin and tungsten in granites from south-west England, *Mineralogical Magazine*, v. 44, p. 354-356.
- Bailey, J. C. (1977), Fluorine in granitic rocks and melts: A review, *Chemical Geology*, v. 19, p. 1-42.
- Bowers, T.S., Jackson, K.J. and Helgeson, H.C. (1984), "Equilibrium Activity Diagrams", Springer-Verlag, New York, 397 p.
- Carten, R. B. (1986), Sodium-calcium metasomatism: Chemical, temporal, and spatial relationships at the Yerington, Nevada, porphyry copper deposit, *Economic Geology*, vol. 81, p. 1495-1519.
- Clarke, D. B. and Chatterjee, A. K. (1988), Physical and chemical processes in the South Mountain Batholith, in R. P. Taylor and D. F. Strong, eds., *Recent Advances in the Geology of Granite-Related Mineral Deposits*, Special Volume 39, The Canadian Institute of Mining and Metallurgy, p. 223-233.
- Clarke, M. C. J. and Beddoe-Stephens, B. (1987), Geochemistry, mineralogy and plate tectonic setting of a late Cretaceous Sn-W granite from Sumatra, Indonesia, *Mineralogical Magazine*, v. 51, p. 371-387.
- Cook, R. B. (1986), Li-Rb-Cs-Be distribution in the McAllister tin-tantalum deposit, *Geol. Soc. Amer. Abstr. w. Prog.*, v. 18, no. 6, p. 570.
- Cook, R. B., Dean, L. S. and Foord, E. E. (1987), Tin-tantalum mineralization associated with the Rockford Granites, Coosa County, Alabama, in M. S. Drummond and N. L. Green, eds., *Granites of Alabama*, Geological Survey of Alabama, p. 209-220.
- Dean, L. S. and Cook, R. B. (1987), Some geochemical aspects of tin mineralization related to granitic rocks of the northern Alabama Piedmont, in M. S. Drummond and N. L. Green, eds., *Granites of Alabama*, Geological Survey of Alabama, p. 209-220.
- Douthitt, C. B. (1985), Boron in graphite: Content, speciation, and significance, *Chemical Geology*, v. 53, p. 129-133.
- Drummond, M. S. (1986), Igneous, metamorphic, and structural history of the Alabama Tin Belt, Coosa County, Alabama, Ph.D. Thesis, Florida State University, 411 p.
- Drummond, M. S., Ragland, P. C., and Wesolowski, D. (1986), An example of trondhjemite genesis by means of alkali metasomatism: Rockford Granite, Alabama Appalachians; *Contrib. Mineral. Petrol.*, v. 93, p. 98-113.
- Drummond, M. S., Wesolowski, D. and Allison, D. T. (1988), Generation, diversification and emplacement of the Rockford Granite, Alabama Appalachians: Mineralogic, petrologic, isotopic (C&O), and P-T constraints; *Jour. Petrology*, v. 29, p. 869-897.

- Eugster, H. P. and Wright, T. L. (1960), Synthetic hydrous boron micas, U. S. Geological Survey, Professional Paper 400-B, p. 441-442.
- Foord, E. E. and Cook, R. B. (1989), Mineralogy and paragenesis of the McAllister Sn-Ta-bearing pegmatite, Coosa County, Alabama, *Canadian Mineralogist*, v. 27, p. 93-105.
- Galbreath, K. C., Duke, E. F., Papike, J. J. and Laul, J. C. (1988), Mass transfer during wall rock alteration: An example from a quartz-graphite vein, Black Hills, South Dakota, *Geochimica et Cosmochimica Acta*, v. 52, p. 1905-1918.
- Ginzburg, A.I. (1956), Certain features of geochemistry of tantalum and types of tantalum enrichment, *Geokhimiya*, English Translation, vol. 1956, no. 3, p. 312-325.
- Hesp, W. R. and Rigby, D. (1971), The transport of tin in acid igneous rocks, *Pacific Geology*, v. 5, p. 135-152.
- Hunter, F. R. (1944), Geology of the Alabama Tin Belt, Geological Survey of Alabama, Bulletin 54, 59 p.
- Jackson, N. J., Halliday, A. N., Sheppard, S. M. F. and Mitchell, J. G. (1982), Hydrothermal activity in the St. Just mining district, Cornwall, England, *in* A. M. Evans, ed., *Metallization Associated with Acid Magmatism*, New York, John Wiley and Sons, p. 137-179.
- Kinnaird, J.A. (1984), Contrasting styles of Sn-Nb-Ta-Zn mineralization in Nigeria, *Journal of African Earth Sciences*, vol. 2, no. 2, p. 81-90.
- LeMaitre, R. W. (1976), The chemical variability of some common igneous rocks, *Journal of Petrology*, v. 17, p. 589-637.
- Luth, W. C., Jahns, R. H. and Tuttle, O. F. (1964), The granite system at pressures of 4 to 10 kilobars, *Journal of Geophysical Research*, v. 69, p. 759-773.
- Manning, D. A. C. (1981), The effect of fluorine on the liquidus phase relationships in the system Qz-Ab-Or with excess water at 1 kbar, *Contributions to Mineralogy and Petrology*, v. 75, p. 257-262.
- Manning, D.A.C. and Pichavant, M. (1988), Volatiles and their bearing on the behavior of metals in granitic systems, *in* R.P. Taylor and D.F. Strong, ed.s, *Recent Advances in the Geology of Granite-Related Mineral Deposits*, Special Volume 39, The Canadian Institute of Mining and Metallurgy, p. 13-24.
- Martin, J. S. (1983), An experimental study of the effects of lithium on the granite system, *Proceedings of the Ussher Society*, v. 5, p. 417-420.
- Montoya, J.W., and Hemley, J.J. (1975), Activity relations and stabilities in alkali feldspar and mica alteration reactions, *Economic Geology*, vol. 70, p. 577-583.
- Ohmoto, H. and Kerrick, D.M. (1977), Devolatilization equilibria in graphitic systems, *American Journal of Science*, vol. 277, p. 1013-1044.

- Orville, P.M. (1963), Alkali ion exchange between vapor and feldspar phases, *American Journal of Science*, vol. 261, p. 210-237.
- Pichavant, M. (1981), An experimental study of the effect of boron on a water-saturated haplogranite at 1 kbar pressure: *Geological Applications, Contributions to Mineralogy and Petrology*, v. 76, p. 430-439.
- Pichavant, M. (1983), (Na,K) exchange between alkali feldspars and aqueous solutions containing borate and fluoride ions; experimental results at P = 1kbar: 3rd NATO Advanced Study Institute on feldspars, feldspathoids and their paragenesis. Rennes, France, p. 102.
- Sams, M. S. and Thomas-Betts, A. (1988), Models of convective fluid flow and mineralization in south-west England, *Journal of the Geological Society of London*, v. 145, p. 809-817.
- Serebryakov, V. A. (1961), Autometasomatic alteration of granitoids and association of tin mineralization with the zone of sodium-potassium metasomatism, *International Geology Review*, v. 3, p. 100-113.
- Taylor, R. G. (1979), *Geology of Tin Deposits*, Elsevier, New York, 543 p.
- Taylor, S. R. (1965), The application of trace element data to problems in petrology, *in* L. H. Ahrens, F. Press, S. K. Runkorn and H. C. Vrey, eds., *Physics and Chemistry of the Earth*, New York, Pergamon Press, 510 p.
- Tischendorf, G. (1977), Geochemical and petrographic characteristics of silicic magmatic rocks associated with rare-element mineralization, *in* M. Stempok, L. Burnoli and G. Tischendorf, eds., *Metallization Associated with Acid Magmatism*, Prague, Geological Survey, p. 41-96.
- Tompa, B. (1987), Stop 11 - Two Bit Pegmatite, *in* M.S. Drummond et al., eds., *The Granites of Alabama*, Alabama Geological Survey, 24th Annual Field Trip Guidebook, p. 41-43.
- Wesolowski, D., Drummond, M. S., and Gomolka, J. (1987), Oxygen and carbon isotope distributions in granitoids and metasediments of the Rockford District and adjacent portions of the northern Alabama Piedmont and Inner Piedmont; *in* M. S. Drummond and N. L. Green (eds.), *Granites of Alabama*, Geological Survey of Alabama, Special Publication, p. 221-238.
- Wilson, G. A. (1986), Cassiterite solubility and metal chloride speciation in supercritical solutions, Ph.D. Thesis, The Johns Hopkins University, 158 p.

Polymetallic Sulfide/Fluorspar Mineralization  
in Western Kentucky: Lead and Zinc Reserves  
for the 21st Century

Ed L. Schrader, D. E. Gann, A. D. Bishop;  
Departments of Geology and Chemistry,  
Millsaps College  
Jackson, MS 39210

ABSTRACT

Fluorspar and galena mining began near Paducah, Kentucky around 1835. Data from recent programs of field mapping, core drilling, mine development, core analyses and test flotation runs are included in this report.

Modes of ore mineralization in the district are: 1) bedded, replacement bodies of fluorspar and calcite in Mississippian aged carbonates; and, 2) veins of fluorspar, calcite, quartz and sulfides within the gouge zones of steeply dipping normal faults. Within the Mississippian sequence, fault-hosted ore "blossoms out" into the country rock and ranges from 20% to 60%  $\text{CaF}_2$  and 3.0% to 6.0% total metals. In four major fault zones, 2,200,000+ tons of reserves ranging from 2.4% to 4.2% Zinc and trace amounts to 1.5% lead were discovered. Vein ore averages about 37%  $\text{CaF}_2$ . With over 10 miles of additional fault trends to be explored, increased reserves are expected. Bedded deposits are restricted to calcite+fluorspar beds, suggesting vertical zonation in the ascending fluids. The bedded sphalerite is not fully delineated, but over 350,000 tons of ore grading 14% Zinc were identified.

Polished section and elemental analyses of the ore indicates low temperature deposition of sulfides with few exotic phases or precious metals. Paragenesis is indicated as: Calcite → Early Fluorspar → Quartz → Sphalerite → Galena → late Fluorspar. Plant tests indicate a 99% sulfide concentrate can be obtained using flotation methods. At 14 tons per hour feed, 35%  $\text{CaF}_2$  and 3% Zn grades, annual production of 32,000+ tons of 97%  $\text{CaF}_2$  and 3,800+ tons of Zinc concentrate is realized. At 20 tons per hour, 46,000 tons of  $\text{CaF}_2$  and 5400+ tons per hour feed results in 17,900+ tons of  $\text{ZnS}_2$  per year. Use of these resources to augment imported  $\text{CaF}_2$  and Zinc appears strategically favorable.

## INTRODUCTION

For many years a sporadic production of high grade fluorite (fluorspar) filtercake concentrate and metallurgical gravel kept the Kentucky Fluorspar District alive in an internationally competitive marketplace. Often, higher grade Zinc ores were considered undesirable since they prohibited "log washing" of gravel ores for metallurgical fluorspar markets and created complications in basic flotation processes. However, several now defunct mines recovered as by-product or major product substantial amounts of Zinc concentrates over the last 100 years. Ozark-Mahoning in Illinois still produces Zinc concentrate.

With the bullish Zinc market of the last 1980's we re-examined this district with the intent to consider Zinc as the major resource and fluorspar as the gangue or, possibly by-product. It is the purpose of this paper to demonstrate:

- 1) The probability of remaining Zinc resources in the district.
- 2) The technical feasibility of Zinc flotation in converted fluorspar mills, and,
- 3) The economic parameters affecting Zinc production.

## REVIEW OF MINING HISTORY AND GEOLOGIC SETTING OF MINERALIZATION

Fluorspar (fluorite) is naturally occurring calcium fluoride ( $\text{CaF}_2$ ) which is deposited along with sulfides as bedded replacements and vein fillings of the local limestone country rock of Mississippian age in the Kentucky Fluorspar District. Fluorspar and lead were known to the early settlers by 1812. Lead mining commenced in 1835 in Crittenden County, Kentucky. This early period of lead mining resulted in the identification of vein structures which later became the principal fluorspar producers. (Crittenden County Courthouse Records.)

Ore is generally located between 150 and 700 vertical feet of depth and occurs as coarse vein-filling crystals. It is mined by sinking shafts alongside the ore bodies and drifting out along the veins. Conventional stoping methods were employed. ZnS and PbS occur disseminated in veins with crystal sizes generally from 0.25 to 5 mm in diameter only.

The geological formations exposed in the Illinois-Kentucky Fluorspar District consist predominantly of limestone with interbedded sandstones and shales of Mississippian age. (Figures 1 and 2.) (After Grogan and Bradbury, 1968). Within

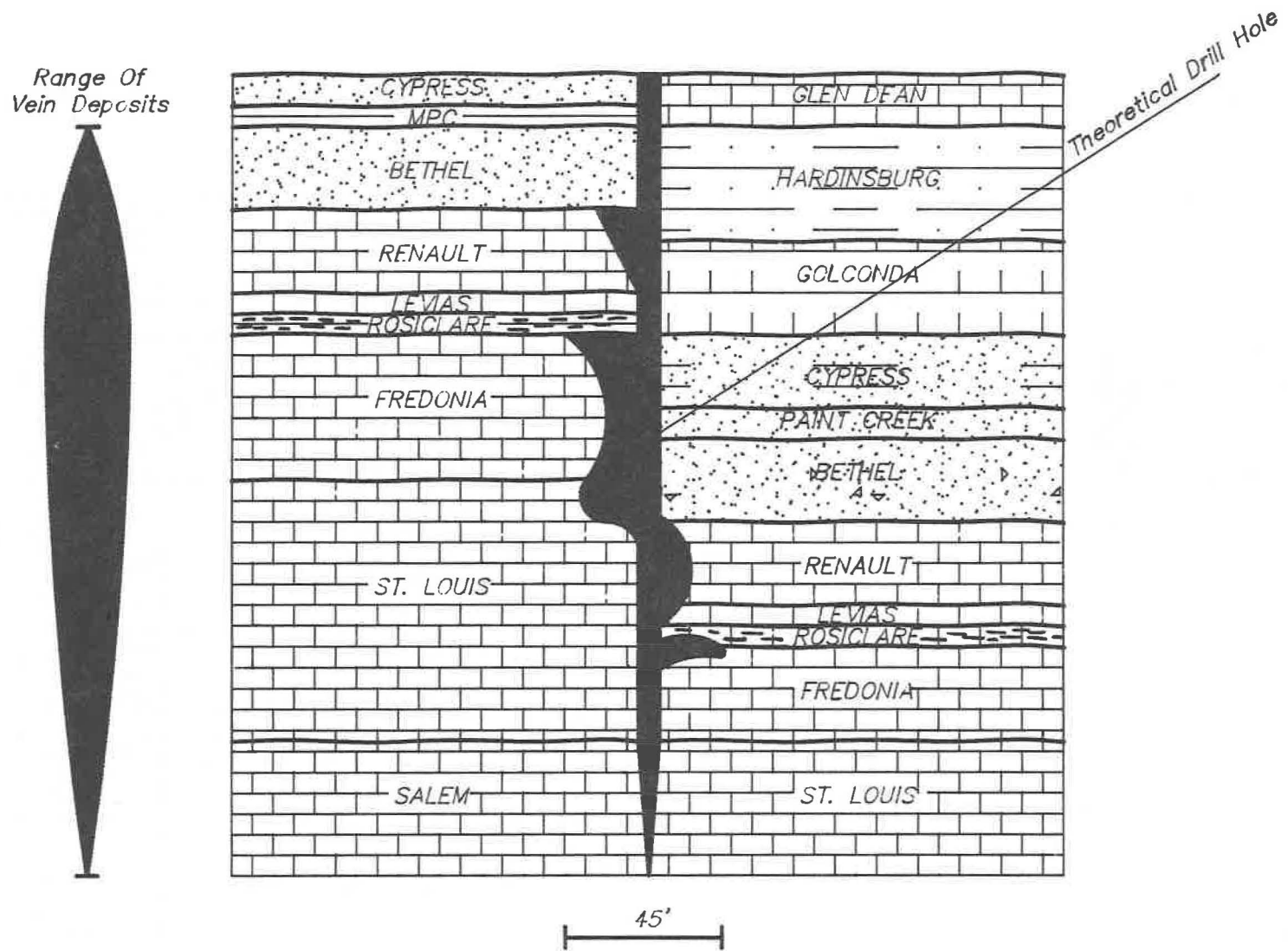


Figure 1. Typical cross-section of a mineralized fault zone through Mississippian strata.

SYS.	FORMATION	MEMBER	Lithologic Description	Range Of Deposits		
				Veins	Bedded	
PENNSYLVANIAN			Sandstone, Shale, Thin Coals			
MISSISSIPPIAN	Kinkaid		Grey Cherty Limestone, Shale			
	Degonia		Shale And Thin Bedded Sandstone			
	Clore		Shale, Limestone, Thin Bedded Sandstone			
	Palestine		Sandstone, Silty Shale			
	Menard		Fine-Grained Limestone, Shale			
	Waltersburg		Shale, Shaly Limestone			
	Vienna		Limestone Shaly Limestone			
	Tar Springs		Sandstone, Shale, Thin Coal			
	Glen Dean		Fossiliferous, Partly Oolitic Limestone, Shale			
	Hardinsburg		Shale, Sandstone			
	Haney		Fossiliferous Limestone, Lime			
	Fralleys		Shale, Thin Limestone			
	Beech Creek		Silty Limestone			
	Cypress		Sandstone, Shale			
	Ridenhower		Shale, Sandy Sandstone			
	Bethel		Sandstone			
	Downey Bif.		Crinoidal, Locally Oolitic Limestone			
	Yankeetown		Shale, Siltstone			
	Renault	Sheltonville				Limestone, Shale
		Levias				Calcareous Sandstone Shale At Base
	AuxVases	Rosiclare				Calcareous Sandstone Shale At Base
	St. Genevieve	Spar Mtn.				Light Colored, Largely Oolitic Limestone, Sandstone Lenses
	St. Louis					Fine Grained, Cherty Limestone
Salem			Dark-Colored Limestone, Foraminiferal Calcarenite			
Ullin			Crinoidal, Bryozoan, Dark-Grey, Fine-Grained Limestone			
Fort Payne			Siltstone, Silty, Cherty Limestone			
Pre-Mississippian			Carbonates and Clastics			

Figure 2. Stratigraphic column of veined formations and range of deposits.

the fluorspar district these sediments are complexly broken by a series of steeply dipping to vertical gravity faults which trend northeast and divide the area into a series of elongated northeast horsts and grabens. Most of the faults are normal and dip 75° to vertical. (Figure 3.)

Vein mineralization occurs in a specific paragenetic sequence depicted on Figure 4. Sphalerite and galena crystals are large, only rarely intergrown, and display mutual surface boundaries with each other as well as the fluorite and gangue. Consequently, milling to liberation size is simple and efficient with liberation coming to about 95% at 80% below 100 mesh. Figures 5 and 6 display typical vein filling textures and sulfide morphologies.

Chemical analyses of selected sulfide crystals and assays of concentrates indicate relatively pure sphalerite and galena with Cu strongly partitioned into sphalerite and Ag partitioned into the galena. (Table I). Samples of galena and sphalerite from the Midway and Babb ores were analyzed with analyses performed on hand-sorted, acid-leached crystals, digested in nitric acid. The resulting solutions were examined by means of atomic absorption spectrophotometry.

A rise in steel production during World War I promoted the development of the Fluorspar deposits. Added demand created by the growth of the aluminum and fluorine chemical industries, coupled with World War II requirements, brought about a period of intense exploration and mine expansion. In the period from 1880 to 1953 the district shipped 6.8 million tons of fluorspar supplying 80% of the total U.S. consumption. Metal production through 1979 was 350,000 tons Zinc and 95,000 tons lead. (U.S. Bureau of Mines Yearbook; and Baster et al., 1973, and Hepser, 1954.

The history of selected properties where mining has been carried out is summarized as follows: (note: Data collated and reviewed by A.C.A. Howe Pty. Ltd.)

Big Four Mines - The La Rue Mine opened in 1874 and up to 1945 a total a 31,750 tons of fluorspar were produced. In 1945 the Woods shaft was sunk to 100 feet (30 m) and from 1945-47 a total of 16,500 tons of fluorspar were produced. In 1953 U.S. Steel corporation resumed operating but it was discontinued in 1954. Many small mines produced ore of undocumented amounts. All ore in this vein system is also Zinc-bearing with 0.5 to +5.00 Zinc.

Lafayette Mine - The main shaft was sunk to a depth of 800 feet (244 m). Workings from the lower level were via two drifts and four stopes producing +26,000 tons per year of 60% fluorspar. Over 1,000,000 tons of ore were removed with Zinc values of 3.0%. Zinc concentrates were recovered in the

Zn = MINES WHERE Zn HAS BEEN RECOVERED.

✕ — ✕ — ✕ — ✕ — ✕ MINE SITES AND MAJOR MINERALIZED FAULT ZONES

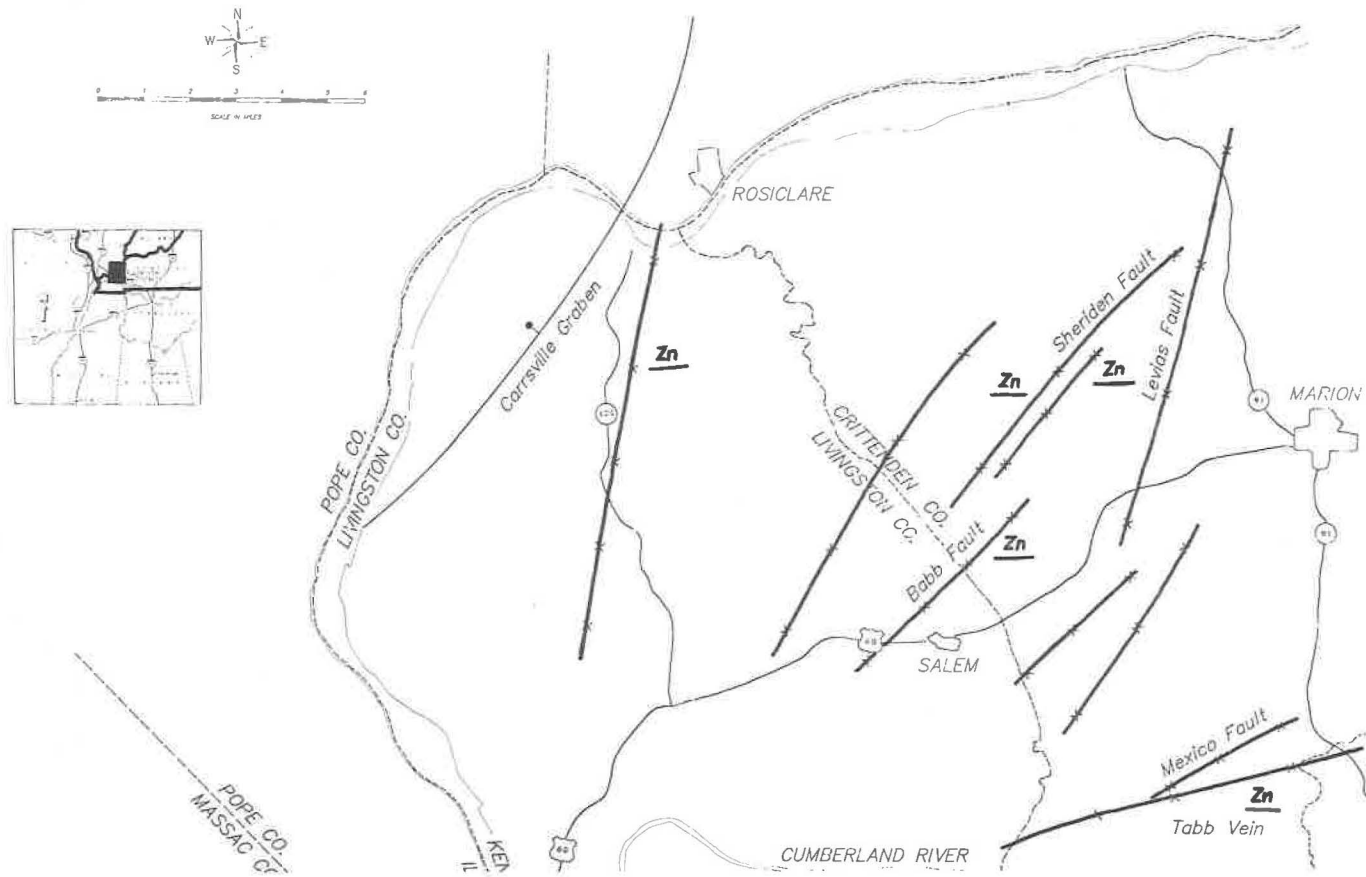


Figure 3. General location of ZnS mineralized fault zones in the Kentucky Fluorspar District.



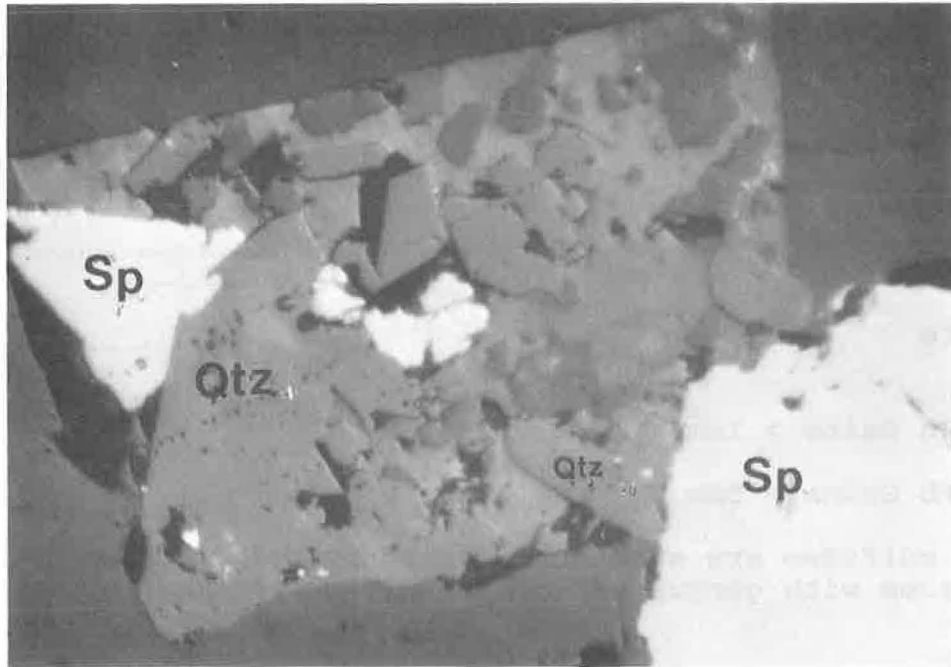


Figure 5. Sphalerite and euhedral quartz filling a "negative cubic" vug in fluorite. Photo taken at 160x.

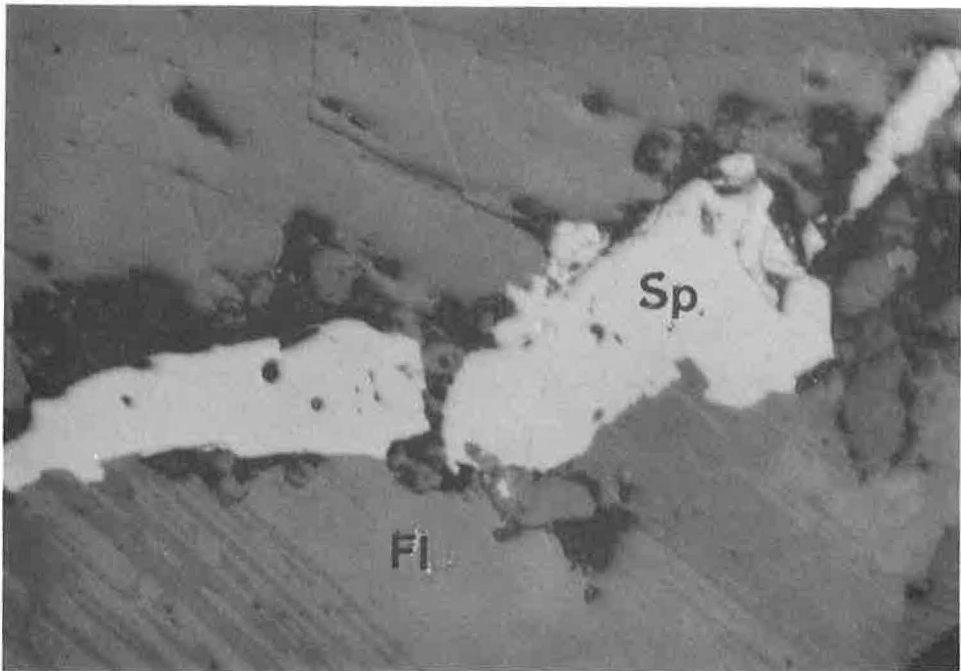


Figure 6. Sphalerite vein filling in fluorite matrix. Photo taken at 160x.

Table 1. Trace metal compositions of Midway and Babb galena and sphalerite

	<u>ppm Cu</u>	<u>ppm Ag</u>
Midway Galena	441	224
Midway Sphalerite	1900	60
Babb Galena	532	307
Babb Sphalerite	1700	44

flotation circuit.

Two miles west of the main shaft the Yandell shaft was sunk to 420 feet (128 m). Only the high grade (>60% fluorspar) was mined. Both of these mines were closed in 1954. The Tabb Fault System veins contain abundant Zinc-bearing zones. 25,000 tons of dumped development muck contain +4.00% Zinc.

In 1963 Minerva Oli Company leased the property, conducted a diamond drill program, rehabilitated the shafts and commenced underground mining. Up until 1975, when production ceased, they had produced a total of +9,300 tons of concentrate.

Babb-Barnes - In the early seventies, 45 angle diamond drill holes were completed. In 1972 a shaft was sunk and production was established at the 500, 600 and 700 foot (152, 183 and 213 m) levels. In 1973 a processing plant was erected. Between August 1973 to December 1978, over 130,000 tons of ore grading 38% CaF<sub>2</sub> and +360 tons of Zinc concentrates averaging 63% were produced. No lead concentrates were recovered.

Levias-Crittenden Fault System - This zone was one of the highest grade fluorspar producers in the U.S. Prior to 1943 over +91,000 tons of fluorspar ore was mined which often ranged above 60% CaF<sub>2</sub> and 4.0% Zinc. In 1946 Alcoa purchased the property and completed an auger and diamond drill program. The surface deposit of +40,000 tons fluorspar was mined but the underlying vein deposit was left intact.

Franklin - Past production is between 37,000 to +55,000 tons from two shafts. The grade is unknown, however, ZnS is abundant in hand samples.

Hutson Zinc Mine - Mined from 1967 to 1971 for high grade Zinc ore, over 400,000 tons of ore of +14% Zinc were produced by Eagle-Picher Corporation. Earlier records indicated over 600,000 tons mined prior to 1967 at about 12% Zinc. This deposit is a bedded replacement with accessory amounts of fluorspar.

Moore Hill Fault System - Past work on the system consists of numerous small shafts, 24 diamond drill holes by Alcoa and 2 by the U.S. Bureau of Mines. Approximately 2,500,000 tons of ore with significant Zinc values have been mined.

Robinson Decline - Between 1965 and 1980 a deposit with bedded and vein features was discovered. A bedded zinc deposit was drill-indicated initially and later discovered were overlying replacement type fluorspar deposits. An exploration decline was completed to the upper fluorspar deposit. Almost 1,500 tons of fluorspar mineralization were

mined. This ore included development muck from the cross-cut connecting the decline to the raise-bored shaft. Bedded Zinc underlies the fluorspar deposit but was not developed.

Claylick Fault - Prior to 1945, production is thought to have amounted to +100,000 tons of fluorspar. Ore was taken from two different underground levels. Zinc values ranged from 2.0% to 4.5% in crude ore.

As shown in Table 2, Zinc production from this district has been significant. About 350,000 tons of contained Zinc metal in concentrates have been produced in the last 100 years. (U.S. Bureau of Mines Yearbook; Baxter et al., 1973.) From this above data and ore reserves predicted in known deposits by A.C.A. Howe Pty. Ltd. (Table 2), additional possibilities can be seen to exist for Zinc production within the district. The question is, "Are production plans based solely on Zinc values practical and economical?" Cash flow studies in this paper address the question of economics and the practicality of processing.

#### ORE PROCESSING FOR FLUORSPAR AND SULFIDE CONCENTRATES

As mined, the fluorspar ore usually contains 15% to 40% of calcium fluoride ( $\text{CaF}_2$ ). The milling process converts this crude ore into a final product containing in excess of 97%  $\text{CaF}_2$  (acid spar).

Mined ore is first crushed. It then may be upgraded to a higher fluorspar content by log washing or a heavy media separation process which removes rock containing little or no fluorspar. The waste rock is often sold as gravel for road construction. The upgraded ore is fed into a ball mill grinding circuit which produces feed pulp for the Flotation Circuit.

Separation of fluorspar is by "froth flotation" in which the contained ore minerals are selectively extracted and concentrated. Lead, then zinc, are extracted as sulphides prior to the concentration of fluorspar.

A vacuum filter reduces the moisture content of the sulfide and fluorspar concentrates to around 10%. Yielding a moist powder called "filtercake". Alternatively, the fluorspar concentrate can be kiln dried and bagged. The ore is processed to concentrate producing different grades ranging from 80% calcium fluoride which is the metallurgical grade, to 97% calcium fluoride which is called acid grade.

Acid grade fluorspar is used in the manufacture of hydrofluoric acid which has numerous uses in the aluminum, chemical, fluorchemical and uranium industries. It is also used in aerosols, fluorinated hydrocarbone refrigerants, and to produce elemental fluorine.

Table 2. Lead and zinc reserves

A) Recorded Metal Production

1880 - 1979; Tons of Metal in Concentrates

Zn	Pb
350,000	95,000

B) Probable Pb & Zn Reserves in District

I) Zn -

Vein Deposits; Grade > 3.0% Zn: 7,000,000 tons

Bedded Deposits; Grade > 12.0% Zn: 1,500,000 tons

II) Pb - (As Co-product with Zn)

Vein Deposits: Grade > 1.0% Pb; 3,000,000 tons

Bedded Deposits: None

C) Possible Metal Tons in Concentrate at 90% Floatation Recovery and 90% Mine Recovery

<u>Zn</u> - Vein: 170,100 tons	Pb - Vein: 30,000 tons
Bedded: <u>145,000 tons</u>	
315,100 tons	

With Zn @ 90c/lb = \$567,000,000 metal value

Lower grade fluorspar is used as a flux in the steel industry; as a basic component in glasses, enamels and fibreglass in the ceramic industry; in specialty areas in zinc smelting; as a clinkering aid in portland cement; in brick and tile manufacture; and in the manufacture of calcium carbide, fibre optics glass strands, teflon and high tech organo-fluorine polymers.

ZnS concentrate is easily produced as a by-product in the flotation mill prior to the flotation pulp reaching the spar conditioners.

#### PROCESS ENGINEERING STUDY AND ECONOMIC FEASIBILITY OF CONVERTING FLUORSPAR MILLS TO ZINC PRODUCTION

##### Economic Parameters:

Bedded zinc deposits in the district are known to contain high zinc ore with grades above 12% Zinc. Values were calculated on estimated pre-tax returns using one case with 20% zinc as feed to the mill and a second case of 14% zinc as feed.

In 1988, a pilot run of +5,000 tons of low grade fluorspar ( $\leq 17\% \text{CaF}_2$ ) and higher grade Zinc ore (+3.5% Zn) was completed at the Babb mill. Results are displayed in Table 3. It can be readily seen that an excellent Zinc concentrate can be produced and maintained with good recovery performance.

One of the major factors influencing the excellent grade and recovery of Zinc concentrates is the ore texture as seen in Figures 7 and 8. The sphalerite grains are clean, rarely showing inclusions of fluorite or galena. Also, since the planar, mutual boundary surfaces between sphalerite, galena and gangue minerals are precise and sharp, ease of grinding to achieve liberation is indicated. Occasionally sphalerite will corrode or embay galena as in Figure 9. This relationship accounts for sometime high amounts of Zinc in pilot plant generated Pb concentrates. On the other hand, galena is not seen to embay or replace sphalerite. These relationships are true in vein and bedded ores.

For the purpose of calculating these tables, certain parameters were held constant in all cases. The mining cost is assumed to be \$22.00 per ton as per estimates by a contractor. The milling costs are based on operating costs developed through the pilot plant operations. These costs

Table 3. Zinc pilot study: crushing and flotation

- a) 5,000 Tons Ore @ 3.5% Zn
- b) 158 Tons Metal = 90.5% Yield  
233 Tons of Concentrate
- c) Concentrate Analysis: 62% - Zn (Pb < 0.1%)  
<0.1%  $\text{CaF}_2$   
37% - S
- d) Production Parameters:  
10 Tons Per Hour Feed  
99% - 80 Mesh Grind  
Conventional Zn Reagents  
Filter Cake < 10%  $\text{H}_2\text{O}$

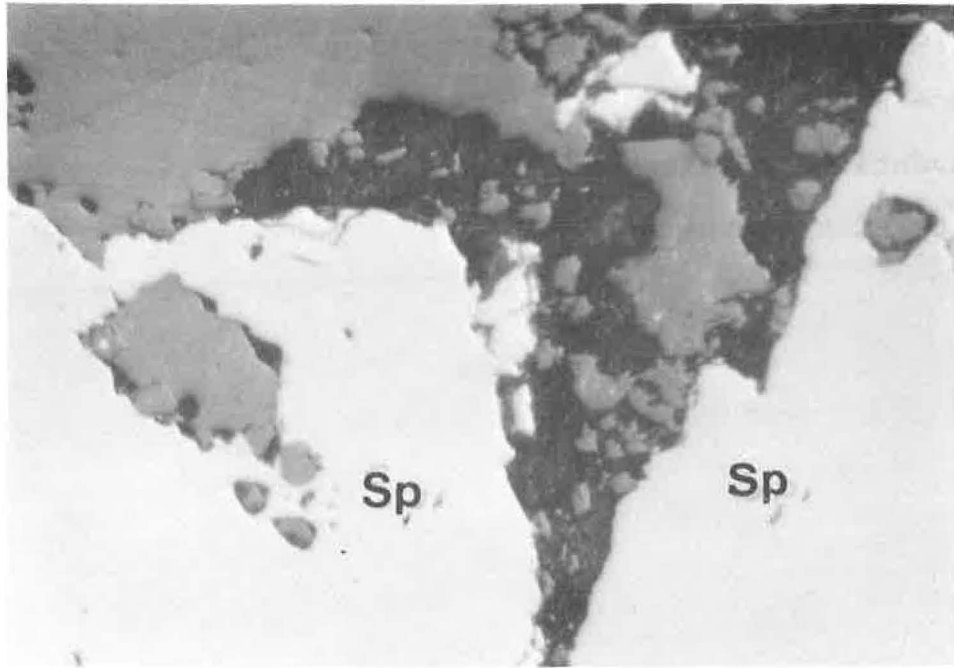


Figure 7. Sphalerite in fluorspar. Photo at 160x.

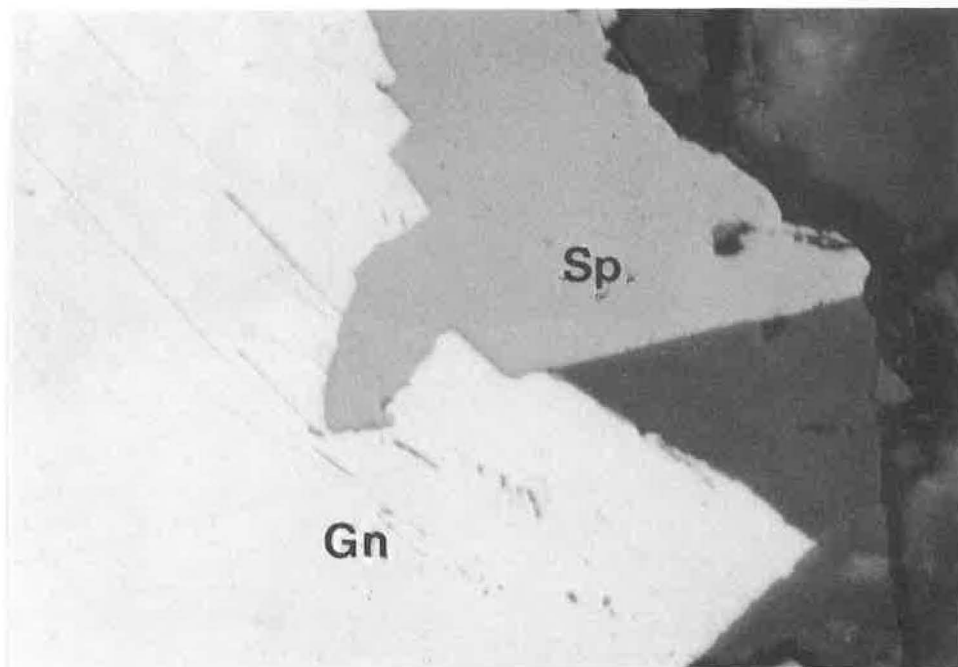


Figure 8. Mutual boundary of galena and sphalerite. Photo at 160x.

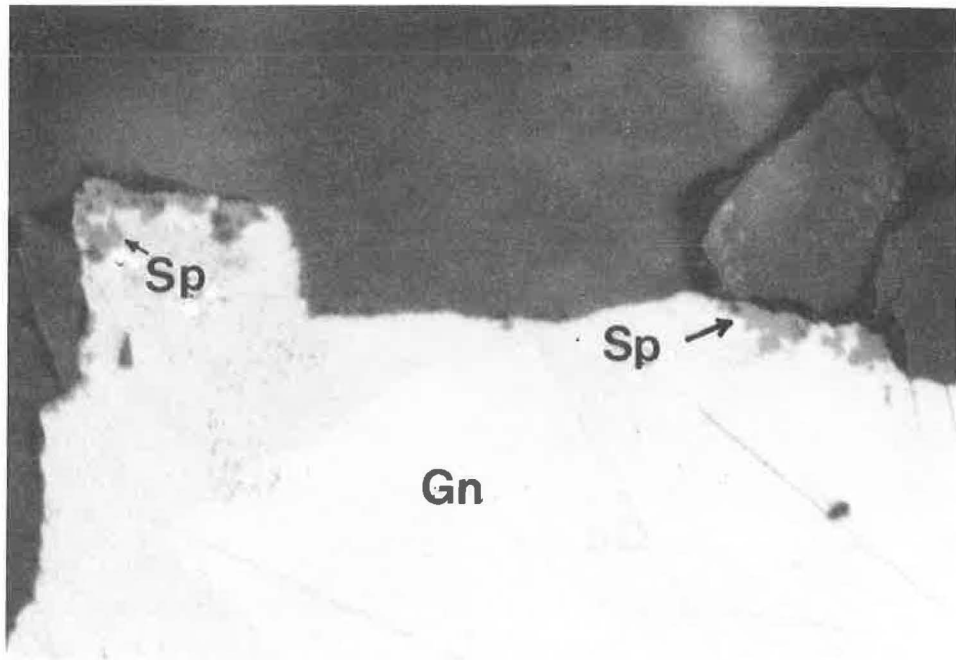


Figure 9. Galena embayed and replaced by sphalerite. Photo at 160x.

include labor, power, reagents, and administrative costs including current taxes. A constant milling rate of 12 tons per hour was assumed which is well within normal capabilities. The results are reported in Table 4.

As can be seen, the worst possible condition of a 14% zinc feed with a 60% recovery and a price of 40 cents per pound for zinc would still yield a profit of \$8,828 per operating day providing the smelter paid for 92% of the contained zinc in the concentrates. Large producers are paid at least 92% of the zinc values contained in concentrates and the possibility exists that a similar contract could be negotiated for a small producer if regular shipments were guaranteed and a high grade of product was maintained. The high grade of product is consistent with by-product zinc concentrate that has already been produced in pilot operations (Table 3.)

A 60% recovery of zinc was achieved in the pilot operations under the worst conditions and over 90% recovery under optimum conditions. The ore that yielded such a low recovery was stockpiled ore that had been mined 40 years previously. The sphalerite contained in this ore had been weathered badly, thus increasing the content of zinc oxide minerals and sulfates. Freshly mined ore yields a higher recovery closer to 80% and better.

A more realistic case would be for 14% zinc in the feed with a recovery of 80% and the smelter paying on 92% of the zinc. This situation would yield an unadjusted return of \$20,698.56 per operating day.

The projected life of a zinc deposit of 400,000 tons would be 4.40 years with a six day operating week, i.e., 12 days on and two days down. This estimate is based on 306 operating days per year, including seven holidays.

Based on the current market for zinc, it is logical to consider whether a small flotations mill should be temporarily converted into a zinc concentrator to take advantage of the current bullish Zinc markets.

#### Conversion of Convention Fluorspar Flotation Mill for Processing of High Zinc Ore

A typical flotation mill designed to produce acid grade fluorspar concentrate generally consists of the following circuits:

Crushing → Heavy Media Up-Grading → Grinding → Pb Circuit  
Tails →  
(Optional)  
Filter

Table 4. Pre-tax return in dollars per operating day

20% Zinc, 288 tons/day, Smelter payment on 92% of contained Zinc

Recovery price/lb Zinc	.50	.48	.46	.44	.42	.40
80	33,416.64	31,720.90	30,025.15	28,329.41	26,633.66	24,937.92
75	30,767.04	29,177.28	27,587.52	25,997.76	24,408.00	22,818.24
70	28,117.44	26,633.66	25,149.99	23,666.11	22,182.34	20,698.56
65	25,467.84	24,090.05	22,712.26	21,334.46	19,956.67	18,578.88
60	22,818.24	21,546.43	20,274.62	19,002.82	17,731.01	16,459.20

20% Zinc, 288 tons/day, Smelter payment on 80% of contained Zinc

Recovery price/lb Zinc	.50	.48	.46	.44	.42	.40
80	27,887.04	26,412.48	24,937.92	23,463.36	21,988.80	20,514.24
75	25,583.04	24,200.64	22,818.24	21,435.84	20,053.44	18,671.04
70	23,279.04	21,988.80	20,698.56	19,408.32	18,118.08	16,827.84
65	20,975.04	19,776.96	18,578.88	17,380.80	16,182.72	14,984.64
60	18,671.04	17,565.12	16,459.20	15,353.28	14,247.36	13,141.44

14% Zinc, 288 tons/day, Smelter payment on 92% of contained Zinc

Recovery price/lb Zinc	.50	.48	.46	.44	.42	.40
80	20,698.56	19,511.54	18,324.52	17,137.50	15,950.48	14,763.46
75	18,843.84	17,731.01	16,618.18	15,505.34	14,392.51	13,279.68
70	16,989.12	15,950.48	14,911.83	13,873.19	12,834.55	11,795.90
65	15,134.40	14,169.95	13,205.49	12,241.04	11,276.58	10,312.13
60	13,279.68	12,389.41	11,499.15	10,608.88	9,718.62	8,828.35

Zinc Circuit Tails to Fluorspar Circuit (2 roughers, 2 cleaners, 2 scavengers,

Final Cleaner) Leaf Filter or Vacuum Filter

A consideration of converting this design to accommodate high grade Zinc ore is presented below. The conversion process is described in terms of the Babb mill where pilot flotation runs were accomplished.

The Babb mill was designed as a fluorspar concentrator to produce fluorspar as the primary product with a zinc concentrate as a by-product. This setup works well as long as the zinc content of the flotation feed does not exceed 4% or the lead content of the feed does not exceed 0.1% of the total. Should the zinc content of the flotation feed increase substantially above this level, several options are available.

a) The first of these is to eliminate the lead circuit and convert it into an additional zinc circuit. This would handle up to 8% zinc in the feed providing the lead content of the feed remained less than .11% lead. In this type of circuit, it would be anticipated that at least 90% of the lead content of the ore would report to the zinc concentrate. If the ore were freshly mined at least a 90% recovery of zinc would be anticipated. If the lead content was above .11% then the zinc concentrate would contain so much lead that it would be difficult to market.

At a fixed feed rate of 200 tons per day through the mill, the lead rougher circuit must be operated as long as the lead content of the feed exceeds .11%. However, it probably would not be economically feasible to operate the lead cleaners unless the lead content of the ore exceeds .6% lead, providing there is a greater need of these cleaner cells for zinc recovery. It is noted that if no use exists for the lead circuit equipment then a lead concentrate could be produced with this equipment and it could contribute to the income as a by-product. In this event a leaf filter would have to be purchased for the lead concentrate.

If the feed to flotation does not exceed .11% lead and 8% zinc, the fluorspar circuit can be operated in a near normal manner. The zinc filter could be utilized to filter only zinc concentrates and the spar filter would remain in service for use in filtering by-product spar concentrate. However, should the lead content of the float feed exceed .11% or the zinc content exceed 8% zinc, then the spar circuit must be shut down for use in the zinc circuit.

b) In the event that the float feed exceeds 8% zinc and/or it is desirable to recover lead concentrate, the lead rougher cells would be used to remove lead and this rougher

concentrate would be pumped directly to the filter or final tailings. With higher zinc grades, the zinc circuit would continue to operate as normal. The zinc rougher tailing at this point would still contain a considerable amount of zinc. The zinc rougher tailing would then be pumped to the head of the spar rougher cells with the spar conditioners being bypassed. The spar rougher cells then would become part of a new zinc circuit. The rougher concentrate being pumped from the former spar rougher cells would not go to the spar second cleaner cells. This pulp would then be upgraded through the 3rd cleaner spar cells with the 2nd cleaner tailing being returned to the head of the rougher cells. The 3rd cleaner concentrate (now 2nd cleaner concentrate) would be pumped to the existing lead cleaners to be further upgraded into an acceptable grade of zinc concentrate. The tailing from these cleaner cells would be returned to the 3rd cleaner spar cell. The concentrate from both the old and new zinc cleaner cells would be pumped to the zinc filter. The filtrate water from this filter should then be rerouted to the spar rougher scavenger cells to recover any fine zinc passing through the filters. The limiting factor of this circuit is the capacity of the disc-type zinc filter. If the zinc content of the float feed exceeded 8% zinc, then it would be necessary to use the spar filter to filter zinc concentrate. Utilizing the complete spar circuit to process zinc would allow any grade of zinc ore to be processed.

Flotation feed with higher zinc content can be processed with the existing Babb concentrator. Up to a 8% zinc ore can be treated with the existing lead and zinc circuits providing the lead content of the feed is less than .11%. All other zinc ores would require the shutdown and conversion of the spar flotation section of the concentrator. The conversion to zinc processing could be made easily during any scheduled two day period.

#### CASH FLOW ESTIMATES BASED ON PILOT OPERATIONS AND DOCUMENTED FIXED COSTS

Variable and fixed costs for a 50 week production year are presented in Table 5. These data are based on a pilot scale run of a rehabilitated flurospar plant for a period of 60 days. Reagent consumptions, power, labor, fuel oil, insurance and lease payments are actual data. Cost of ore to the mill is based on the average of three quotes from mining contractors. It is felt that this number is significantly above probable "in house" costs and reflects the single largest factor that could vary in actual production.

Five cases are presented with the following variations in cost:

Case 1: 14% Zinc ore; \$453.00 net per concentrate ton receipts based on .45 per pound zinc.

Case 2: 14% Zinc ore; \$906.00 per concentrate ton receipts

Table 5. Profit-loss comparison for specific production cases

	Case (1)	(2)	Weekly Cash Flow Estimates		
			(3)	(4)	(5)
	14%	14%	4%	4%	4%
<u>Mill Production:</u>	Zn	Zn	Zn	Zn	Zn
Tons Per Hour Through Mill	20	20	20	20	20
Total Ore Per Week	2880	2880	2880	2880	2880
Contained Zn tons	403	403	115	115	115
Mill Recovery Tons (80%)	323	92	92	92	92
Zn Concentrate Tons	512	512	146	146	146
Total Tails Tons	2300	2300	2700	2700	2700
Total Tons Ore Annual (50 Weeks)	144,000	144,000	144,000	144,000	144,000
Total Tons Concentrate Annual	25,600	25,600	7,300	7,300	7,300
Cost of Ore to Mill/Ton	\$25.00	\$25.00	\$25.00	\$25.00	\$25.00
Weekly Cost of Ore	\$72,000	\$72,000	\$72,000	\$72,000	\$43,200
<u>Sales:</u>					
Zinc Concentrate					
@ \$453.00*	\$231,936	-	\$66,138	-	-
@ \$906.00*	-	\$463,872	-	\$132,276	\$132,276
* \$453. = 45c Zinc					
* \$906. = 90c Zinc					
<u>Costs:</u>					
Fixed	\$10,641	\$10,461	\$10,461	\$10,461	\$10,461
Variable	11,047	11,047	11,047	11,047	11,047
Ore to Mill	72,000	72,000	72,000	72,000	43,200
	\$93,688	\$93,688	\$93,688	\$93,688	\$54,247
<u>Profit/&lt;Loss&gt; Before Tax</u>					
Weekly Profit/<Loss>	\$138,748	\$370,184	<\$27,550>	\$38,588	\$78,029
Annual Profit?<Loss>					
50 Weeks (Million)	\$6.9	\$18.5	<\$1.4>	\$1.9	\$3.9

based on .90 per pound zinc.

Case 3: 4% Zinc ore: \$453.00 net per concentrate for receipts.

Case 4: 4% Zinc ore; \$906.00 net per concentrate ton receipts.

Case 5: 4% Zinc ore; \$906.00 net per concentrate ton receipts; cost of ore to mill is reduced by \$28,800 per week or a 40% reduction in mining and hauling costs.

It is apparent that under the presented parameters, an operation to produce Zinc concentrates is economically feasible under certain constraints: 1) Mining costs must be controlled and preferably below about \$20.00/ton delivered to mill in order to insure a competitive position; 2) Non-union, hourly rates common to Western Kentucky must be employed; 3) Especially with lower grade ores, the high efficiency production of 90%+ recovery of metal must be achieved to provide adequate margins. As Zinc prices soften, the sensitivity of this analysis to receipts is apparent; therefore, a long term contract should be secured with a smelter that provides base price guarantees and concedes a higher margin to the smelter at higher zinc prices.

### Conclusions

The following positions are supportable with scrutiny of available data:

- 1) Zinc resources in the Kentucky Fluorspar District are postulated to exist in sufficient amounts to justify attention of mining corporations;
- 2) It has been demonstrated that high grade Zinc concentrates are produceable from conventional fluorspar circuits at reasonable production costs.
- 3) Financial evaluation of actual pilot scale operations for 60 days allows the conclusion that such a project can be viable within a wide range of Zinc metal prices.

### ADDENDUM:

#### A Note on the United States' Fluorspar Supply and Demand Picture and Environmental Concerns

### Markets and Competition

Of the approximately 700,000 tons of fluorspar consumed in the United States in 1986, only 78,000 tons were produced domestically. Of that tonnage 75,000 tons were produced by Ozark-Mahoning, a subsidiary of Pennwalt Corporation, with mining and milling facilities located in Illinois. (U.S. Bureau of Mines Yearbook.)

Based on verbal data from industrial fluorspar consumers and the U.S. Bureau of Mines commodity expert, Larry Pelham, U.S. consumption of fluorspar for the five years to 1986 is tabulated below (x 1,000 tons):

	<u>1982</u>	<u>1982</u>	<u>1984</u>	<u>1985</u>	<u>1986</u>	<u>1987*</u>
Domestic Production	77	61	72	66	78	78
Imports:						
Acid fluorspar	408	385	521	432	490	470
Metallurgic fluorspar	<u>136</u>	<u>68</u>	<u>182</u>	<u>121</u>	<u>130</u>	<u>110</u>
Total	<u>621</u>	<u>519</u>	<u>775</u>	<u>619</u>	<u>698</u>	<u>658</u>

\*Estimated

Of the import tonnage in acid grades, Mexican producers supply 46% and South African producers supply 43%. Producers in Spain and Morocco are the other main suppliers. Mexican producers also supply nearly 90% of the high grade metallurgical and ceramic fluorspar, bringing the total for Mexican exports to the U.S. to about 67% of the total U.S. market.

Mexican producers sometimes find it difficult to produce high grade fluorspar because of the presence of toxic contaminants such as arsenic, cadmium and antimony. Due to these problems, Spanish ore is being imported at higher costs in order to reduce arsenic levels in hydrofluoric acid production.

A major advantage that Kentucky fluorspar production has over alternative suppliers, is that these deposits are virtually free of arsenic, phosphorous or other toxic contaminants. The presence of a long-term reliable domestic fluorspar source of highest quality should be attractive to U.S. consumers because of the absence of contaminants and advantages in inventory control. Interviews with Allied-Signal, Pennwalt, DuPont, Reynolds, Alcoa and other purchasing staffs confirm this idea.

Chlorofluorocarbons and the Ozone Layer (Based on industry interviews.) Chlorofluorocarbons (CFCs) are inert, odourless, non-toxic and non-flammable chemical compounds in wide use in developed nations. Although their safety and versatility make them excellent industrial chemicals, CFCs are claimed to aid in depletion of the earth's ozone layer.

CFCs which are stable enough to persist in the atmosphere find their way into the upper atmosphere where it is believed by scientists that as they slowly disperse, the chlorine released breaks down the ozone layer which is a protective shield against ultraviolet radiation from the sun. There is a misconception among the general public that the total composition of aerosol cans damages the ozone layer; this idea is incorrect. The damaging reagent is chlorine gas.

International agreements call for a 50% cut in worldwide production of CFCs by 1999. CFC production is a US \$2 billion-a-year industry.

Current estimates for 1988 U.S. and Canada fluorspar consumption are:

Steel (Metallurgical and Acid Grades)	175,000 tons
Aluminium	100,000 tons
Glass, Ceramics and Specialities	65,000 tons
Hydrofluoric Acid	470,000 tons
Total	<u>810,000 tons</u>

About 60% of the Hydrofluoric Acid market is devoted to the production of CFCs. The major uses of CFCs are as coolants in refrigerators and air-conditioners; for making plastic foams used in packaging; and as propellants in aerosol spray cans.

Alternatives to CFCs as aerosol propellants have been in use for some time but substitute gases for other applications are being developed from hydrogen-containing CFC compounds which are less stable than CFCs in current use. Therefore, they decompose before they can reach the stratosphere. The adverse effects on the ozone layer can be reduced as much as 95% by using these alternatives.

The substitute gases are high fluorine fluorocarbons which use up to 50% more fluorite to produce equivalent amounts of the new refrigerants.

The changeover will take probably 3 to 6 years and is likely to increase rather than decrease the market for fluorspar over that period.

## ACKNOWLEDGEMENTS

Obviously, much of the basic data in this report has been compiled by various geologists and engineers over the past 100 years. For keeping the District alive they deserve our appreciation.

Special recognitions are due Mr. Ken Hunt, consulting process engineer, who ran the pilot operations and evaluated the mill for the flotation. Also, the cash flow evaluations are modified from data analyses by James Dorrien-Smith, investment banker.

## REFERENCES

- Baxter, J.W., 1973, Geologic excursion to fluorspar mines in Hardin and Pope Counties, Illinois, Guidebook Series II, Illinois State Geological Survey, 28 p.
- Crittenden County Courthouse - County Clerk and Tax Assessor Records.
- Grogan, R.M. and Bradbury, J.C., 1968, Fluorite - zinc - lead deposits of the Illinois - Kentucky mining districts in Ridge, John D., ed., Ore deposits in the United States, American Institute of Mining, Metallurgical and Petroleum Engineering, pp. 370-399.
- Klepser, H.J., 1954, Fluorspar deposits in western Kentucky, U.S. Geological Survey Bull. 1012-F, Part 3, pp. 115-127.
- United States Bureau of Mines Yearbooks - 1949 through 1981, U.S. Government Printing Office.

APPENDIX: Financial Data for Cash Flow Development

WEEKLY BUDGET FORECAST

<u>CATEGORY</u>	<u>SECTION</u>
FIXED COSTS	1. MILL PERSONNEL 2. CRUSHING & SCREENING PERSONNEL 3. MAINTAINENCE PERSONNEL 4. OFFICE PERSONNEL 5. LABOERATORY PERSONNEL 6. INSURANCE 7. EQUIPMENT LEASE/RENTAL
VARIABLE COSTS	1. FLUORSPAR REAGENTS 2. LEAD/ZINC REAGENTS 3. FUEL OIL 4. ELECTRICITY 5. ADDITIONAL CRUSHING & SCREENING

Note: All data developed from 60 day trial flotation run on rehabilitated beneficiation plant near Salem, Kentucky.

FIXED COSTS

SUMMARY:

	<u>COSTS</u> <u>PER WEEK</u>
1. MILL PERSONNEL	\$3,251.35
2. CRUSHING & SCREENING PERSONNEL	519.18
3. MAINTAINENCE PERSONNEL	1,371.11
4. OFFICE PERSONNEL/GENERAL EXPENSE	1,661.11
5. LABORATORY PERSONNEL	801.80
6. INSURANCE	1,660.00
7. EQUIPMENT LEASE/RENTAL	376.86
	<u>\$9,641.41</u>

1. MILL PERSONNEL

Assumption: 3 shifts of 3 men 6 days per week, 48 hours per man per week.

<u>Position</u>	<u>Hourly Rate</u>	<u>Regular Pay</u>	<u>Overtime Pay</u>	<u>Weekly Pay</u>
Lead Operator	\$6.25	\$250.00	\$75.00	\$325.00
No. 2 Operator	6.00	240.00	72.00	312.00
Helper	5.75	230.00	69.00	299.00
				-----
				\$936.00
				Employer Social Security 70.00
				State & Federal Unemploy. Tax 28.08
				Medical Insurance 49.41
				-----
				Weekly Shift Total 1,083.78
				-----
				Total per Week for 3 Shifts \$3,251.35

2. CRUSHING & SCREENING PERSONNEL

Assumption: 1 Shift per day of 2 men 5 days per week.

<u>Position</u>	<u>Hourly Rate</u>	<u>Regular Pay</u>	<u>Overtime Pay</u>	<u>Weekly Pay</u>
Operator	\$5.50	\$220.00		\$220.00
Operator	5.50	220.00		220.00
				-----
				\$440.00
				Employer Social Security 33.04
				State & Federal Unemploy. Tax 13.20
				Medical Insurance 32.94
				-----
				Weekly Shift Total \$519.18

### 3. MAINTAINENCE PERSONNEL

<u>Position</u>	<u>Hourly Rate</u>	<u>Regular Pay</u>	<u>Overtime Pay</u>	<u>Weekly Pay</u>
Lead Mechanic	\$8.00	\$320.00	\$96.00	\$416.00
Electrician	8.00	320.00	96.00	416.00
Helper	7.00	280.00	84.00	364.00
				-----
				\$1,196.00
				Employer Social Security 89.82
				State & Federal Unemploy. Tax 35.88
				Medical Insurance 49.41
				-----
				Weekly shift Total \$1,371.11

### 4. OFFICE PERSONNEL/GENERAL EXPENSE

<u>Position</u>	<u>Hourly Rate</u>	<u>Regular Pay</u>	<u>Overtime Pay</u>	<u>Weekly Pay</u>
General Manager				\$900.00
Secretary/ Bookkeeper	\$7.00	\$280.00		280.00
				-----
				\$1,180.00
				Employer Social Security 88.62
				State & Federal Unemploy. Tax 35.40
				Medical Insurance 32.94
				-----
				Weekly Shift Total \$1,336.96
				=====

#### Sundry Other

Telephone	\$200.00
Supplies	100.00
Electricity	25.00
Other	100.00
	-----
	\$425.00
	=====

Total for Section	\$1,761.96
	=====

5. LABORATORY PERSONNEL

<u>Position</u>	<u>Hourly Rate</u>	<u>Regular Pay</u>	<u>Overtime Pay</u>	<u>Weekly Pay</u>
Operator	\$8.00	\$320.00		\$320.00
Operator	6.00	240.00		240.00
				-----
				\$560.00
				Employer Social Security 42.06
				State & Federal Unemploy. Tax 16.80
				Medical Insurance 32.94
				-----
				Weekly Shift Total \$651.80
				=====
 <u>Sundry Other</u>				
				Chemicals & Equipment \$150.00
				=====
				Total for Section \$801.80
				=====

6. INSURANCE

	<u>Per Annum</u>	<u>Per Week</u>
General Liability	\$30,000.00	\$600.00
Property	18,000.00	360.00
Workers Compensation	20,000.00	400.00
Umbrella Liability	12,000.00	240.00
Vehicle	3,000.00	60.00
	-----	-----
	\$83,000.00	\$1,660.00

7. EQUIPMENT LEASE

	<u>Per Month</u>	<u>Per Week</u>
Front-end Loader	\$1,250.00	\$300.00
4-wheel Drive Truck	320.00	76.81
	-----	-----
	\$1,570.00	\$376.86

VARIABLE COSTS

SUMMARY:

1. FLUORSPAR REAGENTS
2. LEAD/ZINC REAGENTS
3. FUEL OIL
4. ELECTRICITY
5. ADDITIONAL CRUSHING & SCREENING

<u>Tons Per Hour</u>	<u>Fluorspar Reagents</u>	<u>Zinc/Lead Reagents</u>	<u>Fuel Oil</u>	<u>Electricity</u>	<u>Additional Crushing &amp; Screening</u>	<u>Total</u>
8	\$4,218.76	\$640.48	\$2,232.85	\$3,000.00		\$10,092.09
10	\$5,273.45	\$800.60	\$2,791.07	\$3,100.00		\$11,965.12
12	\$6,328.14	\$960.72	\$3,349.28	\$3,200.00	\$0.00	\$13,838.14
14	\$7,382.83	\$1,120.84	\$3,907.49	\$3,300.00	\$66.00	\$15,777.16
16	\$8,437.52	\$1,280.96	\$4,465.70	\$3,400.00	\$132.00	\$17,716.18
18	\$9,492.21	\$1,441.08	\$5,023.92	\$3,500.00	\$198.00	\$19,655.21
20	\$10,546.90	\$1,601.20	\$5,582.13	\$3,600.00	\$264.00	\$21,594.23

### 1. FLUORSPAR REAGENTS

Useage @ 8 Tons per per Hour	Pounds per Week	Unit Cost	Cost Week
Quebracho	1730	\$0.7900	\$1,366.35
Oleic Acid	2282	0.3750	855.59
Sodium Silicate	1964	0.2045	401.60
Soda Ash	12762	0.1250	1,595.25
			-----
			\$4,218.78
			=====

### 2. ZINC/LEAD REAGENTS

Useage @ 8 Tons per Hour	Pounds per Week	Unit Cost	Cost per Week
Zinc Hydrosulphate	238.2	\$1.0635	\$253.33
Copper Sulphate	381.0	0.6710	255.65
MIBC	48.0	0.7130	34.22
404	11.4	0.8800	10.03
325	17.4	1.0250	17.84
211	28.8	1.4100	40.61
633	57.6	0.5000	28.80
			-----
			\$640.48
			=====

### 3. FUEL OIL

Assumption: Fuel Useage @ 2.88 gallons per ton.  
Price @ \$0.673 per gallon.

Tons per Hour	Gallons per Week	Cost per per Week
8	3318	\$2,232.85
10	4147	2,791.07
12	4977	3,349.28
14	5806	3,349.28
16	6636	4,465.70
18	7465	5,023.92
20	8294	5,582.13

### 4. ELECTRICITY

Electricity costs are based on actual cost incurred during operations.

## 5. ADDITIONAL CRUSHING & SCREENING

Fixed costs provide for 40 hours per week for crushing and screening. At 50 tons per hour this will provide sufficient ore for a milling rate of up to 12 tons per hour, allowing for 10% downtime. Additional hours for higher milling rates result in additional labor costs as follows.

<u>Milling Rate per Hour</u>	<u>Additional Hours</u>	<u>Cost of 2 Men/Hour</u>	<u>Cost per Week</u>
12	0	\$11.00	\$ 0.00
14	6	11.00	66.00
16	12	11.00	132.00
18	18	11.00	198.00
20	24	11.00	264.00



For convenience in selecting our reports from your bookshelves, they are color-keyed across the spine by subject as follows:

Red	Valley and Ridge mapping and structural geology
Dk. Purple	Piedmont and Blue Ridge mapping and structural geology
Maroon	Coastal Plain mapping and stratigraphy
Lt. Green	Paleontology
Lt. Blue	Coastal Zone studies
Dk. Green	Geochemical and geophysical studies
Dk. Blue	Hydrology
Olive	Economic geology
Yellow	Environmental studies
	Engineering studies
Dk. Orange	Bibliographies and lists of publications
Brown	Petroleum and natural gas
Black	Field trip guidebooks
Dk. Brown	Collections of papers

Colors have been selected at random, and will be augmented as new subjects are published.

§ 6652/500

**The Department of Natural Resources is an equal opportunity employer and offers all persons the opportunity to compete and participate in each area of DNR employment regardless of race, color, religion, sex, national origin, age, handicap, or other non-merit factors.**